

# CARBON DIOXIDE AND THE ROCK MASSIF

PETR MARTINEC  
WITH CO-AUTHORS



ÚGN AV ČR, v. v. i., OSTRAVA

CARBON DIOXIDE  
AND  
THE ROCK MASSIF



ÚGN AV ČR, v. v. i., OSTRAVA

## **CARBON DIOXIDE AND THE ROCK MASSIF**

Ústav geoniky AV ČR v. v. i. (Institute of Geonics ASCR),

Studentská 1768, CZ-708 00 Ostrava - Poruba, Czech Republic

Printers: Tiskárna AG TYP, Rudé armády 1468, CZ-514 71 Kostelec nad Orlicí, in 2012

Cover design and graphics: Jan Martinec, Jr.

© Ústav geoniky AV ČR, v. v. i. Ostrava

ISBN 978-80-86407-28-9

CARBON DIOXIDE  
AND  
THE ROCK MASSIF

PETR MARTINEC

WITH CO-AUTHORS:

PETR KOLÁŘ  
VÍT MARTINEC  
BOŽENA SCHEJBALOVÁ  
BOLESLAV TARABA

**Reviewers:**

Prof. Ing. Josef Aldorf, DrSc.  
VŠB-Technical University, Ostrava

Prof. Ing. Petr Bujok, CSc.  
VŠB-Technical University, Ostrava

Ing. Petr Šarboch  
director of Main Mine Rescue Station, Praha, a.s.

**Technical assistance:**

Ing. Vlastimil Kajzar, Ph.D.

**Translation:**

Rudolf Štefec, Anna Žaludová

**Annotation:**

Martinec, P. et al. (2012): Carbon dioxide and the rock massif.  
Ústav geoniky Akademie věd ČR, v. v. i., (Institute of Geonics ASCR, Ostrava).  
Pages: 156, Figures: 72, Tables: 41, Plates: A-F

ISBN 978-80-86407-28-9



**SUPPORT FROM THE FOLLOWING INSTITUTIONS  
IS GRATEFULLY ACKNOWLEDGED:**

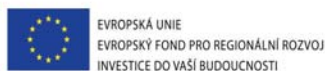
**INSTITUTE OF GEONICS ASCR IN OSTRAVA:  
Long-term conceptual development fund for research organisations, RVO no. 68145535.**



**MORAVIAN-SILESIAN REGION**



and for support of sample analysis from:  
Institute for Clean Technologies for Mining and Utilization of Raw Materials for Energy,  
project no. CZ.1.05/2.1.00/03.0082  
Operational Programme **Research and Development for Innovations** financed by the EU  
Structural Funds and the Czech Republic national budget



The Czech edition of the present work was sponsored by ČEZ Group of Companies:



Support has also been extended by AG TYP Printing House:



*The authors' thanks are also due to the following individuals:*

to **Professor Ing. Josef Aldorf, DrSc., Professor Ing. Petr Bujok, CSc.,**  
and **Ing. Petr Šarboch** for reviewing the manuscript;  
to our colleagues **Ing. Alena Kožušníková, CSc.** and **Dr. Ing. Pavel Konečný,**  
of the Institute of Geonics Academy Sciences, CR, for contributing the data on the permeability  
of rocks and coal that appear in Chapter 2;  
to **Ing. Petr Kříž, Ph.D.,** of DIAMO Corp., and to **Ing. Mgr. Aleš Bouda,**  
for their expert comments and discussions.



# FOREWORD

Carbon dioxide stored within rock massifs has become a topic of worldwide importance, widely discussed today by geologists, geochemists, and geotechnologists as well as environment experts. Within the scope of geology, traditional studies aiming to examine the origins and incidence of carbon dioxide in rock environments have since recently been expanded to also include investigations into the conditions under which carbon dioxide can be captured and stored in underground locations. Geotechnology is concerned with underground occurrence of carbon dioxide because of its impact on mining activities, owing to the fact that mines frequently face formidable problems whenever gases are released during the course of either driving or extraction operations. Currently, intense planning is in progress focused on implementation of the technology of carbon dioxide storage in suitable geological host formations within the framework of the CCS (Carbon capture and storage) technologies. This is reflected, for instance, in the document entitled **Investing in the Development of Low Carbon Technologies (SET-Plan)**, Communication from the European Commission COM (2009) 519.

In this context, the monograph by Professor Petr Martinec and his co-workers is a welcome contribution deserving of attention. This book, focused on the conditions prevailing in the Czech Republic (and also mentioning the adjoining regions of Poland), presents an overview that summarizes important information gathered thanks to the mining activities taking place on the said territories during recent decades. In view of the need to cope with the technical problems being confronted, a sizeable volume of very valuable knowledge has been collected and processed from non-repetitive data which is of interest to Czech Republic's geology as well as to the country's mining industry and its downsizing. Today, this wealth of information is gaining in importance again because of its aspects relating to underground storage of carbon dioxide.

At this point I wish to express my appreciation for the patient and targeted work of Professor Martinec whose efforts and careful research have been focused for years onto a systematic classification of the geological, petrological, and geotechnical information, bringing together not only the latest data but also the results originally obtained in different periods of the past and in different contexts. His previous monographs should be mentioned here; they include his *Atlas of coal from the Czech part of Upper Silesian Basin* (2005, in Czech, with an English abstract); *Termination of underground coal mining and its impact on the environment* (2006, in English); *Geological environment and geotechnical properties of covering strata of Carboniferous in the Czech part of the Upper Silesian Basin* (2008, in Czech, with an English abstract). All these publications, including the monograph hereunder, incorporate the results of his research of many years, with a potential for future use.

May the present monograph gain the attention and appreciation of professionals in the field it deserves, and may it find its well-deserved niche within the expanding body of research devoted to carbon dioxide storage within the framework of the CCS initiative.



Professor RNDr. Radim Blaheta, CSc.  
Director, Institute of Geonics Academy of Sciences of the CR, Ostrava





# CONTENT

## CARBON DIOXIDE AND THE ROCK MASSIF

<b>1. INTRODUCTION</b>	<b>15</b>		
<b>2. CARBON DIOXIDE AND THE ROCK MASSIF</b>	<b>17</b>		
2.1 Natural emissions of carbon dioxide in Bohemian Massif	17		
2.2 The water - carbon dioxide phase diagram	19		
2.3 The H <sub>2</sub> O-NaCl-CO <sub>2</sub> system under the natural conditions of coal deposits	21		
2.4 Sudden liberation of carbon dioxide and methane from the rock massif or from coal seams	23		
2.5 Factors influencing CO <sub>2</sub> and CH <sub>4</sub> adsorption on bituminous coal under laboratory conditions	23		
2.5.1 High-pressure adsorption of carbon dioxide on bituminous coal	24		
2.5.2 Effect of temperature on adsorption of carbon dioxide on bituminous coal	25		
2.5.3 Effect of moisture in coal on adsorption of carbon dioxide	26		
2.5.4 Effect of coal grain size on carbon dioxide adsorption	26		
2.5.5 Comparison of the adsorption properties of carbon dioxide and methane on bituminous coal	27		
2.5.6 Adsorption of carbon dioxide and methane on coal from the Intra-Sudeten Basin	28		
2.6 Nitrogen permeability of rock and coal under triaxial stress	29		
<b>3. CARBON DIOXIDE IN CENTRAL BOHEMIAN CARBONIFEROUS (SLANÝ COAL DEPOSIT)</b>	<b>33</b>		
3.1 Geology, hydrogeology and gas occurrence	33		
3.2 Lithology, mineralogy, physical properties of sedimentary rocks from Mirošov Horizont	37		
3.2.1 Sand-conglomerate to sandstone rock types	39		
3.2.2 Clayey-silty rocks frequently occurring with sandy admixtures	41		
3.3 Physical properties of rocks	42		
3.3.1 Properties of Mirošov horizon rocks in borehole SJ 847 m in the Slaný Mine skip shaft	42		
3.3.2 Porosimetric characteristics of rock determined by high-pressure mercury porosimetry	43		
3.3.3 Residual gas in rocks and gas composition in container samples from borehole SJ 847 m	51		
3.4 Sinking of Slaný Mine shafts and the adoption and effectiveness of certain technical measures taken	51		
3.4.1 Packing of the massif prior to sinking the Slaný Mine shafts	51		
3.4.2 Sinking of the hoisting shaft	57		
3.4.3 Sinking of the skip shaft	57		
3.4.4 Liquidation of the two shafts by backfilling	62		
3.5 Carbon dioxide outbursts experienced during the sinking of Slaný Mine shafts and the manifestations thereof	62		
3.5.1 Outbursts in the skip shaft	62		
3.5.2 Outbursts in the hoisting shaft	66		
3.5.3 Technical measures to limit rock and gas outbursts	67		
3.6 Summary	67		
<b>4. ACCUMULATION OF CARBON DIOXIDE IN BURIED WEATHERED COVER OF CRYSTALLINE BASEMENT AND IN BASAL SEQUENCES OF COVERING STRATA (MOST BASIN, NORTH BOHEMIA)</b>	<b>69</b>		
4.1 Carbon dioxide occurrence in Most basin groundwaters within the Krušné hory (Ore Mts) piedmont basin	69		
4.2 The case of CO <sub>2</sub> liberation during the sinking of the Komořany drainage shaft	70		
4.3 The rock massif and the properties of the rocks therein	72		
4.3.1 The porous system in Upper Cretaceous rocks and porosimetric data	76		
4.3.2 The porous system in fresh and kaolinized gneisses and porosimetric data	76		
4.3.3 Physical properties of the rocks	83		
4.4 Gas conditions in Komořany drainage shaft and in boreholes KO-16 and V2A	84		
4.5 Summary	86		

<b>5. CARBON DIOXIDE AND METHANE IN THE CZECH AND POLISH PART OF INTRA – SUDETEN BASIN</b>	<b>87</b>
5.1 Geology, hydrogeology and gas occurrences	87
5.2 The Czech part of Intra – Sudeten basin	88
5.2.1 Geological situation conducive to the occurrence of carbon dioxide and methane in Zdeněk Nejedlý Mine	88
5.2.2 Occurrences of carbon dioxide and methane, mixed outbursts of coal and gases	89
5.3 Polish part of the Intra – Sudeten basin	96
5.4 Summary	99
<b>6. CARBON DIOXIDE IN THE CZECH PART OF THE UPPER SILESIAN BASIN</b>	<b>101</b>
6.1 Carbon dioxide in basal clastics of Lower Badenian sediments	101
6.2 Coal and gas outbursts in mines in the western part of Ostrava-Karviná Coal District	104
6.3 Carbon dioxide in zones of disturbed tectonics in the Carboniferous massif	106
6.4 Carbon dioxide in mine air and mine gas ascending to surface	106
6.5 Water and gas reservoirs in weathered crust of the Carboniferous	108
6.6 Summary	115
<b>7. INFLUENCE OF CARBON DIOXIDE ON CORROSION OF CONCRETE STRUCTURES IN MINES AND UNDERGROUND CONSTRUCTIONS</b>	<b>116</b>
7.1 Model of concrete corrosion	116
7.2 Summary	118
<b>8. CONCLUSIONS</b>	<b>119</b>
<b>PLATES</b>	
PLATE A	122
PLATE B	124
PLATE C	128
PLATE D	132
PLATE E	138
PLATE F	142
<b>REFERENCES</b>	<b>145</b>

# ACRONYMS IN TEXT, TABLES AND FIGURES

<b>Bpv</b>	– altimetric system Baltic sea after levelling	<b>VOKD</b>	– Výstavba ostravsko-karvinských dolů (Ostrava-Karviná Mines Development OKD Ent.)
<b>CO<sub>2</sub><sup>karbonátový</sup></b>	– CO <sub>2</sub> in carbonates	<b>VKD</b>	– Výstavba kladenských dolů (Kladno Mines Development Ent.)
<b>DP</b>	– mine field	<b>VUD</b>	– Východočeské uhelné doly (East Bohemia Coal Mines Ent.)
<b>DPB OKD</b>	– Důlní průzkum a bezpečnost OKD, k.p. (před rokem 1990) (DPB OKD Ent.) (before 1990)	<b>VVUÚ</b>	– Vědeckovýzkumný uhelný ústav Ostrava-Radvanice (Coal Research Institute)
<b>HBZS</b>	– Hlavní báňská záchranná stanice (Main Mine Rescue Services)	<b>w<sub>u</sub></b>	– moisture content in situ [% weight]
<b>k<sub>p</sub></b>	– coefficient of permeability for gases [m <sup>2</sup> ]	<b>w<sub>L</sub></b>	– moisture content in laboratory conditions [% weight]
<b>ODMG</b>	– Section of Mine Surveyor and Geologist (in mine establishment)	<b>w<sub>n</sub></b>	– moisture content of sample fully saturated by water (= water absorption) [% weight]
<b>OKR</b>	– Ostrava-Karviná Coal District (in the Czech part of the Upper Silesian Basin)	<b>c<sub>CO<sub>2</sub></sub></b>	– concentration of CO <sub>2</sub> in air [% , ppm, ppmv]
<b>p<sub>c</sub></b>	– total porosity [%]	<b>μ</b>	– Poisson number [-]
<b>p<sub>ef</sub></b>	– effective porosity [%]	<b>ρ<sub>o</sub></b>	– bulk weight [kg·m <sup>-3</sup> ]
<b>p<sub>p</sub></b>	– pressure on the sample surface in time of measurement of gas permeability [MPa]	<b>ρ<sub>s</sub></b>	– specific gravity [kg·m <sup>-3</sup> ]
<b>PÚ</b>	– exploration area	<b>σ<sub>D</sub></b>	– uniaxial compressive strength [MPa]
<b>d<sub>vz</sub></b>	– diameter of sample	<b>σ<sub>T</sub></b>	– splitting tensile strength [MPa]
<b>p<sub>r</sub></b>	– residual pressure after packing [MPa]	<b>σ<sub>VTL</sub></b>	– indent strength (poit loading test) [MPa]
<b>p<sub>t</sub></b>	– pressure of packing [MPa]		
<b>p<sub>gmin</sub></b>	– vertical component of geostatic pressure on the top of body with packing [MPa]		
<b>p<sub>gmax</sub></b>	– vertical component of geostatic pressure on the base of body with packing [MPa]		
<b>(p<sub>t</sub>-p<sub>r</sub>) = p<sub>diff</sub></b>	– differential pressure as difference of packing pressure and residual pressure after packing [MPa]		
<b>R<sub>o</sub></b>	– average vitrinite reflectance [%]		
<b>V<sup>daf</sup></b>	– content of volatile matter in coal, dry [%]		
<b>V<sub>COP</sub></b>	– cumulative volume of mercury intrusion into pores [cm <sup>3</sup> ·g <sup>-1</sup> ] or [mm <sup>3</sup> ·g <sup>-1</sup> ]		
<b>ZŽ</b>	– lost of ignition up to 1000°C in oxidation regime of heating [% weight]		
<b>ÚGN</b>	– Ústav geoniky Akademie věd ČR, v. v. i. v Ostravě (Institute of Geonics ASci CR)		



# 1. INTRODUCTION

Carbon dioxide is an integral part of our atmosphere. Its content in air (386 ppm by volume, i.e., 0.04% by volume) is not constant. It kept changing during the course of geological history. Carbon dioxide enters the atmosphere due to volcanic activity, coalification processes and metamorphic processes taking place in the Earth's crust. It is carried up to the surface in the form of emissions of gaseous CO<sub>2</sub> (as „dry gas“) or in springs of underground water (as free gas and also in dissolved form, as Ca(HCO<sub>3</sub>)). However, a great portion of carbon dioxide thus migrating in the Earth's mantle becomes dissolved in deep aquifers. Then the dissolved gas is stored in the pores of rocks or in cracks of the rock massif. Frequently, it is contained in coal seams as adsorbed carbon dioxide, together with methane, or also in rocks rich in dispersed coal matter. It is also believed that carbon dioxide can be generated by the activity of petrophile bacteria present in the rock massif.

Carbon dioxide also enters the atmosphere by oxidation of buried decayed organic matter (bodies of plants and animals). Then, the biosphere proper produces carbon dioxide as a product of metabolic processes (breathing, digestion, and decomposition of metabolic products) on all levels of living organisms – from bacteria to vertebrates. As a result of human activities, carbon dioxide enters the atmosphere as a combustion product of kaustobolites, as a technological product deriving from chemical and petrochemical production, from production of building materials (lime, cement), etc.

**From the point of view of underground mining of raw materials, carbon dioxide is a negative factor; its concentration in mine air must be controlled. Moreover, a number of cases are known where accidents were caused by a sudden outpour of CO<sub>2</sub> or by gas-dynamic effects.** Such gas-dynamic effects are classified as belonging to the category of outbursts of gases and coal or rocks. Sudden outbursts of carbon dioxide and methane together with coal and rock are a constant challenge to coal mining worldwide (Lama and Bodziony (1998), Kidybiński and Patyńska (2008)). On the other hand, a completely **new sector of mining activity came into existence, viz., storage of carbon dioxide in underground permeable rock bodies**, the so-called CO<sub>2</sub> geosequestration.

The aforementioned circumstances became a stimulus for the authors to produce this work, devoted to the natural occurrences and conditions of accumulation of carbon dioxide in natural permeable rock bodies and to the reaction of the mines to the presence of a rock massif containing carbon dioxide. The present study offers a **description of cases of carbon dioxide outbursts in mines of the Bohemian massif, i.e., on Czech Republic territory as well as in adjoining areas on the territory of Poland where the geology is similar.** No information is presented here on carbon dioxide occurring elsewhere in the world and no such comparisons are made.

Present-day technological trends in geosequestration of carbon dioxide stem from the working knowledge of hydrocarbon deposits based on geology and drilling technology; they are oriented on depleted gas and crude oil

deposits in rock massifs containing pores or fissures. Recently, research has focused also on carbon dioxide sequestration in coal seams or abandoned coal mines. On the other hand, mining technologies (or, generally speaking, geotechnologies) make it possible to form new anthropogenic types of carbon dioxide sequestration or to transform technologically abandoned deposits of gas and crude oil into new storage sites for this gas, etc.

The present work deals with situations where miners managed to get into direct contact, even if unexpectedly or unintentionally, with some types of the above mentioned natural accumulation of carbon dioxide. From a historical point of view, this occurred at a time when the possibility to sequester CO<sub>2</sub> in deep geological structures has not been considered yet and all efforts were directed onto ensuring safety of work at the mines. The knowledge acquired and described hereunder reflects the degree of understanding such extraordinary events at the time when they occurred.

The best known locality where carbon dioxide complicated geological surveying work being carried out in the **mine workings in Central Bohemia's Permo-Carboniferous s the bituminous coal deposit Slaný (1979-1990), situated near Kladno in Central Bohemia.** The fact that carbon dioxide is present and tends to cause eruptions in the Slaný coal district had been well-known since the time of surveying by boreholes; springs of salt water with dissolved carbon dioxide had been known there from time immemorial (the name of Slaný town means „Salty“). Carbon dioxide is bound here to the most important water-gas permeable rock body in Mirošov horizon formed of fluvial facies of sandstones and conglomerates in Nýřany Mbr. This is why attention was paid to this phenomenon ever since the preparations were started for sinking the skip and hoisting shafts of Slaný Mine. Considerable effort was made, at a substantial cost, to ensure safe sinking of the shafts (with adequate surveying and prevention boreholes) and to conduct research, by means of laboratory tests, of samples of rocks, water and gases taken in situ. The results of all this work are contained in a number of research reports and specialized papers yet to be presented as a summarized whole.

At the time when the above shafts were being sunk, and in connection with the occurrence of rock and gas outbursts therein, certain hypotheses were put forward concerning the conditions conducive to the occurrence of outbursts and the potential preventative actions was used. A number of such recommendations were implemented when the Slaný Mine shafts were being sunk. Nevertheless, it is obvious from how the sinking progressed that the shaft sinking technology used at Slaný Mine, in a massif which contained carbon dioxide, did not bring results that could be regarded as wholly positive. In case of any future efforts to re-open this deposit, it will be necessary to tackle the problem of outbursts once again, resorting to physical chemistry of gases and water as well as to new, safe technologies.

**Sinking of a dewatering shaft in Obránců Míru open pit mine in Komořany near Most town in the North Bohe-**

mian lignite basin (1989), within the Piedmont Krušné hory basin (Ore Mountain Range tectonic graben), is another case where a natural permeable rock body was encountered and the works passed through it. In that locality, carbon dioxide is accumulated in buried weathered crust of crystalline basement formed by kaolinized gneisses of crystalline complex of the Ore Mts. The covering sediments are silicified conglomerates, sandstones and marlstone of Upper Cretaceous and Tertiary sediments (claystone, coal lignite seam and sands) and tertiary volcanic deposits. These sediments serve to insulate the weathered crust.

Occurrences of carbon dioxide which is bound, together with methane, by adsorption to coal seams, were observed in other coal basins in the Czech Republic and in the neighbouring coal basins in Poland, too. Such occurrences manifested themselves as outbursts of coal and carbon dioxide with methane or outbursts of rocks and carbon dioxide. They were registered not only during the mining in the Czech part of the Intra-Sudeten Basin (in the area of East Bohemia Mines Company) but, first of all, in the Polish part of the Intra-Sudeten Basin where large-scale outbursts of carbon dioxide and methane in Wałbrzych district and Nowa Ruda district in the Intra-Sudeten Basin were encountered.

Sinking of the shaft at Bedřich Mine in Ostrava-Zábřeh town (on 9th April, 1902) probably is our oldest and best-known case of eruption of carbon dioxide. While the sinking was in progress, dissolved carbon dioxide was liberated from basal clastic sediments in Lower Badenian (so-called Czech „detritus“) in the Zábřeh lateral furrow of Bludovice furrow in the Czech part of the Upper Silesian Basin. The cases of mixed outbursts of carbon dioxide and methane bound to coal seams (e.g., at Jan Šverma Mine in Ostrava-Karviná Coal District (hereafter referred to as „OKR“)) are less known. Since 1894, 43 outbursts of coal and CO<sub>2</sub> have occurred here. Equally, carbon dioxide dissolved in mineral water in basal clastic sediments in Lower Badenian deposited in the western section of Bludovice furrow is typical of this zone of the Czech part of the Upper Silesian Basin where Tertiary volcanites (basalt from Petr Bezruč Mine in Ostrava = 19.6 million years) also appear next to deep tectonic faults.

A specific, new problem observed following the closure of mines in the western part of the OKR basin, in an area affected by mining, is the presence of mine gases, containing carbon dioxide and methane, in a massif where mining was terminated. Such gases ascend to surface and represent a serious safety hazard.

The petrological properties of rocks as well as the characteristics of pores in rocks, selected physical properties of rocks and coal, and also structural and textural characteristics of rocks upon which the accumulation of carbon dioxide is contingent are described in detail in the present work for selected localities. The influence of tectonic structure and the linkage if any to sources of Tertiary volcanism in the outer area of Bohemian massif are also shown.

The work also summarizes general knowledge about the behaviour of the H<sub>2</sub>O – CO<sub>2</sub> – NaCl system under temperature and pressure conditions existing in the coal

basins in question. Particular attention is paid to rocks in which carbon dioxide accumulates. New laboratory data on the adsorption of carbon dioxide on coal from the Czech part of the Upper Silesian Basin are presented and compared with the results of the study of CO<sub>2</sub> and methane adsorption on coal in the Polish part of the Intra-Sudeten Basin.

The individual cases described provide an insight into the nature's own brew. In spite of the fact that at the time when these outbursts and gas-dynamic effects took place the sequestration of carbon dioxide was not yet perceived as one of the new mining eco-technologies, such cases reflect, in a historical perspective, the possibilities existing at that time for studying these extraordinary events, mainly in connection with outbursts of coal, rocks and gases.

The information presented hereunder can be put to good use in searching for localities suitable for underground storage of carbon dioxide, for modelling of processes associated with such storage as well as for the practice of mining operations conducted within a rock massif where carbon dioxide may potentially occur. The present work also addresses the rather neglected problems of corrosion of concrete structures due to long-term effects of elevated carbon dioxide concentrations under extreme climatic and aerodynamic conditions encountered in deep mines.

## 2. CARBON DIOXIDE AND THE ROCK MASSIF

### 2.1. NATURAL EMISSIONS OF CARBON DIOXIDE IN BOHEMIAN MASSIF

Natural emissions of carbon dioxide on the surface of the Bohemian massif are linked to springs of mineral waters or mofettes (e.g., dry, gaseous emissions of CO<sub>2</sub>). Emissions also exist which are related to gas-dynamic effects (outbursts of rocks, coal, carbon dioxide, and methane); they occur during exploitation both underground and in quarries, as well as during exploration of deposits by deep boreholes drilled from the surface. Such dynamic effects are accompanied by gas emissions of natural origin which are associated with the rock massif. As stated by numerous authors (e.g., Hynie, 1963; Jetel, Rybářová et al., 1978), such gas-containing and mineralized hot and cold water springs and mofettes are concentrated in tectonic faults located deep underground throughout the Krušné hory (Ore Mountains) tectonic graben in the NW part of the Bohemian massif and in deep tectonic faults of Sudeten directions (extending in the NW-SE direction) skirting the NE rims of the Bohemian massif (*Fig. 2.1*). Thus, carbon dioxide emission sites are clustered along an arc-shaped zone adjacent to the NW and NE parts of the Bohemian massif. They are closely related to deep-seated faults and to localities where Tertiary volcanism is in evidence. Such close association between tectonics and Tertiary volcanism is a rather characteristic feature of all CO<sub>2</sub> emission sites.

Carbon dioxide is part of the geochemical cycle of carbon. It occurs in sedimentary rocks (together with CH<sub>4</sub> and higher hydrocarbons in pores, as a product of coalification processes) as well as in eruptive rocks (as inclusion in minerals); it forms a part of the gas phase present in pores and fissures and is also present as dissolved gas or [HCO<sub>3</sub>] in aquifers or in accumulations in permeable rock bodies of different genesis.

The principal problem is to establish where all this CO<sub>2</sub> comes from. For solving the question of genesis of carbon dioxide, the <sup>13</sup>C/<sup>12</sup>C isotope ratio is used (*see note 1*). However, our understanding of CO<sub>2</sub> genesis, its distribution, and its behaviour under the temperature and pressure conditions prevailing in pores in the rock massif is still insufficient.

#### AS REGARDS CARBON DIOXIDE EMISSIONS, THE SITUATION IN THE BOHEMIAN MASSIF IS AS FOLLOWS:

**The Ore Mountains (in Czech: Krušné hory) Foothills tectonic graben is a rather prominent zone of CO<sub>2</sub> emissions** (Hynie, 1963; Pačes, 1974; Tesař, 1986; Weinlich et al., 1998a, b; Kolářová and Myslil, 1979, Kačura, 1980). The genesis of CO<sub>2</sub> was studied by many authors (Pačes 1974; Polyak et al., 1985; D'Amore et al., 1989; Weinlich et al., 1998a, b). According to Weinlich et al. (1998a,b), the content of the heavier isotope of CO<sub>2</sub> together with the high content of helium (<sup>3</sup>He/<sup>4</sup>He) in the mantle found in the western part of the above basin (near Cheb and

Sokolov) indicates that this gas is of magmatic origin, rising from depths greater than 15 km. The outlets of gas and CO<sub>2</sub> - containing water are closely related to a Y-shaped, ramified structure involving a branch formed by the Main Ore Mountain Range Foothills piedmont fault and the Central Ore Mountain Range Foothills piedmont fault. Nevertheless, in the block between the Central Ore Mountain Range piedmont fault and the Litoměřice fault zone running in parallel with the range, no CO<sub>2</sub> emissions were registered. This is a confirmation that for migration of CO<sub>2</sub> from the mantle, migration paths must first have been formed which had the form of deep-seated tectonic structures.

CO<sub>2</sub> emission sites situated to the SE of the Litoměřice fault zone, towards the center of the Bohemian massif, are linked with the crossing of this great-depth fault with other faults extending in the NW-SE direction (Horní Slavkov fault, Mariánské Lázně fault). A number of CO<sub>2</sub> emission sites is directly linked with the continuation of these faults farther in the SE direction or with faults running in the NNE - SSE direction; this applies to Bezručice fault (cf. Weinlich, 1998, Fig. 4). Tectonic zones with accompanying tectonic faults represent a rock massif of a higher permeability which serves as a migration route whereby gas and gas-containing mineral waters can rise the surface. At the same time, it is evident that a linkage exists with the third volcanic phase (as specified by Kopecký, 1978, 1986-1988). As stated by Weinlich et al. (1998b), it can be estimated that in the western part of Ohárecký rift alone, the volume of emitted free carbon dioxide is 5.31 million m<sup>3</sup> per year and that of dissolved CO<sub>2</sub> and [HCO<sub>3</sub>] - is 8.13 million m<sup>3</sup> per year. In analogous fashion, the genesis and volumes of CO<sub>2</sub> emissions are similar in other places of their occurrence, too, e.g. in the central part of the Ore Mountain Range Foothills tectonic graben (Komořany) and in the NNE part of the same basin (Bílina, Teplice Lázně).

**In the Polish and Czech parts of the Intra-Sudeten Basin,** CO<sub>2</sub> emissions are accompanied by springs of gas-containing mineral water (e.g., Běloves u Náchoda, Libverda Spa (Jetel and Rybářová 1979); in Poland, this includes localities such as Czerniava Zdrój, Świeradów Zdrój, Kudowa Zdrój, Duszniki Zdrój, Polanica Zdrój, etc.). Also of interest are isolated emission sites of mineral water with CO<sub>2</sub> in the Bohemian Cretaceous basin, along the Sudeten fault zones extending in the NW-SE direction; such outlets were confirmed in boreholes in Poděbrady and Všeň (Jetel and Rybářová, 1979).

#### Note 1):

*Isotopic composition of carbon δ<sup>13</sup>C is defined as follows:*

$$\delta^{13}\text{C} = [(^{13}\text{C}/^{12}\text{C})_{\text{sample}} - (^{13}\text{C}/^{12}\text{C})_{\text{standard}}] / (^{13}\text{C}/^{12}\text{C})_{\text{standard}} \cdot 1000$$

*where:*

*(<sup>13</sup>C/<sup>12</sup>C)<sub>standard</sub> corresponds to the PDB international standard.*



CO<sub>2</sub> emissions are also found in coal seams and their accompanying small tectonic structures. Together with methane, carbon dioxide is adsorbed on coal matter in coal seams in the Czech part of the Intra-Sudeten Basin (former Zdeněk Nejedlý Mine in Malé Svatoňovice – Odolov), and in the Polish part of the Intra-Sudeten Basin in mines situated around Wałbrzych and Nowa Ruda. During mining, the presence of CO<sub>2</sub> is manifested by dynamic gas effects as well as by outbursts of CO<sub>2</sub> and coal or mixed outbursts of (CO<sub>2</sub> + CH<sub>4</sub>) and coal.

It is assumed that a close relationship also exists between CO<sub>2</sub> emissions and deep tectonic faults extending in the NW-SE direction (the so-called Sudeten faults). Carbon dioxide migrates via the fractured structures surrounding the main faults. In those parts of the massif where there are coal seams, carbon dioxide adsorbs on the coal matter of the seams or is accumulated in the faulted zones. In the area marked with deep tectonic faults parallel to the system of the Main Marginal Sudeten fault, CO<sub>2</sub> emissions probably are linked to local sources of Tertiary volcanism. This seems to be corroborated by <sup>13</sup>C isotope analyses in CO<sub>2</sub> from the Polish part of the Intra-Sudeten Basin described by Kotarba, 1990. He indicates very low values of CO<sub>2</sub> with δ<sup>13</sup>C, viz., in the range of - 4 to -7‰. This suggests that the gas originates at great depths where volcanic activities are also at play.

**In the area of Jeseník (a part of Hrubý Jeseník Mts, Nízký Jeseník Highlands, Oderské Highlands)** there are numerous, cold springs of CO<sub>2</sub> - containing mineral waters (Karlova Studánka, Karlov, the riverbed of Opavice river, Suchá Rudná, Ondrášov u Moravského Berouna, the Rýmařov and Krnov districts, the Moravice river basin near Jánské Koupele). There are also emission sites here producing dry, gaseous CO<sub>2</sub> which is even pumped for use in food processing (Opavice river valley near Krnov) (Květ and Kačura, 1978). Springs of mineral water and emissions of dry gaseous CO<sub>2</sub> follow deep tectonic faults in this area or the crossing of these faults with geological structures belong to a larger area of Tertiary basalt volcanism on east border of the Bohemian massif. CO<sub>2</sub> emission sites continue towards the western section of the Czech part of the Upper Silesian Basin. This will be analyzed later on.

Emissions of gaseous CO<sub>2</sub> as well as of gas-containing mineral waters are also known from the **Moravian Gate region** (in Czech: Moravská brána), first of all from the Hranice district (Hranice, Macůška Chasm, Zbrašov Caves, and Teplice nad Bečvou Spa). Their relationship with the Sudeten tectonic faults is evident here, too (Šmejkal et al., 1976). For free CO<sub>2</sub> from Zbrašov Cave, this author reports δ<sup>13</sup>C (CO<sub>2</sub>) = -7.1 ‰. This value corresponds to a source of gaseous CO<sub>2</sub> located at a great depth (Květ and Kačura, 1978).

**Analyses of mineral waters published in the reviews of mineral water springs suggest that the sum total of CO<sub>2</sub> emissions (including dissolved [HCO<sub>3</sub>]) can be estimated to be of the order of ≈ 60 – 80·10<sup>6</sup> m<sup>3</sup> per year as a minimum; assuming a CO<sub>2</sub> density equal to 1.9768 kg·m<sup>-3</sup> (at 0°C and normal pressure), the production would be ≈ 120 – 160·10<sup>6</sup> kg CO<sub>2</sub> per year.**

The question of emissions of carbon dioxide in **boreholes and mines of the Czech part of the Upper Sile-**

**sian Basin** has been paid considerable attention in the past (Patteisky and Folprecht, 1928; Říman, 1955; Pišta, 1961) – cf. Chapter 6). In the Czech part of the Upper Silesian Basin, **methane and carbon dioxide are dissolved in highly mineralized water in an aquifer; they are linked to basal detritic facies of Lower Badenian (so-called “detritus”)**. The Lower Badenian basal sediments are deposited at the bottom of deep valleys in the Carboniferous, namely in the southern Bludovice furrow and in the northern Dětmárovice furrow. From a hydrochemical point of view, the above aquifer has a very complicated, closed structure of primarily stagnant marine fossil salt waters saturated with gas; in Dětmárovice furrow and in the eastern part of Bludovice furrow, the gas was CH<sub>4</sub> from coalification process, whereas in the western part of Bludovice furrow it was chemogenic CO<sub>2</sub> (Grmela in Dopita, 1997; Dvorský et al., 2009).

Further, emissions of **CO<sub>2</sub> together with methane occur in coal seams where the gas is adsorbed**. Such cases are encountered only in the western part of the abandoned Jan Šverma Mine exploitation area where CO<sub>2</sub> was adsorbed on coal together with methane (Patteisky and Folprecht, 1928; Šmíd et al., 1989).

In the Czech part of the Upper Silesian Basin, **carbon dioxide is also part of mine air**. The contents of CO<sub>2</sub> in exhaust air from active coal mines in the Czech part of the Upper Silesian Basin range from 0.05 to 1 wt.%. When the mines close down the composition of mine air continues changing constantly because the air is enclosed in a massif disturbed by coal mining in the past (the gases bonded in coal are liberated). At the abandoned mine sites, the gases – a mixture of CO<sub>2</sub> and CH<sub>4</sub> – ascend to surface.

**It follows from the above overview that CO<sub>2</sub> can occur in the rock massif in the following forms:**

- free CO<sub>2</sub>,
- CO<sub>2</sub> dissolved in water (as CO<sub>2</sub> or [HCO<sub>3</sub>]),
- CO<sub>2</sub> adsorbed (together with CH<sub>4</sub>) on coal (mainly, on coal matter in coal seams).

The primary CO<sub>2</sub> originates from mantle sources and migrates along deep faults or in sites where they cross a different system of faults, in the form of free gas or of gas dissolved in water. In coal seams it is adsorbed on coal matter. Some part of the CO<sub>2</sub> in coal basins or in sedimentary coal stratifications is produced by biogenic transformation from methane. After closure of the mines, mine gas remains in the massif. The composition of such mine gas is determined by polygenetic processes.

## 2.2. THE WATER – CARBON DIOXIDE PHASE DIAGRAM

The basic idea on the behaviour of water under different pressures and temperatures can be obtained from the phase diagram of the water – carbon dioxide system where, three basic states – the solid phase (s), the liquid phase (l), and the gas phase (g) are represented within an area bounded by pressure and temperature coordinates. A general form of this diagram is shown in Fig. 2.2.

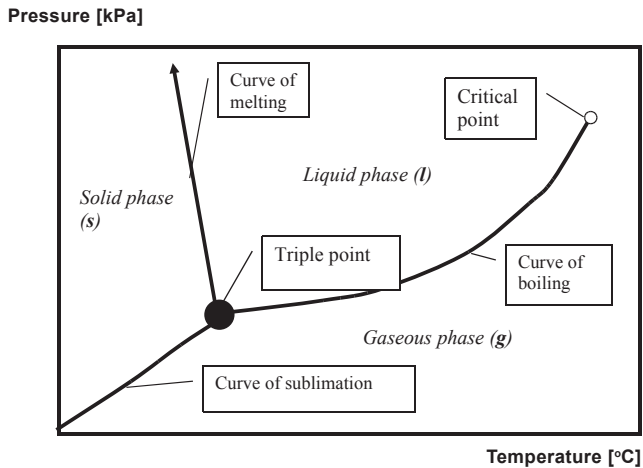


Fig. 2.2. General representation of the water phase diagram (three-phase diagram, pure water)

In the diagram, the ones of stability of the phases are separated by curved phase boundaries which precisely determine the pressures  $p$  and temperatures  $T$  under which the two adjoining phases coexist in a mutual equilibrium (the „melting – solidification“ boundary, the „boiling – condensation“ boundary, and the „sublimation – desublimation“ boundary). The three phase boundary curves intersect in one common point, the so-called triple point. This is a unique point where all the three phases are in an equilibrium and where the vapor tension above the liquid and the solid phase is the same, see Fig. 2.2. The curve which indicates boiling (condensation) ends at the critical point (at „critical temperature“ and „critical pressure“ coordinates); here the critical temperature  $T_K$  denotes the highest temperature under which a given matter is still stable in its liquid phase; at temperatures higher than  $T_K$ , vapors of the given matter cannot be liquefied by action of any – no matter how big – pressure. The coordinates of important points of the phase diagram for pure water are shown in Fig. 2.3.

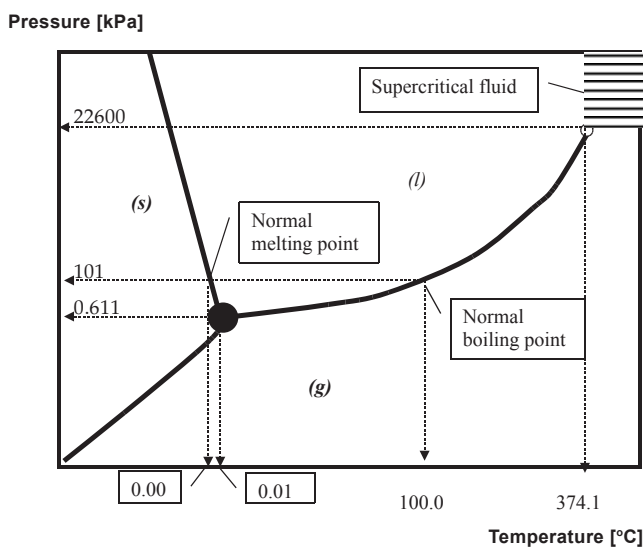


Fig. 2.3. Phase diagram of pure water {gas (g) - liquid (l) - solid (s) states} representing pressures and temperatures up to the critical point

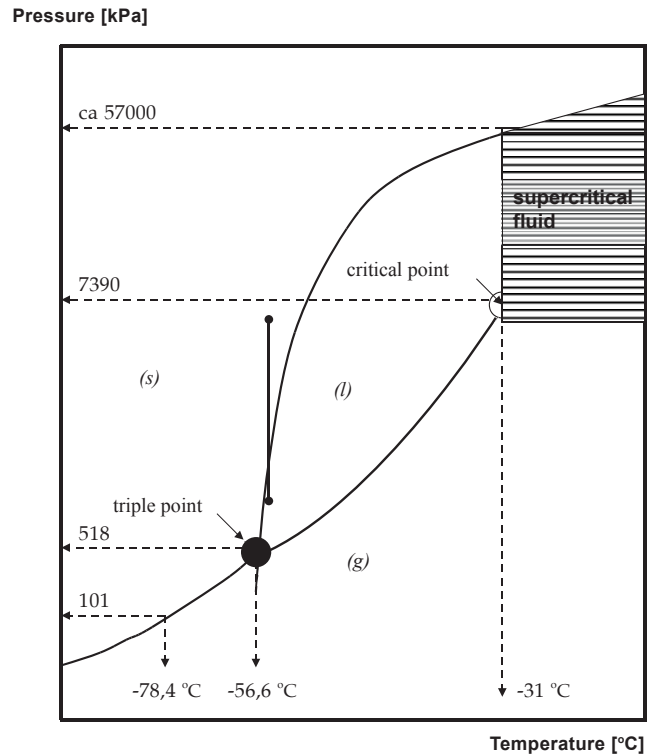


Fig. 2.4. General representation of the phase diagram of  $\text{CO}_2$  {gas (g) - liquid (l) - solid (s) states} at pressures and temperatures up to the critical point

The point of intersection of the isobar of normal pressure of 101.325 kPa with the boiling curve corresponds to the temperature of 100.0°C and is known as the normal boiling point. It is precisely at this temperature of 100°C that the water vapour tension is equal to 101.325 kPa (i.e., the normal atmospheric pressure). The point of intersection of the isobar 101.325 kPa with the melting curve corresponds to the temperature of 0.0°C and is known as the normal melting (solidification) point. The coordinates of the triple point of water (the solid-liquid-vapour triple point: 0.01°C and 0.611 kPa indicate that in at the temperature of 0.01°C, to bring water to the boiling point requires to decrease the ambient pressure precisely to 0.611 kPa; then, a state of equilibrium is reached where the liquid phase coexists with the gas phase but, at the same time, also with ice. A more detailed study of the phase behaviour of water under high pressures proved that depending on pressure and temperature ice can exist in a number of other stable modifications, too. However, the phase diagram of water encompassing an extended scale of pressures is rather complicated and its description would fall outside the scope of this work. A total of 22 modifications of ice, I-XXII, are known. It is worth mentioning that, at the pressure of 2000 MPa, the so called ice VII will only melt at the temperature of +100°C (Atkins and de Paula, 2002). The phase diagram of carbon dioxide ( $\text{CO}_2$ ) is shown in Fig. 2.4. As opposed to the phase diagram of water, the melting (solidification) curve is of a steeply rising (not decreasing) character. This means that isothermic compression of liquid  $\text{CO}_2$  to a pressure above the melting–solidification curve, at constant temperature, brings about a phase transformation where the liquid phase

turns solid, i.e., where freezing of the liquid occurs (see the curve A–B in Fig. 2.4).

**The triple point of CO<sub>2</sub> is defined by the temperature of -56.6°C and the pressure of 518 kPa.** As a result, the isobar of normal pressure of 101 kPa is situated underneath the triple point and intersects the sublimation-desublimation curve (rather than the melting-solidification curve); unlike water (see Figs. 2.3 and 2.4). Therefore, the phase which is stable at the normal pressure of 101 kPa, is solid CO<sub>2</sub> rather than liquid CO<sub>2</sub> and, at temperatures above -78.4°C, it transforms directly into the gas phase (sublimation). Thanks to its low sublimation temperature, solid CO<sub>2</sub> is used as refrigerant and is called „dry ice“; it will transform, at atmospheric pressure, directly to the gas phase.

In the water – carbon dioxide phase diagrams (Figs. 2.3 and 2.4), there are areas, just above the critical point, of supercritical fluids where water or CO<sub>2</sub> combines properties of gases and liquids, making it to something „between gas and liquid“. In supercritical fluids there is no phase boundary that would separate the liquid from the gas phase, i.e., these fluids do not exhibit any surface tension. Thus, the behaviour of supercritical fluids reflects the properties of both the gas phase and the liquid phase. In particular, they are highly capable of penetration (diffusion) in solid matter (as gases); at the same time, they have a considerable capability to dissolve such solid matter (as liquids). Thanks to these properties, the supercritical fluids are used as effective extraction agents; their capacity of acting as a solvent can be effectively controlled by changes in temperature and pressure which influence the supercritical fluid density. At the same time, the extracts obtained by extraction with a supercritical liquid can be separated into useful fractions by stepwise temperature and pressure changes. A number of deposits of mineral raw materials (common crude oil) owe their existence to such processes. Carbon dioxide is indisputably the most frequently used supercritical extraction agent. Here the **supercritical state can be reached already at temperatures above 31°C and at pressures above 7390 kPa** (see Fig. 2.4). Reaching the supercritical state with (“cheaper”) water is much more sophisticated technically and is much more energy-intensive; in practice, this means that the operation would have to proceed at temperatures above 374°C and at pressures exceeding 22600 kPa (see Fig. 2.3): More detail about H<sub>2</sub>O and CO<sub>2</sub> and system H<sub>2</sub>O – CO<sub>2</sub> – NaCl see Clark, 1969.

The solubility of CO<sub>2</sub> in water is dependent on temperature and pressure (Zelvenskii, 1937); at the temperature of 25°C and at normal pressure the amount dissolved is 1.48 g CO<sub>2</sub>·dm<sup>-3</sup>. Solubility at higher temperatures is also influenced by the NaCl concentration (Takenouchi and Kennedy, 1965; Malinin, 1979). Consequently, any model to be adopted will also have to take the NaCl concentration into account. Carbon dioxide is contained in atmospheric air, at a concentration of 0.0337 vol.% (337 ppmv) (= 723 mg CO<sub>2</sub>·m<sup>-3</sup>). In deep mines, and in coal mines in particular, local CO<sub>2</sub> concentrations in poorly ventilated workings may rise as high as several dozen per cent. Its concentrations in exhaust air usually vary from 0.1 to ca. 1% (at OKR mines, they fluctuate between 0.1 and 1 wt.%). The situation is different in ore mining where the CO<sub>2</sub> concentrations in exhaust air are increased only slightly above the value for outdoor air.

### 2.3. THE H<sub>2</sub>O – NaCl – CO<sub>2</sub> SYSTEM UNDER THE NATURAL CONDITIONS OF COAL DEPOSITS

Modeling the above system of aqueous solutions enclosed in pores of rocks under natural conditions of pressure and temperature existing in coal deposits in the Bohemian massif is important for ascertaining the stability conditions of the system. The behaviour of rocks when subjected to deformation is influenced not only by their higher water content but also by the presence of gases in the aqueous solutions present in the pores (e.g., nitrogen, helium); this has been noted e.g. by Gustkiewicz (1990) and Lempp (1993) who conducted experiments on porous rocks saturated with inert gases dissolved in water.

The experimental input data required for the calculation of the H<sub>2</sub>O – NaCl – CO<sub>2</sub> phase equilibrium overlap with the area of interest to chemical engineering (Markham et al., 1941; Wiebe et al., 1941) or, in extreme cases, with the area of geochemical studies of metamorphic processes (e.g., Gehring et al., 1986). Thus, certain extrapolations can be used for those areas where direct experimental data for the above system are absent over a wide range of temperatures, pressures, and concentrations. Kolář and Martinec (1994) published an integrated model capable of providing an exact description of complicated systems containing both subcritical and supercritical components in equilibrium with electrolyte solutions. It has been used to develop a mixed-type model describing a system that involves pressures of 10 MPa and more and temperatures in the 20–40°C range; the model incorporates:

(a) *Nine parameters of the Benedict-Webb-Rubin state equation (Novák et al., 1972) which were used to calculate the properties of state and the fugacity of pure CO<sub>2</sub>. The state equation makes it possible to operate with a critical density of pure CO<sub>2</sub> more than twice as high.*

(b) *The solubility of CO<sub>2</sub> in pure water was calculated by the approximation equation:*

$$\frac{\ln f_{gCO_2}}{x_{CO_2}^l} = \ln H(T) + \left( \frac{Pv_{CO_2}^l}{RT} \right) \quad (2.1)$$

where:

$x^l$  - molar ratio of CO<sub>2</sub> in the liquid phase;

$f_g$  - fugacity of CO<sub>2</sub> in the gaseous phase;

$R$  - universal gas constant 8.314 J·mol<sup>-1</sup>·K<sup>-1</sup>;

$P$  - pressure;

$T$  - absolute (Kelvin) temperature.

$v^l$  - The partial molar volume of CO<sub>2</sub> is given in the equation  $v^l = 37.6 \text{ ml}^3 \cdot \text{mol}^{-1}$ .

This molar volume is considered to be independent of temperature and pressure (Malinin, 1979).

The temperature dependence of Henry's coefficient is given as follows:

$$\ln H(T) = A + \left( \frac{B}{T} \right) + C \ln T + DT \quad (2.2)$$

The parameters of the above function apply over the temperature interval of 273 K > T > 353 K as indicated in Wilhem, 1977.

- (c) *The effect of CO<sub>2</sub> solubility in water can be correlated using the empirical equation (Malinin, 1979).*

$$S_s B = S_o \cdot 10^{-k_s m} \quad (2.3)$$

where:

- $S_s - S_o$  - solubility of CO<sub>2</sub> in mineralized and pure water, respectively;  
 $m$  - molar concentration of NaCl;  
 $k_s$  - salting-out coefficient [-].

The effect of pressure on  $k_s$  is negligible in the first approximation (Krajča, 1977).

As an example, the following two limiting cases were computed using input data deriving from the physical properties as determined for rocks of the Mirošov horizon where a shaft was sunk at Slaný mine:

CO<sub>2</sub> evolved at depths of 875,7 to 888,3 m (for details see Chapter 3) and two possible model cases of CO<sub>2</sub> binding in the rock were explored.

- (aa) *The pore structure of sandstones and conglomerates of the Mirošov horizon was fully saturated with mineralized, NaCl-containing water ( $c_{NaCl} = 35 \text{ g} \cdot \text{dm}^{-3}$ ). At the given pressure and temperature, carbon dioxide is in equilibrium with the solution in the given rock system.*
- (ab) *The pore structure of rocks of the Mirošov horizon is filled with compressed CO<sub>2</sub> gas, under conditions of ambient critical pressure and temperature.*

The results of the simulation, expressed as CO<sub>2</sub> volume (converted so as to correspond to the conditions of normal temperature and pressure) liberated from the rocks, are shown in Figs. 2.5 and 2.6 for different horizons of Slaný Mine.

Due to increasing pressure, the quantity of CO<sub>2</sub> dissolved in water in the pores (see case (aa)) is lower by at least one order of magnitude than the quantity that would correspond to pure CO<sub>2</sub> compressed in the pores (see case (ab)). It should be pointed out that the quantity of CO<sub>2</sub> (case (ab)) is in a good quantitative agreement with the quantity of liberated CO<sub>2</sub> actually registered during the sinking operations (see Table 2.1). The geostatic vertical stress  $S_v$  (2.4) (Zang et Stephanson, 2011)) is:

$$S_v = \rho_o \cdot g \cdot z \quad (2.4)$$

where:

- $S_v$  - geostatic vertical stress [MPa];  
 $g$  - gravitational constant = 9.81 kg.m<sup>-1</sup>;  
 $z$  - depth = 870-900 m;  
 $\rho_o$  - the average bulk volume of overburden massif  
 $\rho_o = 2290 \text{ kg} \cdot \text{m}^{-3}$ .

For Mirošov horizon, the values of calculated geostatic vertical component of stress (in the interval of 19.5-20.2 MPa) were surpassed. The reason for a suddenly increased quantity of CO<sub>2</sub> at pressures of ca. 20 MPa is the nearness of the CO<sub>2</sub> critical point (temperature 31.04°C, pressure 7.384 MPa – Fig. 2.6). Under conditions near to the critical point, the compressibility of gaseous CO<sub>2</sub> increases substantially. The sudden liberation of CO<sub>2</sub> and loosening of rocks was due to the presence of compressed CO<sub>2</sub> gas in the rock pores which was more pronounced than the effect of CO<sub>2</sub> liberation from the pore water. It was found that in case of a sudden shifting of the equilibrium due to mining activities (relating to the change in permeability of sandstones after relieving some of the load acting upon the massif), the evolution of carbon dioxide from disintegrated rocks in the vicinity of the slope of the mine shaft is of the order of 10 000 - 30 000 m<sup>3</sup>. In several degassing cycles, the process of disintegration connected with the fracturing of the massif penetrates deeper into the massif, until a new equilibrium is established. It follows from a study (Martinec and Krajčiček, 1990a) of the properties of rocks in Slaný area that the rock strength and deformation properties are greatly influenced by the moisture level; therefore, this pore pressure surpassing the value of 8 MPa can also exert a critical impact on rock strength and stability at rock moisture levels above 2.5% (see, for example, the degree of fragmentation of rocks or disintegration of massif in the case of outbursts – see Plate D, Figs. D1-D18).

Layer in Mirošov horizon	Thickness of layer [m]	Bulk volume [kg·m <sup>-3</sup> ]	Volume of pores [dm <sup>3</sup> ·Mg <sup>-1</sup> ]	Production of CO <sub>2</sub> [m <sup>3</sup> ]	Temperature [°C]
1.	3.2	2 440	37.2	6 500	33.5
2.	3.1	2 290	61.3	3 400	34
3.	3.2	2 280	63.6	6 200	34
4.	3.1	2 320	61.5	5 500	34

Table 2.1 Physical properties of four sandstone beds of Mirošov horizon, at Slaný Mine skip shaft, at depths of 875.7 to 888.3 m. Shaft diameter, 9.9 m.

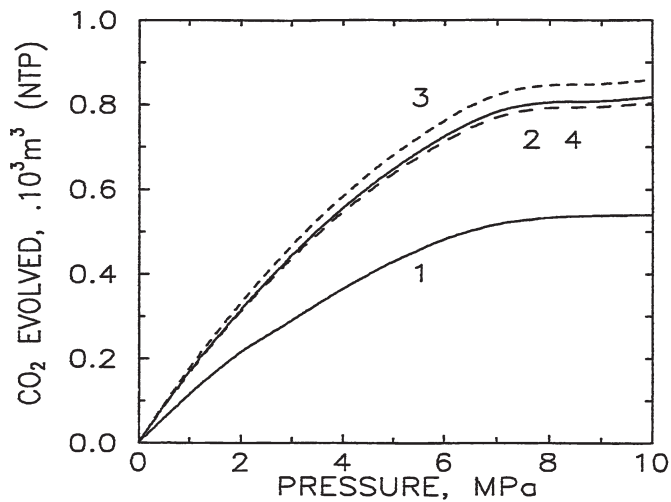


Fig. 2.5 Model calculation of the volume of carbon dioxide liberated from pores in rocks fully saturated with mineralized water containing NaCl ( $35 \text{ g-dm}^{-3}$ ) and with dissolved carbon dioxide (Case (aa)).

Locality: Slaný Mine, Mirošov horizon, depth sequence from 875.7 to 888.3 m (for individual layers, see Table 2.1). The system involved is  $\text{H}_2\text{O} - \text{NaCl} - \text{CO}_2$ ; the volume of liberated carbon dioxide shown corresponds to standard pressure and temperature conditions.

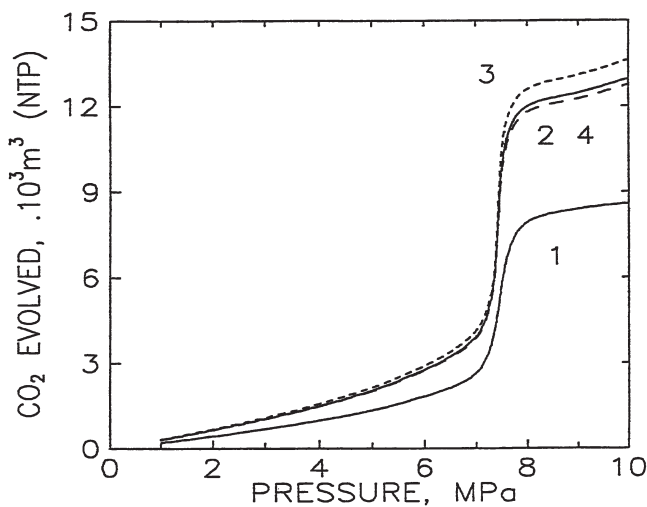


Fig. 2.6 Calculation of the volume of carbon dioxide volume liberated from rock pores containing free carbon dioxide (Case (ab)).

Slaný Mine, Mirošov horizon, depth sequence 875.7 to 888.3 m (for individual layers, see Table 2.1). The system involved is  $\text{H}_2\text{O} - \text{NaCl} - \text{CO}_2$ ; the volume of liberated carbon dioxide shown corresponds to standard pressure and temperature conditions.

Simulation of the conditions existing at Slaný Mine can be applied with advantage to other coal basins (with similar pressure and temperature conditions) as well where the two aforementioned forms of  $\text{CO}_2$  occurrence in the rock pores can be observed. The above thermodynamic analysis shows the importance of the study of phase equilibria of pore fluids at high pressures. This has a direct impact on the reversed situation, too – i.e., on the injection of gas (presumably,  $\text{CO}_2$ ) or liquid into porous permeable rock bodies via boreholes drilled from the surface.

## 2.4. SUDDEN LIBERATION OF CARBON DIOXIDE AND METHANE FROM THE ROCK MASSIF OR FROM COAL SEAMS

In a number of coal deposits, mining operations have to cope with sudden emissions of gases ( $\text{CH}_4$ ,  $\text{CO}_2$  or their mixtures) which were bonded to coal matter of the seam. The gases burst out rapidly into the open, entraining either crushed rock or fine, even dust-like coal debris. This means that e.g., in coal where  $\text{CO}_2$  is adsorbed on the surface of pores existing within the fine inner coal structure (not only on the surface of coal particles delimited by fissures), the gas expands from within and the coal disintegrates to coal dust.

If the quantity of suddenly ejected coal is greater than 0.5 metric ton, such phenomena are defined as “outbursts of coal, rocks and gases” as per Section 2 of the „Instruction for forecasting and preventing coal and gas outbursts in mines prone to outbursts”. If smaller quantities are involved the phenomena are generally classified as “gas-dynamic effects”. Both the outbursts and the gas-dynamic effects furnish valuable information about the forms of accumulation of gases in the seams or, more generally, in the massif.

## 2.5. FACTORS INFLUENCING $\text{CO}_2$ AND $\text{CH}_4$ ADSORPTION ON BITUMINOUS COAL UNDER LABORATORY CONDITIONS

Adsorption of carbon dioxide on coal matter is the fundamental interaction which accompanies  $\text{CO}_2$  occurrence in situ. In the present study, the adsorption behaviour of coal from the Czech part of the Upper Silesian Basin is compared with data on the behaviour of coal from other localities. Adsorption of  $\text{CO}_2$  was studied on selected samples of coal from the seams of the Czech part of the Upper Silesian Basin during the 2008–2009 period (Czech Mining Authority project 57-08).

Type SETARAM C80 calorimeter with calorimetric cells (SETARAM C80) was used to measure the gas flow at an elevated pressure. Thus, data were obtained on high-pressure adsorption of CO<sub>2</sub> and, at the same time, on the importance of factors which influence the adsorption process (moisture content, temperature, grain size). On the basis of such measurements, the thermal effects accompanying adsorption processes were examined. The experimental adsorption heat data were converted (using isosteric heat values for CO<sub>2</sub>) to adsorbed carbon dioxide volumes  $V_{ads}$  [dm<sup>3</sup>·kg<sup>-1</sup>].

The calorimetric measurements were carried out using bituminous coal samples from the following coal seams:

22b (code OKD of coal seam no. 086) – Paskov – Staříč Mine, Ostrava Fm, Petřkovice Mbr; the Natan coal seam (code no. 463) – Lazy Mine, Ostrava Fm, Poruba Mbr; the Prokop coal seam (code no. 504) – Lazy Mine, Karviná Fm, “Sedlové vrstvy” Mbr. The results for these three samples are shown here together with results obtained for a coal sample originating from Darkov Mine (Darkov sample, Poruba Mbr). This latter sample was tested at the Institute of Rock Structure and Mechanics of the Academy of Sciences in Prague (Příbyl et al., 2009). The quality parameters and the elementary composition of all the coal samples are given in *Table 2.2*.

Coal seam	W <sup>a</sup>	A <sup>d</sup>	V <sup>daf</sup>	C <sup>d</sup>	H <sup>d</sup>	N <sup>d</sup>	S <sub>t</sub> <sup>d</sup>
	[%]						
Prokop (No 504)	0.8	10.2	33.7	79.6	4.7	1.0	0.35
Natan (No 463)	1.0	8.2	31.6	81.3	4.5	1.35	0.8
22d (No 086)	1.0	11.7	18.6	80.7	3.4	1.3	0.55

*Table 2.2* Elemental composition and chemical parameters of bituminous coal from the Czech part of Upper Silesian Coal basin

*Explanatory note:* W<sup>a</sup> – moisture of coal in analytical sample; A<sup>d</sup> – content of ash, dry; V<sup>daf</sup> – content of volatile matter; C<sup>d</sup>, H<sup>d</sup>, N<sup>d</sup> – contents of carbon, hydrogen, and nitrogen, dry; S<sub>t</sub><sup>d</sup> – total content of sulphur, dry.

Name / designation and code no. of coal seam in the Czech part of the Upper Silesian Basin (after Dopita et al., 1997).

### 2.5.1 HIGH-PRESSURE ADSORPTION OF CARBON DIOXIDE ON BITUMINOUS COAL

High-pressure CO<sub>2</sub> adsorption was studied experimentally in the sub-critical region, at a temperature of 30°C and at pressures up to ca. 5.5 MPa. The resultant isothermal adsorption curves represent the amounts of adsorbed carbon dioxide as a function of pressure acting on the adsorbate (CO<sub>2</sub>) (*Fig. 2.7*).

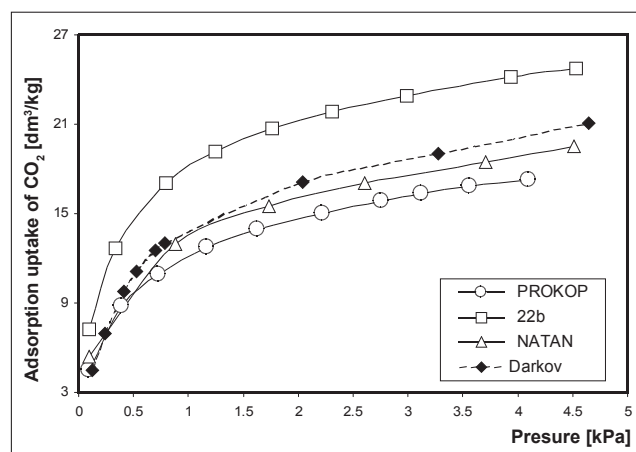


*Fig. 2.7.* High-pressure adsorption isotherms of CO<sub>2</sub> for bituminous coal (from the Czech part of Upper Silesian Basin, Namurian A (Ostrava Fm) and Namurian C and Westphalian A (Karviná Fm).

*Experimental conditions:* temperature 30°C, grain size 0.06 – 0.15 mm, dry coal (cf. *Table 2.2*).

A number of equations and models (see e.g., Perera et al., 2011) were proposed to mathematically express the adsorption isotherms. The Langmuir model is used most frequently. It is based on the theory of a monolayer covering the sorbent surface. The Langmuir isotherm has also been used for the correlation of adsorption data determined for the carbon dioxide – coal system (Medek, 1971; Nodzienski, 2000; Krooss et al., 2002; Goodman et al., 2007; Perera et al., 2011).

In linearized form, the Langmuir isotherm can be expressed as:

$$p/V^{ads} = p/V_m + 1/(V_m \cdot k) \quad (2.5)$$

where:

- $V_{ads}$  – adsorbed volume of CO<sub>2</sub> [dm<sup>3</sup>·kg<sup>-1</sup>];
- $p$  – equilibrium pressure of CO<sub>2</sub> adsorption [MPa];
- $V_m$  – (maximum) adsorption capacity expressing the amount of CO<sub>2</sub> adsorbed at a multilayer cover of the coal surface [dm<sup>3</sup>·kg<sup>-1</sup>];
- $k$  – a constant relating to the rate of the adsorption and desorption processes.

The typical Langmuir shapes, i.e., a steeply increasing amount of adsorbed gas in the low-pressure region up to maximum adsorption in the high-pressure region is also evident from the adsorption isotherms pertaining to adsorption on coal from the seams of the Czech part of the Upper Silesian Basin (*Fig. 2.7*) or the Intra-Sudeten Basin (*Figs. 2.10 and 2.11*). The experimental adsorption isotherms were in excellent agreement with the Langmuir isotherm; this is also attested to by the values of the determination of coefficients R<sup>2</sup> obtained from the linearized isotherms (equation 2.5); in all cases, they were higher than 0.99 (see *Table 2.3*). It follows from *Fig. 2.7* that the maximum amount of adsorbed CO<sub>2</sub> in the samples under study was ca. 20.5 dm<sup>3</sup> CO<sub>2</sub>·kg<sup>-1</sup>. The maximum CO<sub>2</sub> adsorption was obtained for coal from the no. 22b seam

(code no. 086) of Paskov-Staříč Mine ( $26.7 \text{ dm}^3 \text{ CO}_2 \cdot \text{kg}^{-1}$ ), whereas the coal from Prokop seam (code no. 504) of Lazy Mine had minimum adsorption ( $18.8 \text{ dm}^3 \text{ CO}_2 \cdot \text{kg}^{-1}$ ). Thus, it can be stated that, generally, the adsorption capacity of coal – as far as carbon dioxide is concerned – increases with increasing degree of coalification  $V^{\text{daf}}$ , and is also related to the average reflectivity of vitrinite,  $R_v$ , and the  $C^{\text{d}}/H^{\text{d}}$  ratio, which is commensurate with the expected behaviour of coal matter in seams of the Czech part of the Upper Silesian Basin (Martinec and Honěk, 2002; Martinec et al., 2005).

The correlation coefficients  $R^2$  expressing the degree of agreement of experimental data with Langmuir's model is summarized in Table 2.3, together with the absorption capacities  $V_m$  computed for individual samples. The calculated percentages of surface of coal occupied by adsorbed carbon dioxide  $S$  ( $\text{m}^2 \cdot \text{g}^{-1}$ ) is shown here as well. These data were arrived at based on the experimental values of  $V_m$  on the assumption that one  $\text{CO}_2$  molecule covers an area of  $0.253 \cdot 10^{-18} \text{ m}^2$  (Medek, 1971). Generally, it can be stated that the boundary found for the surface coverage values of  $127 - 181 \text{ m}^2 \cdot \text{g}^{-1}$  fully corresponds with our current notions about the area of internal surface of natural bituminous coals (Medek, 1971; Ettinger and Šulman; 1975; Nodzienski; 2000).

Nevertheless, from a practical point of view, what is most important is to compare the adsorption capacities  $V_m$  obtained for coal from the Czech part of the Upper Silesian Basin with the adsorption capacities of coal samples from other localities. In this respect, the study of Busch and Gesterblum (2011) summarizing adsorption data for Australian coals (from Bowen and Sydney basins), Indian coals (from Raniganj, South Karanpurna coalfield), German coals (Ruhr basin), Brazilian coals (Paraná basin), or North American coals (Argonne Premium Coals) is important. For these coal samples which on the coalification scale range from lignite to anthracite, the high-pressure adsorption capacities of  $\text{CO}_2$  were determined to be in the range of ca.  $15 - 50 \text{ dm}^3 \text{ CO}_2 \cdot \text{kg}^{-1}$  of dry coal (Busch and Gesterblum, 2011). It is curious to note that a clear-cut dependence of adsorption capacity on the degree of coalification was not proved. But in any case it is obvious that the limiting adsorption capacities of  $18 - 27 \text{ dm}^3 \text{ CO}_2 \cdot \text{kg}^{-1}$  resulting from our experiments conducted on coal from the Czech part of the Upper Silesian Basin are fully comparable with published coal adsorption capacity data pertaining to other localities.

## 2.5.2 EFFECT OF TEMPERATURE ON ADSORPTION OF CARBON DIOXIDE ON BITUMINOUS COAL

It follows from general thermodynamic notions about the process of physical adsorption that, at a given pressure, the degree of coverage of the surface of coal matter with molecules of a gaseous adsorbate ( $\text{CO}_2$ ,  $\text{CH}_4$ ,  $\text{N}_2$  and other) decreases with increasing temperature (under a given pressure); this is explained by the fact that the kinetic energy of the molecules increases with increasing temperature (Gregg and Singh, 1982). The same was found to apply generally to the adsorption of carbon dioxide

on coal matter; a distinctive decrease of carbon dioxide adsorption capacity was proved to be associated with an increase of temperature (Krooss et al., 2002; Sakurovs et al., 2007; Nodzienski, 2000).

For coal from the Czech part of the Upper Silesian Basin, the effect of temperature on the carbon dioxide adsorption capacity was studied at temperatures of 30 and 50°C. Dry coal samples from Natan coal seam (463) and from no. 22b seam (086) adapted to grain size of 0.06–0.5 mm were measured. The results are summarized in Table 2.3, Fig.2.8; they represent the amounts of carbon dioxide adsorbed at a pressure of 0.1 MPa.

Temperature	30°C	50°C	60°C
Sample from coal seam	$V^{\text{ads}}(\text{CO}_2)$ [ $\text{dm}^3 \cdot \text{kg}^{-1}$ ]		
Natan (No 463)	$5.4 \pm 0.15$	$3.9 \pm 0.15$	$3.0 \pm 0.2$
22b (No 086)	$7.4 \pm 0.15$	$4.6 \pm 0.15$	

Table 2.3 Effect of temperature on carbon dioxide absorption in bituminous coal from the Czech part of the Upper Silesian Basin

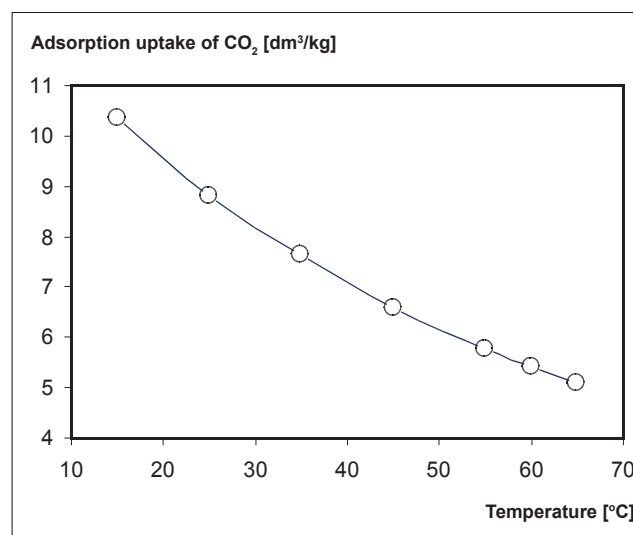


Fig. 2.8 Effect of temperature on adsorption uptake of carbon dioxide at pressure 0.02 MPa.

Sample: bituminous coal, grain size < 0.2 mm, from Poruba Mbr., Ostrava Fm., the Czech part of the Upper Silesian Basin (adopted from ref. Příbyl et al. 2009).

The data in Table 2.4 confirm that the adsorption capacity of carbon dioxide on coal decreases distinctly with increasing temperature; a temperature increase of 20°C produces a ca. 30% decrease in the amount of adsorbed  $\text{CO}_2$ . The same percentage (30%) was obtained by Příbyl et al. (2009) based on their analysis of a Darkov sample using a gravimetric (weight) sorption apparatus.

### 2.5.3 EFFECT OF MOISTURE IN COAL ON ADSORPTION OF CARBON DIOXIDE

Water is the basic component which accompanies coal matter regardless of its origin, place of occurrence, or degree of coalification. The content of water in coal (i.e., moisture) can vary – from a few tenths of a per cent (anthracite) to more than 50% (lignite). The occurrence of water in coal also represents the main, ultimate factor which also influences the capacity of coal to adsorb carbon dioxide.

The effect of moisture in coal from the Czech part of the Upper Silesian Basin on the capacity of coal to adsorb carbon dioxide was determined on samples having 0.06-0.15 mm in grain size, at a temperature of 30°C. The samples were measured in dry and wet condition. The content of water in wet coal was determined immediately after the calorimetric test (Table 2.4).

Sample from coal seam	$V_{\text{ads}}(\text{CO}_2)$ [dm <sup>3</sup> ·kg <sup>-1</sup> ]	$W_{\text{sample}}$ [%]	$V_{\text{ads}}(\text{CO}_2)$ [dm <sup>3</sup> ·kg <sup>-1</sup> ]
	Dry sample	Wet sample	
Natan (no 463)	5.4 ± 0.15	2.0	3.1 + 0.2
Prokop (no. 504)	4.5 + 0,08	3.2	2.8 + 0.15
22b (no 086)	7.4 + 0,15	1.2	5.5 + 0.15

Table 2.4 Effect of coal moisture in samples of bituminous coal from the Czech part of the Upper Silesian Basin on carbon dioxide absorption.

Explanatory note:

$w_{\text{sample}}$  = water content of bituminous coal in calorimetric test conducted on moist coal.  
Name / designation and code no. of coal seam in the Czech part of the Upper Silesian Basin (after Dopita et al., 1997).

It is clear from Table 2.4 that moisture is an important factor that imposes a limit on the capacity of the coal surface to adsorb carbon dioxide; water contents as low as 1 - 2%, which are encountered frequently, bring about a 30 to 40% decrease of CO<sub>2</sub> adsorption compared to dry coal. This dramatic limiting influence of water on CO<sub>2</sub> adsorption has been fully corroborated by other published results (Busch and Gensterblum, 2011; Day et al., 2008). The same was proved by an analysis of carried out on samples of Darkov Mine coal (Příbyl et al., 2009). At a moisture content of 1.1%, the capacity of coal to adsorb carbon dioxide is roughly 40% lower than that of a dry coal sample. A comparison of the CO<sub>2</sub> adsorption isotherms for dry and wet samples of Darkov coal is given in Fig. 2.9.

A number of authors made efforts to arrive at a detailed explanation of the effect of moisture on the process of carbon dioxide adsorption on the surface of coal matter (e.g., Ettinger and Šulman, 1975; Batistuta et al., 2010; Day et al., 2008). Some of these authors studied the differences observed in the adsorption centers depending on whether the species adsorbed was carbon dioxide or water (Kroos

et al., 2002; Příbyl et al., 2009; Busch and Gensterblum, 2011). Other authors believe that the curtailment of CO<sub>2</sub> adsorption on wet coal is the consequence of an adsorption mechanism of volumetric filling of micropores by molecules of water (Sakurovs et al., 2008). A valuable contribution to this subject is the „conventional“ information presented by Ettinger and Šulman (1975); they claim that gas components having higher critical temperatures  $T_k$  are adsorbed preferentially on the coal surface. The value of  $T_k$  of water is 374.1°C, while  $T_k$  for carbon dioxide is (only) 31.1°C. This corresponds to preferential adsorption of that water which carbon dioxide no longer is capable of displacing from the coal surface. On the basis of studies of Australian and Chinese coal, Day et al. (2008) estimate that three molecules of water displace one molecule of carbon dioxide. Another published claim has been that the capacity of coal to adsorb carbon dioxide decreases with increasing water content of moisture only up to a certain, so-called equilibrium value, whereupon it remains more or less constant (Day et al., 2008; Joubert et al., 1974). Such behaviour could not be proved for bituminous coals from the Czech part of the Upper Silesian Basin. It is evident that the above information applies only to hydrophyllous coals with a low degree of coalification and a different maceral composition.

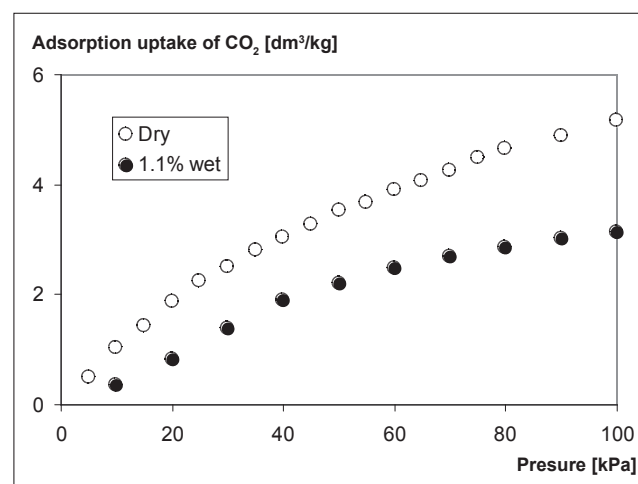


Fig. 2.9 Effect of coal moisture on adsorption uptake of carbon dioxide at 35 °C and grain size < 0.2 mm.

Sample: Bituminous coal from Poruba Mbr, Ostrava Fm, the Czech part of the Upper Silesian Basin (adopted from ref. Příbyl et al. 2009).

### 2.5.4 EFFECT OF COAL GRAIN SIZE ON CARBON DIOXIDE ADSORPTION

Grain size of coal samples is another parameter that can influence the adsorption process on coal in situ. The effect of grain size on adsorption of carbon dioxide on coal from the Czech part of the Upper Silesian Basin was examined using two grain size fractions: (1) 0.06 – 0.15 mm and (2) 0.8 – 1.0 mm. Dry samples were used and the measurements were performed at a temperature of 30°C. The results are summarized in Table 2.5.

Grain size	0.06 – 0.15 mm	0.8 – 1.0 mm
Samle from the coal seam	$V^{ads}(CO_2)$ [dm <sup>3</sup> ·kg <sup>-1</sup> ]	$V^{ads}(CO_2)$ [dm <sup>3</sup> ·kg <sup>-1</sup> ]
Natan (No 463)	5.4 ± 0.15	3.3 ± 0.15
22b (No 086)	7.4 ± 0.15	3.4 ± 0.15

**Table 2.5** Effect of grain size of bituminous coal from the Czech part of the Upper Silesian basin on carbon dioxide absorption

The results in *Table 2.5* show that the grain size of coal (in situ or in a coal sample) is an important parameter influencing its adsorption capacity. With increasing grain size, the adsorbed amounts of carbon dioxide decrease. It follows from the experimental data that a tenfold increase in grain size causes the amount of adsorbed CO<sub>2</sub> to decrease by one half. Roughly the same results were obtained by Přibyl et al. (2009) who used the method of gravitational adsorption of carbon dioxide on samples of Darkov coal which however were of different grain sizes: (1) under 0.2 mm and (2) above 5 mm.

The behavior of the coal – CO<sub>2</sub> system as a function of coal fragmentation is definitely linked with poorly developed pores in the coal matter not allowing free access of adsorbate to the adsorption centers throughout the bulk of the coal particles. Thus, in the real time of the adsorption experiment, the adsorption process proper takes place predominantly on the accessible, external surfaces of the coal grains. The test results indicate that, more precisely, this instantaneous (apparent) adsorption of CO<sub>2</sub> on these accessible surfaces of the coal particles is completed and terminated within ca. 1.5 h from the first contact of carbon dioxide with coal. Then, evidently, any further access of CO<sub>2</sub> molecules into the undisturbed coal matrix takes place by activated diffusion (Busch and Gensterblum 2011) and requires a long time (days, weeks, ...). In this connection, it is worth mentioning that for the diffusion of nitrogen into coal (at the temperature of liquid nitrogen), the time to reach the adsorption equilibrium is of the order of 1,000 years (van Krevelen, 1993).

**Many authors have paid attention to the quantification of the coefficients of CO<sub>2</sub> diffusion into the pore structure of coal. Busch and Gensterblum (2011) present the results of measurements taken by thirteen different authors who studied CO<sub>2</sub> diffusion into coal during the 1993 to 2010 period. In this connection, the following conclusions (Busch and Gensterblum, 2011) ought to be highlighted as being the most interesting:**

- The coefficients of CO<sub>2</sub> diffusion into coal range from 10<sup>-11</sup> to 10<sup>-16</sup> m<sup>2</sup>·s<sup>-1</sup>.*
- The rate of CO<sub>2</sub> adsorption on dry coal is always higher than that on wet coal; a 1-2% increase of moisture brings about a ca. 30-40% decrease of the amount of CO<sub>2</sub> adsorbed.*
- For identical coal samples, the CO<sub>2</sub> adsorption rate is higher than the CH<sub>4</sub> adsorption rate.*
- The CO<sub>2</sub> adsorption rate decreases with increasing fragmentation of the coal, but only up to a certain*

*limit. A tenfold increase in the diameter of coal grains causes the amount of adsorbed CO<sub>2</sub> to decrease to approximately one half.*

- The capacity of coal to adsorb CO<sub>2</sub> decreases with increasing temperature; an temperature increase of 20°C produces a decrease of the adsorbed amount of CO<sub>2</sub> by ca. 30%.*
- The CO<sub>2</sub> adsorption rate manifestly decreases with increasing stress applied onto the coal sample. Strange as it may seem, sporadic attention has been dedicated to that question so far (Pone et al., 2009).*

Detailed study of orientation, intensity and natural susceptibility to cracking (natural cleats) in coal seam and precisely identification of mineralization in cracks and fissures is very important.

### 2.5.5 COMPARISON OF THE ADSORPTION PROPERTIES OF CARBON DIOXIDE AND METHANE ON BITUMINOUS COAL

No analysis of the factors influencing adsorption of carbon dioxide on coal would be complete without elucidating the effect of the presence of methane which often accompanies carbon dioxide in coal seams.

It follows from *Table 2.7* that the capacity of coal to adsorb CO<sub>2</sub> is 4 to 5 times higher than its capacity to adsorb methane. This finding fully corresponds with earlier information by Ettinger and Šulman (1975), to the effect that preferential adsorption can be expected for that gas component which has the higher value of the critical temperature T<sub>k</sub>. The value T<sub>k</sub> for carbon dioxide is 31.1°C (*Fig.2.3*), the value T<sub>k</sub> for methane is -82°C, and the value for water is 385°C (*Fig.2.4*). Therefore, preferential adsorption of carbon dioxide can be expected; this gas should be able to displace methane previously adsorbed on the coal surface. The ability of carbon dioxide to displace methane was proved experimentally (Ottiger et al., 2008; Fitzgerald et al., 2005).

The relative adsorption capacities of carbon dioxide and methane derived from measurements also correspond to the published results. Measurements of CO<sub>2</sub> and CH<sub>4</sub> adsorption performed so far proved that the capacity of coal to adsorb CO<sub>2</sub> is higher than the capacity to adsorb CH<sub>4</sub> (e.g., Battistuta et al., 2010; Sakurovs et al., 2007; Day et al., 2008; Fitzgerald et al., 2005). This fact is illustrated in *Fig 2.10* showing the CO<sub>2</sub>/CH<sub>4</sub> adsorption ratios for coals from lignite to anthracite (Busch and Gensterblum, 2011) having different degrees of coalification (vitrinite reflectance) on the basis of the works of seventeen authors who studied this subject.

While the measurements of adsorption of pure CO<sub>2</sub> and CH<sub>4</sub> proved unambiguously that the capacity of coal to adsorb carbon dioxide is higher, the results of measurements of adsorption of a mixture of carbon dioxide with methane on coal were not so convincing. Alongside works confirming preferential adsorption of carbon dioxide also from the CO<sub>2</sub> – CH<sub>4</sub> gas mixture (Ottiger et al., 2008; Fitzgerald et al., 2005), other results were also

published which claimed that methane adsorbed preferentially (Majewska et al., 2009). However, finding an explanation of this latter preferential adsorption will require further research.

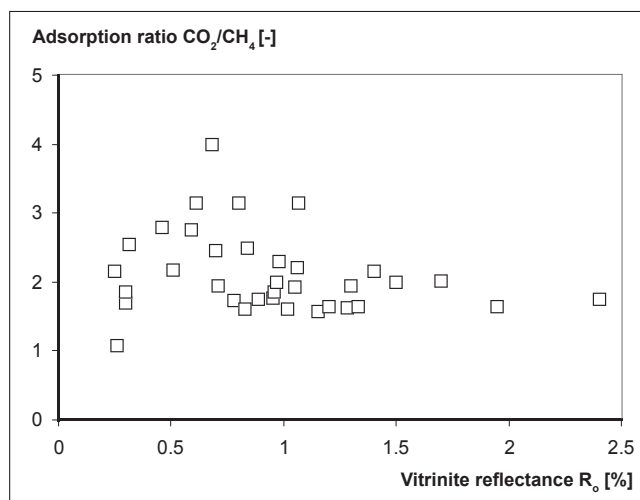


Fig. 2.10 Ratio between adsorption capacities of coal to  $\text{CO}_2$  and  $\text{CH}_4$  as a dependence of coal rank, dry samples (adopted from ref. Busch and Gensterblum, 2011)

### 2.5.6 ADSORPTION OF CARBON DIOXIDE AND METHANE ON COAL FROM THE INTRA-SUDETEN BASIN

As a piece of supplementary information, it should be pointed out that adsorption of  $\text{CO}_2$ ,  $\text{CH}_4$  or ( $\text{CO}_2 + \text{CH}_4$ ) mixtures having variable ratios of the two gases, at a temperature of  $20^\circ\text{C}$  and at pressures increasing progressively up to 50 atm (4.93 MPa), was demonstrated by Tarnowski in Kruk (1969) on samples of coal from the Polish part of the Intra-Sudeten Basin. The authors used coal samples of less than 0.042 mm grain size and of 60 g in weight. The samples came from the following mines: Thorez (coal seams nos. 72, 73, 78); Nowa Ruda, Boleslaw (coal seams nos. 12, 13, 32); Piast (upper and middle coal seams, Frantisek, Roman, Ferdynand, and Wilhelm coal seams). The adsorption isotherms of  $\text{CO}_2$  and  $\text{CH}_4$  mixtures deviated considerably from the Langmuir behavior. For the above coals, Tarnowski (lit.cit.) indicates that the volumes of adsorbed pure  $\text{CO}_2$  (Fig. 2.11), pure  $\text{CH}_4$ , and mixture of both gases (Fig. 2.12) in  $[\text{m}^3 \cdot \text{Mg}]$  (at different  $\text{CO}_2/\text{CH}_4$  ratios) are pressure-dependent (up to 50 atm., i.e., 4.93 MPa). Curves of potential gas absorption capacity of coal from a given seam versus pressure were presented. The graph in Fig. 2.12 shows examples of three adsorption isotherms of  $\text{CO}_2$  and  $\text{CH}_4$  and their mixture, converted to the amount of gas adsorbed, as function of the maximum attained adsorption pressure (50 atm = 4.93 MPa) for selected coal samples. The capacity of coal samples from the Polish part of the Intra-Sudeten Basin for adsorption of pure methane at high pressure is  $17 \text{ m}^3$  methane per kg of coal at  $20^\circ\text{C}$ , at grain sizes under 0.042 mm; the same parameter for  $\text{CO}_2$  is in the range of  $40 \text{ dm}^3 \text{ CO}_2$  per kg of coal.

It was confirmed that in coal from the Polish part of the Intra-Sudeten Basin, namely in coal of a lower coalification with volatile matter  $V^{\text{daf}}$  (22 to 42%, most frequently 35 to 39%), both grain size and temperature have a considerable influence on the amount of  $\text{CO}_2$  adsorbed ( $35\text{--}45 \text{ dm}^3 \cdot \text{kg}^{-1}$ ). This is higher than the amount of  $\text{CO}_2$  ( $18\text{--}27 \text{ dm}^3 \cdot \text{kg}^{-1}$ ) adsorbed on coal from the Czech part of the Upper Silesian Basin, of a higher coalification  $V^{\text{daf}}$  (18.6 – 33.8%). This may be explained by the influence of temperature and, first of all, grain size of the samples used in the experiment.

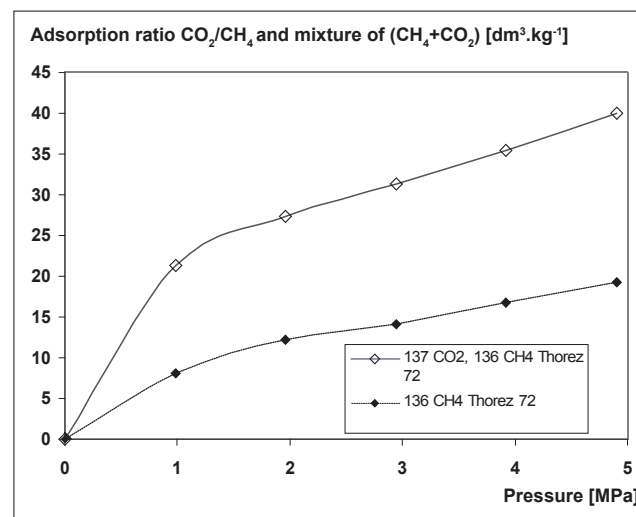


Fig. 2.11 Adsorption isotherms of pure  $\text{CO}_2$  and  $\text{CH}_4$  for a sample of bituminous coal from Polish part of the Intra-Sudeten Basin, Thorez Mine, no. 72 coal seam (Tarnowski in Kruk (1969), adapted).

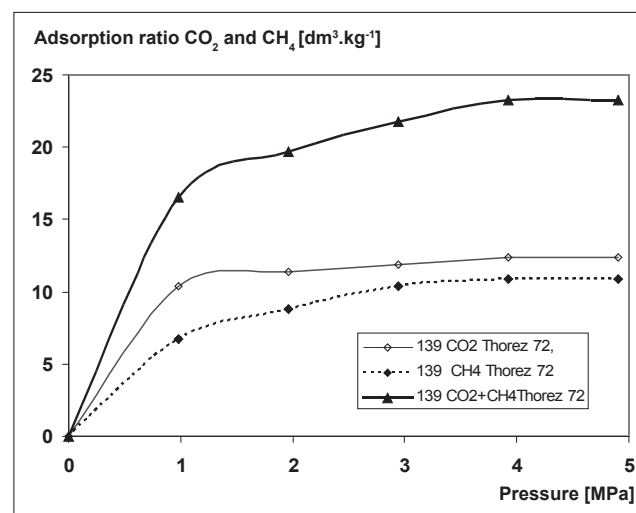


Fig. 2.12 Adsorption isotherms of pure  $\text{CO}_2$  and  $\text{CH}_4$  and their mixture for a sample of bituminous coal, Polish part of the Intra-Sudeten Basin, Thorez Mine, coal seam 75. (Tarnowski in Kruk (1969), adapted).

For coal from the Czech part of the Intra-Sudeten Basin, where mixed outbursts of  $\text{CO}_2$  and  $\text{CH}_4$  occurred in coal seams containing volatile matter  $V^{\text{daf}}$ : 36–39%,  $\text{C}^{\text{d}}$ : 80–84% and  $\text{H}^{\text{d}}$ : 5.2% (Zdenek Nejedlý Mine – (Tásler et al., 1979), corresponding data on the adsorption of  $\text{CO}_2$  or  $\text{CH}_4$  on

coal are missing. In view of the geological analogies, geological age, the coal deposit structure, the coal composition and its maceral composition and coalification, the data on adsorption of pure CO<sub>2</sub>, methane, and CO<sub>2</sub> – CH<sub>4</sub> mixtures at a temperature of 20°C available for coal from the Polish part of the Intra-Sudeten Basin (Tarnowski in Kruk (1969) or Nodziński 2000) may also apply in the Czech part of the basin, bearing in mind all the accompanying factors (water content, grain size, degree of coalification, and temperature and pressure).

## 2.6 NITROGEN PERMEABILITY OF ROCKS AND COAL UNDER TRIAXIAL STRESS

The permeability of rocks or coal microstructures is a complicated phenomenon: it includes both volumetric gas transport through the pores and gas diffusion processes influenced by the temperature at which the process of gas migration occurs. In rocks with dispersed coal matter or in coal, an integral part of the process of gas migration is the process of its adsorption on the coal matter. The adsorption process is influenced by the surface area of the absorbent (e.g., coal or rock) as well as by water content and temperature. Data for Carboniferous rocks and coal of the Czech part of the Upper Silesian Basin according to Konečný and Kožušníková (2011) are listed in Table 2.6 – 2.8.

### The permeability of rocks and coal was tested under the following experimental conditions:

The permeability measuring device of the Institute of Geonics of the Academy of Sciences in Ostrava–Poruba consists of a KTK 100 UNIPRESS triaxial cell, modified to enable the passage of gas. A so-called “false triaxial ap-

paratus” was employed, producing a confining pressure of hydraulic oil ( $\sigma_2 = \sigma_3$ ) of up to 100 MPa upon the testpiece. The axial stress ( $\sigma_1$ ) was exerted by type ZWICK 1494 mechanical press. This experimental arrangement makes it possible to perform basically two main types of experiments: measurements of permeability under increasing hydrostatic pressure and measurements of permeability under increasing axial pressure.

The gas medium used for the measurements of permeability is nitrogen of a dynamic viscosity  $\mu = 1.75 \times 10^{-5}$  Pa·s; its pressure  $P_{up}$  is maintained constant at 3 MPa by the control valve from a gas pressure vessel. The gas is passed through a capillary to the cylindrical part of the apparatus and to a special screen where the gas is distributed to the upper base of the rock specimen. At an atmospheric pressure  $P_{down}$  the gas flows through the screen from the low base of the rock specimen to the output capillary.

From the outlet capillary the gas is passed to a flowmeter or measuring cylinder from which it expulses water; the volume of water corresponds to the volume of gas passed per unit time  $Q$ . Equation (2.6) based on Darcy’s law is applied to calculate the intrinsic permeability of compressible gas (ASTM Standards, D 4525),

$$k = \frac{2Q \cdot \mu \cdot L \cdot P_{down}}{A \cdot (P_{up}^2 - P_{down}^2)} \quad (2.6)$$

where:

- $k$  – permeability coefficient [ $m^2$ ];
- $Q$  – volumetric flow of nitrogen [ $m^3$ ];
- $\mu$  – dynamic viscosity;  $\mu$  for nitrogen =  $1.75 \cdot 10^{-5}$  Pa·s;
- $L$  – length of sample [ $m$ ];
- $P_{down}$  – atmospheric pressure [MPa];
- $A$  – cross-sectional area of specimen  $A$  [ $m^2$ ];
- $P_{up}$  – pressure regulated from the gas pressure vessel by the control valve, so as to be maintained at the constant value of 3 MPa.

Sample	Borehole / Mine	Formation / Member	Petrography	Median grain size of quartz
				[mm]
3327	Čeladná (Č-1)	Sedlové vrstvy Mbr / Karviná Fm	SAMg	0.21
3336	Čeladná (Č-1)	Suchá Mbr / Karviná Fm	SAMg	0.23
3888	Ostravice (O-1)	Poruba Mbr / Ostrava Fm	SAfg	0.15
3946	Ostravice (O-1)	Poruba Mbr / Ostrava Fm	SAMg	0.40
4502	Lazy Mine (C 84 A)	Sedlové vrstvy Mbr / Karviná Fm	SAC	0.59
4512	Lazy Mine (C 84 A)	Poruba Mbr / Ostrava Fm	SAC	0.51
4537	Dukla Mine (D 2197)	Poruba Mbr / Ostrava Fm	SAMg	0.29
4539	Dukla Mine (D 2197)	Poruba Mbr / Ostrava Fm	SAC	0.51
4542	Dukla Mine (D 2197)	Poruba Mbr / Ostrava Fm	SAMg	0.32
4543	Dukla Mine (D 2197)	Poruba Mbr / Ostrava Fm	SAMg	0.44
7567	Darkov Mine (257)	Sedlové vrstvy Mbr / Karviná Fm	SAC	0.58

*Explanatory notes: fine-grained sandstone – SAfg, medium-grained sandstone – SAMg, coarse-grained sandstone – SAC*

**Table 2.6 Permeability of sandstone from the Czech part of the Upper Silesian Basin – characterization of rock samples in Fig. 2.13 (experimental data: Konečný and Kožušníková, 2011)**

Rock	Bulk volume [kg·m <sup>-3</sup> ]	Total porosity [%]	Strenght [MPa]	Splitting tensile strenght [MPa]
Interval (minimum-maximum) / Average				
Sedlové vrstvy Mbr – (Namurian C) Karviná Fm (Namurian C,D and Westphalian A)				
fine-grained sandstone Sfg	2470-2980 2583	1-9 4.0	15-103 67	4.1-13.8 8.3
medium-grained sandstone Smg	2490-2630 2548	3-10 5.0	20-143 69	4.3-7.3 5.7
coarse-grained sandstone Sc	2450-2680 2583	4-10 7	34-174 79	3.8-8.7 4.9
Poruba Mbr (Namurian A, zóne E2b) – Ostrava Fm (Namurian A)				
fine-grained sandstone Sfg	2460-2990 2593	1-7 3.0	39-143 87	5.3-13.5 8.4
medium-grained sandstone Smg	2485-2640 2555	3-8 4.5	45-121 83	3.3-13.3 6.9
coarse-grained sandstone Sc	2445-2692 2585	4-8 5.8	67-110 89	2.8-8.3 5.6

Table 2.7 Bulk volume, total porosity, strength, and splitting tensile strength of sandstones from Sedlové vrstvy Mbr, Karviná Fm and Poruba Mbr, Ostrava Fm (Czech part of Upper Silesian coal basin) (Müller et al. in Dopita et al., 1997, adapted).

Sample no.	Mine, (borehole)	Member	Coal seam name/designation and (code no.)	Vitrinite reflectance Ro [%]	Coal macerals [%]		
					Vitrinite	Liptinite	Inertinite
3284	Lazy (38704)	Sedlové vrstvy Mbr	38 (522)	0.960	64.3	2.0	33.7
3284	Lazy (38704)	Sedlové vrstvy Mbr	38 (522)	0.938	61.9	3.1	35.0
4159	9. květen (SuSto572)	Sedlové vrstvy Mbr	Prokop (507-510+504)	1.054	61.1	8.2	30.7
4160	9. květen (SuSto572)	Sedlové vrstvy Mbr	Prokop (507-510+504)	1.082	45.5	12.1	42.4
4162	9. květen (SuSto572)	Sedlové vrstvy Mbr	Prokop (507-510+504)	1.072	47.0	10.8	42.2
4163	9. květen (SuSto572)	Sedlové vrstvy Mbr	Prokop (507-510+504)	1.077	47.6	23.1	29.3
4166	9. květen (SuSto572)	Sedlové vrstvy Mbr	Prokop (507-510+504)	1.009	61.8	2.1	36.1
4168	Lazy (C 117)	Sedlové vrstvy Mbr	Prokop (504)	0.875	44.5	17.6	37.9
5215	Lazy (C 110)	Sedlové vrstvy Mbr	39 (507-510)	0.828	69.1	7.9	23.0
5216	František (F 3313)	Poruba Mbr	Sek (420)	1.226	87.6	3.8	8.6

Table 2.8 Permeability of bituminous coal from the Czech part of the Upper Silesian basin – characterization of coal samples in Fig. 2.14 (experimental data: Konečný and Kožusniková, 2011)

The cylindrical testpieces used for permeability measurements usually are of a length of  $L = 96$  mm and a diameter of 48 mm defining the cross-sectional area of the specimen,  $A$ . The bases of the cylindrical testpieces are ground. The setup of rock specimens, screen and clamps is protected against ingress of oil by a rubber seal.

### PERMEABILITY MEASUREMENTS AT INCREASING HYDROSTATIC PRESSURE

This measurement method is based on gradually increasing the hydraulic oil pressure in the triaxial cell. The testpiece is clamped in the press. The confining pressure induced by hydraulic oil is increased starting from 5 MPa in stepwise fashion, in 5 MPa steps, up to the maximum of 50 MPa. The axial stress is identical to the confining pressure, thus inducing a hydrostatic three-dimensional stress in the testpiece ( $\sigma_1 = \sigma_2 = \sigma_3$ ). The hydrostatic pressure of 50 MPa corresponds to the hydrostatic pressures encountered in the rock massif at ca. 2000 m depth, calculated from general rock density.

The pressure of the gas medium is regulated by a control valve of a gas pressure vessel so as to be kept constant at 3 MPa throughout the test. Nitrogen was the gas medium used in all experiments. This gas behaves as an inert medium, i.e., it does not react with the rocks, and no adsorption on coal samples was observed during short-time experiments (Konečný and Kožušníková, 2010). Volumetric flow of nitrogen  $Q$  is measured at selected values of hydrostatic pressure, and permeability is calculated according to the formula (2.6). The testpieces are not loaded to rupture during these experiments.

The permeability measuring method at increasing hydrostatic pressure was developed at the Institute of Geonics, in the Laboratory of Petrology and Physical Properties of Rocks (Konečný and Kožušníková, 1998; Konečný, Kožušníková and Nowakowski, 2000).

### PERMEABILITY MEASUREMENTS AT INCREASING AXIAL PRESSURE

In permeability measurements conducted at a constant confining pressure and an increasing axial stress, the testpiece is clamped in the press and the confining pressure is pre-set to the required value, in this case, 5 MPa. The value of axial stress is gradually increased by the movement of the press chucks up to the potential rupturing level ( $\sigma_1 = \sigma_2 = \sigma_3$ ). Again, the nitrogen pressure is regulated by the control valve from a gas pressure vessel and is kept constant at 3 MPa throughout the experiment.

For this type of experiment involving a continuous measurement of the volume of passed gas, volumetric flow has to be recorded at regular intervals. Three flowmeters of different measuring range are employed. At the present, continuous measurements are feasible for flowrates of  $5 \text{ cm}^3 \cdot \text{min}^{-1}$  to  $5000 \text{ cm}^3 \cdot \text{min}^{-1}$ . For reliable registration of the flowrates, an optimal loading regime has to be defined. After an introductory test series, the optimal strain rate was set at  $10^{-5} \text{ s}^{-1}$ .

During these experiments, the permeability values are related to the axial stress by recording the axial and lateral deformations. The axial deformation is recorded by following the position of the cross-beam of the press

and is corrected for the rigidity of the measuring setup. For measurements of lateral deformation under triaxial stressing, special strain gauges were developed at the Institute of Geonics. The sensor consists of a flexible ring segment fitted with strain gauges on both sides, connected to a Wheatstone bridge semiconductor. The nominal range of the shift is 5 mm, the non-destructive range is 7.5 mm, and linearity is 7%. During the measurement, two sensors positioned at an angle of  $90^\circ$  to each other are used, mounted symmetrically to the testpiece axis, at half the specimen height.

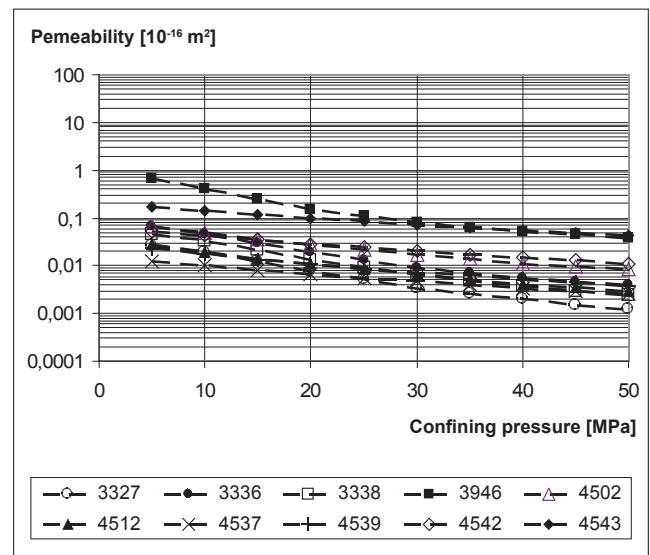


Fig. 2.13 Dependence of permeability coefficient on confining pressure for sandstones. Carboniferous sandstones from the Czech part of the Upper Silesian Basin (data was provided by Pavel Konečný and Alena Kožušníková, adapted)

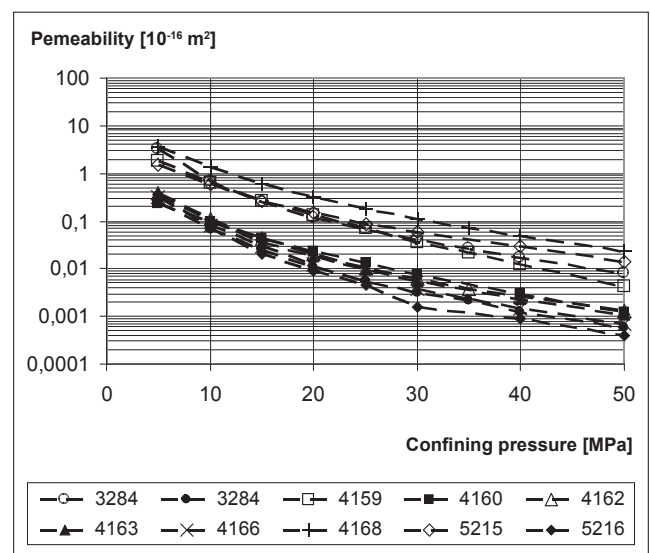


Fig. 2.14 Dependence of permeability coefficient on confining pressure for bituminous coal from the Czech part of the Upper Silesian Basin (data was provided by Pavel Konečný and Alena Kožušníková, adapted)

Sandstones are characterized in more detail in *Table 2.8* and in the graph in *Fig. 2.13*. Clastic sediments from the Carboniferous of the Czech part of the Upper Silesian Basin, originating from the Sedlové vrstvy Mbr (Karviná Fm) and from Poruba Mbr (Ostrava Fm) exhibit similar permeability trends in relation to strain as the medium grained sandstones from Poruba Mbr (Ostrava Fm). For this types of sandstones, the rock permeability values are changed: at the pressure of 3 MPa, permeabilities for nitrogen are within the interval of  $1-0.12 \cdot 10^{-16} \text{ m}^2$ , at the pressure of 50 MPa, permeability is in the interval of  $1 \cdot 10^{-16} \text{ m}^2 - 0.05 \cdot 10^{-16} \text{ m}^2$ . The other sandstones from Sedlové vrstvy Mbr and Poruba Mbr are more homogenous. Their permeabilities are within the interval from  $0.09-0.01 \cdot 10^{-16} \text{ m}^2$  at 3 MPa to  $0.01-0.001 \cdot 10^{-16} \text{ m}^2$  at 50 MPa. The nitrogen permeability changes reflect the influence of pressure not only on the closing of configurative pores, but also on microfissures (Konečný, Kožušníková and Martinec (1999), Konečný and Kožušníková (2011), Konečný and Mlynarczuk (2002)). For claystones and siltstones, which frequently are well represented in dispersed coal matter and clay minerals, the permeability will be much lower.

Pressure has a substantial effect on the permeability coefficient of bituminous coal (Konečný and Kožušníková, 2010, 2011) at the pressure of 3 MPa the permeability coefficients are within the interval of  $6 \cdot 10^{-16} \text{ m}^2 - 0.26 \cdot 10^{-16} \text{ m}^2$ , at the pressure of 50 MPa the interval is  $0.016 \cdot 10^{-16} \text{ m}^2 - 0.0006 \cdot 10^{-16} \text{ m}^2$  (*Fig. 2.14*). This must be taken into consideration when considering carbon dioxide migration in deep coal seams of the rock massif.

Generally, caution must be exercised when adapting published data on transport properties obtained under laboratory conditions onto coal and rocks originating from different basins and onto experiments performed out at different temperatures and with differently prepared samples, even if the degree of coalification is the same. In any specific case, the same experimental conditions must be respected, as well as the geological factors and the composition and texture of rocks and coal in the coal seams.

### 3. CARBON DIOXIDE IN CENTRAL BOHEMIAN CARBONIFEROUS (SLANÝ COAL DEPOSIT)

From the point of view of the occurrence of carbon dioxide, the above part of Central Bohemian Permo-Carboniferous basin is of extraordinary interest because the mine workings opened there have made it possible to study the natural collectors of gas represented by the sandstones and conglomerates of the Mirošov horizon, Nýřany Mbr wherein the gas is dissolved in pore water (Fig. 3.1). The facts that the properties of pores in this permeable rock body with mineralized water were influenced, and that the mineral composition of the rock matrix was altered, by reaction of carbon dioxide with rock-forming minerals during a later (Tertiary) penetration of carbon dioxide from greater depths into the collector with mineralized water is, in a way, a unique experience for geologists, miners, and geo-technologists alike.

#### 3.1. GEOLOGY, HYDROGEOLOGY AND GAS OCCURRENCE

A systematic geological exploration of Slaný deposit by boreholes from surface, undertaken in the 1970s and 1980s, culminated by geological and geotechnical exploration conducted from mine workings in two shafts being opened at Slaný Mine (1979-1989). These shafts however

were never completed, due i.a. to problems connected with CO<sub>2</sub> outbursts within the Mirošov horizon. The shafts were backfilled in 1993.

The latest description of the geology of Slaný deposit was presented by Pešek (1996). The area of Slaný deposit is 49 km<sup>2</sup> covering an approximately square-shaped area of 7.5 by 6.5 km. Four main coal bearing horizons are known there: Kounov seams (which were mined as far back as the 18<sup>th</sup> century), Nýřany seams, the Lubná seam, and the Radnice seam (Fig. 3.1, Table 3.1). Boreholes were drilled and exploration started in the Nýřany and Radnice seams before World War I, but a more detailed geological exploration in the Slaný region has not started until 1960. A total of 59 boreholes drilled from the surface were used to calculate the coal reserves (Žbánek et al., 1978).

#### METAMORPHIC COMPLEX OF THE BASEMENT OF CARBONIFEROUS

The basement of Carboniferous consists of rocks of Upper Proterozoic of the Teplá-Barrandien unit. The relief of the Proterozoic can be considered as a peneplain, the differences in elevation being ca. 80 m. During sedimentation of the Carboniferous, two phenomena manifested themselves: subsidence and tectonic segmentation into blocks during successive stages of development.

Stratigraphy		Formation	Member		Group of coal seams		
Carboniferous	Stephanian	C	Líně				
		B	Slaný	Kamenný Most	Otruby	Kounov	
				Kounov			
				Ledce			
				Hřeble	Malesice		
				Mšeno			
	Jelenice						
	Westphalian	D Cantabrian + AD	Týnec				
				Kladno	Nýřany		Nevřeňe
							Chotíkov
						Nýřany	
	Touškov						
C C		Radnice	Upper Lower	Lubná Radnice Plzeň			

Table 3.1 Lithostratigraphical Carboniferous scheme of the Central Bohemian Permo-Carboniferous basin (after Holub and Pešek, 1991, adapted)

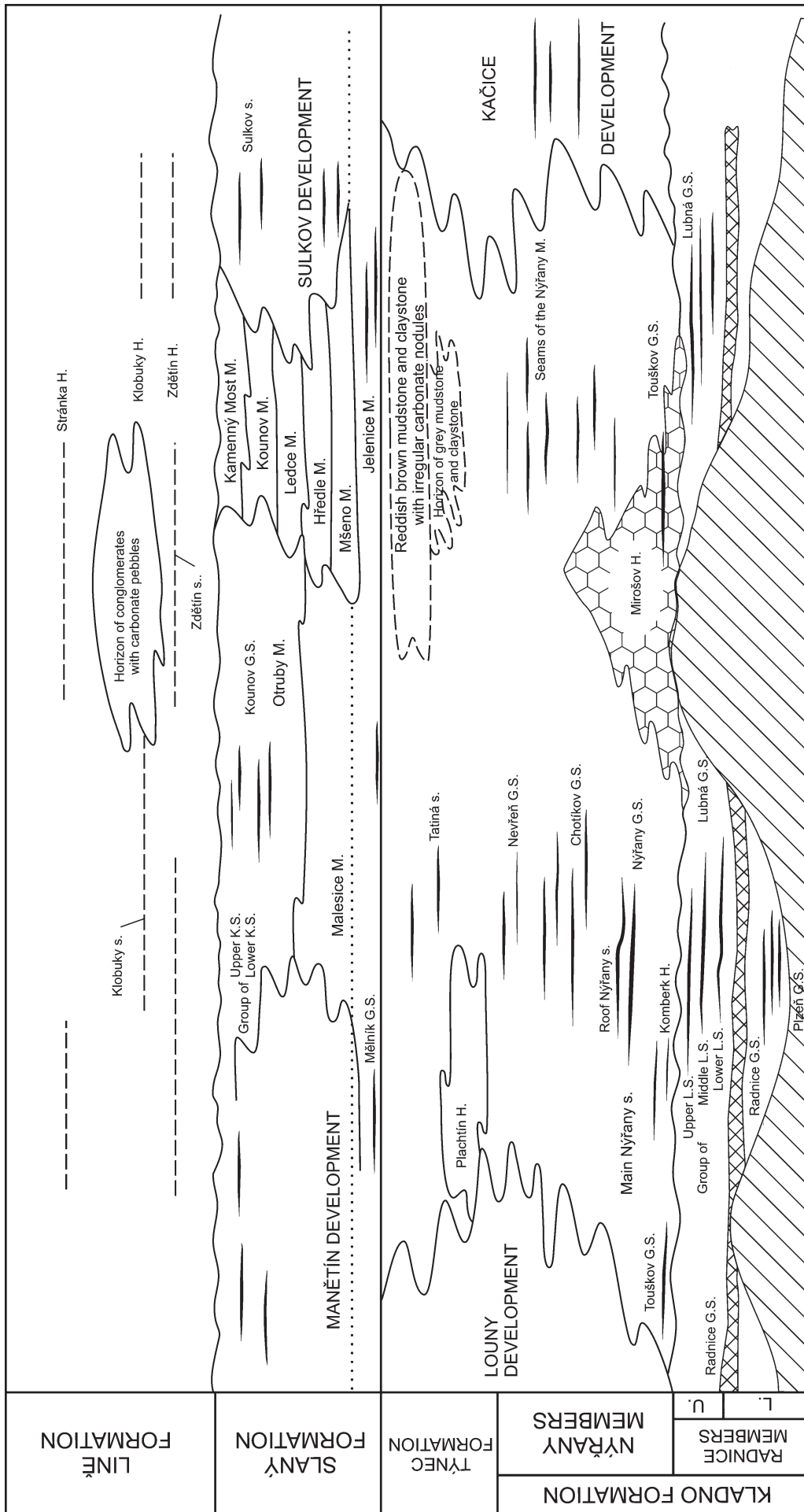


Fig. 3.1 Positional layout of Mirošov horizon in Nýřany Mbr. in the Central Bohemian Permo-Carboniferous basin (Pešek, 1996)

Legend: G.S. Group of coal seams; M Member; S Coal seams; H Horizon.

## THE CARBONIFEROUS

The thickness of Carboniferous on this location is up to 1400m. A detailed description of the geology of the Central Bohemian Permo-Carboniferous Basin was given by Pešek (1996). The Carboniferous consists of four distinct formations (*Fig. 3.1, Table 3.1*). The local names of the formations and members, also used in geological and technical reports by various authors (Leopold, 1985; Leopold and Živor, 1986; Žbánek, 1978; Čichovský et al., 1987), are reproduced in Table 3.2.

The Kladno formation is a basal formation of variable thickness lying on a buried rolling landscape (*Fig. 3.1*). The permeable rock bodies of Radnice Mbr can contain highly mineralized and gas-containing water. Following the deposition of Radnice Mbr, the next phase was intra-Westphalian hiatus, which manifested itself by

the fracturing of an almost leveled paleosurface and by the creation of rolling land with morphological depression of an erosive nature, in which process tectonics as well as subsidence participated. The Radnice and Lubná coal seams were formed (*Fig. 3.1, Table 3.1*). The basal sediments of Nýřany Mbr – Mirošov horizon – were deposited as fluviatile facies in a morphologically rugged terrain. This horizon consists of conglomerates and arcose sandstones, which predominate over layers of siltstones and claystones (Havlena and Pešek, 1975). The Mirošov horizon is limited at its base by the erosive hiatus of Westphalian age. In the overlying strata, the boundary is constituted by the beginning of the coal bearing cycle of Nýřany seams, or by its equivalent (Pešek, 1996). Correlation and continuation of the Mirošov horizon in individual parts of the Central Bohemian Permo-Carboniferous Basin is complicated and remains yet to be clarified.

Stratigraphy		Formation	Member	Lithology	Group of coal seams
Upper Cretaceous	Lower Turonian	Bílá hora		Marlstone and siltstone	
	Cenomanian	Skuteč			
			Vyšerovice		
Upper Carboniferous	Stephanian C	Upper red (Líně)		Litofacies: lacustrine and fluviatile	Klobuky
	Stephanian B	Upper grey (Slaný)	Kounov	Litofacies: lacustrine and fluviatile	Upper and Lower Kounov
			Ledeč	Litofacies: fluviatile	
			Malesice	Litofacies: Two lacustrine	
			Jelenice	Litofacies: lacustrine and fluviatile	
	Stephanian A	Lower red (Týnec)		Litofacies: lacustrine and fluviatile	
	Westphalian D	Lower grey (Kladno)	Nýřany	Siltstone and sandstone	Nýřany (15 coal seams)
				Litofacies: lacustrine and fluviatile with sandstones and conglomerates	<b>Mirošov conglomerates, Mirošov horizon</b>
	Westphalian C		Upper Radnice	4 litofacies: proluvial – deluvial fluviatile and lacustrine, volcanigenous	Lubná
			Lower Radnice		Radnice
Proterozoic basement					

*Table 3.2 Names / designations of formations and members used in geological documentation (reports and documents by Geindustria Co.) of Slaný Mine shafts and boreholes drilled from surface (Leopold and Živor, 1986; Žbánek, 1978; Leopold, 1985; Čichovský, 1987).*

Slaný deposit follows a generally horizontal direction, with a gentle incline to the NE (5°-10°); there are irregularities in this incline in the vicinity of tectonic lines, possibly influenced by the morphology of the underlying strata. Interpretation of the tectonic structure assumed that this forms a cascade, from shallow blocks in the SW part to the deepest blocks in the NE part of Slaný deposit. The cascade-shaped depression is formed by young tectonic faults running in the NNW-SSE direction, with amplitudes up to 110 m and with dips of 40°-80°, and by older transverse tectonic faults following the WWS – NNE direction, with dips of 40°-75°.

These failure zones in NNW-SSE directions probably represent the main routes by which carbon dioxide can ascend. Analogically, as in other areas of Bohemian massif (see Fig. 2.1), there exists a close relationship of carbon dioxide emission and salt water springs to the Tertiary volcanic body of Slánská Hill and Vinařická Hill of Paleogene age. (The name of the town, Slaný, derives from the salt water springs found there).

For temperatures and pressures encountered in the Slaný deposit, the reader is referred to Chapter 2.

The hydrogeology and occurrence of gases in this deposit were studied by Cílek (1971), Kautský in Žbánek (1978), and Hepnar et al. (1987, 1988) based on data from boreholes driven from the surface. In Kladno-Rakovník area, the first CO<sub>2</sub> eruption was registered in Slaný deposit in 1913 when the Zlonice well was being drilled which eventually, attained the depth of 1,340 m from its collar. At the depth of 985 m, an eruption of nearly pure CO<sub>2</sub> with just traces of methane occurred (Cílek, 1971). Exploration by boreholes from surface in the years 1963 – 1965 showed that Slaný deposit represents a unique coal bearing basin which differs from the Kladno-Rakovník area not only by its coal seams, but also by its hydrogeology and incidence of mine gases. The gases mostly dissolved in water but also free, were studied using a methodology common in the research of oil and gas structures. Exploration by boreholes from surface continued in the following years. Exploration from mine workings started in 1979 with the opening of hoisting and skips shafts.

**The following three aquifers (e.g. groundwater permeable bodies) were identified when the area was explored by boreholes from surface:**

- *The first groundwater body is the highest aquifer situated in Cretaceous (Cenomanian–Lower Turonian), with mineralization up to 1 g·dm<sup>-3</sup>, containing calcium hydrocarbonate or sodium bicarbonate water, and with flowrates of the order of n·10<sup>-5</sup> m<sup>2</sup>·s<sup>-1</sup>. This groundwater body did not cause any technical problems when the shaft was being opened.*
- *The second groundwater body is situated in the upper part of Carboniferous with an insulating horizon formed of Malešice shale, with mineralization up to tens of g·dm<sup>-3</sup>, containing sodium bicarbonate or sodium chloride water, with flowrates of the order of n·10<sup>-5</sup> to 10<sup>-6</sup> m<sup>2</sup>·s<sup>-1</sup>.*
- *The third groundwater body is situated in the Lower Carboniferous, constituting the main aquifer of the entire complex of Mirošov horizon on the base of Nýřany*

*Mbr, with conglomerates, sandstones and arkoses of ca. 100 m thickness. Coal seams are situated both above this aquifer (Nýřany seams) and beneath (Lubná and Radnice seams). Water in this groundwater body is highly mineralized (average mineralization 35 g·dm<sup>-3</sup>), sodium chloride water, gas bearing, with the highest CO<sub>2</sub> percentage and a well-developed single-phase water-gas system. The flowrates in all these aquifers are of the order of n·10<sup>-7</sup> to n·10<sup>-5</sup> m<sup>2</sup>·s<sup>-1</sup>; the rate of flow of the main aquifer in Mirošov horizon is n·10<sup>-9</sup> to n·10<sup>-7</sup> m<sup>2</sup>·s<sup>-1</sup>. The main aquifer has a minimum permeability. The piezometric head of the groundwater body of Mirošov horizon ranges from 228 to 270 m above sea level, but most boreholes showed a piezometric head above the level of terrain.*

The Slaný deposit exhibits hydrochemical zonality, which manifests itself mainly in the vertical direction. In the Lower Grey Group in Nýřany and Radnice Mbrs, waters of NaCl type were encountered, with a high mineralization (15-75 g·dm<sup>-3</sup>, average 35 g·dm<sup>-3</sup>) and with dissolved CO<sub>2</sub> and other gases (CH<sub>4</sub>, H<sub>2</sub>, N<sub>2</sub>, H<sub>2</sub>S) (Table 3.3), whereas in the Lower Red Group and Upper Grey Group, mineralization is only ca. 5 g·dm<sup>-3</sup>. The piezometric level is mostly negative, the maximum affluents in the area of the planned shafts (borehole Sa-16) range from 0.1 to 5.2 l·s<sup>-1</sup>, at pressures of 1.0 to 4.3 MPa.

Cuřín and Kautský (1988) called attention to possible risks associated with the shift from a single-phase system (CO<sub>2</sub> dissolved in water) to a two-phase system (CO<sub>2</sub> liberation) which may occur due to a change in any of the state functions (pressure, temperature). Hydrogeological observation boreholes were also drilled in the NW part of the Slaný deposit in connection with opening works there (shaft sinking). Observations from these boreholes were studied by Hepnar, Květoň, and Kautský (1988). Their evaluation of exploratory works brought new information which does not always reconcile with earlier assumptions. It was summarized as follows:

- *“The piezometric head levels of the main aquifer are much more variable than was previously assumed; in many cases, the strata pressure is higher than the hydrostatic pressure.*
- *Vertical development of mineralization is totally irregular; it does not apply that its quantity increases with increasing depth.*

Gas	CO <sub>2</sub>	He	H <sub>2</sub>	N <sub>2</sub>	CH <sub>4</sub>	CO
<b>minimum</b> [%]	85.9	0.001	0.008	0	0.04	0
<b>average</b> [%]	96.5	0.080	0.332	2.03	3.28	0.013
<b>maximum</b> [%]	100.0	0.372	2.000	9.07	11.64	0.033

**Table 3.3** *Minimum, maximum and average contents of CO<sub>2</sub>, He, H<sub>2</sub>, N<sub>2</sub>, CH<sub>4</sub>, and CO in gases from Mirošov horizon (Cuřín and Kautský, 1988).*

- The development of the chemical composition zones of water also is more complicated than previously known. The sodium bicarbonate zone descends, in some places, as far down as to the upper part of Nýřany Mbr (initially, the Malešice Mbr was regarded as constituting the interface).
- Gas was already encountered in the upper part of the second Carboniferous groundwater body, contrary to earlier assumptions.
- For some parts of the aquifers (groundwater bodies), it has been verified that the chemical composition of the gas phase was different in the strata overlying the second Carboniferous groundwater body and in the underlying strata. In the latter case, this is due to the draining function of tectonics, causing the main aquifer to drain continuously.
- The verification of the drainage function of tectonics and of changes in the quantity and quality of the groundwater body arising from this function rank among the most important findings of the study of boreholes in Slaný deposit. With this kind of tectonics, a two-phase system will immediately emerge, causing important changes to the phase impermeability in the surrounding strata. Pulse degassing may occur over a much bigger area of the deposit than would be usual, most probably from a markedly elongated area extending along the tectonic faults and also along the secondary disturbances of the massif. An important aspect is that during this process, the composition of the gas mixture will undergo changes where the percentage of gaseous CO<sub>2</sub> will decrease due to CO<sub>2</sub> dissolution in water while the percentage of the less soluble gases (CH<sub>4</sub>, N<sub>2</sub>) will increase, in spite of their substantially lower quantity.
- Also important has been the verification that even a long-lasting degassing by a borehole does not produce any substantial impact on the surrounding strata, i.e., the resulting radius of pressure depression is negligible, affecting only the immediate vicinity. This is due to the fact that the rocks of the permeable beds have a low permeability for gas (so-called gas colmatage zone). It only remains to verify in the future whether this is a state that will be sustained indefinitely, or a state that is variable in time and in space in the long run, and whether this state can be changed from the outside by available technology. If not, it will be necessary to verify whether safe mine workings can be opened – and under which conditions – in such non-degassed strata.
- The third important piece of information is of significance to petrology rather than hydrogeology. Petrological research confirmed that the main aquifer – the Mirošov horizon had a unique genesis – that of an asynchronous complex of pelitic-psammitic-psephitic sediments mostly of fluviatic origin, from different sections of the flow, from erosive to accumulative sections. Therefore, different sedimentation sites, very limited in size, cannot be interconnected, not even over distance of a few dozen meters, let alone over hundreds or thousands meters. For such

a type of sediments, a large number of modes exists by which the rock matrix may have developed both in quality and in quantity. In addition, the presence of secondary brines with dissolved gas caused important secondary changes to occur both in the rock matrix and in the rock skeleton proper.

- From this point of view, Carboniferous aquifers seem to be completely inhomogeneous bodies of which the low permeable rock body (groundwater body, aquifer) has developed in an entirely irregular fashion. In practice, the hydraulic and other quantities verified at specific, isolated points do not lend themselves to interpolation in space, and even less can they be extrapolated. This cannot be done on the basis of any routine hydrodynamic exploration. Therefore, large-scale petrological exploration has to be relied on, in combination with logging methods and with investigations of the physical and mechanical properties of the sediments. This is how a new synthesis of the hydrogeological and gas conditions in the deposit can be arrived at” – end of quotation (Hepnar, Květoň et Kautský, 1988).

While geological exploration by boreholes from surface was in progress, much attention was also paid to the coal seams from the point of view of their coal bearing capacity, pore volume distribution, and adsorption properties of the coal matter. Based on the results of these explorations, the conclusion was drawn that the threat of coal and gas outbursts cannot be excluded. At the stage of mine prospecting in mine shafts, attention must be paid to a comprehensive prognosis of the propensity of seams to coal and gas outbursts.

### 3.2 LITHOLOGY, MINERALOGY, PHYSICAL PROPERTIES OF SEDIMENTARY ROCKS FROM MIROŠOV HORIZON

Petrography of rocks from Mirošov horizon was studied by Čichovský (1987), Jiráňková (1987, 1989, 1987), Martinec (1987), and Martinec et al. (1989). As mentioned above, the factors exerting the most significant effects upon the properties of more or less permeable rock bodies in the Slaný deposit are secondary porosity and the changes in morphology of the pore spaces which, together with rock microstructure, have the greatest impact on permeability. This applies in particular to the rocks of the Mirošov horizon. From the very outset of the investigations, Mirošov horizon was seen as the source of problems that have to be overcome when sinking the shafts of Slaný Mine. Consequently, the information and opinions of several authors presented below are concerned first of all with the lithology of the said horizon and with the petrological, physical properties of the rocks encountered therein. The character of porosity and the pore spaces is also described in the light of a new analysis of the data obtained by high pressure mercury porosimetry. The structural and textural properties of the Mirošov horizon are summarized in *Table 3.4 and in Fig. 3.2.*

Sedimentary environment	Macrostructure of sedimentary bodyis (bedding)										Lithology	Sorting and grain size distribution	Microtexture Figs. 3.2a,b	Thickness [m]
	Masive, homogenous, graded bedding	Trough cross bedding and nograded sediments	Horizontal bedding	Planar cross bedding	Wavy bedding	Lenticular bedding	Phytogenic sediments	with truns, branches and debries	Coalificate plant remains and coal debries	Micas and plant remains				
Alluvial bench		x	x	x				x			conglomerate, sandy conglomerates	sediment with two fracion of clastic grains	3, 3a, 3b	1-20
River chanel	x	x		x		x		x		x	sandstone with silty laminas	polyfractional sediment	2 + 3	0,1-1
Alluvial plain	x		x	x	x				x	x	medium or fine grained sandstone with micas laminas	mono- and polyfractional sediments	3a, 1 + 2	1-20
Floodplain	x		x		x	x			x		sandstone, siltstone, claystone	polyfractional sediment	1 up to 3	0,1-1
Abandoned meander, oxbow with swamps and peat bog	x		x			x	x	x	x	x	gray fine grained sandstones, claystone and siltstones, lamination with coal matter	monofractional and polyfractional sediment	1	1 up to 10

Table 3.4 Structure and texture of sedimentary rocks from fluviatile facies in Mirošov horizon, in Slaný Mine shafts.

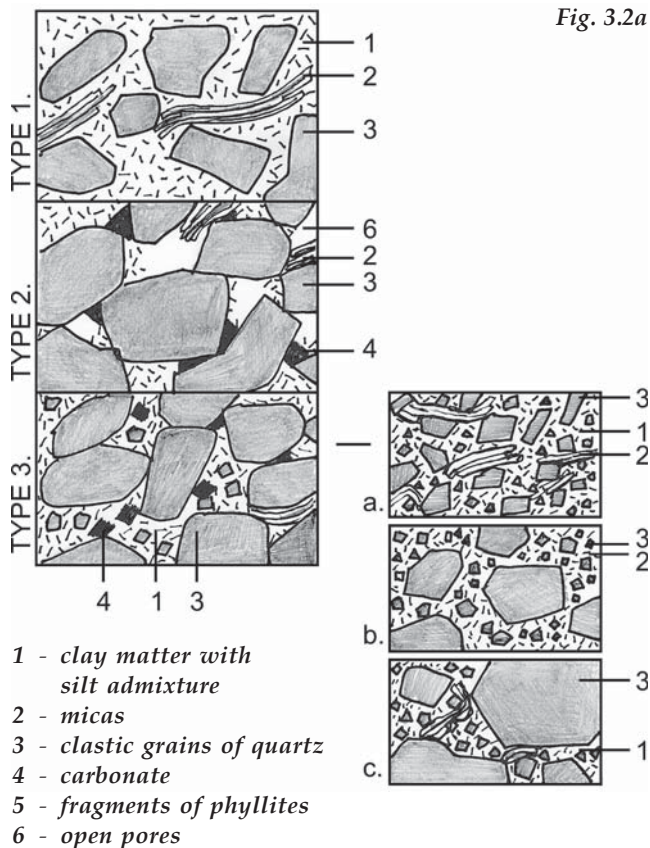


Fig. 3.2a

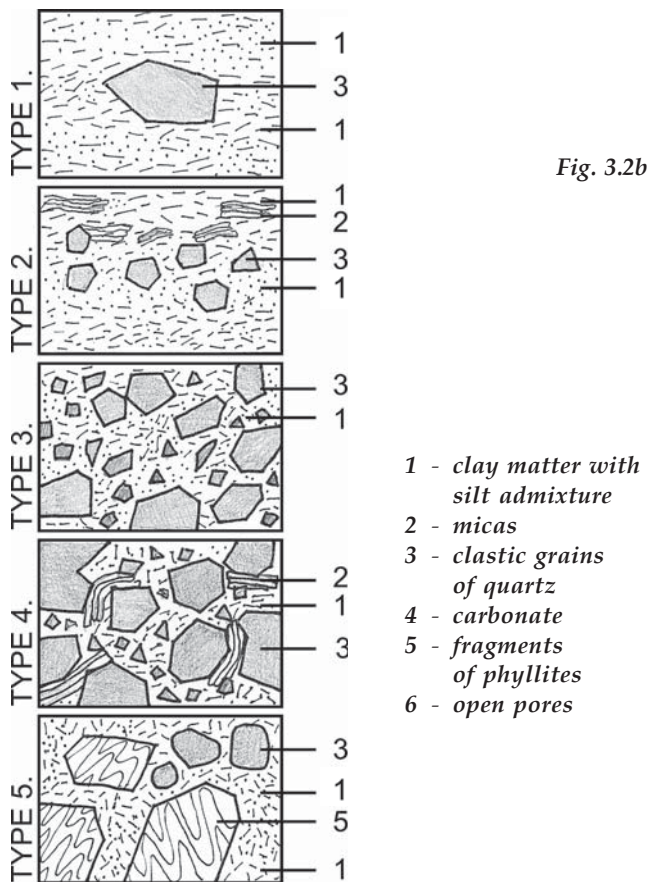


Fig. 3.2b

Fig. 3.2. a, b Major microstructural types of sandy and conglomeration rocks from Mirošov horizon and Nýřany Mbr (Fig. 3.2a) and of rocks from Radnice Mbr (Fig. 3.2b).

For the Mirošov horizon of Slaný deposit, Martinec and Krajíček (1990a) constructed maps showing the percentage contents of the different rocks – claystones, siltstones, fine-grained sandstones, medium-grained to coarse-grained sandstones, and conglomerates, as well as maps illustrating the contents of these rocks according to a classification based on their ratios in a ternary diagram (claystones and siltstones) : (sandstones) : (conglomerates). Similar maps were constructed by the same authors for Lubná and Radnice seams as well as for the characteristics of rocks occurring in the sedimentary environment of Lubná and Radnice seams. Such works find application in geomechanical analysis and in forecasting of outbursts that may occur when coal is extracted from the coal seams. The character of Mirošov horizon rocks is documented by data from the SJ 847m borehole drilled in skip shaft at the depth of 847 m (-530 m according to the altimetric system Baltic sea after leveling, hereafter abbreviated “Bpv”). In the interval from 847.0 m to 952.2 m, this borehole crossed the lower part of Nýřany Mbr in the Mirošov horizon. At the depth of 952.2 to 960.8 m, it crossed the upper part of Radnice Mbr and the Dolín coal seam (at 959.05 to 960.8 m). The borehole (of 114.0 m final length) reached the depth of 960.8 m.

From the petrographic viewpoint, the rocks are formed of the following rock forming mineral associations:

- (a) clastic minerals and rock fragments;
- (b) clay minerals and micas in rock matrix;
- (c) minerals formed by reaction of mineralized pore water solutions with CO<sub>2</sub> with rock forming minerals.

The grain variability of rocks present in the fluvial sedimentation environment was in the center of attention of the works by Martinec (1987) and Martinec and Krajíček (1990a); rather than classifying individual samples from the SJ 847 m borehole, they describe the entire lithological position that consists of types of very similar granularity in spite of a considerable textural and structural variability. The term „sand-conglomerate type“ was coined, describing the type where coarse-grained sandstone changes over to fine-grained conglomerate with a supporting skeleton of arcose-like sandstone; the term „sandstone type“ was used to describe medium-grained arcose-like sandstones with transitions into coarse-grained sandstones; and finally, the term „clayey-silty type“ was used for alternations with transitions of claystone into sandy siltstone with frequent sandy admixtures.

### 3.2.1 SAND-CONGLOMERATE TO SANDSTONE ROCK TYPES

In Mirošov horizon, these types form sequences occurring in a dynamic sedimentary environment of braided river deposits where sand is the dominant component. These types include light-colour, whitish grey to grey coarse-grained sandstones or arcose with graded transitions into coarse-grained sandstones or arcose enclosing isolated quartz pebbles and into sand-conglomerate type to conglomerate type rocks.

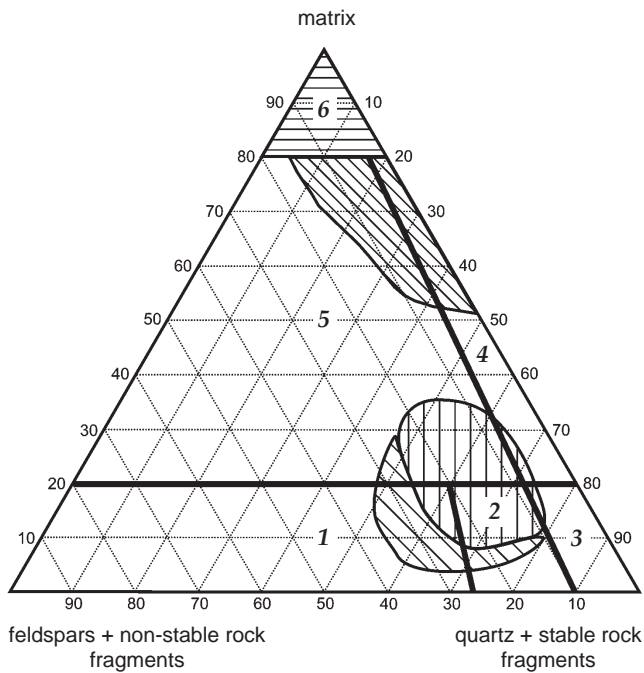


Fig. 3.3 Modal composition of Mirošov horizon rocks in the skip pit and in the hoisting shaft of Slaný Mine.

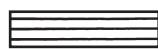
Classification of the rocks by their modal composition is according to Kukul (1985):

1 – arcose; 2 – arcose sandstone; 3 – quartz sandstone; 4 – greywacke sandstone; 5 – greywacke; 6 – claystone.

Classification by granularity:



sandstones



claystones



conglomerates with sandstone matrix



siltstones and silty claystones

The internal structure is rough and massive, crossing over to planar cross-bedded, graded, coarse-grained rock (gravel and sand). The only signs of bedding are the depositions of clastic grains of micas, coal detritus, and graded silt laminae. The textures are psammitic or psammitic-psephitic, with an aleurolithic or aleurolithic-psammitic rock matrix. Sorting is very variable, depending on the dynamics of the sedimentary environment. This sorting corresponds to both single-fraction and poly-fraction sediments. The structural types of sediments can be determined by their relation of the clastic skeleton to the rock matrix (Fig. 3.2). The modal composition of the rocks is shown in Fig. 3.3.

The primary detritic components include quartz, feldspar, muscovite, detritic kaolinite, and illite in the matrix, stable fragments of rocks (quartzite, phyllite), unstable debris (clastic sediments), and detritic coal matter. Unstable contents of variably kaolinized or carbonated feldspars are a typical feature; these being with signs of pre-sedimentary argillitization and end with full pseudomorphosis of the vermicular form of kaolinite after

feldspar. Authigenic minerals are represented, above all, by early diagenetic forms of quartz (see above), by Fe-dolomite or, in fissures, by the youngest calcite, several generations of kaolinite, smectization of muscovite and, rarely, even by zeolite (laumontite).

### QUARTZ GRAINS

Quartz grains are polycrystalline, with a pronounced undulatory extinction, subangular to semi-oval, with sphericity of 0.4 to 0.6. In the case of rocks from the fluvial facies (bed-load channels), sphericity is 0.7 to 0.8. At the base of the Mirošov horizon, there also occur shard-like grains of quartz without undulatory extinction that can be connected to a volcanogenic origin (possibly also to a re-deposition from Radnice Mbr).

### FELDSPARS

Feldspars occur as a regular clastic component that has reached different stages of argillitization. Clear, variably kaolinized or sericitized grains rather reminding of ortho-class occur rather rarely (Plate B, Fig. B8). The pre-sedimentation kaolinization proper of the feldspars involves several stages. The first stage develops alongside cleavage fissures, the form of clastic feldspar is conserved. The middle stage is characterized by a three-dimensional alteration occurring within the grains, which tend to be cloudy. Secondary metasomatic carbonates are frequent, together with fine flakes of phyllosilicates (kaolinite, illite (?)). The primary shape of the clay minerals aggregates is disturbed. The highest, ultimate form is represented by full pseudomorphosis of kaolinite after micas and by authigenic, vermicular forms of kaolinite (Plate B, Figs. B1, B2). The shape of the primary grain may be retained or can be modified, as a pseudomorphous deformed aggregate of vermicular forms of kaolinite, either by transport in an aqueous medium or by post-diagenetic processes. It is evident from the character of the feldspar grains that most of them were subject to some argillitization as early as in the pre-sedimentary stage, or shortly after sedimentation.

### MICAS

Micas are mainly represented by muscovite which is modified, to a greatly variable degree, by different stages of illitization or even smectization on the grain surface (Plate B, Figs. B3, B4, B9a,b).

### CARBONATE

In the group of coarse-grained sediments, carbonate tend to be mostly an integral part of later diagenetic associations. The main carbonate is Fe-dolomite, at contents below 5%. It forms isolated grains in the pore cavities, positioned in such a way as if the given pore mouth were plugged by a dolomite crystal (see note <sup>3)</sup>) (Plate C, Fig. C5, C6). Furthermore, the carbonates cause a metasomatic suppression of both feldspars and altered micas, and corrode the surfaces of the quartz grains. Rarely occurring thin strings of calcite belong to the youngest generation. They fill in the fissures oriented diagonally to the bedding.

## KAOLINITE & ILLITE

Kaolinite, together with illite, is the predominant clay mineral. Kaolinite occurs in a number of generations and takes up various positions in the rock texture (**Plate B, Figs. B1, B2**). By its position, kaolinite influences the communication capacity of the pores, both under the deposition conditions and under conditions where the moisture content of the sediment is changing (e.g., during laboratory testing). These changes bring about a collapse of the kaolinite aggregates or even the transport of loosened flakes of kaolinite via the pores, or they can produce a thixotropic effect (Čichovský et al, 1987). This influences the distribution of pores and the physical properties of the rock.

## DIAGENETIC CHANGES IN SANDSTONES AND CONGLOMERATES

From the point of view of diagenesis, the post-sedimentary mineral associations in the rocks referred to above are multiphase associations depending on recurrent processes tending to establish an equilibrium between the composition of the pore solution, the CO<sub>2</sub> gas concentration, and the mineral phases; these processes occur during the geological development of the sediment. On polished thin sections, small accumulations of clear quartz on clastic quartz grains were observed, or depositions of very fine-grained quartz material in pores (**Plate B, Fig. B7**) or on the edges of clastic quartz grains, wherever the conditions allowed (**Plate B, Figs. B5, B6**). This is the case in such positions where there is evidence of an increased diagenetic argillitization of micas and feldspars accompanied by release of SiO<sub>2</sub> into the pore solution, and also near geochemical barriers, e.g. in the vicinity of relatively poorly permeable, coal-rich sediments classified as belonging to the clayey-silty type. This silicification has affected the various sandy-conglomerate type rocks to an uneven degree. Nevertheless, it has not had any significantly impact on the physical properties of the rocks. This conclusion follows from an analysis of the difference between the total porosity  $p_c$  and the effective porosity  $p_e$ , which depends on the position of sample under the interface with insulators (geochemical barriers) constituted by clayey-silty types of rocks. A more frequent occurrence of lower values of these differences ( $p_c - p_e$ ) is observed in areas located within the distance of up to ca. 3 m away from the interface with the insulating rock.

From a practical point of view, anything that is studied in separated fine fractions represents a mixture of all the various generations of clayey minerals and micas.

### Note 3):

According to the author's experience, sandstones from other outburst-prone localities in the Czech Republic and in other countries which show blocking of the pore mouths by carbonates exhibit one of the typical characteristics of rocks with a texture pre-disposed for gas accumulation and, thus, exhibit the tendency to rock and gas outbursts.

Therefore, when describing the sandy-conglomerate type and clayey-silty type rocks, the following associations can be identified:

- predominance of illite (1.0 nm) over kaolinite and montmorillonite,
- kaolinite with mixed structures of illite-smectite (montmorillonite),
- illite with kaolinite (with either of them predominating).

The youngest association encountered in the Mirošov horizon rocks is the mineral association formed by interaction of mineralized pore solutions containing dissolved CO<sub>2</sub> with the rock forming minerals:

- dissolution of quartz, new crystallization of quartz on surface of detritic grains of quartz (**Plate B, Fig. B6**), and its recrystallization (in the form of fine quartz aggregates) in pores (**Plate B, Fig. B7**),
- formation of dawsonite  $\text{NaAl}[(\text{OH})_2\text{CO}_3]$  (**Plate B, Fig. 10a,b**) in paragenesis with  $\text{Al}(\text{OH})_3$  and  $\text{Al}(\text{SO})_4 \cdot 2\text{H}_2\text{O}$  and kaolinite,
- illitization on the surface of muscovite flakes (**Plate B, Fig. B4**),
- kaolinization of micas and formation of a vermicular form of kaolinite (**Plate B, Figs. B1, B9b**).

The modal composition of sandy-conglomerate type rocks from the Mirošov horizon is shown in **Fig. 3.3** in a triangular classification diagram of psammites (after Kukal, 1985).

## 3.2.2 CLAYED-SILTY ROCKS FREQUENTLY OCCURRING WITH SANDY ADMIXTURES

In Mirošov horizon, such types form sequences produced in a relatively quiet sedimentary environment, in distal brained river deposits with silt and mud deposition in suspended-load channels and oxbow lake sediments. Internal structures are massive and fine laminated by silt, mud, and fine-grained sand. Numerous flakes of mica (with surface illitization / smectitization of muscovite) and fine coal detritus are deposited on the bedding plane. Subhydrous soil with *Stigmara* roots is less frequent. This deposition environment is primarily reductive, which made the conservation of detritic vegetal mass possible. These types consist of dark grey claystones, clay siltstones to sandy siltstones with frequent laminas and with fine detritic coal matter on the top of the laminas. The clastic phase of the sediment is formed of detritic angular quartz grains (sphericity 0.3 to 0.4). A minor share of the grains is poly-aggregate grains with undulatory extinction. Diagenetic corrosion is noticeable on the surface of the quartz grains (**Plate C, Figs. C1, C2**). The modal composition of the silty-clayey rocks of Mirošov horizon was shown in **Fig. 3.3** in the triangular classification diagram (after Kukal, 1985).

Clastic flakes of muscovite are irregularly illitized or smectitized; it cannot be excluded that detritic illite in the rock matrix was also affected by smectitization (**Plate B, Figs. B3, B4**). The matrix of these sediments is fine kao-

linite, generally prevailing over detritic illite. The configuration of flakes of the clay minerals is plane-parallel or grid-like. The over-all reduction environment is also reflected in the presence of an older, micronodular form of siderite and framboidal pyrite. The coal matter is fine detritic, fossilized tissue, probably belonging to the floral root system.

#### DEGREE OF COAL COALIFICATION AND DEGREE OF DIAGENESIS OF THE CLAYEY-SILTY MINERALS

Depending on the degree of coalification of the Nýřany coal seams (in Nýřany Mbr) and of the Dolín coal seams (in Radnice Mbr), the character of the coal found therein ranges from coal metatypes to bituminous coals. The content of volatile matter  $V^{\text{daf}}$  is 40 to 32%. The corresponding degree of diagenesis of clastic sediments corresponds to the stage of early katagenesis (Logviněnko, 1968) with facies of clay mass which persisted unaltered and of hydrated and kaolinized biotite. It is worth pointing out that the process of diagenesis of the Mirošov horizon rocks exhibits certain specific features due to the presence of highly mineralized pore solutions where the water present in the pore interstices of permeable rocks (mainly sandstones or conglomerates) of this horizon belongs to highly mineralized waters of the sodium chloride type (Žbánek et al., 1978); according to Alekin's classification of waters it is classified as Cl-Na IIIa,b. The  $\text{Na}^+$ ,  $\text{Mg}^{2+}$ , and  $\text{Ca}^{2+}$  contents are 21300, 1325, and ca. 690  $\text{mg}\cdot\text{dm}^{-3}$ , respectively. Mineralization has reached a maximum in the eastern section of the deposit. The aquifer incorporates both a single-phase system (water with dissolved  $\text{CO}_2$ ) and a two-phase system of water and  $\text{CO}_2$  with a high pore pressure approaching the geostatic pressure (see Chapter 2). It is highly probable that  $\text{CO}_2$  is generated from the deep mantle sources (juvenile gas) and ascends from greater depths along faults activated in connection with Tertiary volcanism of the Slaný and Vinařice hills situated nearby.

### 3.3 PHYSICAL PROPERTIES OF ROCKS

The physical properties of Mirošov horizon rocks encountered in the Slaný deposit were studied in detail on core drill samples from the boreholes SJ 847m (Martinec, 1987) and Dn-3 (Čichovský, 1987). The original set of testpieces was earmarked for laboratory studies of selected mechanical properties under so-called equilibrium moisture conditions. However, such conditions do not fully correspond with the actual conditions encountered in situ. Therefore, the testing of the strength and deformation properties of rocks was extended so as to also include water-saturated samples, i.e., a state that corresponds to the actual moisture level of a saturated sample ( $w_n$ ). According to Čichovský et al. (1987), other factors affecting mechanical properties include the time elapsed from sample withdrawal from the massif and the actual test as well as changes in moisture of the sample which elude control. Such effects were eliminated in part by conducting the tests of the samples within a short time interval and by the fact that during the test proper, the rock moisture was known.

Therefore, it is recommended that the following measures be adopted when testing samples of a similar composition and rock internal structure in different laboratories:

- ensure that the samples be tested without delay, right after sample withdrawal;
- prevent any changes of moisture level of the rocks from the original moisture level; to carry out the required tests at this moisture level; and re-check the moisture level after each test.

#### 3.3.1 PROPERTIES OF MIROŠOV HORIZON ROCKS IN BOREHOLE SJ 847 M IN THE SLANÝ MINE SKIP SHAFT

Cylindrical samples 48 by 48 mm high were prepared from a drill core. They were tested in laboratory, either at the equilibrium moisture level or fully saturated with water. Data on bulk density, specific weight, total (calculated) porosity, effective porosity, total pore volumes, and the dominant pore size category (pore diameters) for rocks of the Mirošov horizon are given in *Table 3.5*.

#### STRENGTH AND DEFORMATION PROPERTIES

Cylindrical testpieces prepared by slicing a 48 mm diameter drill core were subjected to the following tests:

- uniaxial compressive strength  $\sigma_D$  of a sample having an equilibrium moisture level ( $w_e$ ),
- uniaxial compressive strength  $\sigma_D$  of a water-saturated sample ( $w_n$ ),
- tensile strength  $\sigma_T$  of a sample having an equilibrium moisture level ( $w_e$ ),
- tensile strength  $\sigma_T$  of a water-saturated sample ( $w_n$ ),
- modulus of deformation  $E_p$  of a sample having an equilibrium moisture level ( $w_e$ ),
- modulus of deformation  $E_p$  of a water-saturated sample ( $w_n$ ).

It is evident from the values shown in *Table 3.6* that in rocks of the sandy-conglomerate types (sandstones to conglomerates), both strength and modulus of deformation decrease with increasing moisture level. This is due to changes in the consistency of the clayey matrix in the pores (destruction of primary internal structure of the pore filling; thixotropic effects; transport of clayey particles; etc.). Cracks in the drill core having the form of conchoidal fracture are common in these rocks (*Plates A, Figs. A1, A2, A3, Plates C, Figs. C3, C4*). Thus, suitable testpieces cannot be fabricated.

In clayey-silty rocks, claystones to siltstones, sometimes, with mixed illite-smectite structures and smectite also present, there is observed, during gradual increase of moisture, an over-all solidification is observed as the moisture level increases; this is due to consolidation of the clayey mass in the rock matrix. Then, after attaining

Rocks	Bulk weight $\zeta_0$	Specific gravity $\zeta_s$	Total porosity $P_c$	Effective porosity $P_{ef}$	Total pore volume $V_{COR}$	Distribution of pores after size diameter
	[g·cm <sup>-3</sup> ]	[g·cm <sup>-3</sup> ]	[%]	[%]	[cm <sup>3</sup> ·g <sup>-1</sup> ]	[ $\mu$ m]
Clayes and siltstones	2.45 - 2.6	2.65 - 3.06	2.5 - 14	3 - 4.5	0.014 - 0.029	> 0,5
Sandy conglomerate (arcose)	2.1 - 2.3	2.65 - 3.06	9.3 - 22.3	9 - 17.5	0.04 - 0.066	0,5 - 0,05
Coarse sandstones (incl. arcose)	2.25 - 2.4	2.65 - 3.06	14 - 23	9 - 17.5	0.04 - 0.066	> 0,05

Table 3.5 Review of fundamental properties of sedimentary clastic rocks from Mirošov horizon

Comment: Bulk specific density: only a tight interval of 0.4 g·cm<sup>-3</sup>, e.g. ≈13 % of maximum values was found.

Effective porosity  $p_{ef}$ : High values of  $p_{ef}$  correspond to clastic sediments with better sorting and hard argillitization of feldspars.

Rock	Water content	$\sigma_D$	$\sigma_T$	E*
		[MPa]		
Claystones and siltstones	equilibrium $w_r$	15-35	2.0-3.3	1400-2600
	full saturated $w_{nv}$	40-60	3.3-6.0	3500-5700
Sandstones (arcoses) and conglomerates	equilibrium $w_r$	25-65	3.1-1.0	3600-2000
	full saturated $w_{nv}$	5-32	2.5-0.5	2500-600

Table 3.6 Representative intervals of strength and deformation properties of clastic sedimentary rocks originating from borehole drilled in the shaft of Slaný Mine.

Explanatory note:

$\sigma_D$  – uniaxial compressive strength,  
 $\sigma_T$  – splitting tensile strength,  
E\* – tangent modulus, cylindrical samples (1:2).

Rock	$\sigma_{vit}$	$\sigma_D/\sigma_T$
	[MPa]	[-]
Siltstone	150-800	5-17
Fine-grained sandstone	150-800	6-26
Medium-grained sandstone	250-800	9-25
Coarse-grained sandstones	260-700	10-25

Table 3.7 Indentation strength intervals (point loading test)  $\sigma_{vit}$  and  $\sigma_D/\sigma_T$  ratios for selected sedimentary clastic rocks from Mirošov horizon. Moisture of rocks under laboratory conditions ≈ 1.5-2%.

the peak moisture level (in the tested set, this was ca. 8% moisture), the values decrease again. This phenomenon is generally known from soil processing practice. With siltstones to medium-grained sandstones, the ratio  $\sigma_D/\sigma_T$  (Table 3.7) varies within the interval of 5 to 26. Thus, with some rocks (where the ratios are < 10), even a brittle behavior can be expected when the rock is dry. From the point of view of rock disintegration, the important parameters are the point indentation strength  $\sigma_{vit}$  and the ratio  $\sigma_D/\sigma_T$ . These values are also given in Table 3.7. Detailed results of the study of physical properties of rocks according to their stratigraphy and petrography as well as of the effects of moisture on the properties of rocks of Slaný deposit were presented by Martinec and Krajíček (1990) to whose work the reader is referred.

### 3.3.2 POROSIMETRIC CHARACTERISTICS OF ROCKS DETERMINED BY HIGH-PRESSURE MERCURY POROSIMETRY

Porosimetric tests were performed using a high-pressure mercury porosimeter, under the following conditions: type 2000 Series Macropore 120 Porosimeter, Carlo Erba Instruments; samples cut from core ca. 10 by 5 by 10 to 20 mm, dried at 105°C for 30 minutes and, before measurement, vacuum-treated in a low-pressure unit of the porosimeter; measured pores sizes from 3.6 to 56,000 nm, the pressurization rate to reach 200 MPa in 25 minutes; mercury wetting angle 141.3°; surface tension of mercury 0.480 N·m<sup>-1</sup>. The pore size categories A, B, C and  $\alpha$ ,  $\beta$ ,  $\gamma$  are defined below (Kolář and Martinec, 1991). The Mirošov horizon rocks were analyzed in detail and were compared with analyses performed on Nýřany Mbr rocks originating from outside the Mirošov horizon and on Radnice Mbr rocks. The examples shown hereunder refer to selected rocks from the skip shaft taken at depths of 815 to 824 m (Figs. 3.4 and 3.5) and to rocks from the cage shaft taken from the KJ-3 borehole (Figs. 3.6a,b-3.11a,b).

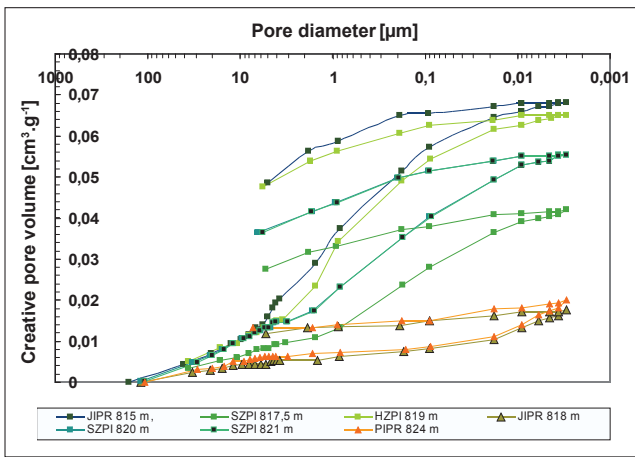


Fig. 3.4 Cumulative pore volume ( $V_{COP}$ ) vs pore diameter ( $\mu\text{m}$ ) and, on the return curve, changes of pore volume as a function of decreasing pressure. Slaný Mine, skip shaft, samples taken at the depths of 815-824 m. High-pressure mercury porosimetry.

Legend: HZPI – coarse-grained sandstone, SZPI – medium-grained sandstone, PRJI-JIPR – sandy claystone to clayey siltstone.

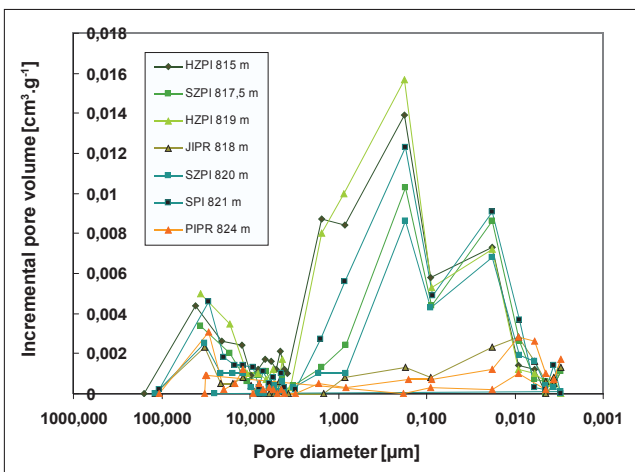


Fig. 3.5 Incremental pore volume ( $\Delta V_{COP}$ ) vs pore diameter ( $\mu\text{m}$ ). Slaný Mine, skip shaft, samples taken at the depths of 815-824 m. High-pressure mercury porosimetry.

Legend: See Fig. 3.4

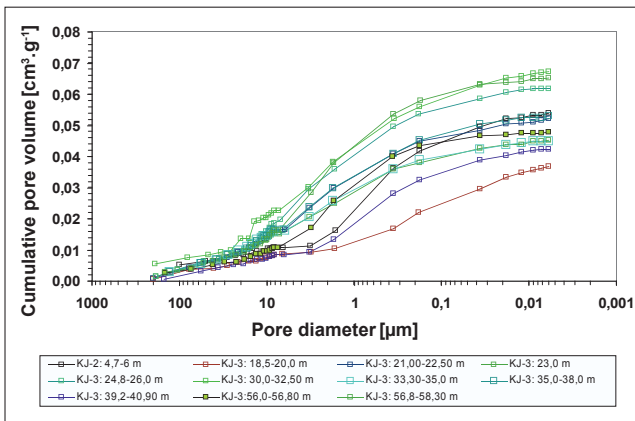


Fig. 3.6a Cumulative pore volume ( $V_{COP}$ ) vs pore diameter ( $\mu\text{m}$ ). Coarse-grained sandstones. Slaný Mine, hoisting shaft. Borehole KJ-3 from the depth of 798.8 m (-408 m according to the Baltic sea altimetric system after levelling) to depth 858 m. Samples were taken at the depths of 803.5-857.6 m within the Nýřany Mbr with Mirošov horizon. High-pressure mercury porosimetry.

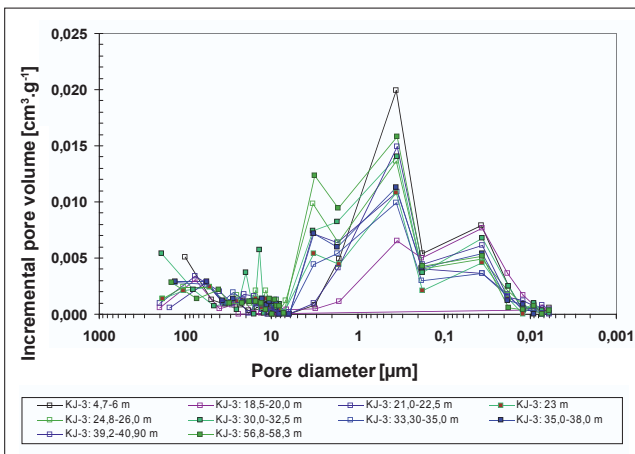


Fig. 3.6b Incremental pore volume ( $\Delta V_{COP}$ ) vs pore diameter ( $\mu\text{m}$ ). Coarse-grained sandstones. Slaný Mine, hoisting shaft. Borehole KJ-3 from the depth of 798.8 m (-408 m according to the Baltic sea altimetric system after levelling) to depth 858 m. Samples were taken at the depths of 803.5-857.6 m within the Nýřany Mbr with Mirošov horizon. High-pressure mercury porosimetry.

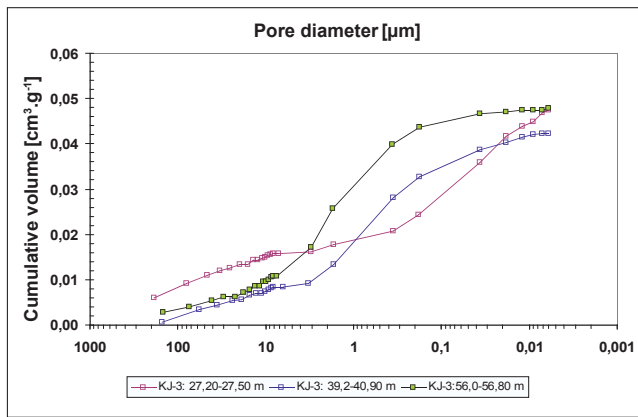


Fig. 3.7a Cumulative pore volume ( $V_{COP}$ ) vs pore diameter ( $\mu\text{m}$ ). Sandy siltstones and fine grained sandstone with silt admixture. Slaný Mine, hoisting shaft. Borehole KJ-3 from the depth of 798.8 m (-408 m according to the Baltic sea altimetric system after levelling) to depth 858 m. Samples were taken at the depths of 803.5-858 m within the Nýřany Mbr with Mirošov horizon. High-pressure mercury porosimetry.

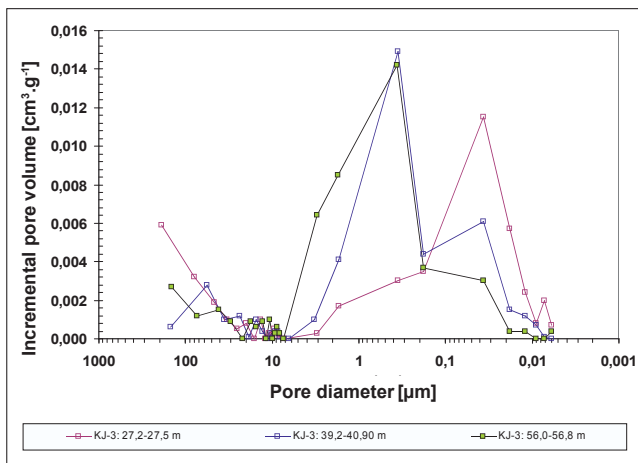


Fig. 3.7b Incremental pore volume ( $\Delta V_{COP}$ ) vs pore diameter ( $\mu\text{m}$ ). Sandy siltstones and fine grained sandstone with silt admixture. Slaný Mine, hoisting shaft. Borehole KJ-3 from the depth of 798.8 m (-408 m according to the Baltic sea altimetric system after levelling) to depth 858 m. Samples were taken at the depths of 803.5-857.8 m within the Nýřany Mbr with Mirošov horizon. High-pressure mercury porosimetry altimetric system after levelling) to depth 858 m. Samples were taken at the depths of 803.5-858 m within the Nýřany Mbr with Mirošov horizon. High-pressure mercury porosimetry.

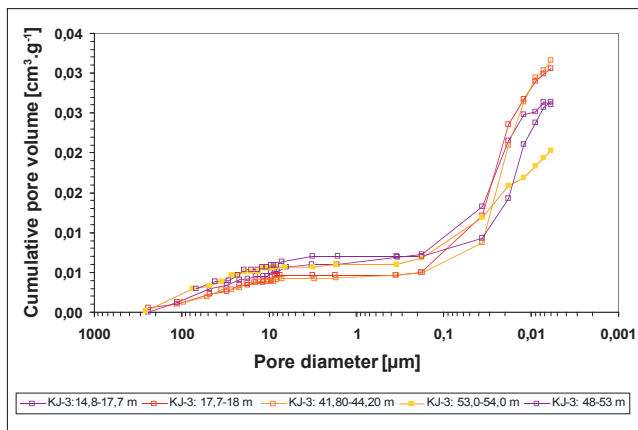


Fig. 3.8a Cumulative pore volume ( $V_{COP}$ ) vs pore diameter ( $\mu\text{m}$ ). Claystones, silty claystones and sandy claystones from Slaný Mine, hoisting shaft. Borehole KJ-3 from the depth of 798.8 m (-408 m according to the Baltic sea altimetric system after levelling) to depth 858 m. Samples were taken at the depths of 803.5-858 m within the Nýřany Mbr with Mirošov horizon. High-pressure mercury porosimetry.

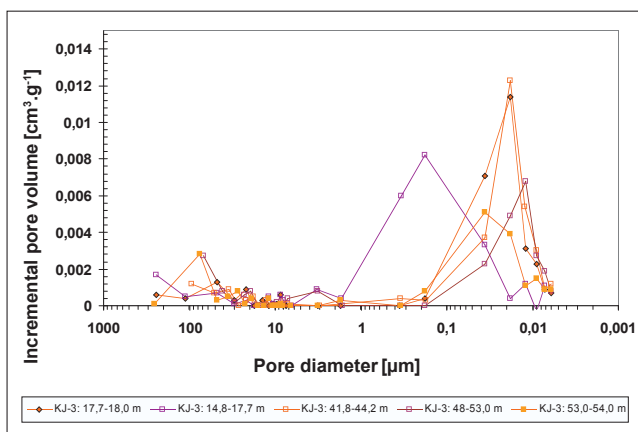


Fig. 3.8b Incremental pore volume ( $\Delta V_{COP}$ ) vs pore diameter ( $\mu\text{m}$ ). Claystones, silty claystones and sandy claystones from Slaný Mine, hoisting shaft. Borehole KJ-3 from the depth of 798.8 m (-408 m according to the Baltic sea altimetric system after levelling) to depth 858 m. Samples were taken at the depths of 803.5-857.8 m within the Nýřany Mbr with Mirošov horizon. High-pressure mercury porosimetry.

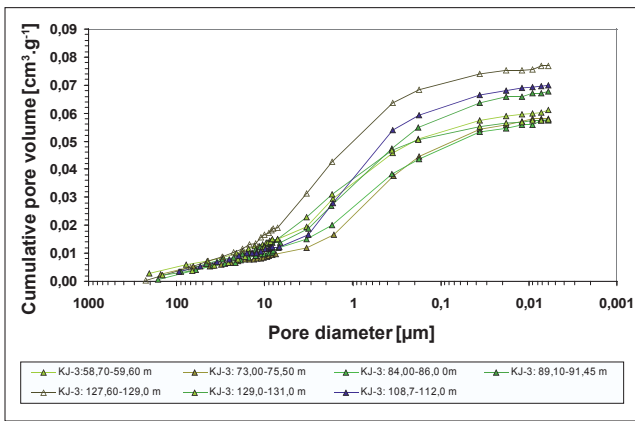


Fig. 3.9a Cumulative pore volume ( $V_{COP}$ ) vs pore diameter ( $\mu\text{m}$ ). Coarse-grained sandstones from Slaný Mine, hoisting shaft. Borehole KJ-3 from the depth of 858 m (-467 m according to the Baltic sea altimetric system after levelling) to depth 933 m. Samples were taken at the depths of 803.5-857.6 m within the Radnice Mbr. High-pressure mercury porosimetry.

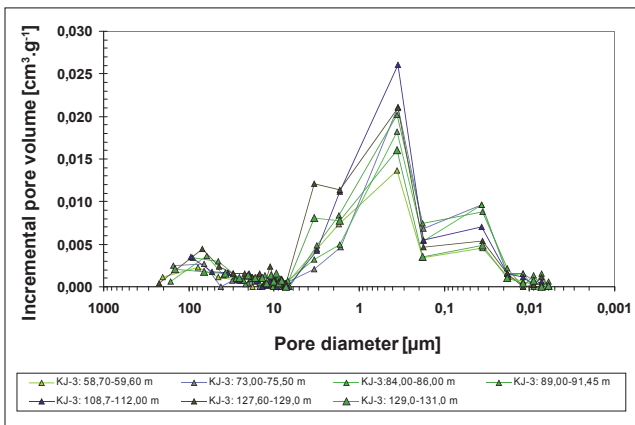


Fig. 3.9b Incremental pore volume ( $\Delta V_{COP}$ ) vs pore diameter ( $\mu\text{m}$ ). Coarse grained sandstone from Slaný Mine, hoisting shaft. Borehole KJ-3 from the depth of 858 m (-467 m according to the Baltic sea altimetric system after levelling) to depth 933 m. Samples were taken at the depths of 857.5-932,8 m m within the Radnice Mbr. High-pressure mercury porosimetry.

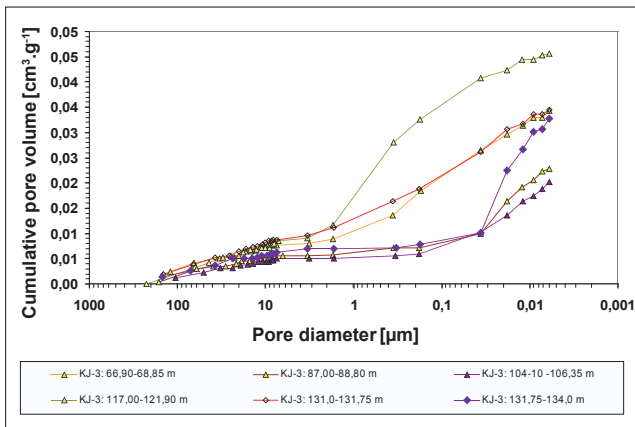


Fig. 3.10a Cumulative pore volume ( $V_{COP}$ ) vs pore diameter ( $\mu\text{m}$ ). Sandy siltstones and fine grained sandstone with silt admixture Slaný Mine, hoisting shaft. Borehole KJ-3 from the depth of 858 m (-467 m according to the Baltic sea altimetric system after levelling) to depth 933 m. Samples were taken at the depths of 803.5-857.6 m within the Radnice Mbr. High-pressure mercury porosimetry.

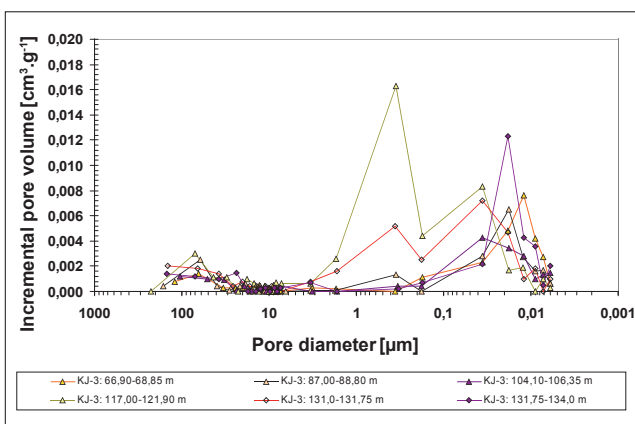


Fig. 3.10b Incremental pore volume ( $\Delta V_{COP}$ ) vs pore diameter ( $\mu\text{m}$ ). Sandy siltstones and fine grained sandstone with silt admixture Slaný Mine, hoisting shaft. Borehole KJ-3 from the depth of 858 m (-467 m according to the Baltic sea altimetric system after levelling) to depth 933 m. Samples were taken at the depths of 857.5-932.8 m within the Radnice Mbr. High-pressure mercury porosimetry.

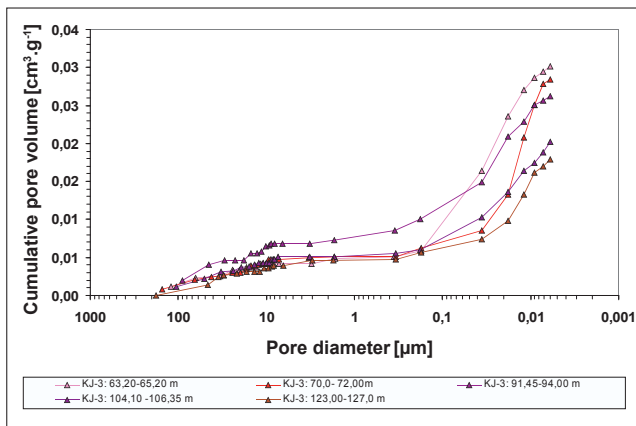


Fig. 3.11a Cumulative pore volume ( $V_{COP}$ ) vs pore diameter ( $\mu\text{m}$ ). Claystones and siltstones, frequently with a sand admixture, from Slaný Mine, hoisting shaft. Borehole KJ-3 from the depth of 858 m (-467 m according to the Baltic sea altimetric system after levelling) to depth 933 m. Samples were taken at the depths of 857.5-932.8 m within the Radnice Mbr. High-pressure mercury porosimetry.

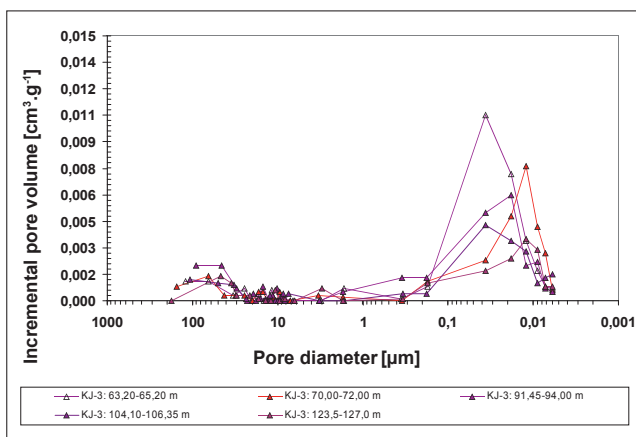


Fig. 3.11b Incremental pore volume ( $\Delta V_{COP}$ ) vs pore diameter ( $\mu\text{m}$ ). Claystones and siltstones, frequently with a sand admixture from Slaný Mine, hoisting shaft. Borehole KJ-3 from the depth of 858 m (-467 m according to the Baltic sea altimetric system after levelling) to depth 933 m. Samples were taken at the depths of 857.5-932.8 m within the Radnice Mbr. High-pressure mercury porosimetry.

### CUMULATIVE PORE VOLUMES $V_{COP}$ AND THE PORE SIZE DISTRIBUTION

Pore size data obtained by high-pressure mercury porosimetry are given here as diameters ( $\mu\text{m}$ ) of pores. Considering that forecasts of the susceptibility of rocks to rock and gas outbursts are based on the classification of pore sizes according to Chobot, the distribution used is the percentages of the cumulative pore volume  $V_{COP}$  that can be allocated to the partial pore volumes  $V_A - V_B - V_C$  for the respective pore size categories A ( $> 0.5 \mu\text{m}$ ), B ( $0.05-0.5 \mu\text{m}$ ), C ( $< 0.05 \mu\text{m}$ ):

$$A = V_A / V_{COP} \cdot 100 [\%]$$

$$B = V_B / V_{COP} \cdot 100 [\%]$$

$$C = V_C / V_{COP} \cdot 100 [\%]$$
(3.1)

$$V_{COP} = V_A + V_B + V_C = 100\%$$
(3.2)

where:

- $V_{COP}$  - cumulative pore volume [ $\text{cm}^3 \cdot \text{g}^{-1}$ ]
- $V_A$  - share of pore volumes belonging to pores having diameters  $> 0.5 \mu\text{m}$  [ $\text{cm}^3 \cdot \text{g}^{-1}$ ]
- $V_B$  - share of pore volumes belonging to pores having diameters of  $0.05$  to  $0.5 \mu\text{m}$  [ $\text{cm}^3 \cdot \text{g}^{-1}$ ]
- $V_C$  - share of pore volumes belonging to pores having diameters  $< 0.05 \mu\text{m}$  [ $\text{cm}^3 \cdot \text{g}^{-1}$ ].

Using the above classification, the field characterizing the allocation shares of pore volumes to the different pore diameter categories existing in the rocks encountered in the Nýřany Mbr (outside the Mirošov horizon) is shown in Fig. 3.12.

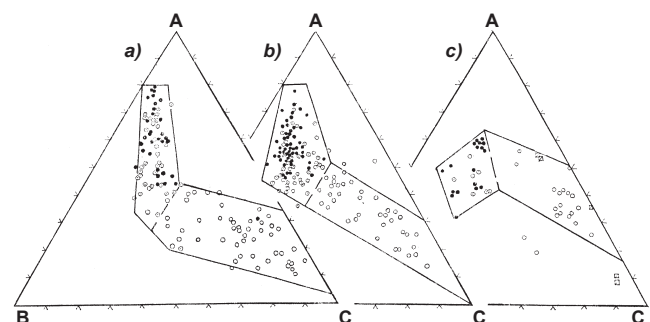


Fig. 3.12 Ratio of partial pore volumes  $V_A + V_B + V_C = V_{COP}$  (100 %) for the following pore diameter categories: A ( $> 0.5 \mu\text{m}$ ), B ( $0.05$  to  $0.5 \mu\text{m}$ ), C ( $< 0.05 \mu\text{m}$ ). Rocks from Nýřany Mbr excl. the Mirošov horizon (a), from the Mirošov horizon (b), and from Radnice Mbr (c).

Legend:

- $o$  -  $V_A$  ( $< 0,045 \text{ cm}^3 \cdot \text{g}^{-1}$ )
- $x$  -  $V_B$  ( $0,045 - 0,550 \text{ cm}^3 \cdot \text{g}^{-1}$ )
- $\bullet$  -  $V_C$  ( $> 0,550 \text{ cm}^3 \cdot \text{g}^{-1}$ )

Taking the pore size distribution and the different morphologic groups of pores specific for different types of rocks into account, the classification used is described below. Detailed analysis of the porosimetric curves) has proved that the following three pore size (diameter) categories are a better approximation of the real pore space found in cement-clastic rocks of the Mirošov horizon:

$\alpha$  ( $> 5 \mu\text{m}$ )  $\beta$  (0.08 up to  $5 \mu\text{m}$ ),  $\gamma$  ( $< 0.08 \mu\text{m}$ ) (see Note 4))

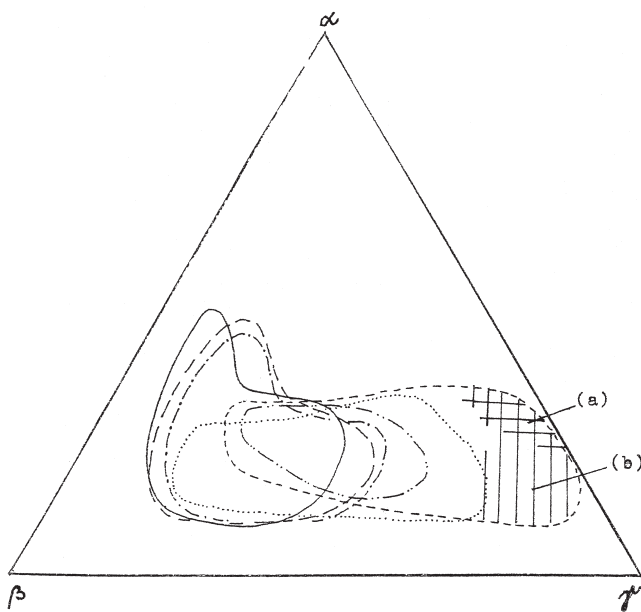
**On the reverse curve, the diameters of open-mouthed pores existing in in the all rocks studied are within the 5 to  $10 \mu\text{m}$  range.**

$$\alpha = V_{\alpha} / V_{\text{COP}} \cdot 100 [\%]$$

$$\beta = V_{\beta} / V_{\text{COP}} \cdot 100 [\%]$$

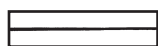
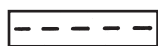
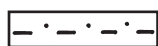
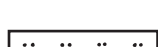
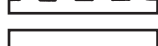
$$\gamma = V_{\gamma} / V_{\text{COP}} \cdot 100 [\%]$$
(3.3)

$$V_{\text{COP}} = V_{\alpha} + V_{\beta} + V_{\gamma} = 100\%$$
(3.4)



**Fig. 3.13 Ratio of partial pore volumes  $V_{\alpha} + V_{\beta} + V_{\gamma} = V_{\text{COP}}$  (100 %) for the following pore diameter categories:  $\alpha$  ( $> 5 \mu\text{m}$ ),  $\beta$  (5 to  $0.08 \mu\text{m}$ ),  $\gamma$  ( $< 0.08 \mu\text{m}$ ), for clastic rocks from Nýřany Mbr incl. the Mirošov horizon and from Radnice Mbr.**

Legend:

-  conglomerate
-  grained sandstone
-  medium grained sandstone
-  fine grained sandstone including silty fine grained sandstone
-  siltstone, sandy siltstone,
-  siltstone, sandy siltstone, claystone

- a) claystone with smectite a mixed structure illitelsmectite;
- b) claystone with domination of kaolinite and illite.

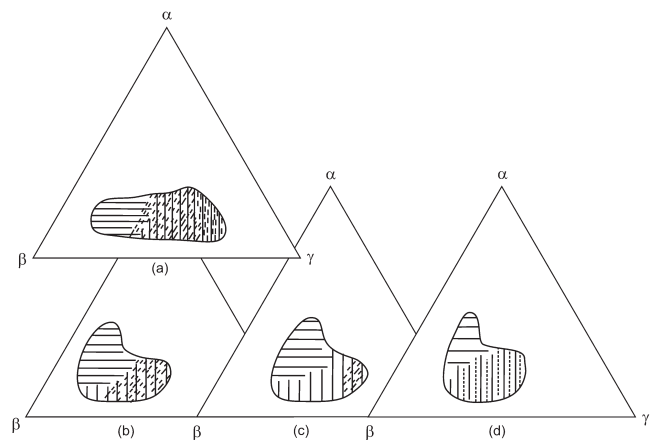
where:

$V_{\alpha}$  - volumetric share of pores having diameters  $> 5 \mu\text{m}$  (out of the cumulative pore volume [ $\text{cm}^3 \cdot \text{g}^{-1}$ ])

$V_{\beta}$  - volumetric share of pores having diameters of 5 to  $0.08 \mu\text{m}$  (out of the cumulative pore volume [ $\text{cm}^3 \cdot \text{g}^{-1}$ ])

$V_{\gamma}$  - volumetric share of pores having diameters  $< 0.08 \mu\text{m}$  (out of the cumulative pore volume [ $\text{cm}^3 \cdot \text{g}^{-1}$ ]).

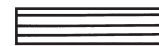
The field characterizing the distribution of pores in different rock types based on the above classification is shown in Fig. 3.13. The position of the point which characterizes the relative share of pore volumes belonging to pores of a given category of pore diameters in the triangular diagram showing the categories  $\alpha$ ,  $\beta$ , and  $\gamma$  is influenced, i.a.,



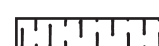
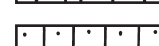
**Fig. 3.14 Ratio of partial pore volumes  $V_{\alpha} + V_{\beta} + V_{\gamma} = V_{\text{COP}}$  (100 %) for the following pore diameter categories:  $\alpha$  ( $> 5 \mu\text{m}$ ),  $\beta$  (5 to  $0.08 \mu\text{m}$ ),  $\gamma$  ( $< 0.08 \mu\text{m}$ ), for clastic rocks from Nýřany Mbr incl. the Mirošov horizon and from Radnice Mbr, also showing the influence of sorting of sediments (sorting coefficient according to Folk) and the influence of an admixture of clastic grains of a different grain size.**

Legend:

Sorting of sediments (Folk):

-  medium to very good sorting
-  medium to very poor sorting

Admixture of grains of a different grain size:

-  silty admixture
-  clayey admixture
-  sandy admixture

Note 4):

A more detailed sub-categorization of the pores by their size is also possible: diameter  $> 5 \mu\text{m}$  – (5 to  $0.8 \mu\text{m}$ ) – ( $0.8$  to  $0.08 \mu\text{m}$ ) – ( $0.08$  to  $0.005 \mu\text{m}$ ) and  $> 0.005 \mu\text{m}$ . This classification is not as robust as the  $\alpha$ - $\beta$ - $\gamma$  classification given above.

by the ratio of clasts to matrix, by grain size, and by sorting. In view of the fact that sandstones and conglomerates of Slaný deposit often tend to be silty or have variable contents of the clayey fraction in the matrix and, conversely, claystones and siltstones often tend to be sandy, the corresponding fields are relatively large. For sandstones and conglomerates of Nýřany and Radnice Mbrs in Slaný deposit, the effects of sorting and of the percentage of silty (clayey) fraction in the sediment are shown in Fig. 3.14.

**In sandstones and conglomerates (where the clayey or silty rock matrix is poorly represented), the pore size categories  $\alpha$ ,  $\beta$ , and  $\gamma$  can be interpreted as follows:**

- The  $\alpha$  category pores correspond primarily to pores formed by a particular configuration of clastic grains and cement and, in the case of sandstones, also to fissures (cracks);
- The  $\beta$  category pores correspond to the internal pore space within clastic grains - the grains are often broken (quartz) or altered (feldspar, mica) - or to pores formed by a particular configuration of clastic grains and the clayey mass;
- The  $\gamma$  category pores correspond to particular configurations of fine particles of clayey minerals, mica, and cement. In this category, the pore volume increases with the amount of clays in the rock matrix.

**In claystones and siltstones, the pore size categories  $\alpha$ ,  $\beta$ , and  $\gamma$  can be interpreted as follows:**

- The  $\alpha$  category pores correspond primarily to microfissures in the rock structures (due e.g., to drying), to pores remaining after the originally present mineral particles or altered coal matter was dissolved;
- The  $\beta$  category pores correspond, most probably, to a particular configuration of larger-sized mica flakes and clayey minerals in the matrix;
- The  $\gamma$  category pores correspond to a particular configuration of fine particles of the clayey mass, often cemented together within the rock matrix.

In the case of sandstones and conglomerates of the Slaný deposit which often are silty-clayey, or in the case of claystones which often are sandy or silty, the final structural pattern of the pores reflects both the basic models mentioned above. For example, siltstones with a sandy admixture, silty claystones etc. belong to the „mixed“ model of pore distribution that combines features of sandy rocks with those of clayey rocks.

The pore space in rocks is the result of all the changes that took place in the sediment during all its geological history. Thus, the information about the character of the pore space should not be generalized only in terms of total pore volume or of calculated total porosity; the distribution of pores in the particular sediment under scrutiny has to be taken into account, too.

The pore distribution and the total pore volume can serve as criteria for forecasting the susceptibility of a given rock structure to rock and gas outbursts (Fig. 3.15). Or, conversely, these parameters can be used to estimate the gas storage capacity represented by the pore space in permeable rocks (at the given temperature and pressure).

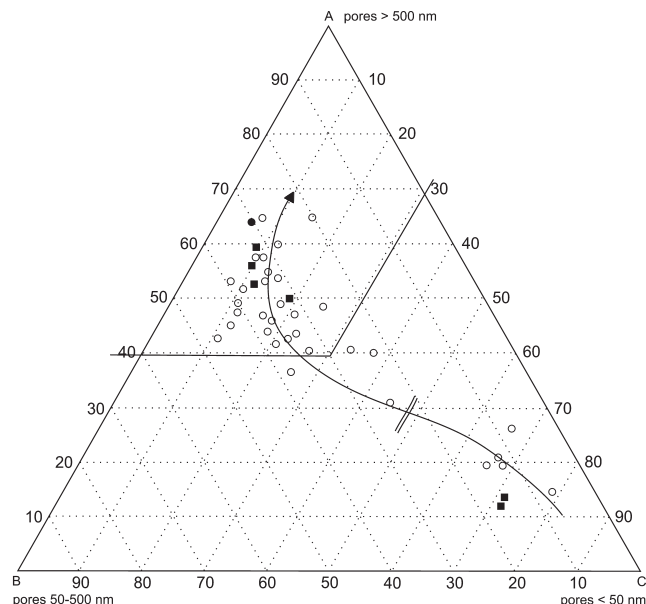


**Fig. 3.15** Relative percentages of category A, B, and C pores in the rocks encountered within the borehole drilled in sandstones and siltstones in the skip shaft, at outburst sites no. 1 (●) and no. 2 (□), and in the rocks encountered in the skip shaft at the depth of 847 m (○), † – showing the borderline between siltstones and sandstones with conglomerates. The trend followed by the relative percentages of these pores in the clastic rocks of Mirošov horizon and Nýřany Mbr is indicated by an arrow.

The cumulative pore volumes ( $V_{COP}$ ) were found to be within the interval from 0.01 to 0.07  $\text{cm}^3 \cdot \text{g}^{-1}$ . For clayey-silty rock types of the Mirošov horizon, the  $V_{COP}$  values ranged from 0.014 to 0.029  $\text{cm}^3 \cdot \text{g}^{-1}$ ; for conglomerate and sandstones they ranged from 0.04 to 0.066  $\text{cm}^3 \cdot \text{g}^{-1}$ , with 70% of the values within the range from 0.047 to 0.065  $\text{cm}^3 \cdot \text{g}^{-1}$ . A good agreement with the pef values was found too (Fig. 3.16).

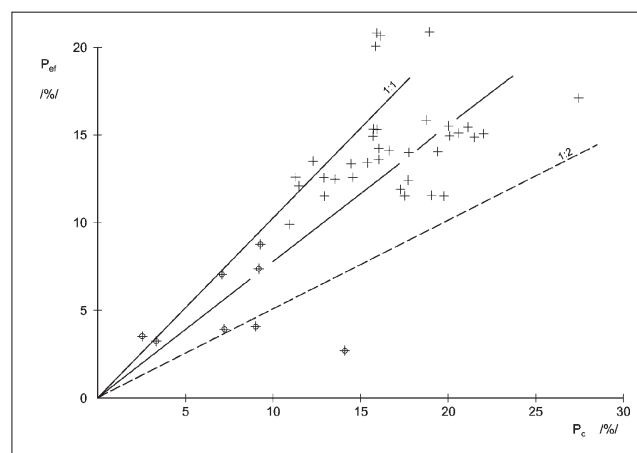


**Fig. 3.16** Total (calculated) porosity of rocks  $p_c$  versus the effective porosity  $p_{ef}$  for clastic rocks of Nýřany and Radnice Mbrs in the Slaný Mine shafts.

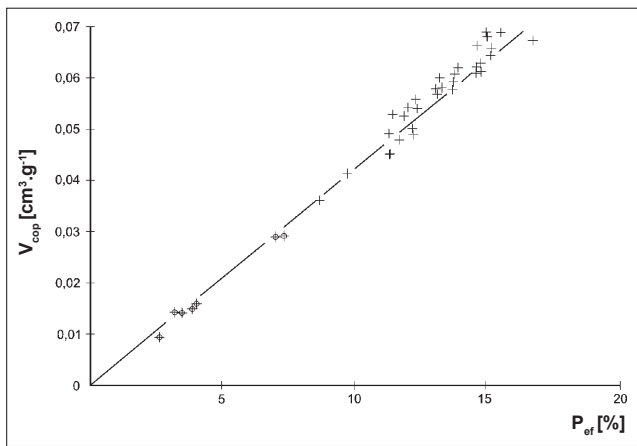


**Fig. 3.17** Cumulative pore volume  $V_{\text{COP}}$  versus effective porosity  $p_{\text{ef}}$  for clastic rocks of Nýřany and Radnice Mbrs in the Slaný Mine shafts.

The relation between the values of total (calculated) porosity  $p_c$  and those of effective porosity  $p_{\text{ef}}$  (Fig. 3.17) makes it evident that there is a difference between the clayey-silty types of rocks and the sandy-conglomerate types with which the sandy types merge. It is also evident that for the granulometric series of claystone – siltstone – sandstone – conglomerate, there exists a continuous succession of  $p_c$  and  $p_{\text{ef}}$  values, corresponding to continuous changes in the rock structure and in the morphology of pore spaces formed by configurations of the detritic grains, the matrix, and diagenetic cement. Also, the relationship between  $p_c$  and  $p_{\text{ef}}$  (Fig. 3.17) shows that with relatively scarce data, it is not possible to reliably decide on the type of this interdependence; however a direct linear dependence is conceivable considering that due to the rock structure the values are greatly scattered. This fact impacts the relationships among all the parameters involved.

An analogous statement would apply to the relationship between  $V_{\text{COP}}$  and  $p_c$  where clayey-silty rock types are distinctly separate from the sandy-conglomerate types (Fig. 3.16). The linear relationship between  $V_{\text{COP}}$  and  $p_{\text{ef}}$  could be used for forecasting.

#### Cumulative pore volume $V_{\text{COP}}$ in rocks with carbonate cement yield the following information:

- The loss due to calcination,  $[(ZZ) - \text{CO}_2^{\text{carbonate}}]$ , is proportional to the percentage of layered silicates (mainly, kaolinite) in the rock and to the value of the difference  $(p_c - p_{\text{ef}})$ .
- At low contents of normative carbonate (computed from chemical analysis), of up to ca. 3% (82% of samples), there is no significant effect on the over-all distribution characteristics of the pores.
- The contents of kaolinite, illite, mixed structures illite/smectite, muscovite, and dispersed coal matter impact the distribution characteristics substantially. The group of clayey-silty rocks is clearly separated from the sandy-conglomerate type rocks. Further, the value  $(ZZ - \text{CO}_2^{\text{carbonate}})$ , which reflects the content of clayey minerals, directly impacts the percentage of category C pores and also, is inversely proportional to the shares of A and B category pores. The type of clayey mineral involved also plays a role (Martinec and Kolář, 1989).

- The total pore volumes  $V_{\text{COP}}$  related to the position of the projection point representing the volumetric shares of A, B, and C category pores, show a growing tendency from the clayey-silty rock samples with values below  $0.0450 \text{ cm}^3 \cdot \text{g}^{-1}$  to the sandstone and sandy-conglomerate type samples with values of  $0.045$  to  $0.055 \text{ cm}^3 \cdot \text{g}^{-1}$  and  $0.055$  to  $0.065 \text{ cm}^3 \cdot \text{g}^{-1}$ , respectively. The higher  $V_{\text{COP}}$  values tend to concentrate along the line corresponding to a 10-20% share of category C pores. It is important to note that the projection points for sandy-conglomerate types from the nos. 1 and 2 outbursts also fall in this area (Fig. 3.15).
- The values of the difference  $(p_c - p_{\text{ef}})$  related to the ratios of category A, B, and C pores merely suggest that values higher than 5% tend to accumulate within the zone delimiting the shares of 5 to 25% of category C pores and above 40% of category A pores. As already mentioned, the effect of a slowly progressing silicification of the basic mass of the sediments adjacent to geochemical barriers will also manifest itself.
- It can be concluded from the above confrontation that the configuration of detritic grains reflecting the sorting, grain size, and content of the clayey-sandy matrix exerts a dominant effect on the size of the pores and on their distribution.

#### The parameters which characterize the properties of the pore space in rocks indicate that, from this aspect, the massif is formed of two groups of rocks:

- Rocks with relatively low values of effective and total porosity and with lower values of total pore volume; which correspond to earlier defined rocks of the distal braided river deposits with silt and mud deposition in suspended-load channels and oxbow lake sediments. The internal structures are massive and finely laminated silt, mud and fine-grained sand acting as hydrogeological isolating barriers.
- Rocks showing a relatively well developed total and effective porosity, with higher values of total pore volume. They correspond to a dynamic sedimentary environment of distal braided river deposits with sand domination, minor lithofacies of the alluvial plain, an active watercourse as well as river bed and river bench sediments, exhibiting the character of hydrogeological reservoir rocks.

The difference between these two types of sediments is also evident from their different relationships between pore volume and pore size (the pressure of mercury injected during the porometric measurement). The character of the curves obtained for aquifer rocks (e.g., of sandy-conglomerate types) can be followed in Figs. 3.4 and 3.5, Figs. 3.6 and 3.7, Figs. 3.8 and 3.9. For isolating rocks (e.g., clayey to silty) the situation is illustrated in Figs. 3.10 to 3.11. In fine-grained, isolating sediments there is a well-developed ultra-fine pore structure, which was formed and modified by the properties of the clay matter (mixed I/S structures, montmorillonite, 1.0 nm micas, kaolinite). However, this pore structure cannot be detected by high pressure mercury porosimetry.

### 3.3.3 RESIDUAL GAS IN ROCKS AND GAS COMPOSITION IN CONTAINER SAMPLES FROM BOREHOLE SJ 847 M

When the borehole SJ 847 m was being drilled, the drill core sections obtained were being transferred into containers as quickly as possible, so as to be able to verify the composition of the released gases (*Plate E, Fig. E12*). The gas volumes were related to the volumes of the samples. It has been found that the dominant component of the pore space was CO<sub>2</sub>, with minimal amounts of CH<sub>4</sub> and N<sub>2</sub>. The gas volumes found were smaller than would correspond to the total pore volume in the rock. This difference may be accounted for by changes in porosity in samples originating from a site where the rock was affected by the no. 2 outburst that occurred in the skip shaft; however the more probable cause was that some of the gas escaped while the samples were being handled prior to being placed in the container. The interesting aspect was is that in a number of samples, the detected volumes of released gas were twice as high as the pore volume of the particular rock.

### 3.4 SINKING OF SLANÝ MINE SHAFTS AND THE ADOPTION AND EFFECTIVENESS OF CERTAIN TECHNICAL MEASURES TAKEN

The progress of the sinking operations, including geological and technical documentation, is described in pertinent reports (Leopold, 1985, 1986, 1987; Živor, 1986, 1988, 1989; Leopold and Živor, 1986; Techn. report by Energie Kladno Co., 2002).

The perimeters of the Slaný deposit exploitation area, of 5,603.83 hectares in size, were approved by the Federal Ministry of Fuels and Energy (ref. no. 31/84Ko/My/80 of 19 February, 1980), on the basis of the results of exploratory works and of calculation of reserves (Order form KKZ ref. no. 277-05/18-79 of 9 April, 1979).

The opening of Slaný Mine was started by a period of detailed mine exploration by means of mine workings. The first stage of this geological exploration by mining included the erection of surface structures and facilities. At the same time, works also progressed underground: at this stage, the skip and cage shafts were sunk and the essential connecting and large-sized workings were mined in the vicinity of the two shafts. The collar of the skip shaft was at an elevation of +317.0 m (Baltic sea after leveling); the planned shaft depth was 1,182 m; the collar of the cage shaft was at an elevation of +318.0 m; and the planned depth thereof was 1,293 m (*Table 3.8*). The planned second stage of geological exploration by mining should have included the driving of level and inclined galleries and the mining of level and inclined workings of investment and exploratory character, to their final cross-sections.

	Hoisting shaft	Skip shaft
X [m]	1 022 650.0	1 022 570.0
Y [m]	764 330.0	764 330.0
Z [m]	318.0	317.0

*Table 3.8 Coordinates of Slaný Mine hoisting and skip shafts.*

#### 3.4.1 PACKING OF THE MASSIF PRIOR TO SINKING THE SLANÝ MINE SHAFTS

Soon after the start of sinking of the skip and hoisting shafts, during the period from 01/1982 till 11/1985, a large-scale packing operation was undertaken to pack the adjoining massif, the USSR method of "Spectampon-azhgeologiya" (Special Packing Geology) in order to prevent any ingress of water into the shafts. A large quantity of packing mass was injected into the massif at a pressure higher than the expected geostatic pressure (10 – 40 MPa). The packing operation was conducted via boreholes from surface (six boreholes symmetrically distributed around each shaft at a distance of 17 to 25 m from the shaft axis). In skip shaft, the packing operation was also led from the shaft bottom. A total of ca. 17,000 m<sup>3</sup> of packing mass was injected within the zone adjoining the hoisting shaft; the amount injected within the zone adjoining the skip shaft was 17,700 m<sup>3</sup> (*Table 3.9*). During the sinking, this packing mass was indeed found in the cracks of the Mirošov horizon rocks encountered (Leopold and Živor, 1985). The greatest amount of packing was found in the skip shaft (at the depth of ca. 600 m). Adoption of this measure has prevented any major water inflows into the shaft. Comprehensive logging and hydrodynamic tests were carried out at each borehole. However, the question remains how the stress and strain fields of the massif have changed in the area surrounding the shafts. In any case, the results of the packing operation have to be regarded as reflecting a specific response of the massif to the injected packing mass, even though the interpretation is neither simple nor unambiguous. In the values of packing pressure, residual pressures, differences between packing pressure and residual pressure in boreholes S1 to S6 for the case of packing the horizon in the vicinity of the Slaný Mine skip shaft at the depth of 717 – 981 m from the shaft collar, and the average values for the packing horizons are given in *Figs. 3.18 and 3.19*.

The distribution of packing pressures, residual pressures, and volumes of injected packing mass is shown in *Fig. 3.20* for the different boreholes and packing depth levels. When the shafts were being sunk in the Mirošov horizon, packing mass was found to have penetrated into fractures, especially in those segments of the shaft where outbursts occurred. Comparison with the orientation of tectonic faults in the Slaný basin (NW-SE) shows that the outbursts tend to be aligned with the direction of the lowest average packing pressures and residual pressures. Similarly, the outbreaks in the skip shaft tended to follow an orientation aligned with the direction of low volumes of injected packing mass.

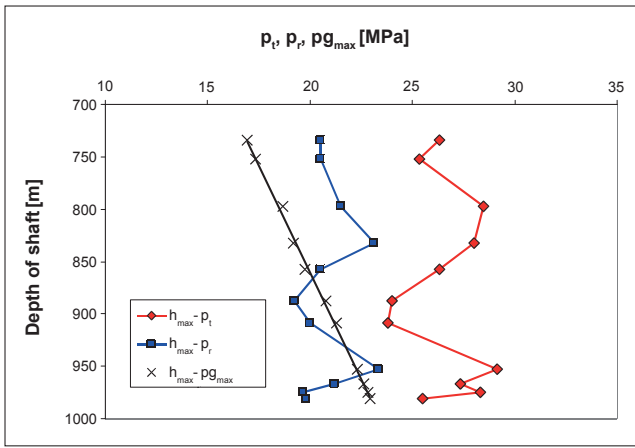


Fig. 3.18 Packing pressures ( $p_t$ ), residual packing pressures ( $p_r$ ), and computed vertical component of the geostatic pressure within the Mirošov horizon of Nýřany Mbr, before and after the packing operations. Skip shaft of Slaný Mine. The distances of the packing boreholes from the central point of the shaft range from 17 to 20 m.

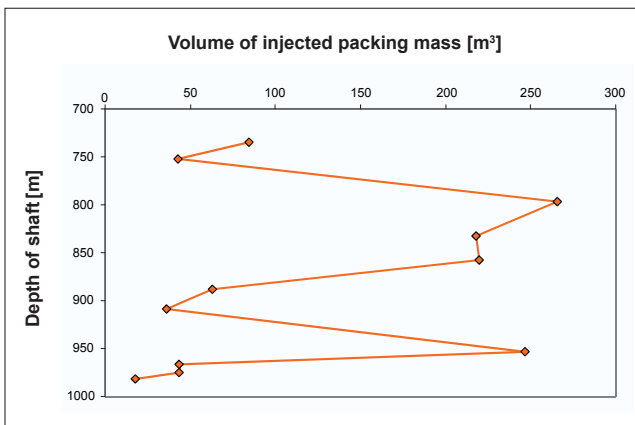


Fig. 3.19 Average volumes of injected packing mass under pressure conditions as rendered in Fig. 3.18 and in Table 3.9. Skip shaft of Slaný Mine. Depth of packing interval: 760-955 m.

Packing horizon	Depth below the shaft mouth		$P_t$	$P_r$	Volume $V_t$	Difference ( $p_t - p_r$ )	$P_t/P_r$	$P_{gmin}$	$P_{gmax}$
	[m]	[m]							
19	717.67	734.50	26.33	20.50	84.67	6.33	1.28	16.54	16.93
19a	745.17	752.33	25.33	20.50	42.77	4.83	1.25	17.18	17.34
20	764.00	797.17	28.50	21.50	265.83	7.00	1.33	17.88	18.66
21	806.00	832.67	28.00	23.17	218.00	4.83	1.21	18.58	19.20
22	834.00	857.83	26.33	20.50	219.50	5.83	1.29	19.23	19.78
23	858.50	887.83	24.00	19.25	62.87	4.75	1.28	20.09	20.78
24	889.67	909.17	23.83	20.00	36.22	3.83	1.19	20.82	21.28
25	913.67	953.17	29.17	23.3	246.75	5.83	1.25	21.38	22.31
26	961.00	966.67	27.33	21.17	43.22	6.17	1.29	22.49	22.63
27	970.33	975.17	28.33	19.67	43.52	8.67	1.53	22.71	22.82
28	977.17	981.00	25.50	19.80	17.72	9.00	1.29	22.87	22.96

Table 3.9 Average values of packing pressures, residual (post-packing) pressures, and volumes of injected packing mass in horizons nos. 19-28 in the boreholes S1-S6, at a distance of 17-20 m from central axis of Slaný Mine shafts. (Lat, 1987, recalculated).

Explanatory note:  $p_t$  – packing pressure,  $p_r$  – residual pressure,  $V_t$  – volume of packing mass injected into horizon,  $p_t/p_r$  – ratio of packing pressure to residual pressure,  $p_{gmin}$ ,  $p_{gmax}$  – geostatic pressure calculated for average bulk weight of  $2350 \text{ kg.m}^{-3}$ .

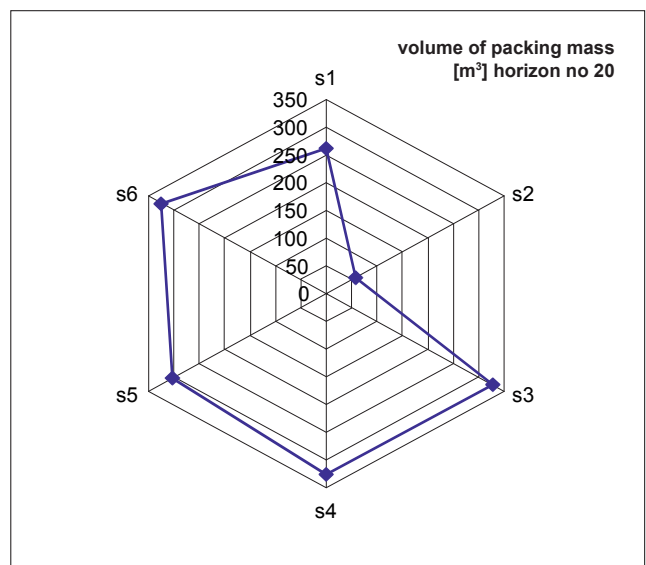
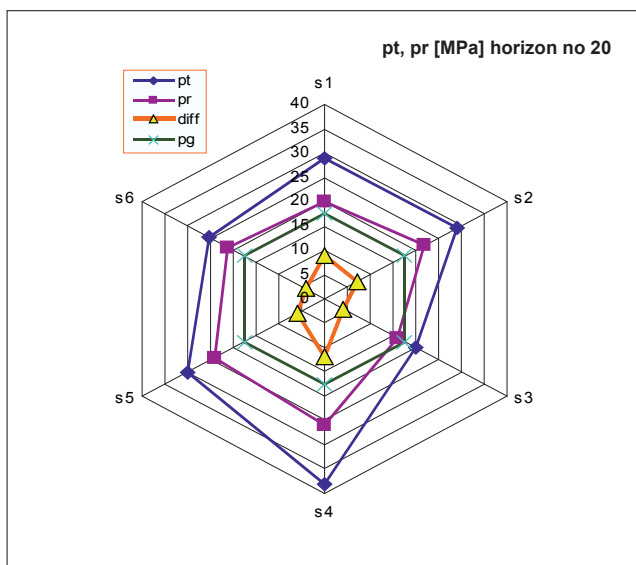
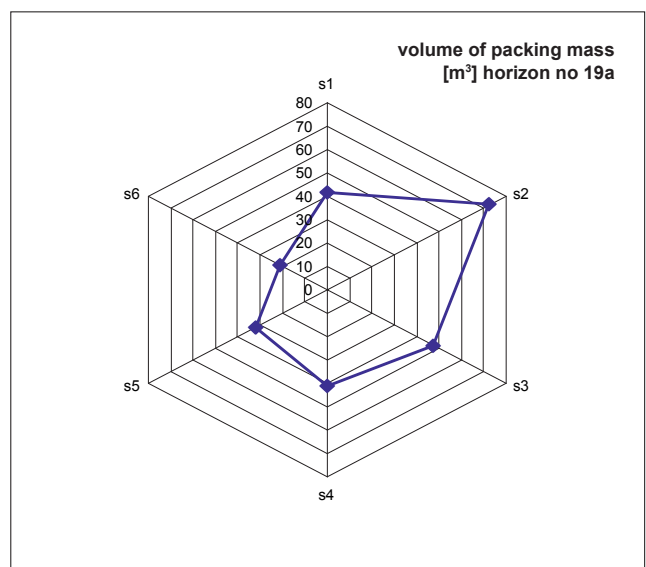
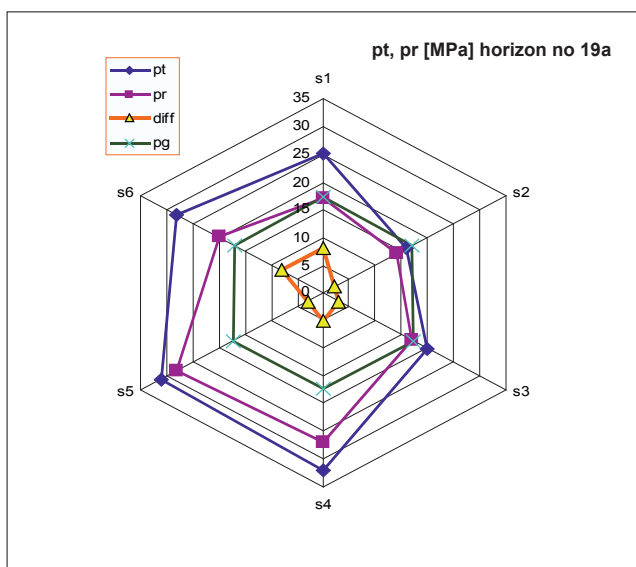
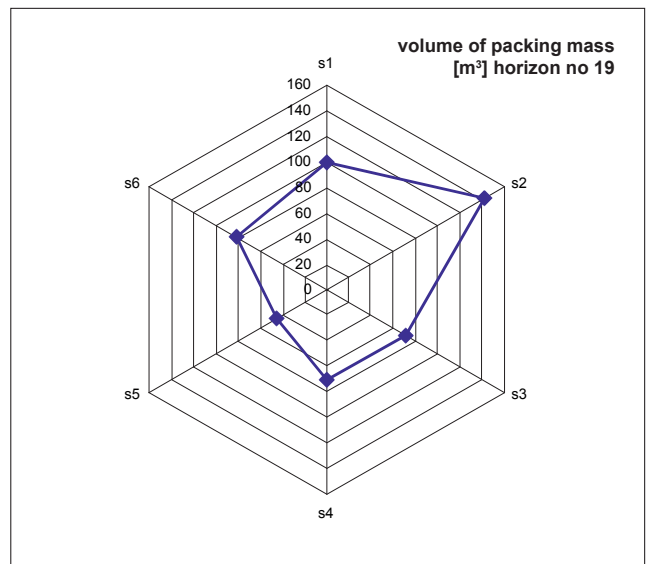
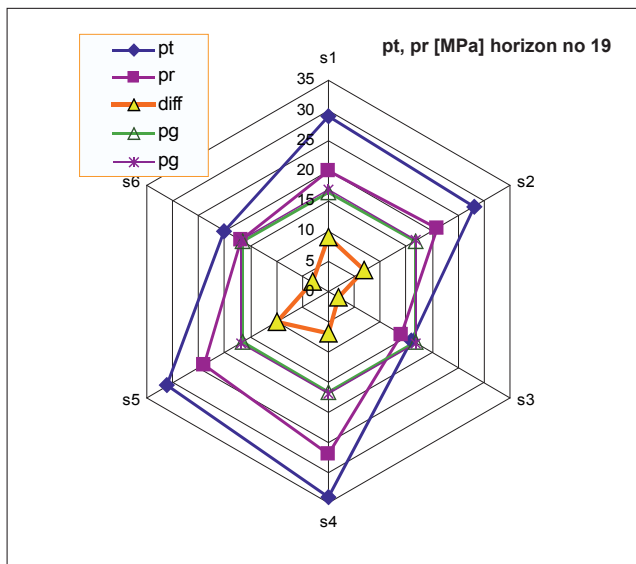


Fig. 3.20a Packing pressures ( $p_t$ ), residual pressures ( $p_r$ ), the differential pressure ( $p_t - p_r$ ), and the vertical component of geostatic pressure ( $p_g$ ) (left-hand column). The volume of packing mass injected into the boreholes (right-hand column). Skip shaft of Slaný Mine, interval of packing depths 760-955 m. The boreholes S1 and S6 are located symmetrically around the shaft center, the borehole S1 is oriented to northwards.

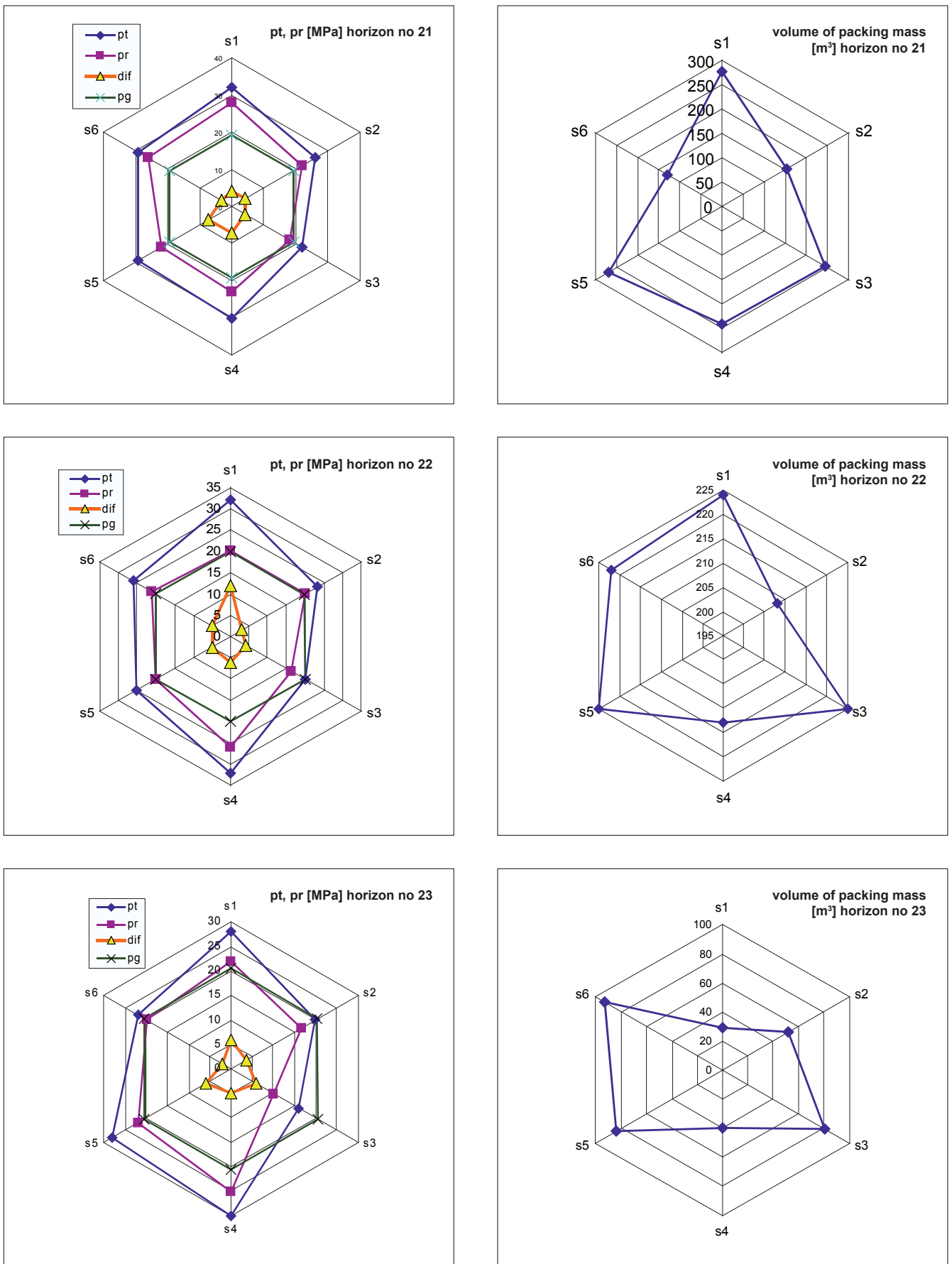


Fig. 3.20b Packing pressures ( $p_t$ ), residual pressures ( $p_r$ ), the differential pressure ( $p_t - p_r$ ), and the vertical component of geostatic pressure ( $p_g$ ) (left-hand column). The volume of packing mass injected into the boreholes (right-hand column). Skip shaft of Slaný Mine, interval of packing depths 760-955 m. The boreholes S1 and S6 are located symmetrically around the shaft center, the borehole S1 is oriented to northwards.

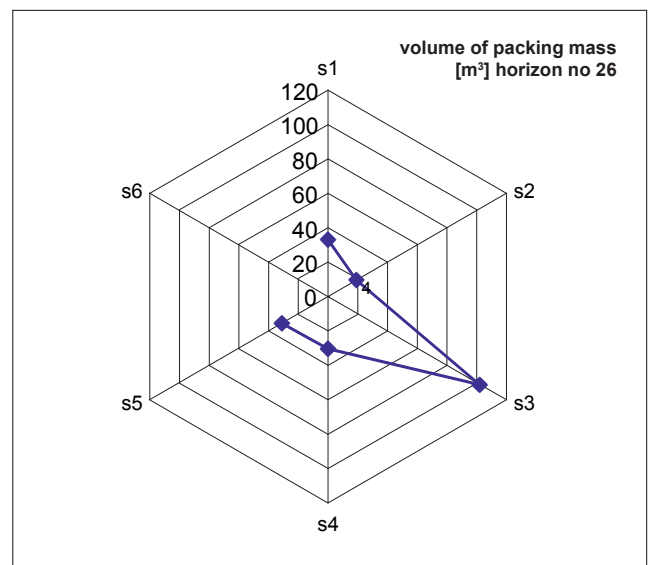
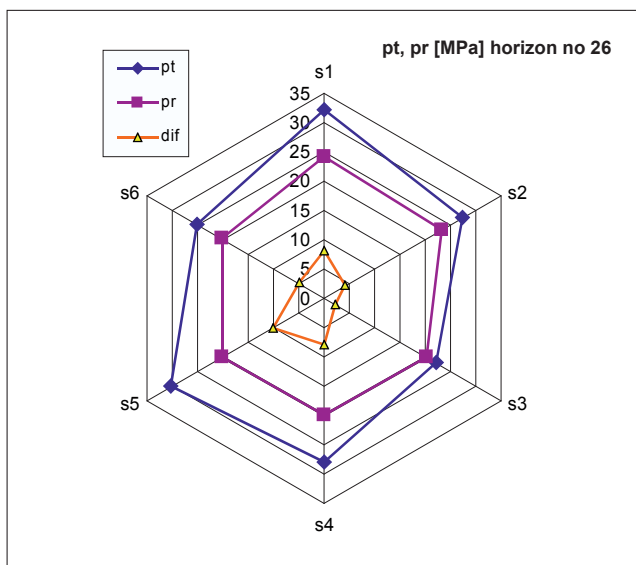
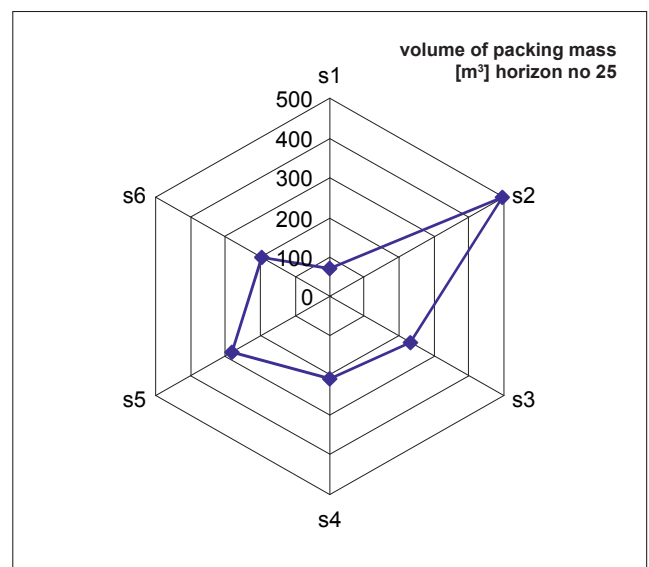
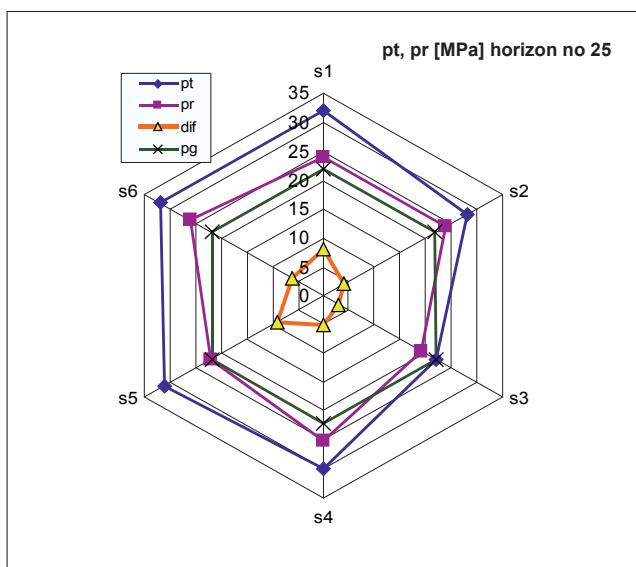
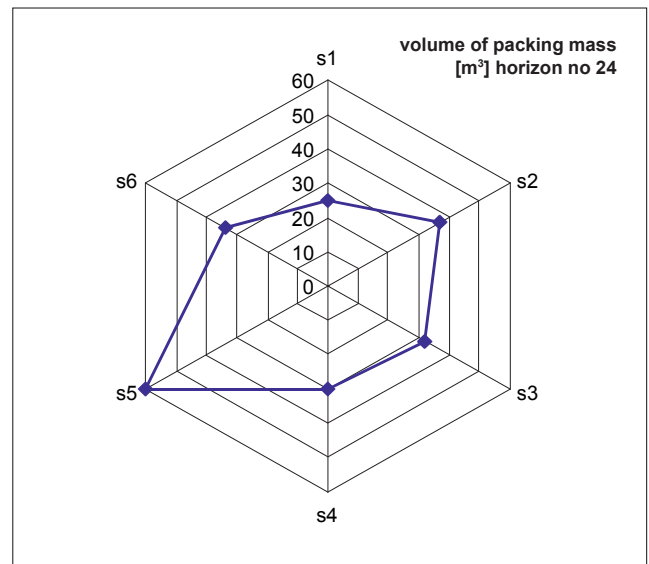
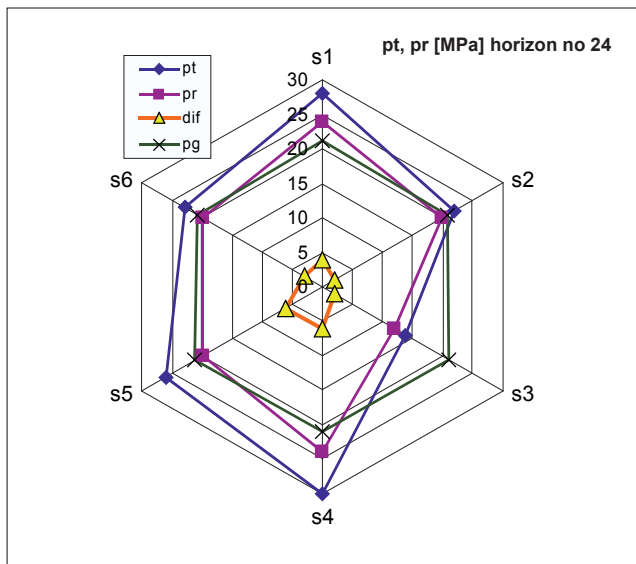


Fig. 3.20c Packing pressures ( $p_t$ ), residual pressures ( $p_r$ ), the differential pressure ( $p_t - p_r$ ), and the vertical component of geostatic pressure ( $p_g$ ) (left-hand column). The volume of packing mass injected into the boreholes (right-hand column). Skip shaft of Slaný Mine, interval of packing depths 760-955 m. The boreholes S1 and S6 are located symmetrically around the shaft center, the borehole S1 is oriented to northwards.

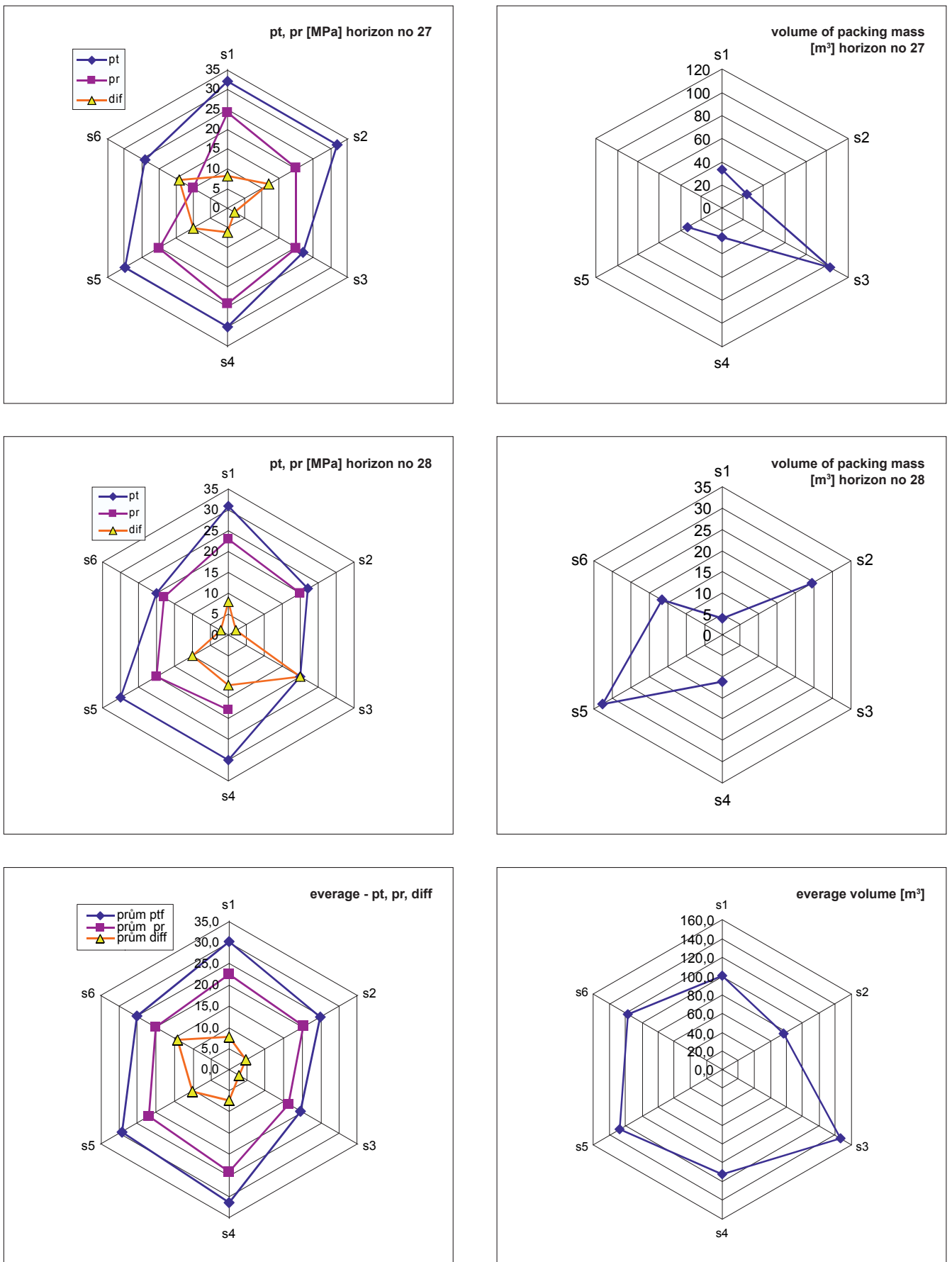
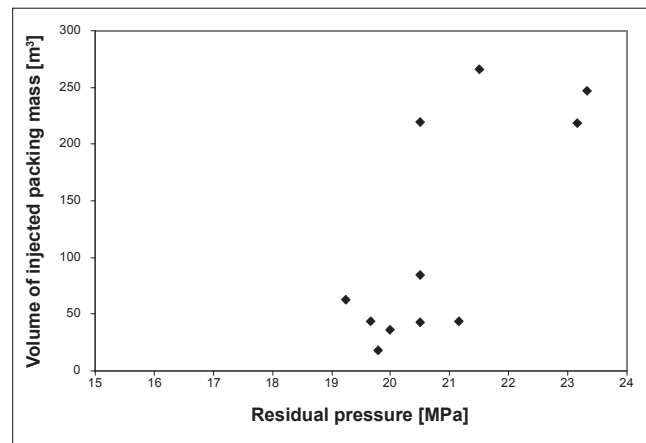
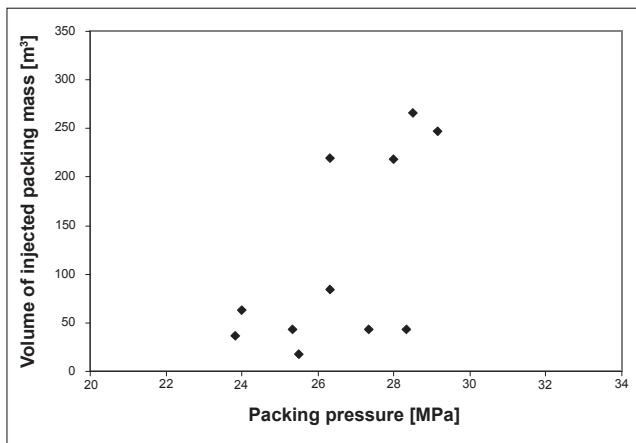


Fig. 3.20d Packing pressures ( $p_t$ ), residual pressures ( $p_r$ ), the differential pressure ( $p_t - p_r$ ), and the vertical component of geostatic pressure ( $p_g$ ) (left-hand column). The volume of packing mass injected into the boreholes ( $V_{sp}$ ) (right-hand column). Skip shaft of Slaný Mine, interval of packing depths 760-955 m. The boreholes S1 and S6 are located symmetrically around the shaft center, the borehole S1 is oriented to northwards.



a)

b)

Fig. 3.21 a,b Volume of injected packing mass versus the packing pressure (a) and the residual pressure (b) on termination of the packing operation. Skip pit of Slaný Mine, interval of packing depths 760-955 m. Boreholes S1 through S6.

The relationships between the amount of packed mass and the packed pressure and between the packing mass volume and the residual pressure are illustrated in Fig. 3.21a and Fig. 3.21b, respectively.

### 3.4.2 SINKING OF THE HOISTING SHAFT

As a preliminary step, the hoisting shaft was sunk to the depth of 62.2 m during the period from 12/1979 to 06/1981. Going down it passed the Quarternary, Turonian, and Cenomanian before reaching the depth of 50.3 m. Carboniferous rocks were encountered further down. Water inflow ranged from 40 to 80 dm<sup>3</sup>·min<sup>-1</sup>, and increased to as much as 225 dm<sup>3</sup>·min<sup>-1</sup> at the interface with the Carboniferous where it was stopped-off completely by adopting appropriate technical measures. The sinking works continued in 1986 down to 372.8 m. Chambers for drilling machine were opened and indication boreholes drilled. Two core drill holes (KJ-1, KJ-2) were drilled in the hoisting shaft at the depth of 686.7 m (from the shaft collar), and a third core drill hole (KJ-3) was drilled at the depth of 798.8 m (-480.8 m below Baltic sea after leveling). The production of water and gas as well as the increase of pressure with time were monitored during these drilling operations. Gas samples were taken and drill cores analyzed. The samples were stored in containers to determine their gas storage capacity. The maximum gas pressure of 3.15 MPa was recorded in the borehole KJ - 3 at the depth of 134.6 m. The maximum gas production of 35.9 dm<sup>3</sup>·min<sup>-1</sup> was recorded in the hole KJ-1 at the depth 39.3 m.

Breakup-free blasting was used as an outburst preventing measure, in line with the recommendation of the Ostrava-Radvanice VVUU Coal Research Institute (L. Štěpán); the blasting works were inspected by a number of horizontal, transversal, and vertical boreholes.

The Mirošov horizon was encountered here at the depth of 815 m (Fig. 3.22); coarse-grained sedimentation began to be the dominant mode starting at the depth of 830 m. A major water and sand outburst occurred when a hole required for the blasting works was being drilled. At the depths

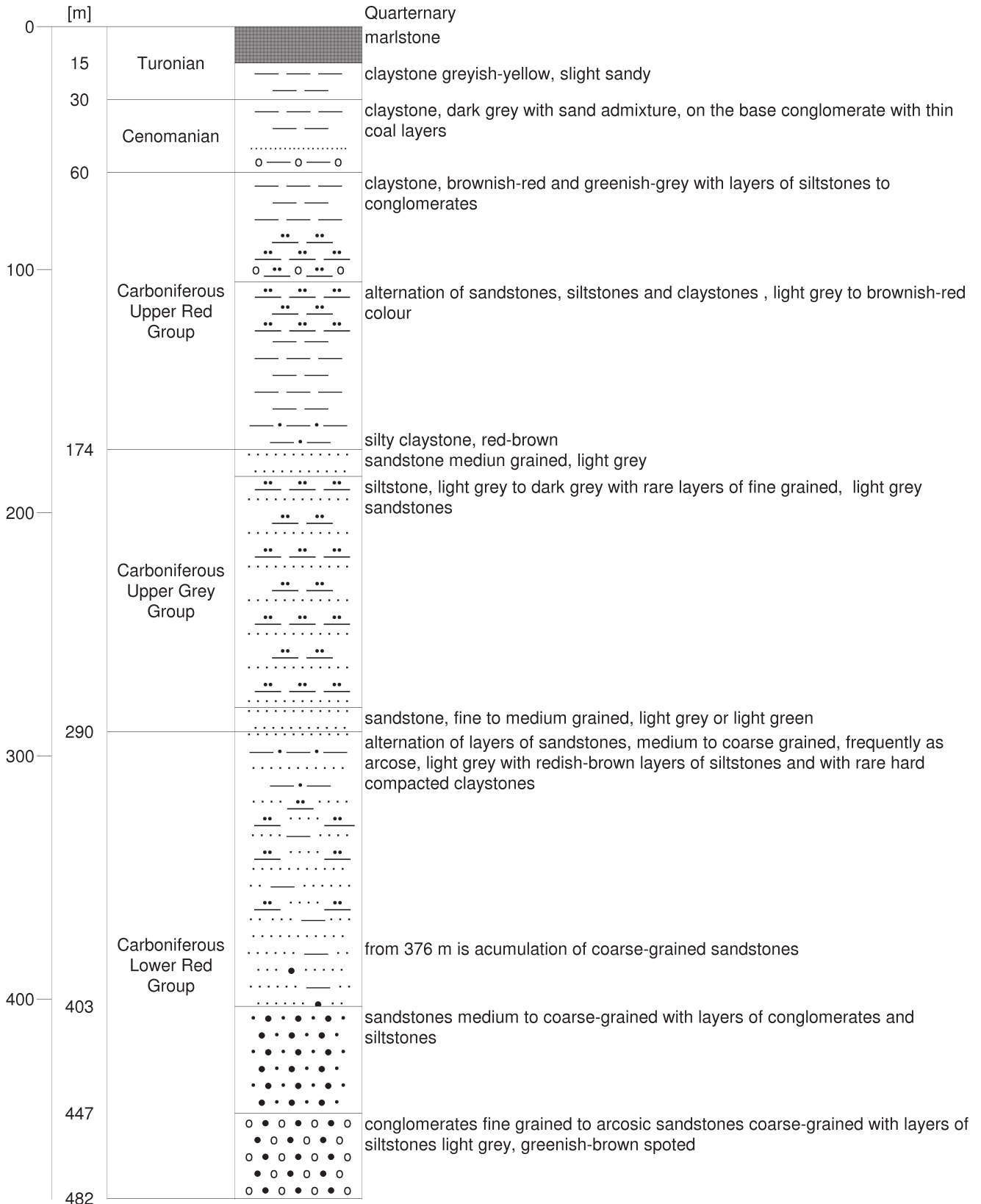
of 775.2 to 777.6 m, 782.8 to 784.7 m, and 804.5 to 806.0 m, an increased CO<sub>2</sub> concentration (4.6%) was observed, together with a number of smaller caverns (after removal of loosened rock) and with rock platelets. In all the boreholes drilled for the purpose of surveying in sandstones and conglomerates, a distinctly coup-shaped or disc-shaped separation was observed on the drill core. According to the so-called Freiburg gas and rock outburst forecasting test, this is considered to be an indicator of the susceptibility to outbursts. In conglomerates, including those with a sandy supporting skeleton, the discs are 10-30 mm thick with a slight vaulting; in coarse-grained sandstones, they are 3-10 mm thick, with a pronounced vaulting (*Plate A, Figs. A1, A2, A3*). As a rule, the discs are concentrated in the central part of sandy-conglomerate parts in drill core. It can be noticed on thin sections that the fracture plane goes across the quartz grains regardless of the grain contours or the sediment structure (*Plate C, Figs. C3, C4, C7*). The first outburst of rocks and gases was registered in the hoisting shaft on 16 February, 1989 at the depth of 855.0 m; the second occurred on 15 March, 1990 at the depth of 901.0 m. These rock and gas outbursts are described further on. The hoisting shaft depth actually attained was 921.2 m (-603, 20 m below the Baltic sea level).

### 3.4.3 SINKING OF THE SKIP SHAFT

As a preliminary step, the skip shaft was sunk to the depth of 58.6 m during the period from November, 1979 until January, 1981. The sinking operation proper was launched in January, 1983. As the works progressed, the formations penetrated by the shaft included the Quarternary (0 - 1.0 m), Cretaceous (1.0 - 55.8 m), Upper Grey Group (55.8 - 130.5 m), Ledec Mbr (130.5 - 198.0 m), Malešice Mbr (198.0 - 279.8 m), Jelenice Mbr (279.8 - 295.3 m), Lower Red Group (295.3 - 456.8 m), and Nýřany Fm down to 856.0 m, a which depth the third rock and gas outburst was registered on 21 October, 1986. **The Mirošov conglomerate horizon was passed at the depth of 813.3 - 856.0 m (Fig. 3.23)** (Leopold and Živor, 1986).

# Hoisting Shaft

x - 1 022 650,00 m  
 y - 764 330,00 m  
 z - 318,00 m Bpv.



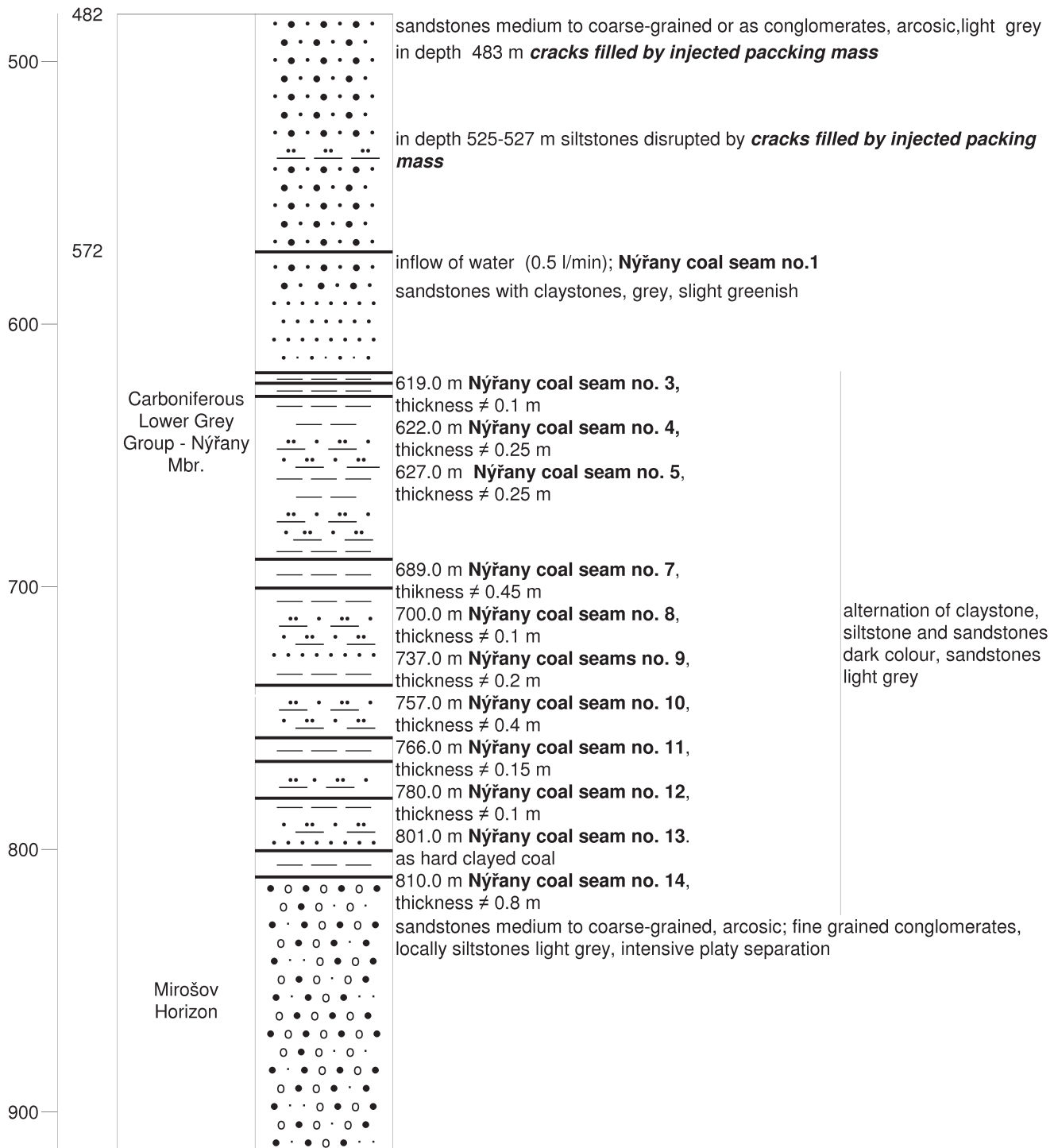
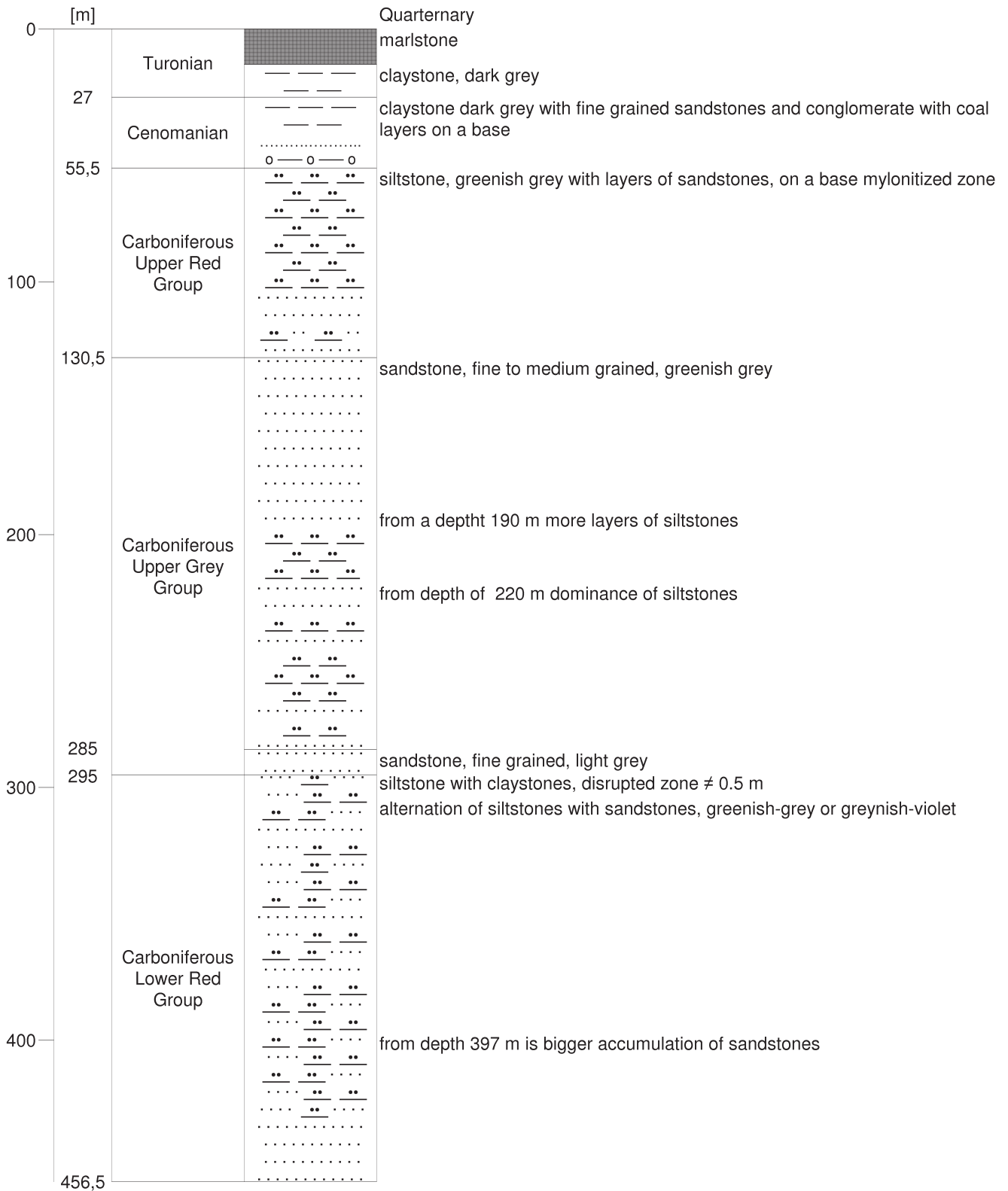


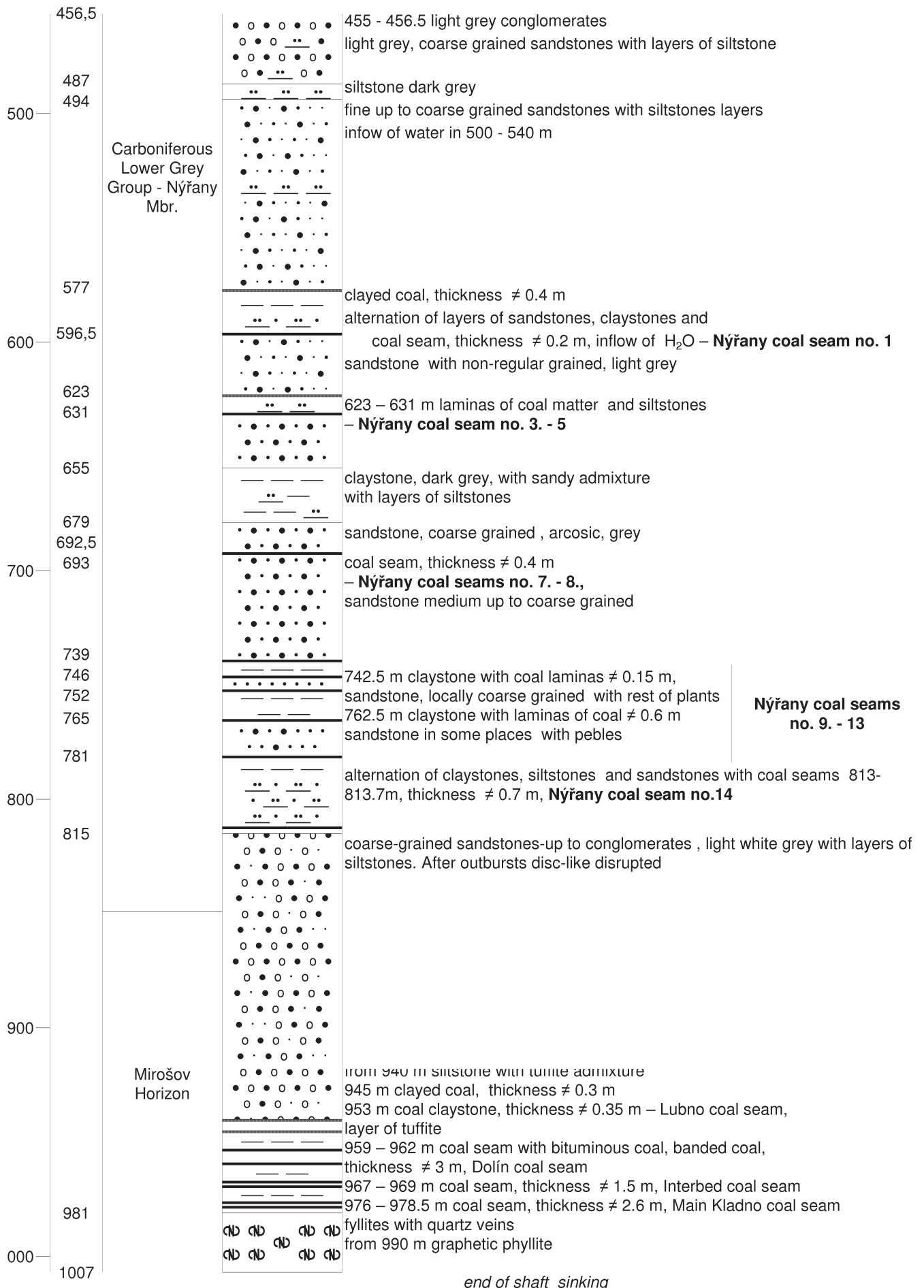
Fig. 3.22 Geological section of the hoisting shaft of Slaný Mine in depth from 0 to 900 m from (simplified, based on documentation from VUD, Kladno). See pages 58 - 59.

Fig. 3.23 Geological section of the skip shaft of Slaný Mine in depth from 0 to 1007 m (simplified, based on documentation from VUD, Kladno). See pages 60 - 61.

# Skip Shaft

x - 1 022 570,00 m  
y - 764 330,00 m  
z - 317,00 m Bpv.





A tectonic discontinuity was encountered at 905 to 940 m; in some parts it exhibited fissures running in the Sudeten NW-SE direction of ca. 76°, with dips of 85-90°. They were at least partly filled with packing mass and were partly open. The discontinuity came to an end on a thick bed of siltstone, at the depth of 940 m from the shaft collar. At the depth of 944.5 m, the Lubno coal seams 30 cm thick were encountered, and at the depth of 952.4 m another Lubno coal seam of 55 cm thickness. At the depth of 961 m it was the Dolín coal seam, 305 cm thick. The interjacent Kladno coal seam, 180 cm thick, was found at the depth of 968 m and the Main Kladno coal seam 225 cm thick at the depth of 977.3 m. A total of eight rock and gas outbursts were registered in this shaft at depths of 814.5 m to 946.0 m from the shaft collar. Their detailed description is given further on. The skip shaft depth actually attained was 1007 m (-690.00 m below the Baltic sea level).

#### 3.4.4 LIQUIDATION OF THE TWO SHAFTS BY BACKFILLING

Czech Republic Government resolution no. 691 of 9 December, 1992 ordered the Slaný Mine to be liquidated. Backfilling and final closure of the two shafts started in March, 1993 (Kurial et al., 2006). The mine liquidation ruling was issued by the Kladno District Mining Office on 29 March, 1993 under the ref. no. 5515/94/469/Le/Vch, with a supplement of 16 May, 1995 of the same reference number (Energie Kladno Corp., 2002).

Both shafts were liquidated by backfilling from surface, using spoil from the Slaný Mine dumpsite as backfilling material. The pertinent mine surveying and geological documentation is kept with Energie Kladno Corp.'s Geotectic services department.

### 3.5. CARBON DIOXIDE OUTBURSTS EXPERIENCED DURING THE SINKING OF SLANÝ MINE SHAFTS, AND THE MANIFESTATIONS THEREOF

Outbursts of rocks and gaseous carbon dioxide were registered in both shafts of Slaný Mine. Even though they share the same features and geological position, their volumes and depths were different in each shaft.

#### 3.5.1 OUTBURSTS IN THE SKIP SHAFT

The *first outburst* of rocks and carbon dioxide occurred on 9 April, 1986 at the depth of 814.5 m (measured from the shaft collar). A total of ca. 160 m<sup>3</sup> of rock and 4,000 m<sup>3</sup> of gas were ejected. The loosened rock filled the shaft up to the level of 811 m under the shaft collar. After removal of loosened rock, an overbreak cavern was found on the western side, under the last concrete ring. The rock which

broke loose consisted of medium-grained to coarse-grained, white-grey sandstone showing a characteristic plate-like disintegration (*Plate D, Figs. D1-D9, Fig. 3.24*). The *second outburst* of rock and carbon dioxide occurred on 24 June, 1986 after a blasting performed at the depth of 831.5 m from collar. A total of 1,000 m<sup>3</sup> of rock and 62,000 m<sup>3</sup> of CO<sub>2</sub> broke loose. Loosened rock filled the shaft to a depth of 809 m under the collar. After removal of loosened rock, only local overbreak caverns were found under the last concrete ring on the western side of the shaft, with loose rock on the shaft sides; these were filled in by injection later (*Plate D, Fig. D10*). In terms of petrography the rock corresponded to the type described above. Pursuant to an order issued by the Kladno District Mining Authority, a core borehole of 76 mm in diameter and 114 m in length was drilled for the purpose of securing the working, from the depth of 847 m under collar. The drill core was analyzed independently by Kladno Mine Development and the Ostrava-Radvanice Coal Research Institute (VVUÚ). No phenomena which could be classified according to the existing Instructions for the prevention of outbursts or which would indicate any danger of a rock or gas outburst were observed while this securing borehole was being drilled. On completion of the drilling operation, the production of water and gas as well as the gas pressure trend in the borehole were monitored. The maximum gas pressure in the borehole was 0.92 MPa. According to estimates, ca. 60 to 85 dm<sup>3</sup>·min<sup>-1</sup> of gas escaped from the borehole during the monitoring period.

The *third outburst* of rock and carbon dioxide occurred at the depth of 856 m on 21<sup>st</sup> October, 1986, immediately after blasting works. The volume of CO<sub>2</sub> released was 105,000 m<sup>3</sup> and the shaft technology and accessories were demolished to a depth of 759 m from the collar. Loosened rock filled the shaft to a depth of 797 m under the collar. The destruction caused by this rock and gas outburst was put to rights in 1987. Photographic documentation from the refurbishment works was produced by Kladno Main Rescue Service Station (*Plate D, Figs. D11 – D18, Fig. 3.25*).

On attaining the depth of 882 m, testing boreholes SJ 847 and SJ 882, of 113.8 and 134.0 m in length, respectively, were drilled from the bottom of the shaft up to the metamorphic complex of the Proterozoic. The maximum gas pressure of 0.80 MPa was recorded at the depth of 9.0 m, whereas the highest gas production, 25.0 dm<sup>3</sup>·min<sup>-1</sup>, was found at the depth of 36.0 m. The drill core was sampled into containers, for evaluation of its gas bearing capacity. Three more rock and gas outbursts occurred in 1988 during further sinking of the shaft, at the depths of 886.2 m, 897.2 m, and 908.7 m; these were followed by two more outbursts in 1989.

The *fourth outburst* of rock and CO<sub>2</sub>, which occurred at the depth of 886.2 to 890.7 m under the collar level, released 49,190 m<sup>3</sup> of gas containing 92 % carbon dioxide.

The *fifth outburst* of rock and carbon dioxide occurred after distress blasting works at the depth of 897.2 to 899.0 m, releasing 10,020 m<sup>3</sup> of gas containing 41.9 % CO<sub>2</sub>. The distress blasting was preceded, in the section of 895.7 to 900.2 m, by rupturing blasting works. After removal of loosened rock, a cavern 12 m wide and 8 m deep was found in the NW to NE section of the shaft.

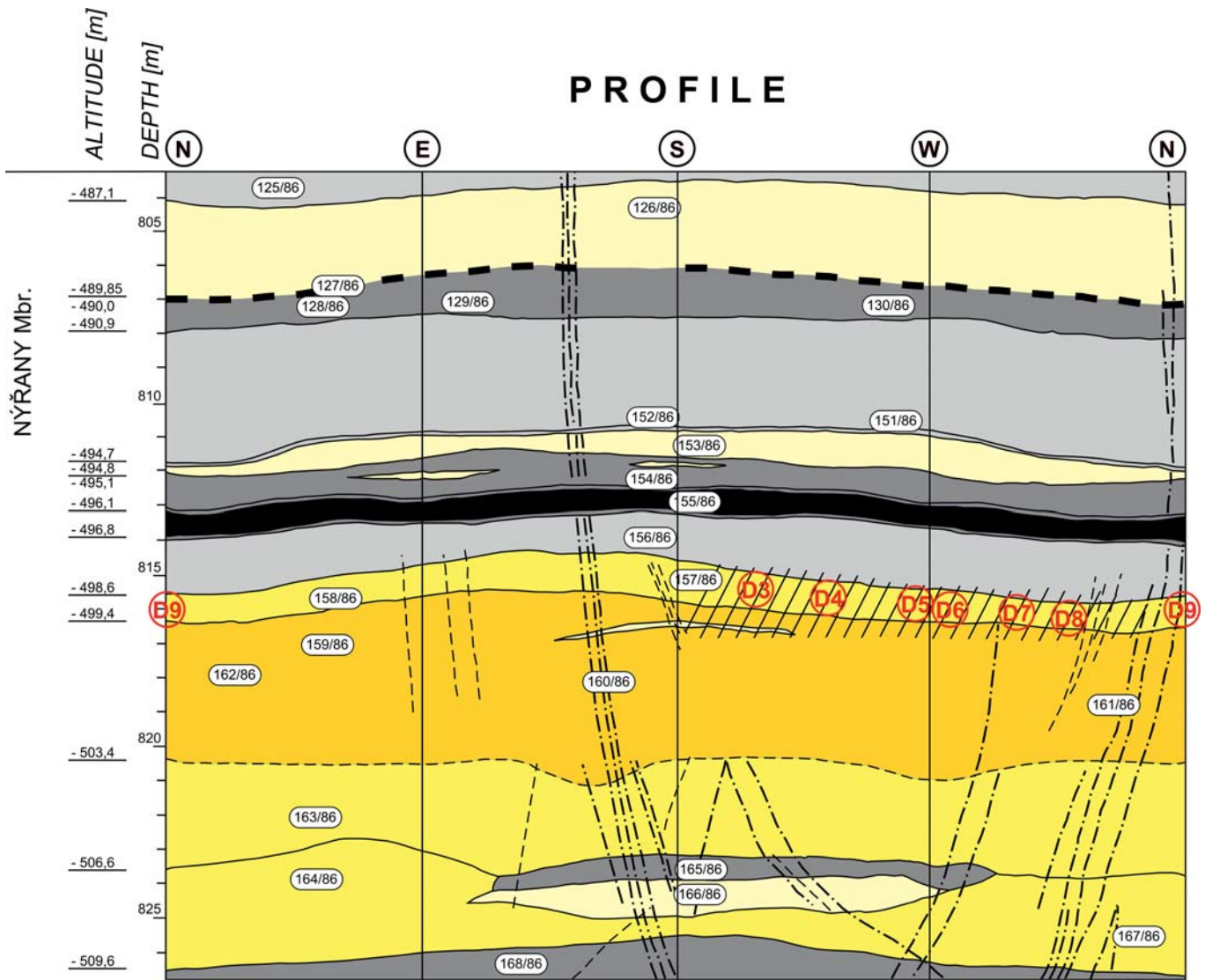


Fig. 3.24 Geological documentation of the no. 1 outburst site at the depth from 803 to 827 m. The outburst occurred on 9. 04. 1986. Skip shaft of Slaný Mine (simplified, based on documentation by ODMG VDK – Slaný Mine)

Legend: Hatched area: indicates the extent of massif affected by the outburst.

• - • - • - cracks filled in with packing mass,

- - - - cracks without packing mass.

Red circle refers to the photograph of the outburst as shown in Table D, Figs. D1 through D9.

1125/86	Siltstone, dark grey, fine sandy type	158/86	Sandstone, medium-grained to coarse-grained
126/86	Sandstone, fine-grained, light grey, low silty	159/86	Sandstone, coarse grained, locally interspersed with fine-grained conglomerate
127/86	Coal, clayey	160/86	Conglomerate, fine-grained
128/86	Claystone, grey-to-black	161/86	Sandstone, coarse-grained, locally interspersed with fine-grained conglomerate
129/86	Claystone, grey, with silty admixture	162/86	Sandstone coarse grained, local with fine grained conglomerate
130/86	Claystone, grey to brownish grey	163/86	Sandstone, medium-grained, white grey
151/86	Sandy siltstone, light grey, with sandy lamination	164/86	Sandstone, medium-grained to coarse-grained
152/86	Siltstone, dark grey, with fine sandy lamination	165/86	Claystone, grey, massive
153/86	Sandstone, fine grained, with silty lamination, grey	166/86	Sandstone, fine-grained, with silty lamination, light grey
154/86	Claystone, dark grey, with marked brownish grey lamination	167/86	Sandstone, medium-grained to coarse-grained
155/86	Coal, lustrous and dull, bedded with interlayers	168/86	Claystone, rich in silt to fine sand, grey
156/86	Siltstone, grey, laminated		
157/86	Sandstone, medium-grained to coarse-grained		

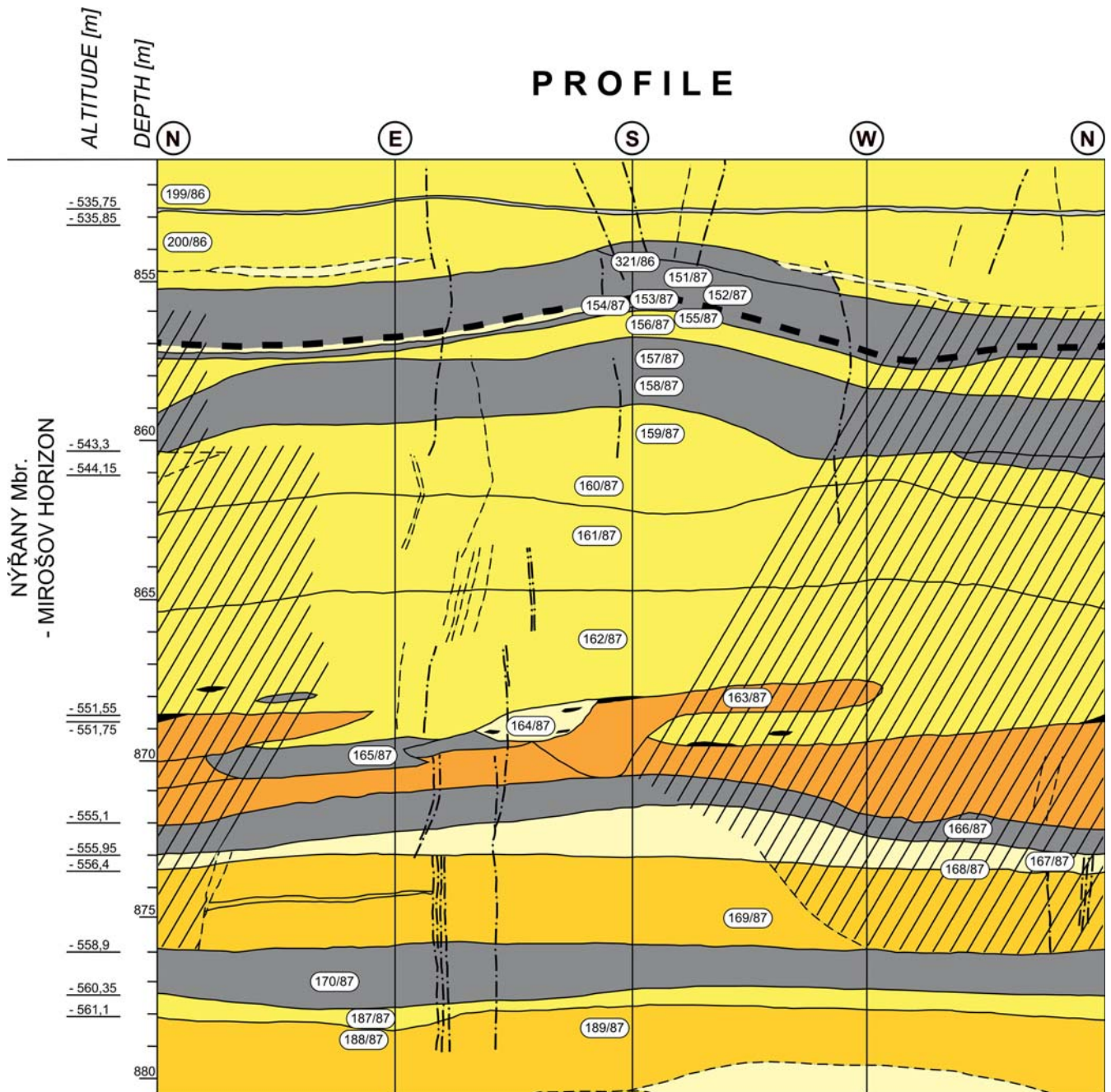


Fig. 3.25 Geological documentation of the no. 3 outburst site at the depth of 851 to 880 m. The outburst occurred on 21. 10. 1986. Skip pit of Slaný Mine (simplified, based on documentation by ODMG VDK – Slaný Mine)

199/86	Sandstone, medium-grained to coarse-grained	163/87	Conglomerate, fine-grained to medium-grained
200/86	Sandstone, medium-grained to coarse-grained	164/87	Sandstone, fine-grained to medium-grained
321/86	Silty claystone, dark grey to black	165/87	Claystone, grey to brownish grey
151/87	Silty claystone, dark grey	166/87	Claystone, dark grey
152/87	Silty claystone, dark grey	167/87	Sandstone, medium-grained to fine-grained
153/87	Claystone rich in coal, dark grey to black	168/87	Sandstone, medium-grained to fine-grained
154/87	Sandstone, fine-grained, light grey	169/87	Sandstone, coarse-grained, light grey, with interstratified bed of conglomerates
155/87	Silty claystone, dark grey	170/87	Silty claystone, dark grey, to clayey siltstone
156/87	Sandstone, coarse-grained, light grey	187/87	Sandstone, coarse-grained, light grey
157/87	Claystone, grey	188/87	Sandstone, coarse-grained, light grey, with transitions to conglomerates
158/87	Claystone, grey	189/87	Sandstone, coarse-grained, light grey, with transitions to fine grained conglomerates
159/87	Sandstone, coarse-grained, light grey		
160/87	Sandstone, medium-grained to coarse-grained		
161/87	Sandstone, coarse-grained, light grey		
162/87	Sandstone, coarse-grained to medium-grained		

The *sixth outburst* of rock and carbon dioxide with methane occurred at the depth of 908.7m measured from the collar, releasing 83,200 m<sup>3</sup> CO<sub>2</sub> and 1,000 m<sup>3</sup> CH<sub>4</sub>. The maximum concentration of CO<sub>2</sub> was 88.8%, the CH<sub>4</sub> concentration after 1.45 hours was 0.9%.

The *seventh outburst* of rock and carbon dioxide with CH<sub>4</sub> occurred on 26<sup>th</sup> August, 1989, at the depth of 936.0m under the shaft collar. A volume of 8,300 m<sup>3</sup> of CO<sub>2</sub>, plus ca. 50 m<sup>3</sup> of CH<sub>4</sub> were released, and ca. 150 m<sup>3</sup> of rock broke loose. The shaft technology remained unscathed.

The *eighth outburst* of rock and carbon dioxide with methane occurred on 16<sup>th</sup> October, 1989, at the depth of 946.0m under the shaft collar, during a blasting operation. A total of 825 m<sup>3</sup> of CO<sub>2</sub> and 50 m<sup>3</sup> of CH<sub>4</sub> were released. The volume of loosened rock was 80 m<sup>3</sup>. The conditions in the vicinity of the shaft were verified by horizontal, inclined as well as vertical boreholes.

Outburst no.	Date	Spot height „Z“	Depth below shaft mouth	Volume of liberated CO <sub>2</sub> / time (minutes)	Volume of liberated CO <sub>2</sub> per minute	Volume of rocks extracted
		[m]	[m]	[m <sup>3</sup> · min <sup>-1</sup> ]	[m <sup>3</sup> · min <sup>-1</sup> ]	[m <sup>3</sup> ]
1	9.4.1986	-497.5	814.5	7,100 over a period of 210 min.	33.81	450
2	24.6.1986	-514.5	831.5	20,300 over a period of 420 min.	48.33	2930
3	21.10.1986	-539.0	856.0	30,600 over a period of 420 min.	72.86	4480
4	13.1.1988	-569.2	886.2	49,190 over a period of 420 min.	117.12	2550
5	5.5.1988	-580.2	897.2	10,020 over a period of 420 min.	23.86	700
6*	10.8.1988	-591.7	908.7 - 909.0	83,200 over a period of 420 min.	198.09	3160
7**	26.8.1989	-619.0	936.0	6,100 over a period of 420 min.	14.53	245
8**	16.10.1989	-629.0	946.8	1,220 over a period of 420 min.	2.90	239
<b>Total</b>			814.5 - 946.9	207 730 m <sup>3</sup>		

**Table 3.10** Time sequence, depth, volumes of carbon dioxide and methane liberated due to outbursts, and rock volumes loosened during gas and rock outbursts at Slaný Mine skip shaft.

**Comments:** \* In the sixth rock and gas (CO<sub>2</sub> with CH<sub>4</sub>) outburst, the volume of CH<sub>4</sub> released within 420 minutes was 1000 m<sup>3</sup>.

\*\* In the seventh and eighth rock and gas (CO<sub>2</sub> with CH<sub>4</sub>) outbursts, the volumes of CH<sub>4</sub> released within 420 minutes were 50 m<sup>3</sup> in each case.

Outburst no.	Date	Spot height „Z“	Depth below shaft mouth	Volume of CO <sub>2</sub> liberated	Volume of rocks extracted
		[m]	[m]	[m <sup>3</sup> ]	[m <sup>3</sup> ]
1	16.2.1989	-628.5	855.0	79,215 over a period of 420 min.	3 280
2	15.3.1990	-674.5	901.0	96,200 over a period of 480 min.	3 465

**Table 3.11** Time sequence, depth, volumes of carbon dioxide and methane liberated due to outbursts, and rock volumes loosened during gas and rock outbursts at Slaný Mine hoisting shaft.

**Comments:** In the first rock and gas (CO<sub>2</sub> with CH<sub>4</sub>) outburst in the hoisting shaft, the volume of CH<sub>4</sub> released during 420 minutes was 197 m<sup>3</sup>. In the second outburst, the volume of CH<sub>4</sub> released over a period of 480 minutes was 1350 m<sup>3</sup>.

### 3.5.2 OUTBURSTS IN THE HOISTING SHAFT

The *first outburst* of rock and carbon dioxide with methane occurred in the hoisting shaft on 16<sup>th</sup> February, 1989, at the depth of 855.0m under the collar, after the firing of misfires from blasting works. The volume of CO<sub>2</sub> released was 79,15 m<sup>3</sup> over 420 minutes, and the volume of removed i.e., extracted rock was 3,280 m<sup>3</sup>. Finely fragmented outburst rock filled the shaft up to a depth of 798 m, and some equipment in the shaft was destroyed. The second outburst of rock and carbon dioxide with methane occurred on 15<sup>th</sup> March, 1990, at the depth of 901m under the shaft collar, while large-scale blasting works and also with contour distress blasting was in progress at the depth of 901.0 to 919.5m under the collar. Some 96,200 m<sup>3</sup> of CO<sub>2</sub> were released in 480 minutes and the volume of removed rock was 3,465 m<sup>3</sup>. The shaft was filled with finely fragmented outburst rock up to the depth of 842.0m under the collar; and some additional equipment in the shaft was put out of operation.

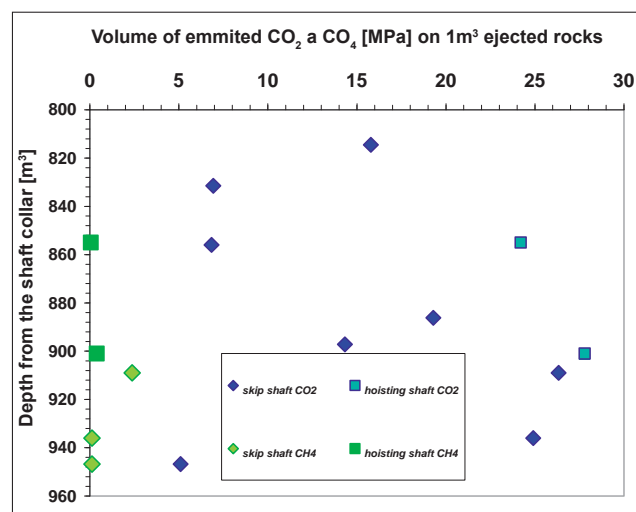


Fig. 3.26 Volume of CO<sub>2</sub> a CH<sub>4</sub> per 1 m<sup>3</sup> of extracted and outburst-ejected rocks in Mirošov horizon, in the hoisting and skip shafts of Slaný Mine, related to outburst depth.

Outburst no.	Depth below shaft mouth	Volume of liberated CO <sub>2</sub> / time (minutes)	Volume of CO <sub>2</sub> liberated per minute	Volume of rocks extracted	Volume of liberated CO <sub>2</sub> per 1 m <sup>3</sup> of loosened rocks	CH <sub>4</sub> /CO <sub>2</sub> ratio
	[m]					
1	814.5	7,100 over a period of 210 min.	33.81	450	15.78	-
2	831.5	20,300 over a period of 420 min.	48.33	2 930	6.93	-
3	856.0	30,600 over a period of 420 min.	72.86	4 480	6.83	-
4	886.2	49,190 over a period of 420 min.	117.12	2 550	19.29	-
5	897.2	10,020 over a period of 420 min.	23.86	700	14.32	-
6*	908.7 – 909.0	83,200 over a period of 420 min.	198.09	3 160	26.33	2.38/26.33 <b>0.09</b>
7**	936.0	6,100 over a period of 420 min.	14.53	245	24.90	0.119/24.9 <b>0.00478</b>
8**	946.8	1,220 over a period of 420 min.	2.90	239	5.10	0.119/5.10 <b>0.023</b>
<b>Total</b>	814.5-946.9	207,730 m <sup>3</sup>				

Table 3.12 Volumetric balance of gases and rocks during the outbursts in Slaný Mine skip shaft.

Outburst no.	Depth below shaft mouth	Volume of liberated CO <sub>2</sub> / time (minutes)	Volume of CO <sub>2</sub> liberated per minute	Volume of rocks extracted	Volume of liberated CO <sub>2</sub> / 1 m <sup>3</sup> of loosened rocks	CH <sub>4</sub> /CO <sub>2</sub> ratio
	[m]					
1	855.0	79,215 over a period of 420 min.	188.6	3,280	24.2	0.059/24.2 <b>0.0025</b>
2	901.0	96,200 over a period of 480 min.	200.4	3,465	27.8	0.39/27.8 <b>0.014</b>
<b>Total</b>		175,415 m <sup>3</sup>		6,745 m <sup>3</sup>		

Table 3.13 Volumetric balance of gases and rocks during the outbursts in Slaný Mine hoisting shaft.

### 3.5.3 TECHNICAL MEASURES TO LIMIT ROCK AND GAS OUTBURSTS

Following the third rock and gas outburst in the skip shaft, subsequent sinking operations conducted at the depth of 870.8 to 882.0m from the collar level were being performed in line with the „*Model recommendation for special blasting works in rock*“ elaborated by the Coal Research Institute (VVUÚ) in Ostrava-Radvanice. In the hoisting shaft, breakup-free destress blasting was applied from the depth of 732.0m downwards, aiming to ensure degassing of the massif and lowering its state of stress in the forefield of the shaft. By destress blasting, ca. the rock was disturbed to a distance of ca. 20m into the forefield and, subsequently, breakup (cavern) blasting was applied making use of shorter (1.6m) blast holes. The effectiveness of this procedure was checked by vertical as well as horizontal inspection boreholes. No problems that would be related to rock and gas outbursts were encountered down to the depth of 855m, not even when horizons were being crossed where rock and gas outbursts had previously occurred in the skip shaft. Prior to the first outburst, five destress blasting operations were undertaken in the cage shaft, plus two in the skip shaft. The procedure lends itself to an assessment only in the cage shaft which was sunk under conditions sufficiently removed from those prevailing in the ship shaft in terms of time and depth. According to a technical report by Energie Kladno Co. (2002), the destress blasting works undertaken represented „*a preventative method successfully verified in practice under the conditions of sinking the Slaný Mine shafts*“.

### 3.6. SUMMARY

The Slaný deposit of bituminous coal when regarded from the point of view of its geology and mining conditions poses a range of formidable natural and technical problems not yet encountered in the Czech mining industry. Analyses of the conditions of stressing of the massif before and after packing as well as of the pressure and temperature conditions under which CO<sub>2</sub> is held in the pores in permeable sandstone and conglomerate beds prior to and after opening of the critical **Mirošov horizon**, coupled with the manifestations of rock and gas outbursts make it possible to formulate the summary of results as follows:

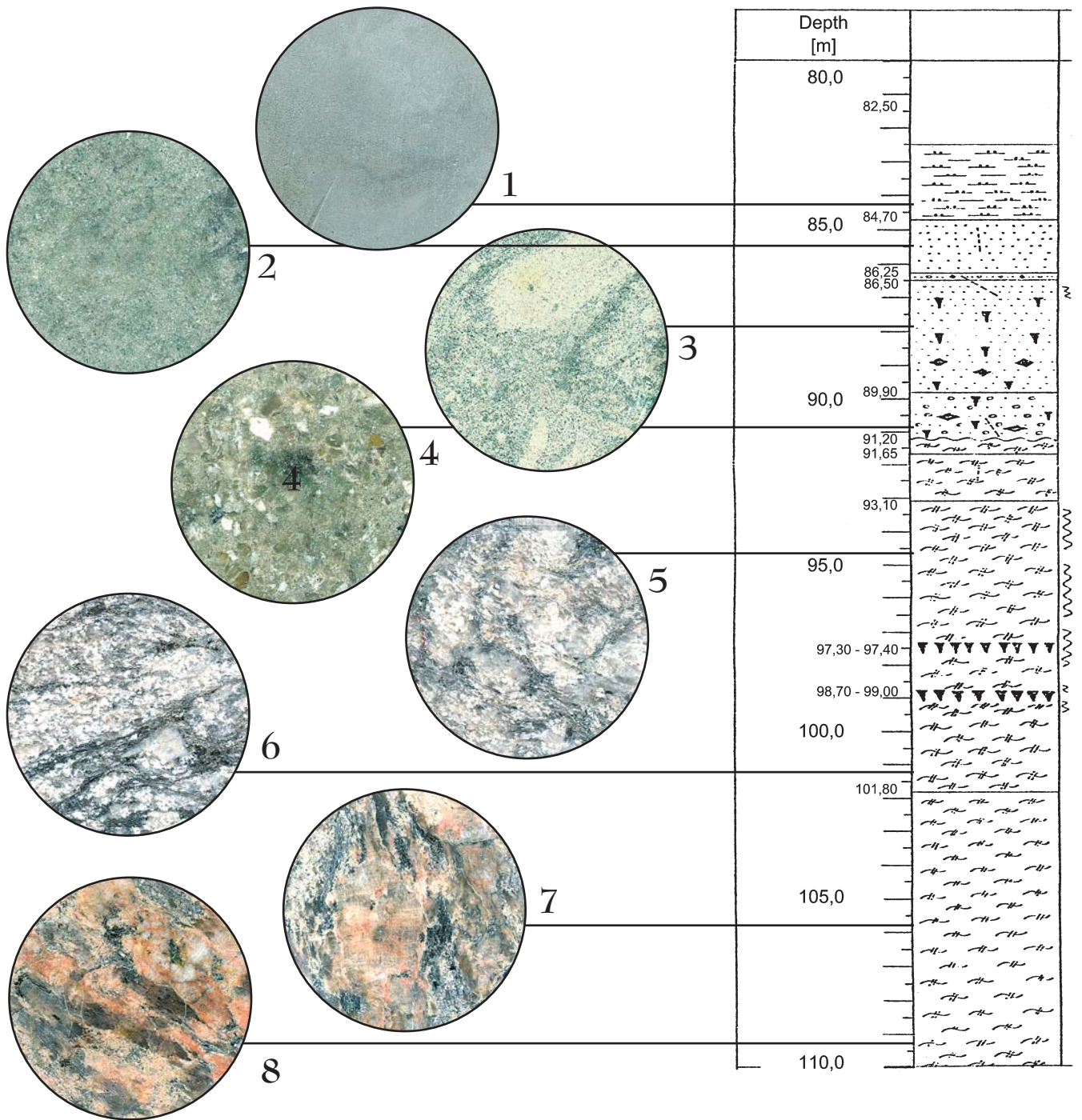
**The assumptions concerning the conditions of existence of CO<sub>2</sub> conditions in the pores of sandstones and conglomerates in the Mirošov horizon at depths of 875.7 to 888.3 m were put to a test in the following two alternatives:**

- (a) *The pore space of sandstones and conglomerates in the Mirošov horizon is fully saturated with mineralized water containing NaCl ( $c_{\text{NaCl}} = 35 \text{ g} \cdot \text{dm}^{-3}$ ). Carbon dioxide was in equilibrium with the solution under the given pressure and temperature conditions prevailing in the pores of the given rock system.*
- (b) *The pore structure of the Mirošov horizon rocks is filled with compressed CO<sub>2</sub>.*

However, the actual situation in the Mirošov horizon is influenced by the local properties of rocks; situations may be encountered where both cases, sub (a) as well as sub (b), can coexist and overlap. In Chapter 2, the reader may find the results of a simulation which are expressed, under normal conditions of temperature and pressure, in terms of the volume of CO<sub>2</sub> released from the rocks. The simulation relates to different horizons of the Slaný shafts.

The volume of carbon dioxide dissolved in pore water in the case mentioned as per (a) is lower by at least one order of magnitude than what would correspond to the volume of pure CO<sub>2</sub> compressed in pores as per the case sub (b). It should be pointed out that the volume of carbon dioxide as per (b) is in a good quantitative agreement with the registered carbon dioxide volume released during the sinking of the shaft (*see Table 2.1*). The reason for a sudden increase of the volume of carbon dioxide at geostatic vertical stresses > 7-8 MPa is the proximity of the CO<sub>2</sub> critical point (temperature of 31.04°C, pressure 7.384 MPa - *Fig. 2.2*).

The balance of the volumes of gases released from rock and gas outbursts shows, in both shafts of Slaný Mine, that in the Mirošov horizon these are rock outbursts releasing pure carbon dioxide or, in the case of outbursts occurring at greater depths, CO<sub>2</sub> with a small admixture of CH<sub>4</sub> of thermogenic origin (coalification of coal seams). With increasing depth, the content of CH<sub>4</sub> also increases (*Tables 3.12 and 3.13, Fig. 3.26*); this is in line with the existence of coal seams in the given sequence. It is true that the trend of increasing volume of carbon dioxide per 1 m<sup>3</sup> of ejected rock is not significant statistically (anomalous value of 5.10 m<sup>3</sup> CO<sub>2</sub>·m<sup>-3</sup> of rock in the no. 8 outburst in the skip shaft), but with increasing depth, the CO<sub>2</sub> volumes can increase. As the sinking progresses to greater depths, complications can arise due to an increased volume of released methane, with all its consequences for coal mining.



Upper Cretaceous rocks in borehole KO-16: marlstone (1)  
sandstones (2)  
conglomerate (3)  
conglomerate with silicification (4).

Crystalline basement:  
intensive kaolinized gneis (4)  
low kaolinized gneis (5)  
and fresh gneis (6)  
and (7).

## 4. ACCUMULATION OF CARBON DIOXIDE IN BURIED WEATHERED COVER OF CRYSTALLINE BASEMENT AND IN BASAL SEQUENCES OF COVERING STRATA (MOST BASIN, NORTH BOHEMIA)

Occurrence of free carbon dioxide during the sinking of the drainage shaft for underground drainage of Oubánců míru Open Pit Mine (hereafter referred to as Komořany shaft), in Komořany near Most town, is an example of migration of carbon dioxide along tectonic faults (or adjacent joint zones) and of its subsequent accumulation in the weathered cover of crystalline basement in underlying Cretaceous and Miocene sediments which exhibit a structure that fulfils an isolating function. The structure of Most Basin as well as of Sokolov and Cheb Basins belongs to important geological structures of the Bohemian massif where carbon dioxide occurs (*Fig 2.1*). The geological structure of Krušné hory (Ore Mts Range) Piedmont Basin was described by Malkovský et al. (1985). Contemporary notions regarding the deep structure of Ohře rift (Cheb basin), the sources of deep CO<sub>2</sub> and heavy isotope He and the migration thereof to the surface were outlined by Babuška and Plomerová (2010). The notions concerning the deep structure of the territory between Saxon granulite massif, České Středohoří Mts and Doupov Mts (Novotný, Skácelová and Mlčoch, 2010) and of the territory between the central part of České Středohoří Mts and the Most basin within the North Bohemian Basin were described by Cajz and Valečka (2010). The main tectonic structures are represented by the Marginal Krušné hory (Ore Mts) fault and the Central fault. These are deep tectonic structures along which emissions of mineral waters saturated with carbon dioxide occur, mainly in the parts of the graben extending over the Cheb - Karlovy Vary and Teplice v Čechách areas (Chapter 2). In Krušné hory Piedmont structure, numerous occurrences of this kind are also tied to accompanying faults between the aforementioned major faults or are linked with small failures in the deep base which communicate with strata up to Miocene. Tectonic zones with accompanying tectonic faults represent a higher-permeability rock massif which constitutes a migration route for emissions of gas and for percolation of gas-bearing mineralized water to the surface. At the same time, it is obvious that CO<sub>2</sub> emissions are connected with the third phase of Tertiary volcanism as described by Kopecký (1978, 1987-1988). The same is also assumed by Polish authors who have addressed the issues of CO<sub>2</sub> and coal outbursts in the Polish part of the Intra-Sudeten Basin.

### 4.1 CARBON DIOXIDE OCCURRENCE IN MOST BASIN GROUNDWATERS WITHIN THE KRUŠNÉ HORY PIEDMONT BASIN

In the Most Basin, Hurník (2004) distinguishes “shallow circulation” and “deep circulation” groundwaters. In both these types of groundwater, CO<sub>2</sub> occurs as free gas as well as a gas bonded to or tied up with other substances. Groundwater of deep circulation is attached to permeable rocks – hydrogeological reservoirs – or to systems (zones) of joints, sometimes reaching considerable depths. Depending on the nature of permeability, he distinguishes between reservoirs with pore permeability and reservoirs with joint permeability. In hard rocks (igneous rocks, metamorphic rocks, compact sedimentary rocks), the water-bearing capacity of the rock is linked, as a rule, with fissure zones accompanying the main faults that run in the NE – SW direction. Both types of permeability are observed in the case of basal Cretaceous conglomerates and sandstones and in the basement of weathered and kaolinized Krušné hory (Ore Mts) crystalline complex.

#### The following hydrogeological reservoirs occur in the Most Basin:

- *Krušné hory (Ore Mts) crystalline complex in the basement of Tertiary basin,*
- *Cretaceous sandstones, conglomerates and calcareous marl*
- *Tertiary (Miocene), underlying and interlayered with sandstones, lignite coal seams and overlaying sandstone.*

Most of these aquifers operated in their own, independent hydrodynamic modes. It is an exception if they are connected with each other, and if so then these are only local interconnections, e.g., the aquifer in Krušné hory (Ore Mts) crystalline basement is interconnected with that of the basal Cretaceous sediments (Hurník, 2004). Waters tied up within the Krušné hory (Ore Mts) crystalline complex are, according to Hurník (2004), either cold natural waters – of little mineralization and with low gas contents – or rather hot mineral waters exhibiting high contents of dissolved salts and rich in free CO<sub>2</sub>. During mining operations, mineralized and gas-containing waters were encountered in the deepest part of the basin situated eastwards of Most town as well as in the western part of Komořany area in Oubánců Míru open pit mine. This is where, in 1984, an inflow was observed of thermal water from the basal crystalline complex composed partly of kaolinized orthogneisses. Such occurrence of mineralized,

gas-containing waters was observed when a drainage shaft was being sunk in the above pit during the 1989-1990 period; first came the outbursts of gas from basal Cretaceous sandstones and these were followed by inrush of water into the shaft which for a period of time attained a constant flow rate of up to  $25 \text{ dm}^3 \cdot \text{s}^{-1}$ . The initial volumetric gas emission rate was  $5.4 \text{ m}^3 \cdot \text{min}^{-1}$ ; the gas pressure was 3 kPa and the  $\text{CO}_2$  concentration was 90 vol.%.

## 4.2 THE CASE OF $\text{CO}_2$ LIBERATION DURING THE SINKING OF THE KOMOŘANY DRAINAGE SHAFT

The shaft was sunk to drain the Obránců Míru open cast mine in Komořany. The sinking was begun from the bottom of the extracted area. The shaft coordinates are  $x = 984,100.012 \text{ m}$ ;  $y = 797,054.997 \text{ m}$ ;  $z = + 196.25 \text{ m}$  (above Baltic sea after leveling). The design depth was 250 m. According to plan, drainage crosscuts should be taken from the shaft to the level of the seat of the lignite coal seam in the underlying crystalline complex. The corresponding geological column down to the depth of 135 m is shown in *Table 4.1* and the geological cross-section of contact of Upper Cretaceous sediments with the weathered surface of the crystalline complex at the depth of 84 to 95 m under the shaft mouth is shown in *Fig. 4.1*. The final depth of the shaft was 220 m (Hurník, 2004). On 24. 09. 1989 at 22.30, an extraordinary incident occurred in the Komořany shaft at the depth of 84.3 m while miners were traveling to the bottom of the shaft in a hoisting bucket. Some 20 m above the shaft bottom, the miners experienced breathing difficulties and two of them lost consciousness. Fortunately, one of them acted with agility (prior to loosing consciousness himself, he

issued the departure command), so that there was no loss of life. Within three quarters of an hour (at 23.13), samples of air in the shaft were taken at the depth of 84 m, with the following results: 68%  $\text{CO}_2$ , 7%  $\text{O}_2$ , 0.007%  $\text{CO}$ , 0%  $\text{CH}_4$  and 0%  $\text{H}_2$ .

Before the incident, the last rock blasting operation took place there on 22. 09. at 13.30. Subsequently, during the afternoon shift, some of the rock loosened by blasting was extracted. Some  $8 \text{ m}^3$  of loose rock remained at the shaft bottom. However, no data is available for the period after the above-mentioned rock blasting operation regarding any suspension or interruption of ventilation (the system used there was ventilation by an independent blower), and likewise, no data is available on the  $\text{CO}_2$  concentration, if any, in the individual sectors of the shaft. Thus it is not possible to form any idea on the development of gassing before the incident.

In view of the fact that there also is no data available on  $\text{CO}_2$  emissions during the sinking of the Komořany drainage shaft until the incident on 24. 09. 1989, there is no way how the volume of gas emitted from the massif until that date could be estimated.

In the same shaft, another incident connected with high concentration of carbon dioxide occurred after rock blasting which took place on 6. 10. 1989. As a consequence of this, the Regional Mining Authority in Most town ordered the Komořany open pit mine to introduce inspection measurements of air quality in the shaft as well as measurements of the intensity of  $\text{CO}_2$  emissions in the face (Protocol of OBÚ - Regional Mining Authority in Most town of 11. 10. 1989).

Subsequently, measures were introduced to intensify ventilation by means of two ventilation tubes, and trials were made to detect the intensity of gassing in the shaft. Nevertheless, all this has helped neither to prevent gassing of the face during the loading of loosened rock after rock blasting nor to determine the amount of actual gas production in the shaft.

Deep	Stratigraphy	Rocks	Colour	Rock structure
0-20 m	Tertiary	Basanite hard argillized, primarily analcime-nefeline basanite	grey, grownish	foam, flow, pellet like
20-34.5 m	Tertiary	Bazanite	red and red pink-violet	flow like, packed
34.5-36 m	Upper Cretaceous, Upper Turonian	Contact of volcanic rocks with underlying limestone	light grey	
36-57 m	Upper Cretaceous, Upper Turonian	Marl	light grey	at depth of 57 m coprolite layer
57-92 m	Upper Cretaceous, Lower Turonian-Cenomanian	Marly and calcareous siltstone, from depth 81 m silty claystones, from depth 86 m sandstones and sedimentary quartzites There was $\text{CO}_2$ emission from a sandstone bed (Fig. 4.1)		subhorizontal bedding
92-135 m	Crystalline complex of Krušné hory Mts	Leaf-gneisses, on fissures and joints kaolinization, secondary siderite deposition, impregnation of siderite, gradual transition to metagranite		foliated or pencil like gneisses

*Table 4.1 Geological situation in Komořany drainage shaft (after Jan Žižka 1989).*

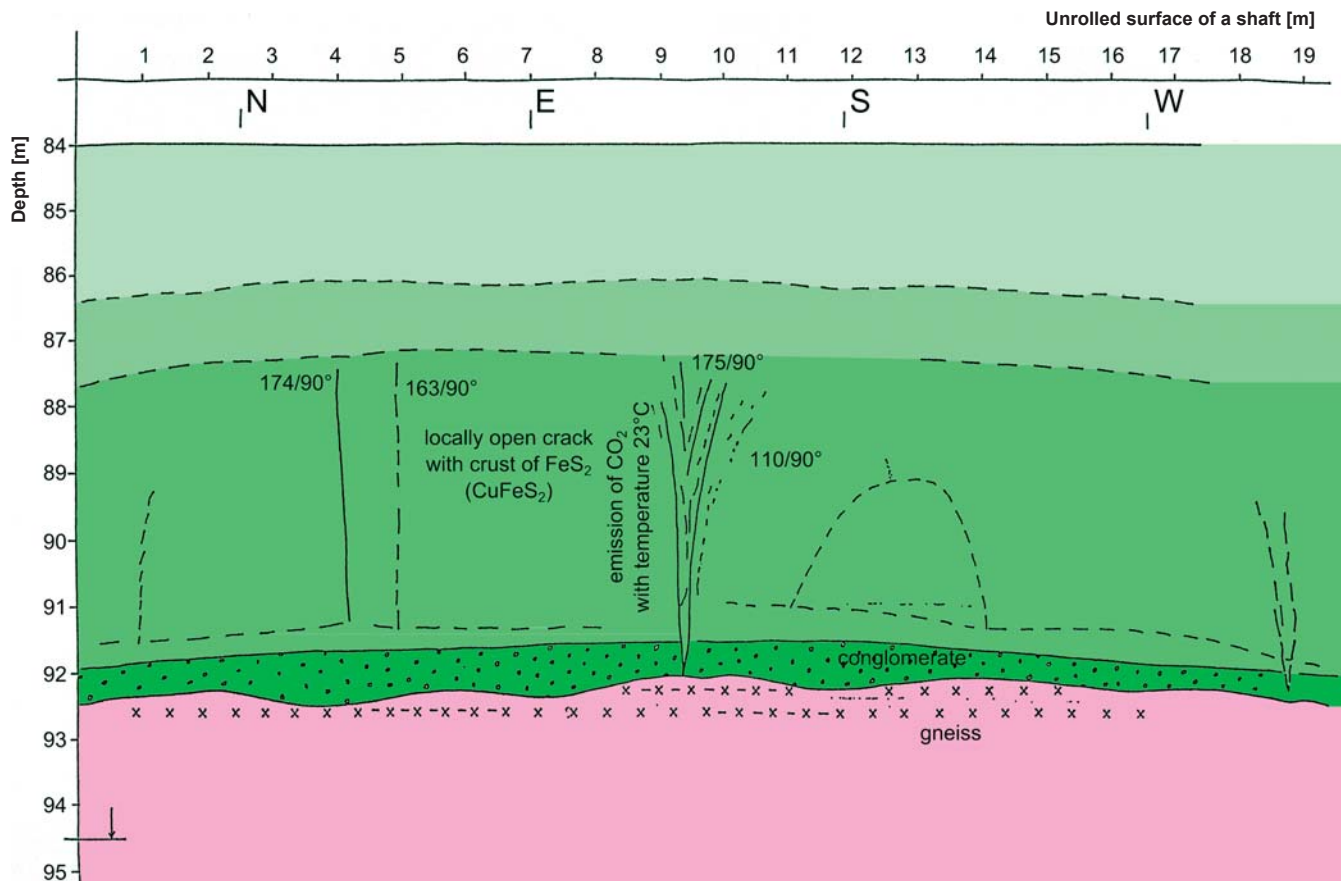


Fig. 4.1 Plane development of the geological profile of the interface of Upper Cretaceous sediments with the surface of partially weathered kaolinized gneisses and metagranites at the depth of 84 to 95 m in the Komořany shaft (situation as of 24. 09. 1989 – 1. 03. 1990).

Legend: UPPER CRETACEOUS:

- glauconitic sandstones with low silicification
- silicified sandstones passing into glauconitic quartz sandstones
- glauconitic quartzite sandstones with hard silicification (secondary quartzites)
- hard silicified conglomerates (secondary quartzites)

CRYSTALLINE BASEMENT:

- gneisses of biotite-muscovite type with irregular kaolinization, of Kateřinská hora Dome type
- cracks and fracture zones

Rough calculation of gas production was made as follows: gas production for the period from 9. 11. 1989 until 28. 02. 1990 was calculated from the actually measured volume of mine air on the downcast side of ventilation tubes and from CO<sub>2</sub> concentrations measured at the depth of 8.5m under shaft mouth which were verified by laboratory analyses of samples from the same depth. The volume of mine air corresponding to the period from 22. 09. until 8. 11. 1989 was recalculated based on the average value of daily gas production found during the period of 9. - 30. 11. 1989. This has resulted in a certain undervaluation of the actual gas production in the shaft. The total volume of gas produced during the period of 24. 09. 1989 – 28. 02. 1990 was 1,101 101 m<sup>3</sup> CO<sub>2</sub>.

The above occurrence of gas in the mine was classified by Šmíd in Pipek et al. (1990) and by Šmíd et al. (1990) as a dynamic gas effect rather than as an outburst of rock and gas because the defining conditions for an outburst as set out in Section 2 of the Instruction for ČBÚ (Czech Mining Authority) Ordinance ref. no. 6000/77 were not met, i.e. no outburst of rock weighing at least 0.5 ton occurred and no open space (cavity) was produced that would surpass an advance per round after rock blasting. Therefore, the Authority decided to allow the shaft to advance only by such sections that would not endanger the miners or that could be made secure by additional preventive safety measures.

To test the tendency of the massif to outbursts of rock and carbon dioxide at shaft depths under 84.3 m, three boreholes nos. 1, 2 and 2A were drilled from the shaft bottom. Outside the shaft, the borehole KO-16 was drilled to the depth of 111.0 m. All these boreholes were core boreholes. From the point of view of the directives and regulations existing at that time, no signs indicating a potential occurrence of outbursts were found during the drilling. Based on geological investigation of the massif in the shaft, the examination of bore cores, the results of laboratory analyses and, first of all, the values of permeability of Cretaceous rocks as well as rocks of the crystalline basement complex, the conclusion was drawn that the main CO<sub>2</sub> migration routes within the massif were tectonic faults and joints. The intensity of CO<sub>2</sub> emissions from the massif was also confirmed by the fact that during subsequent shaft sinking down to the final depth of 220 m, the gas flow rate in the drainage borehole was permanently 3.5 m<sup>3</sup>·min<sup>-1</sup> and the CO<sub>2</sub> content increased to 95 %.

### PUMPING TEST

Pumping tests (i.e., rising and dropping tests) were made in the borehole KO-16 from the depths of 113.5 m and 145 m under the shaft mouth (Pipek and Martinec, 1990) and at the depth of 245 m (in which case the pertinent data could not be located by the authors in the archives). During the rising pumping test conducted at 113.5 m, water was pumped to the level of 109.2 m under the shaft mouth, whereupon low specific mine inflows of ca. 9.0·10<sup>-4</sup> dm<sup>3</sup>·s<sup>-1</sup> were observed. These were interpreted as a capture of local groundwater in joints under the static level of groundwater (98.3-98.6 m). The test took 24 h. The dropping pumping test continued after the rising test and showed an absorption capacity in uncased borehole of a length of 24.5 m (on the premise that the cased borehole was watertight). The pressure gradient from the beginning of the test represents a difference of 0.98 MPa up to the static level. For the interval of 89 – 113.5 m, the bore holding capacity coefficient *k* was 1.4·10<sup>-4</sup> dm<sup>3</sup>·s<sup>-1</sup>·m<sup>-1</sup>, a relatively low value for the holding capacity of joint systems. The second test was made at the depth of 145 m.

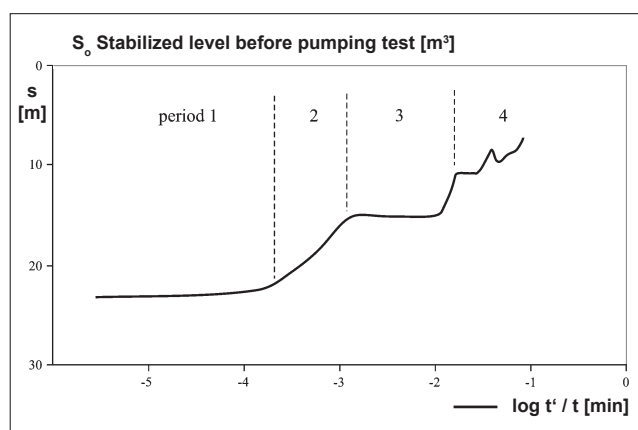


Fig. 4.2 Ascendant curve from pumping test conducted at Komořany shaft, employing a logarithmic time scale *t* – total duration of pumping test, *t'* – time elapsed after completion of ascendant pumping test (according to Hurník, 2004)

It was followed by a decrease of the level to 140.5 m under the mouth of the borehole. In the first minutes, the specific inflow ranged from 2.4·10<sup>-3</sup> dm<sup>3</sup>·s<sup>-1</sup> to 3.1·10<sup>-3</sup> dm<sup>3</sup>·s<sup>-1</sup> and this was interpreted as an occurrence of water-saturated faults and joint systems. This dropping test had a linear development until reaching a drop value of 28,19 m per 24 h; in the section of 89 – 145 m, the bore holding capacity coefficient *k* was 6.3·10<sup>-4</sup> dm<sup>3</sup>·s<sup>-1</sup>·m<sup>-1</sup>. Migration of water and gases took place in zones of joints or tectonic faults, making it difficult or impossible to arrive at any local forecasts of water inflow rates and of gas (CO<sub>2</sub>) volumes. In 1992, a long-term pumping test was performed at the Komořany shaft, aiming to check on the hydraulic functionality of the shaft (Hurník, 2004). The result of the test is shown in Fig. 4.4 which illustrates the effect of CO<sub>2</sub> on the drainage process in a predominantly joint-type collector.

Four sections can be distinguished on the above curve. Section 1 points to a so-called skin effect that indicates an increased permeability of the wall of the shaft compared to the rock massif bulk. Section 2, which is almost linear, reflects a stable permeability of rock massif over the given depth interval. Curve deformation in section 3 reflects the existence of extensive accumulation caverns in the rock massif and the existence of a siphon, in which CO<sub>2</sub> could have accumulated. The caverns could fill with water only after a sudden escape of gas. Unstable course of the curve in section 4 points to an uneven distribution of joints within the reach of the depression zone and to variability of their volumes. The distinct oscillations on the curve can be due to the existence of the aforementioned siphon or of other siphons above it (Hurník, 2004).

### 4.3 THE ROCK MASSIF AND THE PROPERTIES OF THE ROCKS THEREIN

The structure of the rock massif is known thanks to the sinking of shaft and to three boreholes drilled in its vicinity: the borehole KO-17, NNE 11.5 m from the shaft axis; the borehole HJI 275, 14.5 m SW from the shaft axis; and the borehole KO-16, SEE 10 m from the shaft axis. Additionally, the boreholes V1 (1.8 m NW from axis) and V2A (2 m SE from axis) were drilled starting from the bottom of the shaft, at the depth of 84.3 m from the shaft mouth. In all these boreholes and in the shaft, the sequences of the Cretaceous and basal crystalline complex at the same depth level are similar to each other. The structure of the Cretaceous sequence on the surface of the basal crystalline complex with biotitic gneisses of hard and deep kaolinization is illustrated in Fig. 4.1 and can also be followed on the geological cross section of the KO-16 borehole (Fig. 4.3).

#### BOREHOLE KO-16

In the borehole KO-16 (Fig. 4.3), the sequence of Upper Cretaceous sediments is present in the following samples: anal. no. VVUÚ 4465a: 82.5 to 84.7 m, glauconitic marlstone; anal. no. VVUÚ 4466a: 84.7 to 86.25 m, low sandy

siltstone with glauconite; anal. no. VVUÚ 4467a: 86.25 to 89.8 m, silicified sandstone; anal. no. VVUÚ 4468a: 89.8 to 91.2 m, silicified conglomerate (*PLATE C, Figs. C9, C10, C11*).

The Upper Cretaceous sediments overlying the basal crystalline complex consist of marlstone, low calcareous siltstone and clastic sediments – sandstones to conglomerates (Cenomanian – Lower Turonian). The grey glauconitic marlstones are slightly calcareous or micaceous; the matrix is composed of kaolinite, illite and glauconite with calcite cement. The clastic phase is composed of quartz and flakes of muscovite. The rocks are characterized as having low permeability (acting as hydrogeological isolators). The sequence with silicified sandstones containing glauconite and conglomerates is hard silicified (quartz as cement) on its base, with all the consequences to their physical properties and to the development of pore cavities.

In the interval of 91.5 - 110 m (and deeper), the basal crystalline complex is formed of biotite-muscovite gneisses, porphyroclastic with lepidogranoblastic structure, fresh as well as intensely kaolinized (91.2 to 245.6 m: samples anal. nos. VVUÚ 4469a-4471a, 4481a - 4488a, 4508-4510 and VVUÚ 12, 32, 52, 62, 72). By their petrographic nature and metamorphism, they correspond to pink gneisses of Kateřina Dome of Krušné hory (Ore Mts) crystalline complex. The composition of rocks in the borehole referred to above is shown in *Figs. 4.3 to 4.4*. The rocks show a very variable degree of kaolinization which increases towards the surface of the basal crystalline complex. Generally, kaolinization (together with chloritization of biotite) is common in the vicinity of joints.

#### BOREHOLE 2A

Borehole 2A was bored from the depth of 84.3 m from the mouth of the Komořany shaft. According to documentation, its geological profile (Plášil, 1989) is not different from those of the surrounding boreholes and the shaft, and can be described as follows:

#### Upper Cretaceous (Cenomanian ?) – Lower Turonian (?):

- 84.3 – 85.3 m - glauconitic sandstone, medium-grained, very hard, heavily silicified, fractured by continuous joints dipped at 70-90°;
- 85.3 – 87.9 m - quartzzy sandstone, glauconitic, fine-grained to medium-grained, silicified to high hardness;
- 87.9 – 88.5 m - quartzzy sandstone (see above) with a lower content of glauconite;
- 88.5 – 89.9 m - quartzzy sandstone, grained, changing to conglomerate, quartzzy, silicified, glauconitic. Silicification is very irregular. Rocks are fractured, joints are uneven and abrupt.
- 89.9 – 90.4 m - conglomerate, light grey, silicified, with subangular quartz pebbles of 3-6 cm in size, of low porosity, very hard.

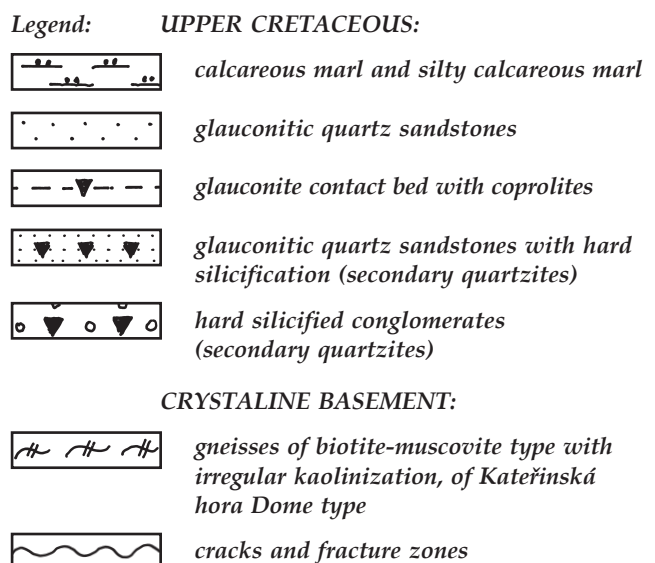
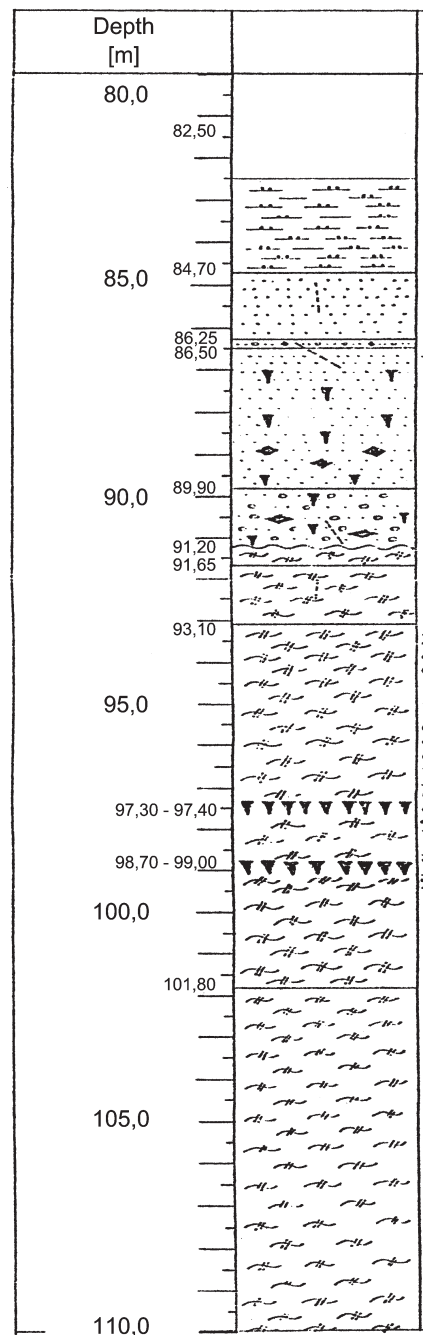


*Fig. 4.3*  
Geological cross-section of borehole KO-16 at Komořany shaft (according to M. Smékal in Pipek et al., 1990).

The whole sequence of Upper Cretaceous has a structure that is typical of basal Cretaceous sediments and does not differ from the situation in the surrounding boreholes. It is formed of individual beds of sandstones and conglomerates. From the point of view of their structure they are of variable grain size and also have various contents of clayey matter (glauconite). The composition of the rocks is shown in *Table 4.2*. Silicification increases towards overlying strata, but is irregular, probably as a reaction to primary textural inhomogeneity. Porosity is 4.2%, determined by well logging in the borehole HJI-275 for glauconitic sandstone with silicification. Glauconitic sandstone is characterized by low silicification and, as a consequence, by a high primary porosity of up to 25.4%. Quartzite sandstone in the basement has the nature of secondary quartzites and its porosity decreases, according to well logging, to 5.4% (Martinec et al., 1990).

From a hydrogeological point of view, the complex of basal Cretaceous sediments is, in the entire shaft area, out of the horizon of deep mineral waters but within the zone of accumulation of gaseous CO<sub>2</sub> between the static groundwater level ( $z = +90$  m above Baltic sea after leveling) and the isolating sediments – marlstone (Cenomanian – Lower Turonian). Therefore, it represents a joint-type or porosity / joint type aquifer. The permeability of these rocks is low (they act as hydrogeological isolators).

Petrographical type of rocks Sample No. depth in borehole	Quartz grains with young regeneration	Cement with quartz with clayed matter	Pyrite	Glauconite	Detritic flakes of mica	Detritic feldspars	Loss of ignition	CO <sub>2</sub> in carbonates	Loss of ignition - CO <sub>2</sub> in carbonates (difference)
	[% volume]						[% weight]		
<b>BOREHOLE 2A</b>									
Conglomerate with silicification 4448 89.4-90.4 m	62	30	2	2	2	2	1.37	0.35	1.02
Conglomerate with silicification VVUÚ 2 88.7-89.0 m	75	20	1	2	1	1	1.25	0.20	1.05
<b>BOREHOLE KO-16</b>									
Glauconitic siltstone 4465a 82.5-84.7 m	20	calcite 5% matrix 59%	1	10	5	+		2.34	
Glauconitic siltstone 4466a 84.7-86.3 m	35	calcite 5% matrix 45%	1	10	5	+		2.55	
Sandstone, coarse-grained, glauconitic 4467a 87- 88.3 m	62	16	+	8	6	8			
Conglomerate (secondary quartzite) 4468a 89.8-91.2 m	71	11	+	6	3	9		0.22	

*Table 4.2 Modal composition of Cretaceous rocks, loss of ignition and content of CO<sub>2</sub> (in carbonates). Borehole 2A and borehole KO-16. Sinking of Komořany drainage shaft.*

*Legend: Depths are given in metres under shaft mouth.*

*Optical planimetry analysis of thin section perpendicular to bedding; 3000 – 5000 points.*

*Feldspars in conglomerates were coloured. + - occurrence of mineral under 1%.*

**Crystalline Basement: 90.4 – 111.0 m**

90.4 – 91.9 m - *biotite-muscovite gneiss, medium-grained, with platy parting, kaolinized, folded, dip of foliation plane mostly 30-40°;*

91.9 – 92.6 m - *biotite-muscovite gneiss, medium-grained, weathered, slightly kaolinized;*

92.6 – 111.0 m - *biotite-muscovite gneiss, coarse-grained, porphyroclastic, slightly kaolinized.*

By their petrographic character and metamorphosis, they correspond to red gneisses from Kateřina Dome of the Krušné hory (Ore Mts) crystalline complex. These are muscovite-biotite gneisses, banded (stromatolite, nebulitic stromatolite), kaolinized, tending to an increase in secondary porosity in altered rocks when compared with fresh ones. In the borehole, the massif contains uneven, rough, abrupt joints with surface alteration. **Tables 4.3 and 4.4** show the modal (mineral) compositions of rocks from the crystalline complex in the boreholes KO-16 and V2A.

Petrographical type of rocks Sample no Depth in borehole	Quartz	Orthoclase	Plagioclase	Kaolinite	Biotite	Muskovite	Chlorite	Carbonate	Garnet	Zirkone	Hematite (+) or pyrite (py)
	[% volume]										
Gneiss bi-mu, kaol. 4469a 99.0-101m	48	11	2	21	<1	13	1	3*	-	-	+++
Gneiss bi-mu, kaol. 4470a 101.8-110.0 m	33	35	14*	2	8	7	<1	+	++	++	-
Metagranite, fresh 4487a 112.2-112.9 m	36	12	28	3	8	11	-	2***	-	++	+++
Gneiss bi-mu, kaol. 4486a 118.5-119 m	49	27	7	5	2	8	-	2*	-	-	+++
Gneiss bi-mu, fresh 4485a 128-128.7m	30	40	12	+	3	12	-	3*	-	+	-
Gneiss bi-mu, fresh 4483a 131.3-131.4 m	51	20	15*	+	5	8	-	<1**	+	+++	++
Gneiss bi-mu, fresh 4482a 138.3-139 m	45	12	12	5	10	8	-	8*	++	+++	-
Gneiss bi-mu, kaol. 4481a 142.5-143 m	43	12	2	20	8	14	-	<1*	+++	++	-
Gneiss bi-mu, fresh VVUÚ12 148-149 m	37	27	12	<1	13	10	-	<1*	++	+++	py
Gneiss bi-mu, kaol. 4508a 162.2-163.3m	46	10	5	15	9	14	-	<1*	<1	++	py
Gneiss bi-mu, kaol. 4509a 185.3-186.5 m	46	14	8	11	8	12	<1	<1*	++	+++	+
Gneiss bi-mu, slight kaol. VVUÚ72 231.7-232.6 m	41	24	15	2	7	11	<1	-	-	+++	++
Gneiss bi-mu, kaol. chlor. 4510a 240.2-241.7 m	21	41	12	7	8	11	-	-	<1	++	++

**Table 4.3** Modal composition of biotite-muscovite gneisses and metagranites. Types: Kateřinská hora Dome in Krušné hory (Ore Mts). Borehole no. KO-16 in Komořany shaft.

**Legend:** Depths are given in meters under shaft mouth.

Optical planimetry analysis of thin sections is perpendicular to metamorphic foliation; 3000–5000 points. Feldspars were colored.

Carbonates: \* fine grained aggregates in matrix; \*\* as a filling in cracks; \*\*\* metasomatic reactions in feldspars;

Relative occurrence of accessory minerals: + individual grains; ++ frequent grains; +++ very frequent grains.

Bi-mu – biotite-muscovite, kaol. – kaolinized, chlor. – chloritized.

Petrographical type of rocks Sample no Depth in borehole	Carbonate	Quartz	Biotite	Muscovite	Orthoclase	Argilized micas and kaolinite	Plagioclase	Loss of ignition (1000°C)	CO <sub>2</sub> in carbonates	Difference (Loss of ignition- CO <sub>2</sub> in carbonates)
	[% volume]									
Gneiss bi-mu kaol. 4449B 90.4-94 m	3 <sup>*</sup>	54	5	3	11	15	9	4.72	1.27	3.45
Gneiss bi-mu kaol. 4450 94-97 m	3	40	8	6	17	22	4 <sup>***</sup>	3.98	1.36	2.62
Gneiss bi-mu kaol. 4451 97-100 m	-	-	-	-	-	-	-	3.56	0.47	3.09
Gneiss bi-mu kaol. 4452 97.3-98.2 m	2 <sup>**</sup>	50	6	13	11	17	1	4.03	1.0	3.03
Gneiss bi-mu kaol. 4453 100-104 m	-	-	-	-	-	-	- <sup>***</sup>	3.01	0.50	2.51
Gneiss bi-mu 4454 108-111 m	*	40	4	6	15	20	15	3.36	0.36	3.00

Table 4.4 Modal composition of biotite-muscovite gneisses and metagranite. Type: Kateřinská hora Dome in Krušné hory (Ore Mts). Borehole no. 2A (depth under shaft mouth 90.4 -111 m)

Legend: Depths are given in meters under shaft mouth. Optical planimetry analysis of thin sections is perpendicular to metamorphic foliation; 3000–5000 points. Feldspars were not colored.

Carbonates: \* fine grained aggregates in matrix; \*\* as a filling in cracks; \*\*\* metasomatic reaction in feldspars.

Bi-mu – biotite-muscovite, kaol. – kaolinized, chlor. – chloritized.

#### 4.3.1 THE POROUS SYSTEM IN UPPER CRETACEOUS ROCKS AND POROSIMETRIC DATA

Silicification of sandstone and conglomerate resulted in the reduction of the primary system of configurative pores (primary porosity) produced by suitable configurations of clastic quartz grains. This primary system of pores is filled-in completely with newly formed quartz and there exist only cavities created by ex-solution (leaching out) of minerals due to circulation of solutions. The shapes of the porosimetric curves (Figs. 4.4a,b and 4.5a,b) are non-standard, pointing to irregular blocking of primary configurative pores due to intensive secondary silicification of matrix and regeneration of quartz grains (PLATE E, Figs E1 - E11). The size distribution of pores (the percentages attributable to the size categories A, B, C and  $\alpha$ ,  $\beta$ ,  $\gamma$ ) was given in Chapter 3.

Figures 4.4a,b and 4.5a,b presented the porosimetric curves, cumulative pore volume  $V_{\text{COP}}$  vs. pore diameter, and the incremental pore volume  $\Delta V_{\text{COP}}$  vs. pore diameter, for Cretaceous sediments.

#### 4.3.2 THE POROUS SYSTEM IN FRESH AND KAOLINIZED GNEISSES AND POROSIMETRIC DATA

In all the boreholes under examination, the rocks of the crystalline complex - porphyroblastic, coarse-grained, foliated gneisses to metagranites - became medium to hard kaolinized on their contact with the Cretaceous basement. Kaolinization affects, first of all, fine-grained feldspars in quartz-feldspars metatekt, and to a smaller extent, porphyroblasts in K-feldspars where kaolinization has only reached the edges of porphyroblasts and the vicinity of cracks. At the same time, coarse-grained carbonate deposited in pore cavities. The pore system of all the medium or slightly and hard kaolinized gneisses (Figs. 4.6a,b – 4.7a,b) – in contrast to fresh and very slightly kaolinized gneisses (Figs. 4.8a,b) – indicates that by argillitization processes, cavities or split pores are formed at sites where minerals dissolve; later, they are filled with newly formed minerals – kaolinite, carbonates, or quartz (PLATE E, Figs. E6 - E11). In spite of the fact that these rocks have a relatively high pore volume, their porosity values can change – as a result of irregular kaolinization – within the distance of decimeters to centimeters.

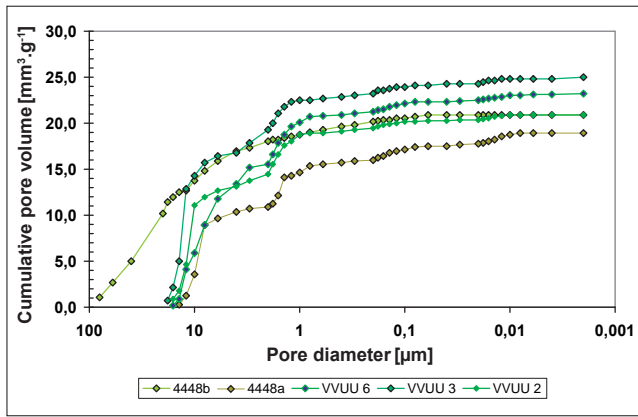


Fig. 4.4a Cumulative pore volume ( $V_{COP}$ ) vs pore diameter ( $\mu\text{m}$ ) for Cretaceous rocks - silicified conglomerates in boreholes KO-16 and V2A. High pressure mercury porosimetry. Drainage shaft Komořany.

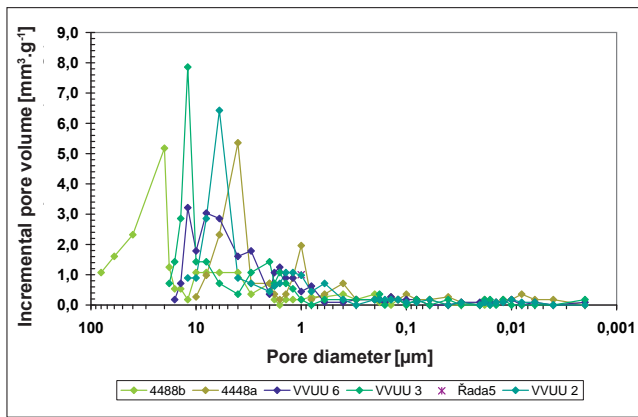


Fig. 4.4b Incremental pore volume ( $\Delta V_{COP}$ ) vs pore diameter ( $\mu\text{m}$ ) for Cretaceous rocks - silicified conglomerates in boreholes KO-16 and V2A. High pressure mercury porosimetry. Drainage shaft Komořany.

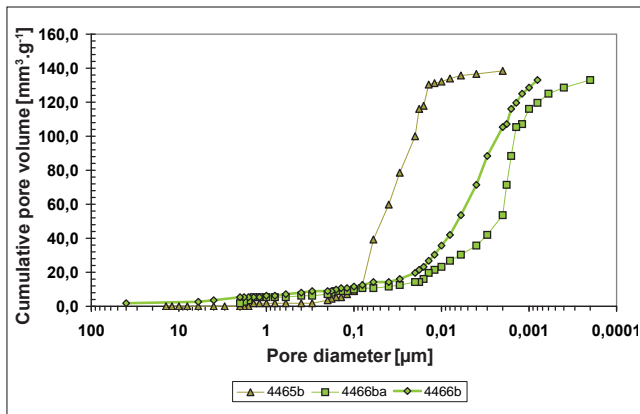


Fig. 4.5a Cumulative pore volume ( $V_{COP}$ ) vs pore diameter ( $\mu\text{m}$ ) for Cretaceous rocks - marlstone to glauconitic silty marlstone in boreholes KO-16 and V2A. High pressure mercury porosimetry. Drainage shaft Komořany.

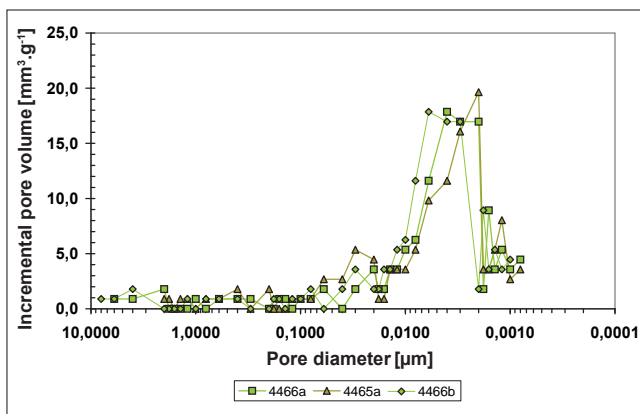


Fig. 4.5b Incremental pore volume ( $\Delta V_{COP}$ ) vs pore diameter ( $\mu\text{m}$ ) for Cretaceous rocks - marlstone to glauconitic silty marlstone in boreholes KO-16 and V2A. High pressure mercury porosimetry. Drainage shaft Komořany.

Petrographical type of rocks Sample no Depth in borehole	$V_{COP}$	$\rho_o$	$\rho_{sp}$	$P_{ef}$	Categories of pores			Categories of pores		
					A	B	C	$\alpha$	$\beta$	$\gamma$
	[mm <sup>3</sup> .g <sup>-1</sup> ]	[g.cm <sup>-3</sup> ]	[g.cm <sup>-3</sup> ]	[%]	[%V <sub>COP</sub> ]					
<b>BOREHOLE V2A</b>										
Sandstone glauconitic VVUÚ1 83 m	128.4	1.976	2.647	25.4	11	52	37			
Conglomerate VVUÚ 2 88.7-89.0 m	20.9	2.583	2.731	5.4	92	5	3			
Conglomerate VVUÚ 4448 89.4-90.4 m	18.97	2.579	2.711	4.89	84	10	6	62	30	8
	20.98	2.516	2.657	5.28	98	9	2	70	26	4
Conglomerate VVUÚ6 89.4-90.4 m	23.2	-	-	-	92	5	3			
<b>BOREHOLE KO-16</b>										
Marlstone 4465a 82.5-84.7 m	139.97	2.210	3.200	30.93	3	27	70	1	3	96
	139.21	1.872	2.531	26.06	2	27	71	2	3	95
Siltstone glauconitic 4466a 84.7-86.25 m	52.61	2.128	2.396	11.20	9	20	71	5	17	78
	53.76	2.275	2.592	12.23	8	15	77	5	9	86

Table 4.5 Porosimetric data for Cretaceous rocks from boreholes nos. V2A and KO-16 in Komořany shaft. High-pressure mercury porosimetry.

Conditions of measurement:

Porosimeter 2000 series Macropore 120, Carlo Erba Instruments. Samples cut from core 10 by 5 by 10 to 30 mm, dried at 105°C for 30 minutes and evacuated, before measurement, in low-pressure unit of porosimeter.

Interval of measured pores 3.7-56 000 nm, rate of pressure increase:

the pressure of 200 MPa was reached within 25 minutes; wetting angle of mercury 141.3°, surface tension of mercury 0480 N.m<sup>-1</sup>. Pore size categories A, B, C and  $\alpha$ ,  $\beta$ ,  $\gamma$  are shown below.

Legend:  $V_{COP}$  – cumulative pore volume;  $\rho_o$  – bulk weight,  $\rho_{sp}$  – specific gravity,  $p_{ef}$  – effective porosity. Kaol. – kaolinization.

Petrographical rock types	Total pore volume $V_{COP}$ [mm <sup>3</sup> .g <sup>-1</sup> ]	Effective porosity $p_{ef}$ [%]
Marlstone	139.9 - 139.2	26.06 - 30.9
Siltstone glauconitic	52.6 - 53.7	11.20 - 12.23
Sandstone glauconitic	128.4	25.4
Conglomerates silicified	19 - 23.2	4.89 - 5.4

Table 4.6 Porosimetric data for Cretaceous rocks in borehole no. KO-16 determined by high-pressure mercury porosimetry

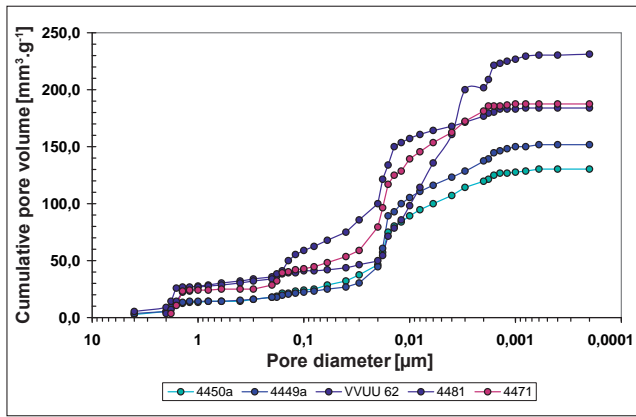


Fig. 4.6a Cumulative pore volume ( $V_{COP}$ ) vs pore diameter ( $\mu\text{m}$ ) for intensive kaolinized gneisses and metagranites from Cretaceous basement in boreholes KO-16 and V2A. High pressure mercury porosimetry. Drainage shaft Komořany.

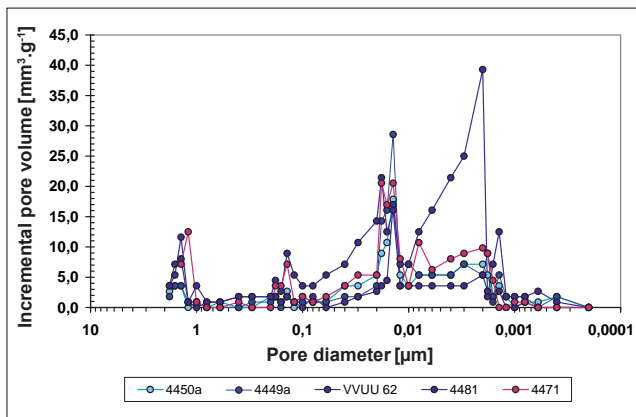


Fig. 4.6b Incremental pore volume ( $\Delta V_{COP}$ ) vs pore diameter ( $\mu\text{m}$ ) for intensive kaolinized gneisses and metagranites from Cretaceous basement in boreholes KO-16 and V2A. High pressure mercury porosimetry. Drainage shaft Komořany.

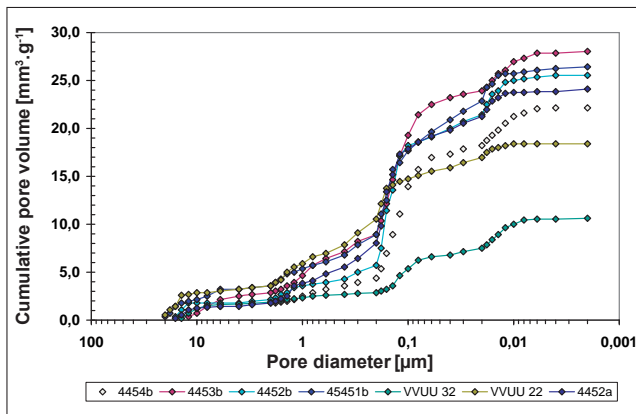


Fig. 4.7a Cumulative pore volume ( $V_{COP}$ ) vs pore diameter ( $\mu\text{m}$ ) for medium kaolinized gneisses and metagranites from Cretaceous basement in boreholes KO-16 and V2A. High pressure mercury porosimetry. Drainage shaft Komořany.

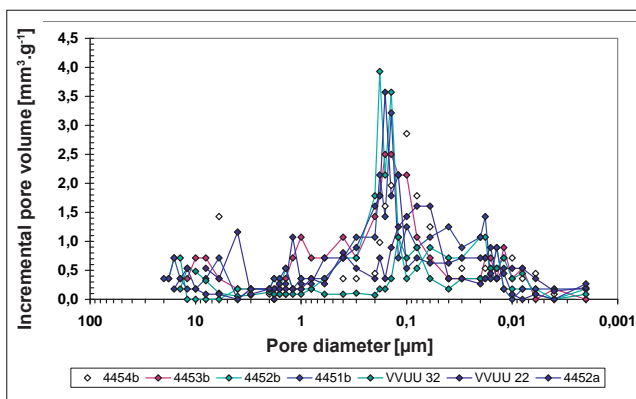


Fig. 4.7b Incremental pore volume ( $\Delta V_{COP}$ ) vs pore diameter ( $\mu\text{m}$ ) for medium kaolinized gneisses and metagranites from Cretaceous basement in boreholes KO-16 and V2A. High pressure mercury porosimetry. Drainage shaft Komořany.

Petrographical type of rocks Sample no Depth in borehole	$V_{\text{COP}}$	$\rho_o$	$\rho_{\text{sp}}$	$P_{\text{ef}}$	Category of pores			Category of pores		
					A	B	C	$\alpha$	$\beta$	$\Gamma$
					[% $V_{\text{COP}}$ ]					
<b>Borehole V2A</b>										
Metagranite kaol. VVUU4 92.5-92.9 m	39.5	2.381	2.628	9.41	19	56	25			
Gneiss bi-mu, kaol. 4449A 90.4-94.0 m	29.54	2.462	2.655	7.27	19	57	24	11	51	38
	30.43	2.451	2.648	7.46	17	57	26	10	48	42
Gneiss bi-mu, kaol. 4449B 90.4-94.0 m	38.42	2.418	2.666	9.29	22	53	25	11	50	39
	36.81	2.525	2.783	9.30	23	55	22	10	55	35
Gneiss bi-mu, kaol. 4450 94-97 m	26.05	2.500	2.675	6.52	22	53	25	12	47	41
	22.24	2,475	2.619	5.51	18	52	30	10	45	45
Gneiss bi-mu, kaol. 4451 97-100 m	28.35	2.472	2.659	7.01	22	48	30	11	40	49
	26.62	2.474	2.648	6.59	23	52	25	13	46	41
Gneiss bi-mu, kaol. 4452 100-104 m	24.16	2.522	2.685	6.09	22	60	18	7	64	29
	25.64	2.433	2.595	6.24	17	61	22	10	56	34
Gneiss bi-mu, kaol. VVUU5	44.02	2.410	2.697	10,65	46	41	13			
Gneiss bi-mu, kaol. 4453 104-108 m	45.32	2.399	2.692	10.87	37	49	14	8	70	22
	28.20	2.452	2.634	6.92	39	48	13	12	68	20
Gneiss bi-mu, kaol. 4454 108-111 m	17.54	2.547	2.666	4.47	24	56	20	12	59	29
	22.27	2.544	2.670	5.67	26	58	16	10	65	25
<b>Borehole KO-16</b>										
Gneiss bi-mu, kaol. 4469a 99-101.8m	42.90	2,449	2.737	10.51	35	50	15	8	67	25
	42.76	2.368	2.633	10.13	39	45	16	9	62	29
Gneiss bi-mu, kaol. 4470a 101.8-110.0 m	24.16	2.446	2.622	5.96	52	38	10	15	70	1
	24.55	2.699	2.776	6.38	45	44	11	17	66	17
gneiss bi-mu, kaol. 4471a 101.8-110.0m	7.49	2,611	2,663	1,95	25	55	20	14	49	37
	13.57	2.553	2.645	3.47	37	43	20	25	46	29
Gneiss bi-mu, fresh 4483a 131.3-131.45 m	8.56	2.613	2.674	2.24	44	38	18	29	43	28
	10.32	2.609	2.681	2.69	37	40	23	23	42	35
Metagranite fresh 4487a 112.2-112.9 m	20.93	2.502	2.640	5.24	19	53	28	14	44	42
	14.44	2.561	2.660	3.70	25	46	29	17	40	43
Gneiss bi-mu, fresh 4485a 128.0-128.7 m	10.77	2.658	2.736	2.86	32	39	29	17	41	42
	8.27	2.599	2.656	2.15	38	34	28	26	34	40
Gneiss bi-mu, kaol. 4481a 142.5-143.0 m	37.32	2.463	2.712	9.19	38	52	10	18	63	19

gneiss bi-mu, fresh VVUÚ 12 148-149 m	12.51	2.567	2.652	3.21	43	39	18	29	44	27
Gneiss bi-mu, kaol. 4508a 162.2-163.3 m	18.56	2.623	2.758	4.87	38	46	16	17	59	24
Gneiss bi-mu, kaol. VVUÚ 32 171.1-172.3 m	10.67	2.622	2.697	2.80	27	44	29	18	41	41
Gneiss bi-mu, low kaol. 4509a 185.3-183.45 m	17.61	2.583	2.706	4.55	32	55	13	16	64	20
Gneiss bi-mu, kaol. VVUÚ 52 206,-206.6 m	30.41	2.451	2.649	7.45	20	49	31	11	37	52
Gneiss bi-mu, kaol. VVUÚ 62 222-223.8 m	23.18	2.545	2.704	5.90	16	33	51	12	17	71
Gneiss bi-mu, low kaol. VVUÚ 72 231.7-232.6 m	9.58	2.641	2.719	2.60	48	32	20	38	29	33
Gneiss bi-mu, low kaol., chlorit. 4510a 240.2-241.7m	38.66	2.484	2.748	9.60	24	62	14	11	65	24

Table 4.7 Porosimetric data for crystalline basement rocks in boreholes V2A and KO-16. For conditions, see Table 4.5. Legend: Bi-mu – biotite-muscovite, kaol. – kaolinized, chlor. – chloritized.

Petrographical type of rock	Total pore volume $V_{COP}$ [mm <sup>3</sup> ·g <sup>-1</sup> ]
Gneiss biotite-muscovite, fresh or slight kaolinized	7.2 - 14
Gneiss biotite-muscovite, fresh or low, medium to hard kaolinized	10.3 - 28
Gneiss biotite-muscovite, intensive	130 - 225

Table 4.8 Comparison of total pore volume  $V_{COP}$  for non-kaolinized (fresh) or medium kaolinized and intensive kaolinized gneisses and metagranites in borehole no. KO-16. High-pressure mercury porosimetry

Figures 4.6a, 4.7a and 4.8a show porosimetric curves,  $V_{COP}$  vs. pore diameter. Figures 4.6b, 4.7b and 4.8b show incremental pore volume  $\Delta V_{COP}$  vs. pore diameter, for hard kaolinized gneisses, for slightly or medium kaolinized gneisses and metagranites and for fresh or very slightly kaolinized gneisses and metagranites.

Under propitious conditions, CO<sub>2</sub> can accumulate in these pore spaces by diffusion, first of all in zones adjacent to a joint system. Areas of metamorphic foliation can be considered as a migration route, too. Nevertheless, such areas need not be permeable throughout the whole block. The kaolinized surface of the crystalline complex in contact with basal Cretaceous sediments can be denoted as a joint/porous type reservoir of gas developed above the static groundwater level of mineralized and gas containing waters. In reality, the main medium that ensures

the permeability of a rock massif for gas and water is the system of open joints, thin fissures as well as fractured zones with local carbonate or quartz - hematite filling and surrounding alterations (chloritization of biotite, hematization of micas and feldspars, silicification, kaolinization of micas and feldspars, new pyrite formations). The open joints may be vertical and ramify themselves with changes in the size of the joint space in the vertical direction. The joints represent the main directions of CO<sub>2</sub> and water migration.

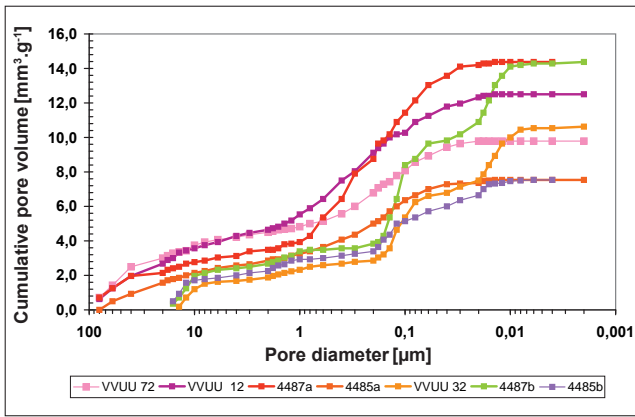


Fig. 4.8a Cumulative pore volume ( $V_{COP}$ ) vs pore diameter ( $\mu\text{m}$ ) for low kaolinized or fresh gneisses and metagranites from Cretaceous basement in boreholes KO-16 and V2A. High pressure mercury porosimetry. Drainage shaft Komořany.

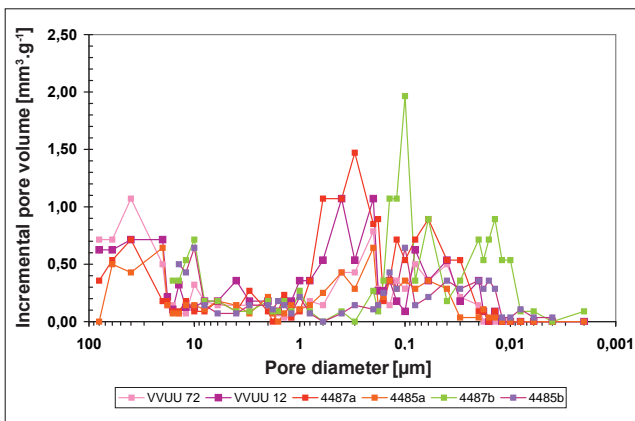


Fig. 4.8b Incremental pore volume ( $\Delta V_{COP}$ ) vs pore diameter ( $\mu\text{m}$ ) for low kaolinized or fresh gneisses and metagranites from Cretaceous basement in boreholes KO-16 and V2A. High pressure mercury porosimetry. Drainage shaft Komořany.

Petrographical type of rocks Sample no Depth in borehole	Depth of sample in borehole V2A and KO16	Bulk weight $\rho_0$	Uniaxial compressive strength $\sigma_{Pd}$	Splitting tensile strength $\sigma_{Pdt}$	Ratio $\sigma_{Pd}/\sigma_{Pdt}$	Tangent modulus $E_{pr}$	Poissons ratio $\mu$	Ultrasonic velocity
	[m]							
<b>BOREHOLE V2A</b>								
Conglomerate 4448	89.4-90.4	2510	154.9	9.00	17.21	60.51	0.11	5.346
<b>BOREHOLE KO – 16</b>								
Marlstone 4465a	82.5-84.7	1905	18.7	1.05	2.62	0.15	1.759	1.759
Glauconitic sandstone 4466a	84.7-86.25	2396	103.3	5.63	30.35	0.22	3.667	3.667
Conglomerate with hard silicification 4467a	86.5-89.8	2424	160.1	10.35	84.57	0.19	4.334	4.334
Gneiss bi-mu, slight kaol. 4468a	89.8-91.2	2469	154.2	12.9	74.50	0.15	4.397	4.397

Table 4.9 Average values of selected physical parameters of Upper Cretaceous rocks in boreholes nos. V2A and KO-16.

Legend: Depths are given from the mouth of shaft.

Bi-mu – biotite-muscovite, kaol. – kaolinized, chlor. – chloritized.

### 4.3.3 PHYSICAL PROPERTIES OF THE ROCKS

The physical properties of the rocks were tested using samples prepared from the bore core, on cylindrical bodies diameter 48 by 48 mm high, at a controlled laboratory humidity of ca. 2-3%. Bulk weight was determined according to the ČSN standard 72 1010 in force at the time; uniaxial compressive strength according to the ČS ON standard 44 11 11; splitting tensile strength according to the ČS ON standard 44 11 15. The results are shown in

*Tables 4.9 and 4.10* (Pipek et al., 1990; Martinec and Pipek, 1991). While Cretaceous rocks show a strengthening of the structure of clastic grains structure in sandstones and conglomerates by silicification, which manifests itself by high values of uniaxial compressive strength and splitting tensile strength, the rocks of the crystalline basement – gneisses and metagranites – show, on the contrary, a decrease of uniaxial compressive strength and splitting tensile strength with increasing kaolinization and, generally, argillitization of feldspars and micas (*Tables 4.9, 4.10*).

Petrographical type of rocks Sample no Depth in borehole	Depth of sample in borehole V2A and KO16	Bulk weight $\rho_0$ [kg·m <sup>-3</sup> ]	Uniaxial compressive strength $\sigma_{pd}$	Splitting tensile strength $\sigma_{pdt}$	Ratio $\sigma_{pd}/\sigma_{rat}$	Tangent modulus $E_{pr}$	Poissons ratio $\mu$ [-]	Ultrasonic velocity $v$ [km/s]
<b>BOREHOLE V2A</b>								
Gneiss bi-mu, kaol. 4449a	90.4-94.0	2400	33.3	2.82	11.80	10.64	0.26	3.288
Gneiss bi-mu, kaol. 4450a	94.0-100.0	2480	26.5	3.41	7.77	7.29	0.18	3.107
Gneiss bi-mu, kaol. 4451a	94.0-100.0	2450	25.2	2.61	9.65	7.42	0.21	3.330
Gneiss bi-mu, kaol. 4452a	100.0-104.0	2440	22,8	2.70	8.44	7.94	0.21	3.153
Gneiss bi-mu, kaol. 4453a	104.0-108.0	2410	31.7	2.93	10.80	11.90	0.22	3.019
Gneiss bi-mu, kaol. 4454a	108.0-111.0	2400	22.9	2.88	7.95	7.02	0.19	3.086
<b>BOREHOLE KO-16</b>								
Gneiss bi-mu, kaol. 4469a	99.0-101.8	2279	19.7	1.67	6.15	11.8	0.16	3.107
Gneiss bi-mu, kaol. 4470a	101.8-110.0	2499	52.1	3.55	18.76	14.7	0.31	4.063
Gneiss bi-mu, kaol. 4471a	101.8-110.0	2557	59.3	4.87	22.71	12.2	0.31	4.115
Gneiss bi-mu, kaol. 4481a	142.5- 143.0	2472	43.2	-	15.0	-	0.20	4.281
Gneiss bi-mu, fresh 4482a	138.2-139.0	2567	58.1	4.43	15.44	13.1	0.19	4.222
Gneiss bi-mu, fresh 4483a	131.3-131.45	2600	78.2	5.74	25.84	13.6	0.23	4.852
Pegmatite-metagranite fresh 4484a	126.0-126.2	2521	49.6	-	14.55	-	-	4.581
Gneiss bi-mu, fresh 4485a	128.0-128.7	2589	77.5	5.50	18.91	9.1	0.20	4.830
Gneiss bi-mu, kaol. 4486a	118.5-119.0	2514	46.0	6.26	13.39	7.3	0.16	3.740
Metagranite fresh 4487a	112.2-112.9	2563	69.3	5.10	17.74	13.6	0.22	4.571
Gneiss bi-mu, slight kaol. 4488a	107.5-108.0	2455	35.7	3.56	6.51	10.1	-	3.495
Gneiss bi-mu, slight kaol. 4508a	162.2-163.3	2470	54.9	4.61	17.59	11.9	0.18	4.159
Gneiss bi-mu, slight kaol. 4509a	185.3-186.45	2480	53.9	3.47	15.47	15.3	0.19	4,105
Gneiss bi-mu, kaol., chlor. 4510a	240.2-241.7	2420	46.6	3.26	15.33	14.3	0.19	3.843

Table 4.10 Average values of selected physical parameters of gneisses and metagranite in crystalline basement from boreholes nos. V2A and KO-16 (Pipek et al., 1990).

Legend: Bi-mu – biotite-muscovite, kaol. – kaolinized, chlor. – chloritized.

#### 4.4 GAS CONDITIONS IN KOMOŘANY DRAINAGE SHAFT AND IN BOREHOLES KO-16 AND V2A

When the Komořany drainage shaft was being sunk to the depth of 130 m under the shaft mouth, the production of carbon dioxide was 200 m<sup>3</sup> per 24 h; at the same time, the local concentration of CO<sub>2</sub> at the shaft bottom and under the shaft mouth was maintained, thanks to intensive ventilation, at 0.2-0.3% CO<sub>2</sub>. The permeability coefficients of two samples of concrete used for shaft lining, which were tested under face pressures of 3 MPa and 1 MPa, are given in *Table 4.11*. They served for estimating the sealing and isolating qualities of concrete when in contact with carbon dioxide. Such measurements indicated that the testpieces of concrete had a permeability higher by one order of magnitude than that of the surrounding rocks. Results of further measurements of gas permeability at a face pressure of 3 MPa for rock samples from the borehole KO-16 (Pipek et al., 1990) are given in *Tables 4.12 and 4.13*. It is evident that, on the scale of the rock structure with regard to the size of the samples (i.e., without any major influence of fracturing of samples along the foliation planes or joints) and at the indicated face pressure acting on the samples, fresh or even kaolinized gneisses or metagranites are impermeable or very little permeable. This very low permeability corresponds to the dimension of the pore system in these rocks.

#### RESIDUAL GASES IN ROCKS FROM BOREHOLE KO-16

The method proposed by the Coal Research Institute (VVOÚ) of Ostrava-Radvanice was employed where the core samples were enclosed in a gas-tight canister (*PLATE E, Fig. E12*) immediately after their separation from the core barrel. The content and qualitative composition of residual gases in the rock were determined using the above method, too. The results are given in *Tables 4.14 and 4.15*.

The analytical results can be interpreted as follows:

- The sequence of Upper Cretaceous basal sediments shows higher contents of CO<sub>2</sub>, viz., up to 0.16 cm<sup>3</sup>·g<sup>-1</sup>. The content of hydrocarbons is negligible.
- The sequence of the crystalline complex situated underneath the sequence of basal sediments of Upper Cretaceous and Miocene sediments, formed by more or less altered gneisses (kaolinization, carbonatization), contains small quantities of carbon dioxide (0.8% max.), carbon monoxide (0.55·10<sup>-4</sup> cm<sup>3</sup>·g<sup>-1</sup> max.), methane (10.3·10<sup>-4</sup> cm<sup>3</sup>·g<sup>-1</sup> max.) and higher hydrocarbons (1·10<sup>-4</sup> cm<sup>3</sup>·g<sup>-1</sup> max.).

It has to be pointed out that because of the high strength of rocks in the Cretaceous basement and of gneisses in the crystalline complex, disintegration of these rocks by grinding in the gas canisters was incomplete, and this

Samples	Coefficient of permeability		Diameter of sample	Length of sample
	[m <sup>2</sup> ] in pressure 3 MPa	[m <sup>2</sup> ] in pressure 1 MPa	[mm]	[mm]
Concrete I	0.797·10 <sup>-15</sup>	0.175·10 <sup>-14</sup>	58	49.6
Concrete II	0.770·10 <sup>-14</sup>	0.157·10 <sup>-13</sup>	58	26.4

Table 4.11 Gas permeability of concrete (type of concrete: B250) used for shaft lining – Komořany (Pipek et al. 1990)

Petrographical type of rocks / Sample no	Depth of sample in borehole KO-16 [m]	Coefficient of permeability	
		[m <sup>2</sup> ]	
		Perpendicular to core axis	Parallel to core axis
Glauconitic marlstone 4465	83.0-82.5-84.7	Destruction	0.336 · 10 <sup>-16</sup>
Conglomerate with silicification 4468	89.9-91.2	0.57 · 10 <sup>-16</sup>	0.172 · 10 <sup>-15</sup>
Gneiss bi-mu, kaol. 4469	99.0-101.8	Non-permeable	0.66 · 10 <sup>-16</sup>
Gneiss bi-mu, kaol. 4470	101.8-110.0	Non-permeable	Non-permeable
Gneiss bi-mu, slight kaol. 4471	101.8-110.0	Non-permeable	Non-permeable
Metagranite, fresh 4487	112.2-112.9	Non-permeable	0.73 · 10 <sup>-16</sup>
Gneiss bi-mu, fresh 4485	128.0-128.7	Non-permeable	Not determined
Gneiss bi-mu, fresh 4483	131.3-131.45	Non-permeable	Non-permeable
Gneiss bi-mu, kaol. VVOÚ 62	222.0-223.8	Non-permeable	Non-permeable

Table 4.12 Gas permeability under face pressure of 3 MPa for rock samples from borehole KO-16 (analyses by B. Hedvábný and M. Musilová in Pipek et al., 1990)

may have influenced the results of the canister tests. In addition, free gas contained in the massif in fissures and joints could not be accounted for in the canister tests (the core well is degassed rapidly and only the gas adsorbed on pore walls remains conserved). Therefore, the composition and quantity of gases tied up in joints, fissures and small-sized caverns in the rocks (representing

the main accumulation and migration system in the rock massif as a whole) cannot be established based on the above analyses.

Petrographical type of rocks Sample no Depth in borehole no 1A and 2A	Face pressure on sample	Coefficient of permeability	
		[m <sup>2</sup> ]	
	[MPa]	Perpendicular to core axis	Parallel to core axis
Glaukonitic sandstone 4400 84.3m	1	$1.768 \cdot 10^{-16}$	Not determined
Conglomerate with silicification 4405 88.7-89m	1	$0.329 \cdot 10^{-15}$	$0.245 \cdot 10^{-15}$
	2	$0.231 \cdot 10^{-15}$	$0.179 \cdot 10^{-15}$
	3	$0.226 \cdot 10^{-15}$	$0.172 \cdot 10^{-15}$
Gneiss bi-mu, kaol. 4406 91.0-91.4 m	1	$0.698 \cdot 10^{-16}$	Not determined
	2	$0.461 \cdot 10^{-16}$	
	3	$0.435 \cdot 10^{-16}$	
Gneiss bi-mu, kaol. 4407 92.5-92.9 m	5	$0.123 \cdot 10^{-17}$	Non-permeable
	6	$0.115 \cdot 10^{-17}$	
	7	$0.104 \cdot 10^{-17}$	
Gneiss bi-mu, kaol. 4408 106-107 m	2	$0.460 \cdot 10^{-17}$	Non-permeable
	3	$0.340 \cdot 10^{-17}$	
	4	$0.270 \cdot 10^{-17}$	
Gneiss bi-mu, kaol. 4320 96 m	1	$0.594 \cdot 10^{-14}$	Destruction
	2	$0.557 \cdot 10^{-14}$	
	3	$0.560 \cdot 10^{-14}$	

Table 4.13 Gas permeability under face pressure of 1 to 7 MPa for rock samples from boreholes 1A a 2A in Komořany shaft (analyses by B. Hedvábný and M. Musilová in Pipek et al., 1990)

Legend: bi – biotite, mu – muscovite, kaol. – kaolinization

Petrographical type of rocks/ Depth in borehole	CO <sub>2</sub>	CH <sub>4</sub>	C <sub>2</sub> H <sub>6</sub>	C <sub>2</sub> H <sub>4</sub>	C <sub>3</sub> H <sub>8</sub>	n-C <sub>4</sub> H <sub>10</sub>	i-C <sub>4</sub> H <sub>10</sub>	C <sub>3</sub> H <sub>6</sub>	CO	Σm	Frag
	[%]	[10 <sup>-4</sup> cm <sup>3</sup> · g <sup>-1</sup> ]							[g]	[%]	
<b>BOREHOLE V2A</b>											
Glauconite sandstone 85.0-85.1 m	0	1.90	0.26	0.13	0.19	0.06	0.07	0.12	0	652.5	89
Conglomerate with silicification 89.0-89.1 m	0.1	3.53	0.48	0.44	0.32	0.14	0.16	0.30	0.36	511.1	81
Conglomerate with silicification 91.3-91.4 m	0.16	4.75	0.61	0.33	0.48	0.08	0.12	0.22	0.22	673.8	16

Table 4.14 Contents and composition of residual gases in Cretaceous rocks from borehole no. V2A in Komořany shaft (canister tests with grinding of rock sample in canister).

Legend: Σm – total weight of sample in grams, frag – percentage of natural fragments of rock (above 3 cm)

Petrographical type of rocks Depth in borehole	CO <sub>2</sub>	CH <sub>4</sub>	C <sub>2</sub> H <sub>6</sub>	C <sub>2</sub> H <sub>4</sub>	C <sub>3</sub> H <sub>8</sub>	n-C <sub>4</sub> H <sub>10</sub>	i-C <sub>4</sub> H <sub>10</sub>	C <sub>3</sub> H <sub>6</sub>	CO	Σm	Frag
	[%]	[10 <sup>-4</sup> cm <sup>3</sup> · g <sup>-1</sup> ]								[g]	[%]
<b>BOREHOLE V2A</b>											
Gneiss bi-mu, kaol. 95.0-95.1 m	0.01	9.73	1.12	0.75	0.73	0.18	0.258	0.52	0.82	249,7	-
Gneiss bi-mu, kaol. 97.8-98.0 m	0	6.09	1.00	1.00	0.85	0.15	0.26	0.80	0.41	284.7	4
Gneiss bi-mu, kaol. 100.0-100.2 m	0,01	10.3	0.61	0.25	0.14	0.01	0.03	0.26	1.19	262.0	10
Gneiss bi-mu, kaol. 103.0-103.2 m	0,01	8.16	1.16	0.82	0.54	0.03	0.11	0.65	0.13	348.3	8
Gneiss bi-mu, kaol. 106.0-106.2 m	0,01	2.10	0.10	0.10	0.04	0.01	0.11	0	0.03	343.1	65
<b>BOREHOLE KO-16</b>											
Gneiss bi-mu, kaol. 109.0-109.15m	0.80	1.64	0.35	0.19	0.29	0.03	0.05	0.19	0.25	640.1	18.9
Metagranite fresh 112.0-112.15m	0.45	1.35	0.43	0.17	0.30	0.02	0.07	0.20	0.10	652.6	22
Gneiss bi-mu, kaol. 124.0-124.15m	0.26	0.95	0.48	0.21	0.41	0.05	0.14	0.25	0.04	636.2	30
Gneiss bi-mu, kaol. 133.0-133.15m	0.30	4.34	0.56	0.20	0.35	0.02	0.09	0.23	0.24	594.6	17
Gneiss bi-mu, kaol. 145.0-145.15m	0.30	7.06	1.04	0.69	0.48	0.03	0.05	0.55	0.55	597.0	2,5
Gneiss bi-mu, fresh 160.0-160.15m	0.21	2.50	0.46	0.46	0.33	0.05	0.08	0.27	0.13	652.5	2,4

Table 4.15 Contents and composition of residual gases in crystalline rocks (gneisses and metagranite) from boreholes nos. V2A and KO-16 (canister tests with grinding of rock sample in canister).

Legend: Σm – total weight of sample in grams frag – percentage of natural fragments of rock (above 3 cm), kaol. – kaolinization, bi – biotite, mu – muscovite.

## 4.5 SUMMARY

The example of the Komořany drainage points to the great importance of natural layers permeable for gases, tied to buried weathered crusts covered with isolating rock bodies where carbon dioxide can accumulate. The collector rocks as such (kaolinized gneisses and Cenomanian sandstones) exhibit structural changes (pore space morphology) provoked by interaction of groundwaters containing dissolved carbon dioxide with the rocks. When prospecting for collectors of this type and when examining their properties, due attention has also to be paid to the properties of the isolating rock horizons and of any changes thereof due to rock-groundwater-gas interactions. Any assessment of the suitability of potential gas reservoirs of this type for the sequestration of carbon dioxide must also bear in mind the influence of natural regional accumulation of this gas upon the storage capacity of the geological body).

## 5. CARBON DIOXIDE AND METHANE IN THE CZECH AND POLISH PARTS OF INTRA-SUDETEN BASIN

### 5.1 GEOLOGY, HYDROGEOLOGY AND GAS OCCURRENCES

The Intra-Sudeten Basin is divided into a Czech part and a Polish part (Fig. 5.1). This limnic basin corresponds to Lower Carboniferous – Viséan up to Permian. In the Czech part of the basin, coal seams are linked with the Žacléř Fm (Westphalian A-C), at the Lampertice Mbr (Šverma group of coal seams); the Prkenný Důl-Žďárky Mbr (group of coal seams Vilemína, Šrumfbach coal seam horizon, Strážkovice and U Buku groups of coal seams),

the Petrovice Mbr (Závřchy and Petrovice coal seam horizons). Also in the Odolov Fm (Westphalian D – lower part of Stephanian B), the Svatoňovice Mbr (Svatoňovice group of coal seams) and the Jívka Mbr (Radvanice group of coal seams and Vítovy doly group of coal seams) (Tásler et al., 1979) In the Polish part of the basin, the coal seams are linked with the Wałbrzych Fm (Namurian A) and the Žacléř Fm (Westphalian A-C) (Augustiniak, 1970, Augustiniak et Grocholski 1968, 1970; Nowak, 1992; Bossowski in Zdanowski et al., 1995). Occurrences of CO<sub>2</sub> or CO<sub>2</sub> and methane in the mines of the Intra-Sudeten Basin are shown in Fig. 5.1.

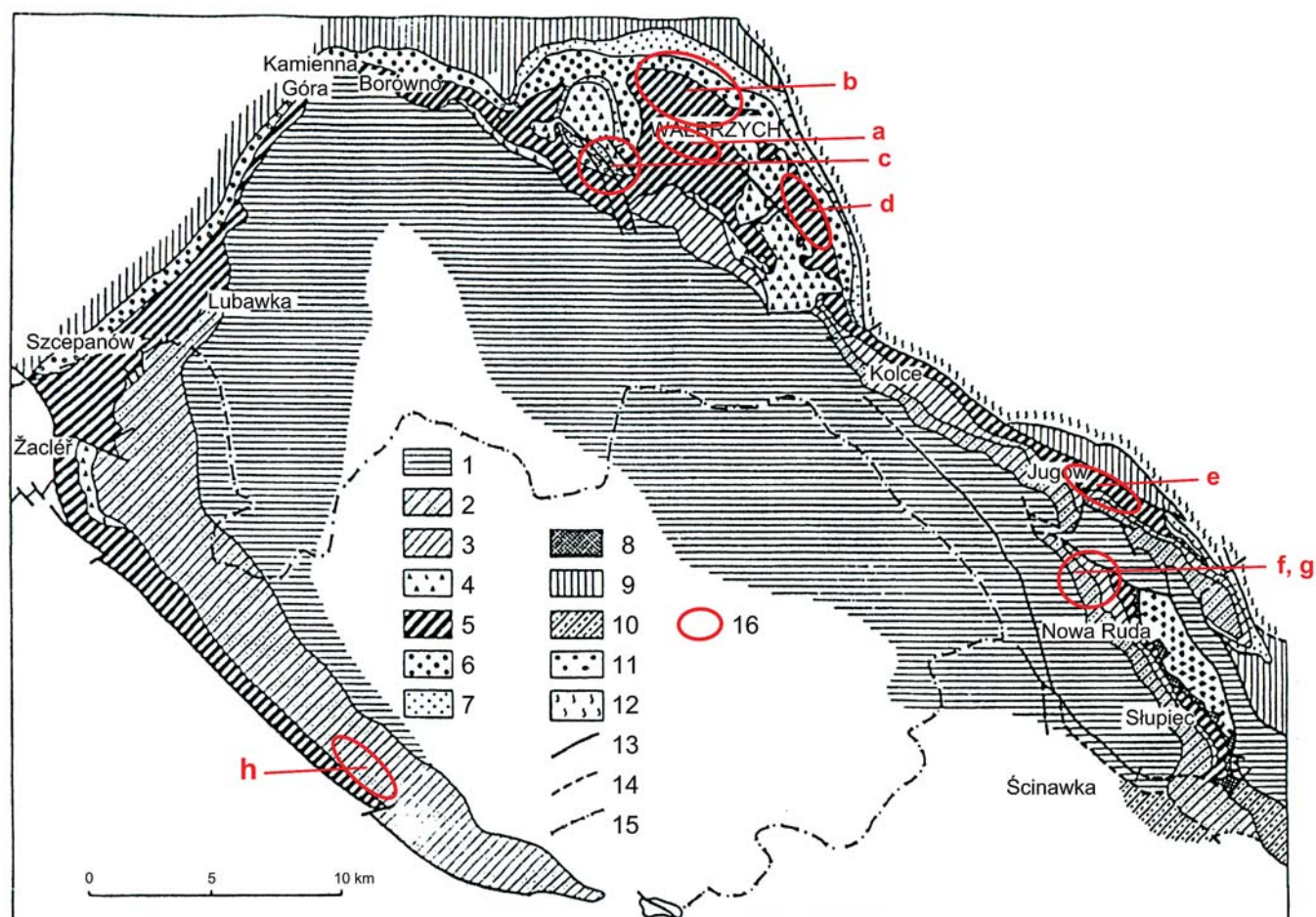


Fig.5.1 Geological map of the Intra-Sudeten Basin (adapted after Augustiniak, 1970, and Kruk et al., 1963)

Legend: red – gas, rock and coal outburst sites in mines.

Polish part: Sobiecin basin: a – Victoria Mine.

Wałbrzych district: b – Thorez Mine; c – Bolesław Chrobry Mine; d – Cezar - Zofia Mine.

Nowa Ruda district: e – Wacław Mine; f – Nowa Ruda – Bolesław Mine; g – Nowa Ruda - Piast Mine.

Czech part: h – Zdeněk Nejedlý Mine.

Geological units: 1 – Permian and younger strata; 2 – Chvoalč Fm (Stephanian C, Lower Autunian);

3 – Glink Fm (Westphalian D, Stephanian A); 4 – volcanic series above Carboniferous;

5 – Žacléř Fm (Upper Namurian C, Westphalian A-C); 6 – Odolov Fm, Svatoňovické and Jívec Mbr (Biało-Kamień Fm in Poland) (Namurian B-C); 7 – Wałbrzych Fm (Namurian A);

8 – weathering crust on Nowa Ruda gabro-diabase massif; 9 – Szczawen (Blażkow) Fm (Upper Viséan);

10 – crystalline basement – phyllites, 11 – gabro and diabase in Nowa Ruda massif;

12 – verified faults, 13-14 – assumed faults; 15 – the Czech-Polish frontiers.

CZECH PART OF THE INTRA-SUDETEN BASIN				POLISH PART OF THE INTRA-SUDETEN BASIN							
				NOWA RUDA		WAŁBRYCH		STUPIEC			
System Stage - Substage	Formation	Member	Coal seams key horizon	Formation	Coal seam No.	Formation	Coal seam No.	Formation	Coal seam No.		
Carboniferous	Stephalian	C									
		B	Odolov	Jívka	Radvanické	Glink	Glink	Glink			
		A									
		Cantabrian		Svatoňovice	Svatoňovice						
	D										
	Westphalian	C	Žaclěř	Petroviče							
		B		Prkenný důl Žďárky	Strážkovické Žaclěř	Žaclěř	301 425	Žaclěř	301 321 423 448	Žaclěř	301 304 409 415
		A		Lamprechtice	Dolu Jan Šverma						
	Namurian	C			Biały Kamień						
		B			Wałbrzych	601 623	Wałbrzych	655	Wałbrzych		
		A									
	Viséan		Blažkova				Szczawno				

Table 5.1 Stratigraphy of the Permo-Carboniferous in the Czech and Polish parts of the Intra-Sudeten basin and occurrences of methane and carbon dioxide (for the Czech part, after Tásler et al., 1979, adapted; for the Polish part, after Bossovski in Zdanowski et al., 1995 adapted).

## 5.2. THE CZECH PART OF INTRA-SUDETEN BASIN

The Czech part of the Intra-Sudeten Basin, namely the coalfields of what used to be Východočeské uhelné doly (East Bohemian Coal Mining Company), is comprised of the following four mining districts: Žaclěř District with Šverma Mine, Svatoňovice District with Zápotocký and Důl Pětiletka Mines, Radvanice District with Kateřina (Stachanov) Mine, and Žďárky District with the abandoned Vilemína Mine (1922). The history of mining of bituminous coal in these districts encompasses the period from 1576 (in Žaclěř District) until 1990, the end point of all coal mining in the region. Nowadays, all these mines are completely closed down.

Occurrences of methane (without CO<sub>2</sub>) were registered only in Jan Šverma Mine, mainly in the lower part of the Lampertice Mbr in the Žaclěř Fm (Westphalian A, Namurian B - C). In the borehole 20/71 in Jiří coalfield, a high content of methane was registered in the underlying bed of no. 11 lower coal seam, together with crude mineral oil of light paraffin base type (Franke and Středa, 1975). When coal was mined in the SE part of the coalfield at the former Zdeněk Nejedlý Mine (Malé Svatoňovice – Odo-

lov), in the vicinity of no. 3 Žďárky coal seam, dynamic gas effects and outbursts were observed, accompanied by evolution of CO<sub>2</sub> and methane. Such dynamic gas effects and outbursts of carbon dioxide and methane have not been studied yet in detail because of poor access to primary documentation. That is why special attention is paid to these cases.

### 5.2.1 GEOLOGICAL SITUATION CONDUCIVE TO THE OCCURRENCE OF CARBON DIOXIDE AND METHANE IN ZDENĚK NEJEDLÝ MINE

In the Prkenný Důl – Žďárky Mbr (Westphalian B, Žaclěř Fm), the coalfield of Zdeněk Nejedlý Mine includes 8 (or 9) developed coal seams, denoted as Žďárky coal seams (Hošek, 1968a); they are numbered from the base to the roof of the members. J. Středa in Tásler et al. (1979) describes these seams under the name of the Strážkovice group of coal seams. In the Prkenný Důl – Žďárky Mbr, the most important seam is no. 3 Žďárky coal seam (identical to the no. 3 coal seam of Strážkovice group of coal seams as designated by Tásler et al., 1979).

## PROPERTIES OF COAL AS A MEDIUM FOR SORPTION OF CARBON DIOXIDE AND METHANE

The seams of Strážkovice group in the Prkenný Důl – Žďárky Mbr (in the area of former Zdeněk Nejedlý Mine) are characterized by a maceral composition of coal with predominance of vitrinite-collinite, with a smaller quantity of telecollinite. Among inertinites, the most frequent ones are fusinite and semifusinite; also present are sklerotinite, mikrinite, and inertodetrinite; among exinites, microsporinite is abundant, while cutinite, rezinite and macro-sporinite occur more sporadically. In most cases, the coal seams contain medium to high contents of vitrinite which indicates the presence of petrologic facie with vitrinite-fusinite, characteristic of forest peat bogs. The chemical and technological parameters for no. 3 Žďárky coal seam show average values of ash content  $A^d = 28.35\%$ , volatile matter  $V^{daf} = 31.02\%$ , at seam thicknesses ranging from 0.53 to 2.04 m (Honěk and Schejbal, 1972; J. Středa and B. Žáková in Tásler et al., 1979). In the framework of the Prkenný Důl – Žďárky Mbr, the coalification of the Strážkovice group of coal seams is expressed by an interval of  $V^{daf}$  contents (33.08 to 29.07 %). The elemental composition of dry and moisture-free matter in coal of the no. 3 Žďárky coal seam,  $C^{daf} = 84.89\%$ ,  $H^{daf} = 5.16\%$ ,  $O^{daf} = 7.48\%$ ,  $N^{daf} = 1.09\%$ ,  $S_{pr}^{daf} = 1.38\%$ , also corresponds, at  $V^{daf} = 31.02\%$  as mentioned above, to the composition of the Strážkovice (Žďárky) group of coal seams (J. Středa and B. Žáková in Tásler et al., 1979). The maceral composition of the coal, its chemical properties, and the degree of coalification are very favourable for the sorption of methane and  $CO_2$  on the coal matter.

## SANDSTONE AND CONGLOMERATE AS A NATURAL RESERVOIR OF CARBON DIOXIDE

In the Czech part of the Intra-Sudeten Basin there are rocks that could in the future be used as reservoir rocks in gas storage installations. They exhibit porosities of several per cent and are located in the deeper parts of the Lampertice – Žďárky Mbrs, which are formed of dominant conglomerates and sandstones with layers of aleuropelites and coal in the Kralovec – Žaclěb area; the same applies to the deepest parts of the Lampertice – Žďárky Mbrs (conglomerates with sandstones) (62%) with layers of aleuropelites (~27%) and coal (~0.3%) in that part of Zdeněk Nejedlý Mine which is far removed from the Hronov thrust. The psammites have a favourably high ratio of stable rock fragments and pebbles rich in quartz; the rock cement is carbonate-clayed. Carbonates are represented by calcite or siderite, clay matter is a mix of illite and kaolinite. Data on rock properties are scarce. The suitability of aquifer rocks for possible  $CO_2$  storage should be verified in the above localities by lithofacial analysis as well as by determining the porometric parameters of reservoir and insulation rocks and by examining the tectonic structure. The sorption properties of coal in the coal seams are propitious; therefore, it is also possible to consider the possibility of sorption of gas on coal seams.

## WHAT MAKES NO. 3 ŽĎÁRKY SEAM TO A NATURAL $CO_2$ RESERVOIR?

The occurrences of  $CO_2$  and methane in the SE section of Zdeněk Nejedlý Mine are linked with no. 3 Žďárky seam (no. 3 Strážkovice seam), at depths of 130 m to 364.8 m under the sea level. That is an area with a relatively undisturbed deposition of seams in the Prkenný důl – Žďárky Mbrs (Žaclěb Fm) with dips of 20-35° approximately towards NE, in an area not affected by the Hronov thrust. In this area, tectonic faults of a small amplitude run in the NNW-SSE direction, dipping to NNE and NE-SW, with a shear dip towards the NW. The heavy disturbance and shear dip of seams and of the Prkenný důl – Žďárky Mbrs in the vicinity of the Hronov thrust were favourable for a deep degassing of the massif. On the contrary, the deeper parts situated out of this tectonically active zone in the SW section of Zdeněk Nejedlý Mine, where there is a favourable sedimentary development of overburden of a Carboniferous complex, were sufficiently insulated (Fig. 5.2). Nevertheless, the origin of gases ( $CH_4$  and  $CO_2$ ) in the Carboniferous massif is unknown here, too. Potential sources of the gases include: younger Permo-Carboniferous volcanism; diagenetic processes connected with coalification (thermogenic methane and  $CO_2$ ); mantle sources; and  $CO_2$  linked to Tertiary volcanism of the third volcanic phase. No evidence (isotopic  $CO_2$  and  $CH_4$  compositions) from this mining district is available. Occurrences of methane and carbon dioxide in the above mining district show that, in certain geological environments, there exist natural conditions for the accumulation of both gases in reservoir in coal seams, in rock pores or in fissures present in the rock massif. Whether this is the case of a purely sorption type reservoir (coal seams) or a porous sorption type reservoir (rocks – coal seams), cannot be deduced from the documentation on the presence of these gases produced at the time when the events of gas occurrence were investigated.

### 5.2.2 OCCURRENCES OF CARBON DIOXIDE AND METHANE, MIXED OUTBURSTS OF COAL AND GASES

According to the legacy documentation obtained from Zdeněk Nejedlý Mine, no cases of evolution of  $CO_2$  and methane were known before 4<sup>th</sup> July, 1985 which could have been qualified as „outbursts of coal and gas” – as documented by the letter of 1<sup>st</sup> September, 1990 authored by VUD s.p. (East Bohemian Coal Mining Company, State Enterprise), ref. no. 1159/90/Ce)<sup>5)</sup>. Nevertheless, after that date, seven mixed outbursts of coal and gas or gaseous dynamic effects occurred in the SE part of the Zdeněk Nejedlý Mine coalfield, namely in the no. 3 Žďárky seam area. The area prone to outbursts of coal and gas in the SE part of this coalfield is delimited by the boundary of the Rtyně v Podkrkonoší coalfield and, in the SE, by the area extending from the straight line connecting the co-ordinates  $y = 620\ 155$  m,  $x = 1\ 009\ 665$  m and  $y = 616\ 299$  m,  $x = 1\ 007\ 318$  m. Zdeněk Nejedlý Mine was classified as belonging to Danger Class One Mines; the no. 3 Žďárky

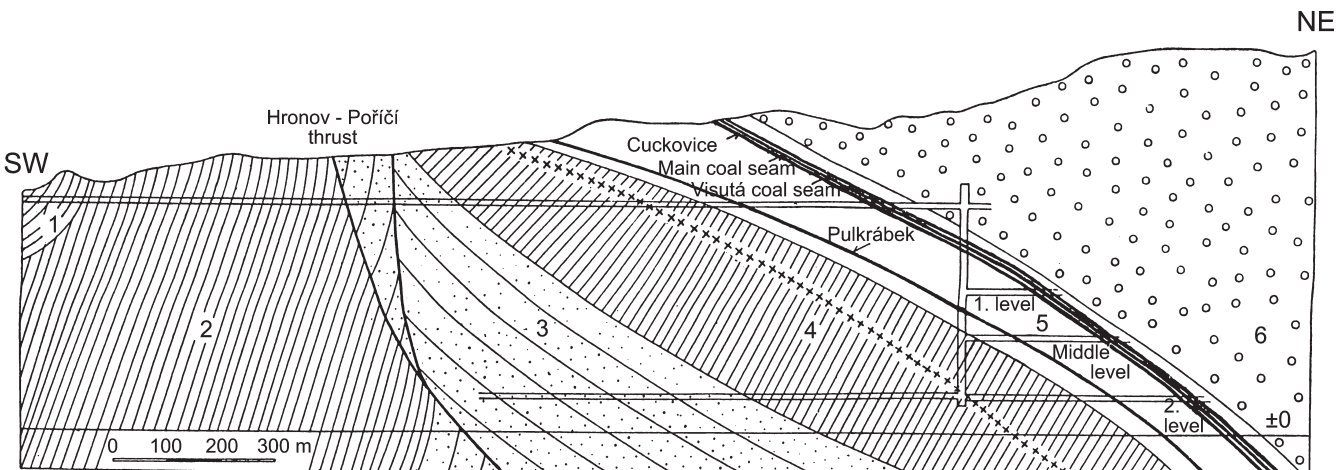


Fig. 5.2 Geological cross-section of Hronov-Poříčí fault (according to Prouza in Havlena, 1964, adapted).

Legend: 1 – Upper Cretaceous; 2 – Permian; 3 – Žalčář Fm with Prkenný Důl - Žďárky Mbr; 4 – lower part of Svatoňovice Mbr; 5 – upper part of Svatoňovice Mbr ; 6 – Žaltman facies of Jívka Mbr.

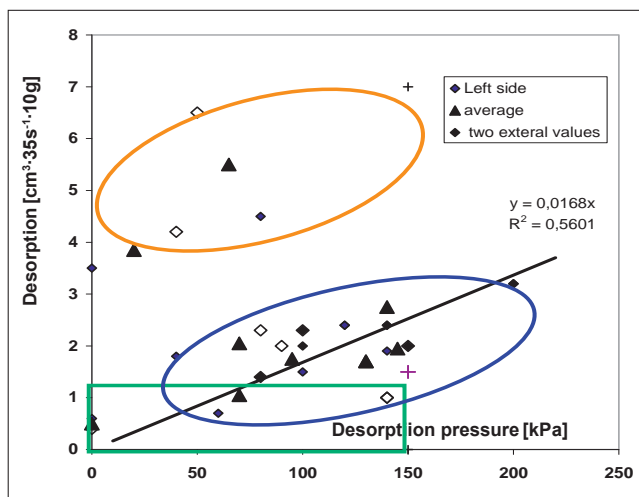


Fig. 5.3 Relationship between desorption pressure and volume of desorbed (evolved) gas (more than 88% CO<sub>2</sub>) in boreholes in left-hand and right-hand walls of the gallery, and average values.

Zdeněk Nejedlý Mine, galleries no. ch3-5212-4 (21. 06. - 27. 06. 1988) and no. ch3-5001 (1. 07. - 3. 07. 1987).

For gas composition, refer to Table 5.2. Green field denotes the area of subcritical pressures and of gas desorption as per the VUD Instruction.

coal seam was classified, in its SE part of the coalfield, as belonging to the category of seams threatened by outbursts of coal and gases.

Existing mine documentation relating to the aforementioned outbursts of coal and gas or to dynamic gas effects lacks any detailed geological and geomechanical evaluation of the localities, such as a determination of the physical properties of rocks and coal from the outburst sites, data on petrographical (maceral) composition of coal, on the properties of seams at the outburst sites, the intensity and type of tectonic faults in the seams and in surrounding rocks, the tectonic structure in the surroundings, etc. Data on gas desorption measurements carried out by a method specified in a VUD Instruction (see Note 3) are available from some outburst sites (e.g., from the four outbursts and the site of the third dynamic gas effect; these are shown, for the sake of completeness, in Fig. 5.3. It is evident from Fig. 5.3 and from the analysis of gas liberated from test boreholes (Table 5.2) that the gas which was dominant in the coal matter of the seam was adsorbed CO<sub>2</sub> (more than 95 %), while the methane content was up to 1%. The gas composition in the cavern at the site where the gas desorption measurements were carried out was as follows: 13.8% CO<sub>2</sub>, 3.9% CH<sub>4</sub>, and 17% O<sub>2</sub>.

In all cases, the critical values of desorbed gas pressure and desorbed gas volume specified by the Instruction were exceeded. In the relationship between the values of desorbed gas pressure and of desorbed gas volume, two phenomena could be identified: one would indicate normal conditions of CO<sub>2</sub> desorption (at the temperature and pressure prevailing in the coal seam) – (Fig. 5.3 – violet field), and the other would indicate anomalous values of desorbed gas (Fig. 5.3 – blue field). Further data required for a detailed analysis are not available.

**Note 5):**

VUD (East Bohemia Coal Mining Company) Instruction relating to ČBÚ (Czech Mining Authority) Regulation 6000/77 (concerned with the prevention of outbursts) gives this the critical parameters:

Critical values for stress relieving blasting works according to the Instruction:  $p > 150 \text{ kPa}$ ,  $\text{desorption} > 1.5 \text{ cm}^3 \cdot 10\text{g}^{-1} \cdot 35\text{s}^{-1}$  (Desorbometer DES-bl). The blasting charges used for stress relief blasting were of a weight of 0.6-1.6 kg/borehole, 5 m long; alternatively, as a preventative measure, the pillar was disintegrated by applying pressurised water.

**OUTBURSTS OF COAL AND GASES AND DYNAMIC GAS EFFECTS**

Sources for reference to data from this locality are missing. The only information available includes unpublished archival materials of the Central Mine Rescue Station of East Bohemian Coal Mining Company and eyewitness accounts which document these cases of coal and gas outbursts and dynamic gas effects that occurred at the mines.

**FIRST COAL AND GAS OUTBURST**

On 20<sup>th</sup> November, 1986 after a rock blasting operation performed at 1.48 h at the face of no. 412 crosscut, a mixed outburst of coal and gas occurred at the stationing point 1,462.8 m, at an elevation of -130 m under the sea level, some 5 m into the overburden of the no. 3 Žďárky coal seam. The outburst site is situated in the SE part of Zdeněk Nejedlý Mine. The crosscut no. 412 passed nos. 6 and 5a,b Žďárky coal seams (Žďárky Fm) and, at the stationing point 1473 m, should have reached the no. 3 Žďárky seam. At the distance of 1360 m into the no. 412 crosscut, a NE-SW thrust was encountered which had a dip of 88° towards NW and a displacement of 3.0 m. In-between this fault and the gas outburst site at the stationing point 1,462.8 m, the strata ran in a fairly regular fashion, with a dip of 19-30° towards NE.

The drifting progressed in sandstone with an irregularly developed strip of coal 5 to 18 cm thick and with siltstone (in overburden) and grey claystone (in base). The strip ran through the middle of the face and had a total thickness of 15 to 20 cm. After having drilled the boreholes for rock blasting, no methane or CO<sub>2</sub> was detected in the boreholes. A gaseous mixture of methane and CO<sub>2</sub>

was liberated due to the rock blasting operation. In the face where the siltstone, coal and claystone layers continued and were in contact with a steeply sloping tectonic surface, there appeared a cavern in the sandstone at the right-hand side of the face. The cavern was delimited by the tectonic surface on the right-hand side of the face; its size was 1.5 by 0.2 m; within the depth of 2 m it shrank to 0.5 m; its length was 4.5 m; it was elongated in the direction of a minor tectonic fault (Fig. 5.4a, b). Water was flowing out of the cavern. According to data obtained from continuous-action methane and carbon dioxide analyzers, of type UNOR (CO<sub>2</sub>) and type IREX (CH<sub>4</sub>), respectively, a total of 211 m<sup>3</sup> CO<sub>2</sub> and 608 m<sup>3</sup> methane were liberated. The maximum instantaneous CO<sub>2</sub> content was estimated to have been 2.6%. It took one hour for the CO<sub>2</sub> content to decrease below 1%. A total of 1.5 ton of coal and coal dust were ejected.

**SECOND COAL AND GAS OUTBURST**

The second coal and gas outburst occurred on 7<sup>th</sup> June, 1987 after a rock blasting operation performed at 17.30 h in the no. 3/5001 mine working, at stationing point 1548.5 m, at spot elevation -241 m (y = 618 773 m, x = 1 001 537 m), in the SE part of the coalfield. The working was drifted in the no. 3 Žďárky coal seam 1.8 m (1.5-2.5 m) thick dipped 25° towards ENE, with siltstones in the base and sandstones in the overburden. A thrust was encountered in the forefront of the face, at the stationing point 1425 m, and a small dip-slip fault was found at the stationing point 1525 m. In this section, the bedding had a general dip of 20-25° towards ENE. Composition of natural gases in testiry bozeholes is in Table 5.2.

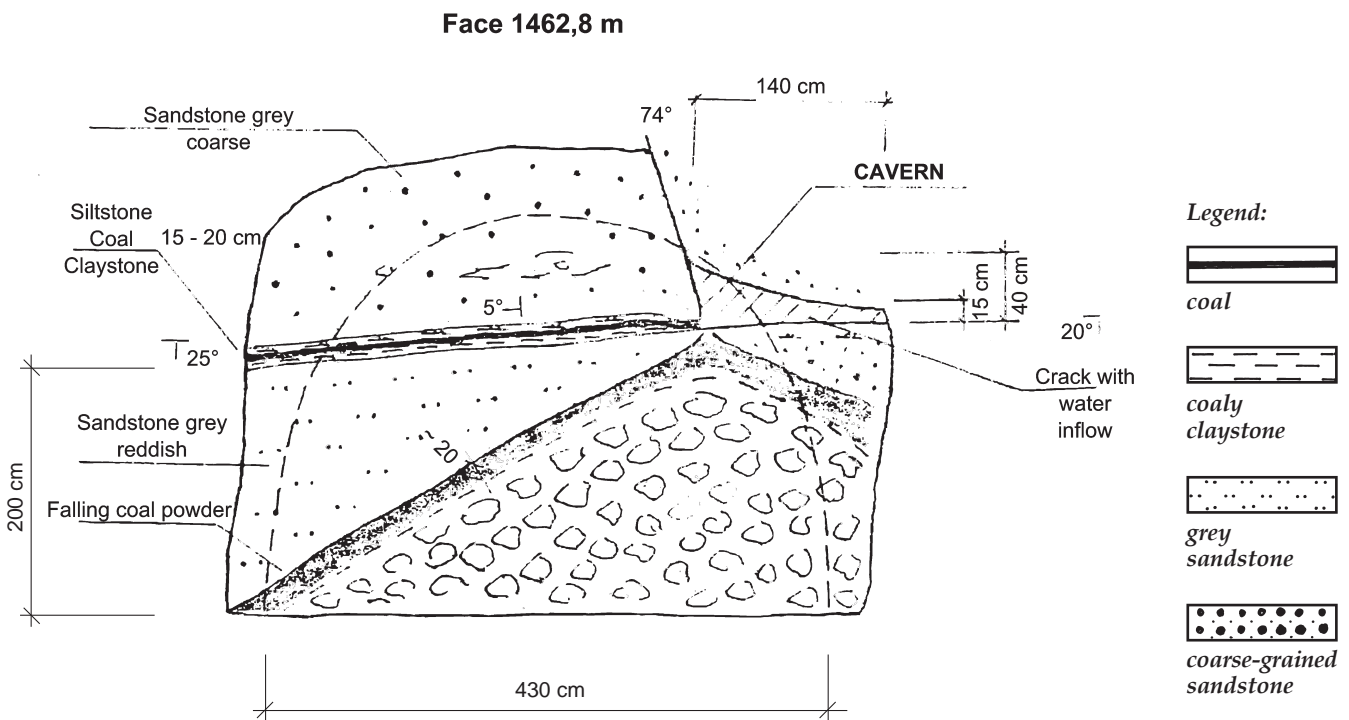


Fig. 5.4a The no. 1 outburst of gases and coal. Face and ground plan of cross-heading no. 412 at the distance of 1462.8 m, elevation -130.3 m, following an outburst in the SE area which is an area threatened by gas and coal outbursts. Documentation by ODMG VUD, Zdeněk Nejedlý Mine in Malé Svatoňovice – adapted.

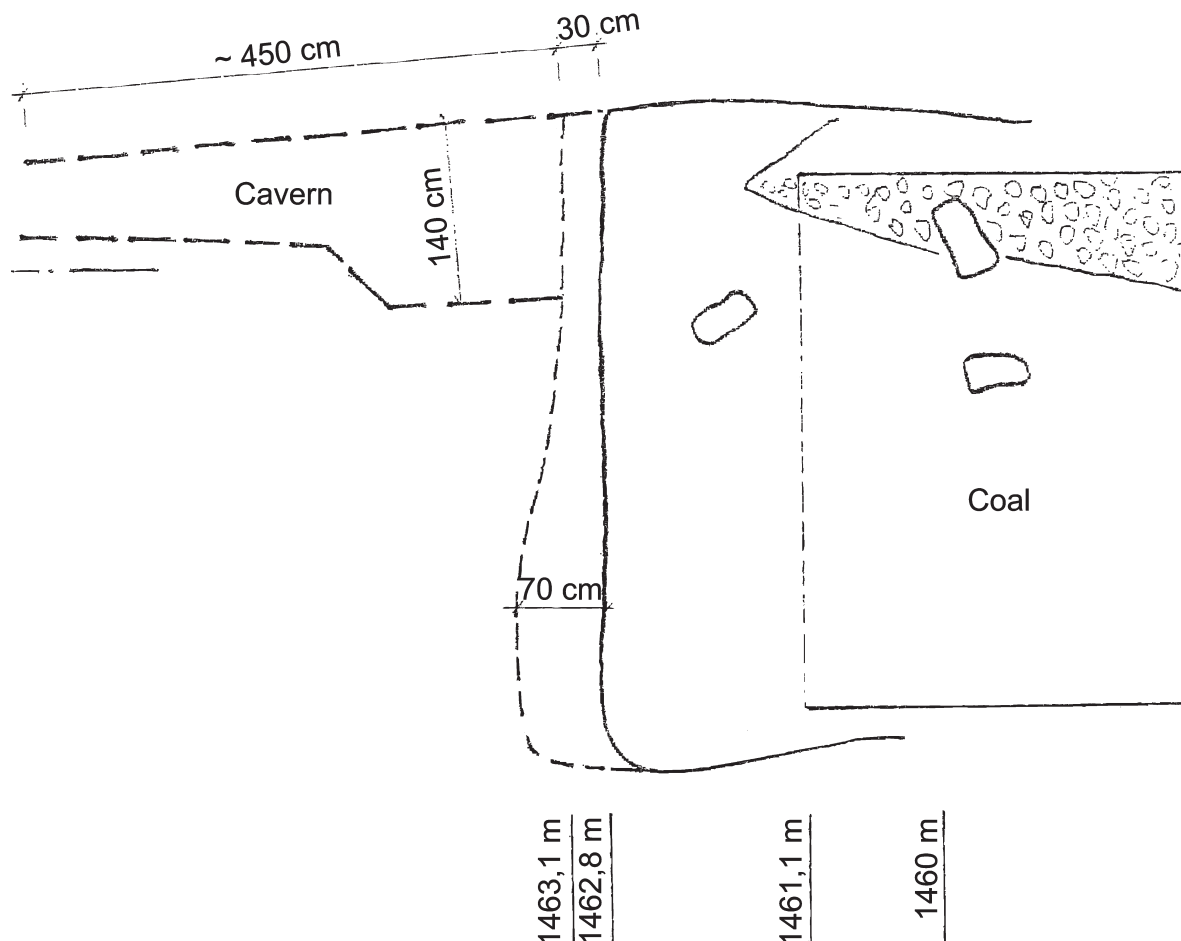
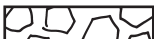


Fig. 5.4b The no. 1 gas and coal outburst. Face and ground plan of cross-heading no. 412 at the distance of 1,462.8 m, elevation -130.3 m, following an outburst in the SE area which is an area threatened by gas and coal outbursts. Documentation by ODMG VUD, Zdeněk Nejedlý Mine in Malé Svatoňovice – adapted.

Legend:

 rock inrush with dusty coal

After having drilled 25 blasting holes for rock blasting, for which a total of 12 kg of Ostravite charge was used, gas burst out in the working. Within approximately 3 hours after aerating the site, an atmosphere containing 2% of CO<sub>2</sub> / methane mixture was detected in the zone of breathing, 20 m away from the face, and a 4% gas mixture was present at the face proper. The outburst opened a cavern at the seam / overburden interface, in absence of any obvious tectonic pre-disposition. The opening of the cavern having 0.5 by 0.7 by 5 m in size was accompanied by a heavy disturbance of the overburden rocks (*PLATE F – Figs. F1, F2, F3, F4*). Due to the outburst, 130 m<sup>3</sup> CO<sub>2</sub> and 1.5 ton of fine-sized coal and coal dust were ejected. The following gas contents were found by analysis of gas samples taken from the test boreholes at the depth of 3 m.

### THIRD DYNAMIC GAS EFFECT WITH SLIDE-UP OF ROCKS AND WITHOUT ANY SIGN OF OUTBURST

On 6<sup>th</sup> July, 1988 at 0.40 h, in the no. 3/5212 drifting gallery, after blasting (2.8 kg of Ostravite C and 7 pieces of

DEMZb electric blasting caps) performed at 23.15h on the day before, a weak roof was discovered in the no. 3 Žďárky coal seam, and a slide-up of coal was observed together with an upsurge of gas at the face (to a concentration higher than 10% of CH<sub>4</sub>+CO<sub>2</sub>). This event was managed without complications and was not classified as an outburst. The slide-up involved some 10 tons of rocks, and the gases liberated amounted to 20 m<sup>3</sup> of CO<sub>2</sub> and 10 m<sup>3</sup> of CH<sub>4</sub>. In the overbreak, the recorded gas contents were CO<sub>2</sub> 1.2%, CH<sub>4</sub> 0.6%, O<sub>2</sub> 20.4%, CO 0%, and hydrogen 0.6% (according to the protocol from Zdeněk Nejedlý Mine dated 28<sup>th</sup> July, 1988).

### FOURTH COAL AND GAS OUTBURST

A slide-up of coal from the no. 3/5212 face occurred again on 23<sup>rd</sup> July, 1988 at 3.45 h on the 5<sup>th</sup> level of no. 3 Žďárky coal seam, at the stationing point 45.3 m; the slide-up was 1.5-2 m long and took place again in the SE part of the coalfield (*Fig. 5.5, PLATE F, Fig. F5, F6*). The drifting operation involved raising, at an angle of 20°, at the depth of 232.1 m under the sea level. Prior to rock

Date	Distance	CO <sub>2</sub>	CH <sub>4</sub>	O <sub>2</sub>	CO	Face: left-hand or right-hand side
	[m]	[%]				
1.07.1987	1543.5	88.0	0.8	3.1	0	left
		98	0.8	0.8	0	right
2.07.1987	1546.5	95.0	1.0	2.0	0	left
		98.0	0.5	1.0	0	right
3.07.1987	1548.5	98.0	0.6	0.8	0	left
		96.0	0.4	1.5	0	right
3.07.1987	1548.5	13.8	3.9	17.0	traces	cavern after outburst

Table 5.2 Composition of natural gases in testing boreholes  
(VUD, Zdeněk Nejedlý Mine, attachment to Protocol by OBÚ Trutnov, dated 3. 07. 1987)

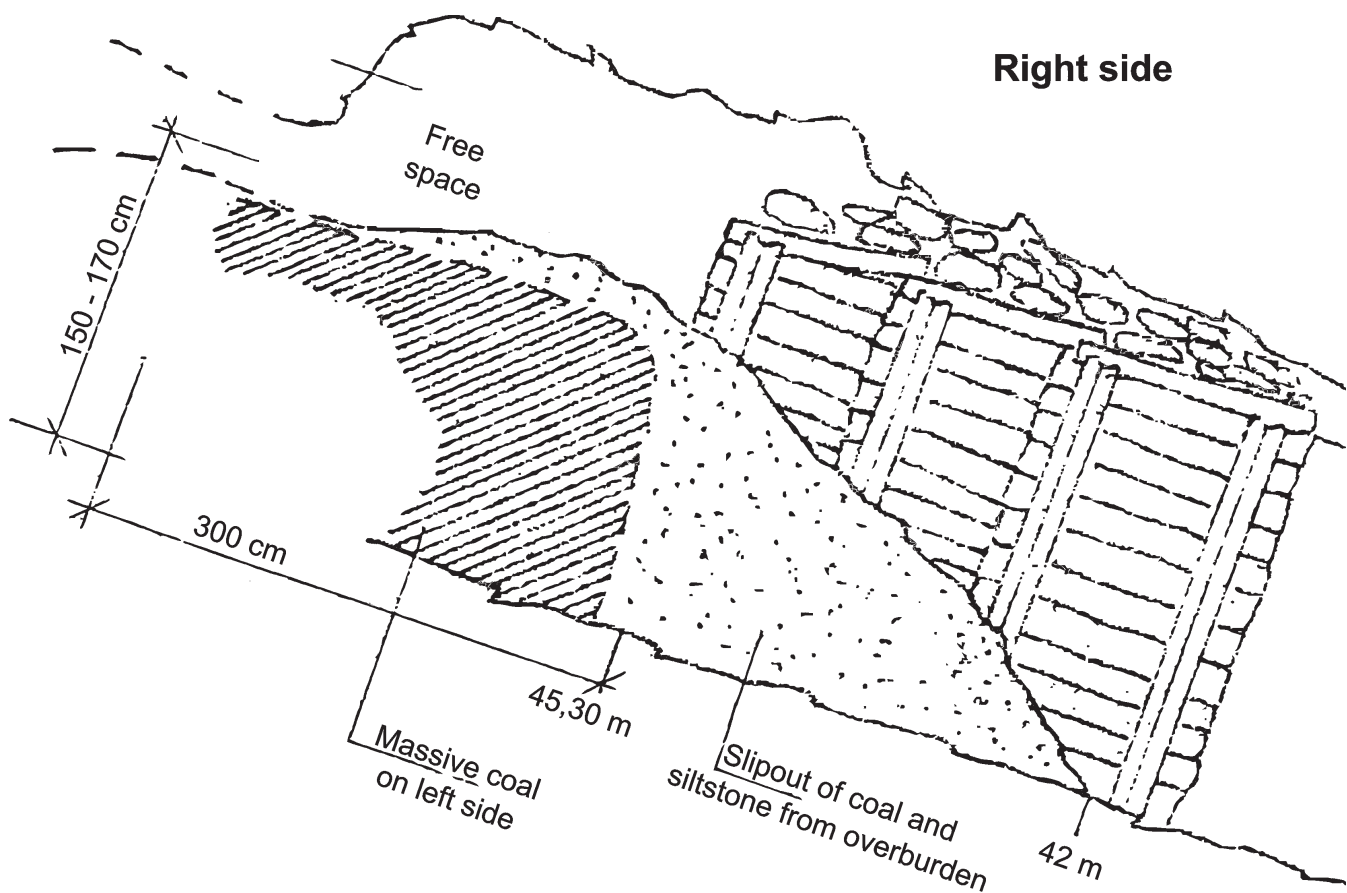


Fig. 5.5 The no. 4 coal and gas outburst on 23. 06. 1988 at 3.45 h in the excavation face no. 3/5212.  
Situation in the gallery no. 3/5212 at the distance of 45.2-42 m, following an outburst which took place  
at the distance of 45.30 m, elevation -232.1 m, in the SE section of the coalfield.  
ODMG VUD, Zdeněk Nejedlý Mine in Malé Svatoňovice – adapted.

blasting, the gas concentrations detected were 0.5% CH<sub>4</sub> and 0.5% CO<sub>2</sub>. The blasting (using 2.4 kg of Ostravite C and 6 pieces of DEM Zb electric blasting caps) took place on the day before, at 23.40 h. Gases were liberated, and the gas concentration readings taken at a distance of 10 m from the face indicated more than 10% of the CH<sub>4</sub>/CO<sub>2</sub> mixture. At 3.53 h, the concentrations recorded in the inlet ventilation air ducts of no. 3/5212 mine working were 1.9% CO<sub>2</sub> and 1.1% CH<sub>4</sub>. At this point the no. 3 Žďárky coal seam is 2.5 m thick; its overburden is formed of tectonically fissured, folded and mylonitized siltstone. The dip of the seam is 22 – 26° towards NEE. The outburst produced a cavern having 1 m in diameter and 3 – 4 m in length. It is situated on the right-hand side of the profile and is accompanied by an overbreak of 0.65 m. The ejected coal had the character of powder coal breeze of ca. 15 tons weight (*PLATE F, Fig. F5*). Based on the ventilation parameters and on air duct gas analysis, the quantities of methane and carbon dioxide liberated over the period of 8 hours were 30 m<sup>3</sup> and 142 m<sup>3</sup>, respectively (according to the report on nos. 3-5 coal and gas outbursts as per the Zdeněk Nejedlý Mine protocol dated 28<sup>th</sup> July, 1988).

#### FIFTH DYNAMIC GAS EFFECT COMBINED WITH A COAL SLIDE-UP AND SUBSEQUENT CAVE-IN OF THE ROOF

On 26<sup>th</sup> July, 1988 at 11.58 h, a slide-up of unstable rocks and coal occurred at the face of no. 3/5212 gallery. The concentration of the CO<sub>2</sub> + CH<sub>4</sub> mixture on the outlet of the air duct exhaust was 8%. No blasting operations took place in that location. The amount of liberated gases included 601 m<sup>3</sup> of CO<sub>2</sub> and 122 m<sup>3</sup> of methane; the quantity of loosened rock was estimated to be 30 tons (according to the report on nos. 3-5 coal and gas outbursts as per the Zdeněk Nejedlý Mine protocol dated 28<sup>th</sup> July, 1988).

#### SIXTH DYNAMIC GAS EFFECT COMBINED WITH ACOUSTIC EFFECTS AND COAL FLAKING

On 16<sup>th</sup> August, 1989, phenomena resembling an outburst (*Fig. 5.6, Fig. 5.7*) were reported by the gang members present at the no. 3/506 coalface, at the stationing point 169.8 m within the no. 3/5018 extraction gate of no. 3 Žďárky coal seam having a thickness of 2.4 m and including a bed of intergrown coal. As the cutter loader went

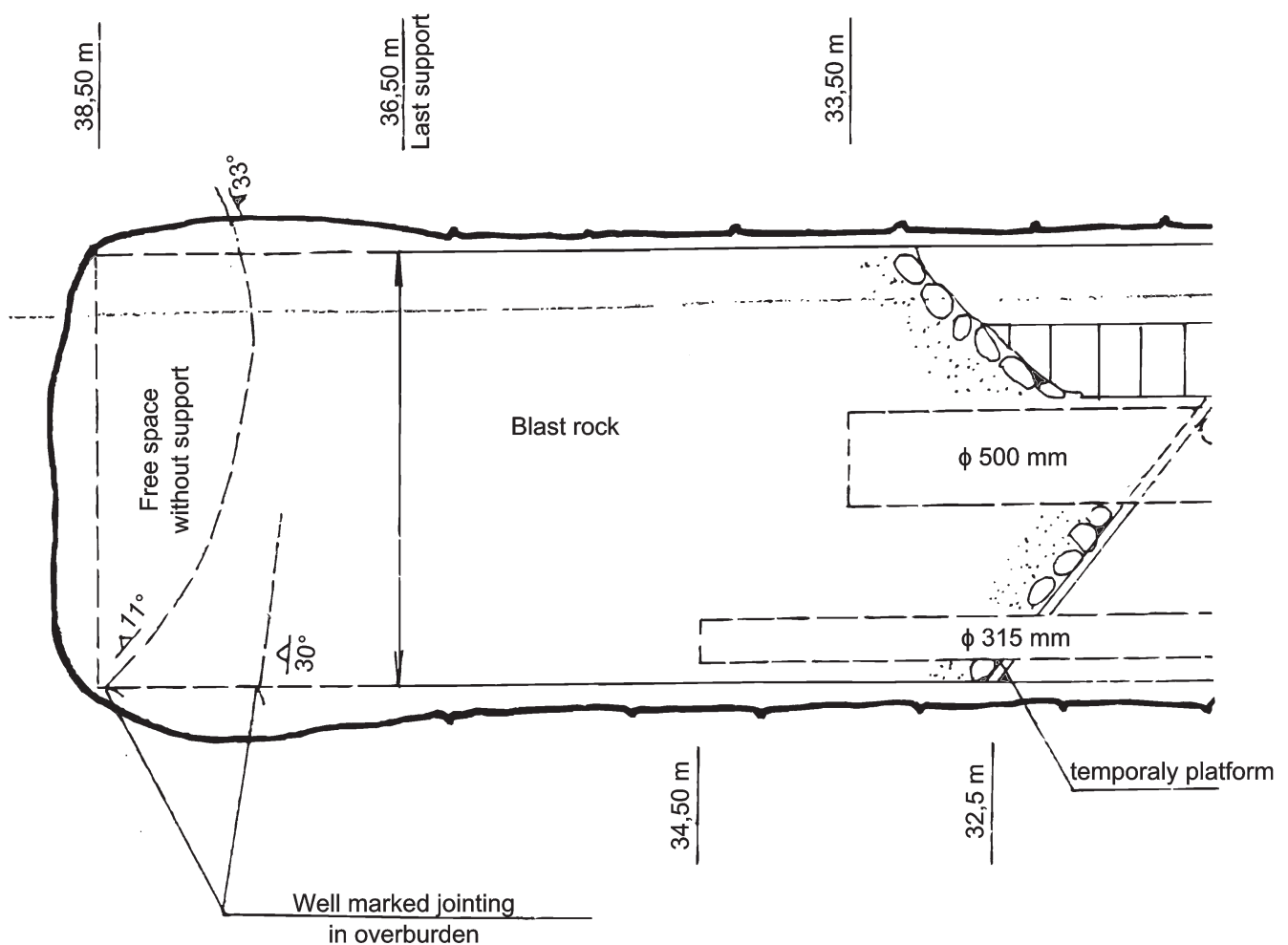


Fig. 5.6 The no. 5 gas and coal outburst. Ground plan of gallery no. 3/5212, at the distance of 30-38.5 m, with an overbreak and a cave-in at the face following the gas and coal outburst, at the stationing point 38.5 m, elevation -232.1 m which occurred on 26.7.1988 during a blasting operation conducted in the gallery no. 3/5212, in the SE section of the coalfield. ODMG VUD, Zdeněk Nejedlý Mine in Malé Svatoňovice – adapted.

downhill along the lower part of the strike face, the pillar was cracking, coal was flaking off and gas was audibly escaping from the pillar. Rock blasting using boreholes 5 m long was applied to release the pressure. Carbon dioxide in concentrations of 0-0.2% CO<sub>2</sub> was detected at the outlet from the working face.

The investigation has revealed that the Žďárky seam in those locations had „different physical and mechanical properties“. Nevertheless, no details are mentioned in the pertinent protocols (Protocol from inspection made underground by OJP VUD Commission for Investigation of Coal and Gas Outbursts at Zdeněk Nejedlý Mine, dated 17<sup>th</sup> August, 1989).

### SEVENTH COAL AND GAS OUTBURST RESULTING IN THE MINE WORKINGS BECOMING FILLED WITH GAS CAUSING SUFFOCATION OF THREE MINERS

On 11<sup>th</sup> August, 1989 at 16.51 h, while a blasting operation was in progress at no. 3/6002 gallery, at the stationing point 14.8 m, during the preparation for opening the no. 3 Žďárky coal seam on the 6<sup>th</sup> level, there occurred a mixed outburst during which the area became overcharged with gases (Fig. 5.8). Driving work was in progress in the SE part of the coalfield classified as „prone to coal and gas outbursts“. The no. 600 cross drift runs under

the 5<sup>th</sup> level in the SE part of the extraction area, at the level of -362.8 m. The rocks present in the overburden of no. 3 Žďárky coal seam include non-cohesive fine bedded siltstones and claystones changing to fine grained sandstones of up to ca. 3.0 m thickness; higher up there are coarse-grained sandstones 1-1.5 m thick. At the site of the outburst, the no. 3 Žďárky coal seam has a thickness of 0.65-2.0 m and a dip of 20° towards NE. The seat of the seam is formed of fine-grained sandstones with siltstone admixture, 1.0-1.2 m thick. At the crossing of no. 3/6002 mine working with no. 600 cross drift, the gas concentrations recorded on 12<sup>th</sup> August, 1989 at 3.47 h were 6% CO<sub>2</sub> and 7% CH<sub>4</sub>. At the no. 3/6002 face, a bottled sample was taken for which the composition was determined as 4.8% CO<sub>2</sub>, 4.7% CH<sub>4</sub>, and 18.9% O<sub>2</sub>. The ejected material comprised fine coal dust which deposited at a distance of up to 13 m. The total quantity ejected was 200 tons of broken to fine coal. Subsequently, three miners suffocated when the shelter in no. 6/5002 face, 200 m away, became filled with gas. (Protocol from an inspection underground by the Commission for Investigation of Coal and Gas Outbursts at Zdeněk Nejedlý Mine, undertaken on 11<sup>th</sup> August, 1989, during the night shift).

The situation was documented by the District Mine Rescue Station (PLATE F, Figs. F6, F7 and E8).

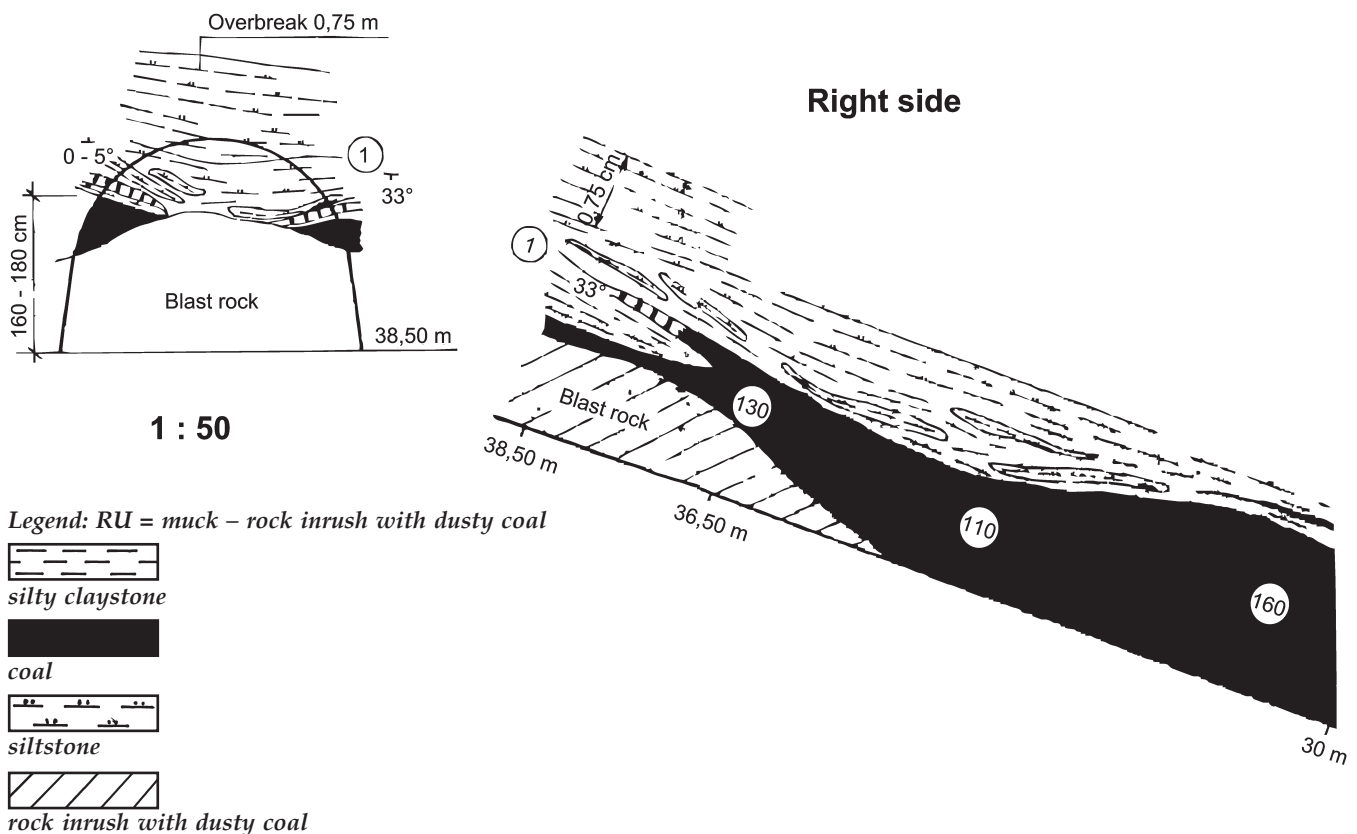


Fig. 5.7 The no. 5 gas and coal outburst on 26.7.1988. Geological section of the right-hand wall of gallery no. 3/5212, at the distance of 30-38.5 m, with an overbreak and a cave-in at the face following the gas and coal outburst, at the stationing point 38.5 m, elevation -232.1 m which occurred on 26.6. 1989 during a blasting operation conducted in the gallery no. 3/5212, in the SE section of the coalfield.

ODMG VUD (A. Bouda), Zdeněk Nejedlý Mine in Malé Svatoňovice – adapted.

### 5.3. POLISH PART OF INTRA-SUDETEN BASIN

The characteristics of deposits and geology in the Carboniferous in the Polish part of the Intra-Sudeten Basin (= Lower Silesian Coal Basin or Intra-Sudetic Depression) were summarized by Bossowski in Źdanowski et al., 1995; those interested in this subject are referred to their work. The following coal seams are found in the Wałbrzych stratification (*Table 5.1*): nos. 655-668 seams (Polish numbering of coal seams) in the Wałbrzych Fm (Namurian A – Lower part B), minor no. 549 seam in the Biały Kamień Fm (Upper part of Namurian B, up to Lower part of Westphalian A) and, above all, nos. 301-321 and 423-448 seams in the Źacléf Fm (Upper part of Westphalian A, up to Lower part of Westphalian C). The coal seams contain medium to high contents of vitrinite, which is a sign of a petrological facie with vitrinite-fusinite typical of forest peat bogs (Nowak 1992a, 1993).

In Nowa Ruda district, nos. 601-632 coal seams and nos. 301-425 seams (Polish numbering of coal seams) are concentrated in the Wałbrzych Fm and in the Źacléf Fm, respectively. Coal in this district is rich in vitrinite (first of all, nos. 415 and 405 seams); again, they correspond to forest peat bogs (Nowak 1992a, 1993). In Słupiec district, to the SE of Nowa Ruda, nos. 301 – 415 seams (Polish numbering) (see *Table 5.1*) are linked to the Źacléf Fm. These coal seams are different from those in the above-mentioned districts. They have a medium content of vitrinite and a high content of inertinite. According to petrological delimitation of the desmosporinite facie,

they correspond, by their origin, to floral pig swamps and bogs (Nowak 1992, 1993).

Unquestionably, the Polish part of the Intra-Sudeten Basin is an area where outbursts of coal and gases in the presence of carbon dioxide are very frequent. The case histories of such outbursts are documented in detail in the works by Kruk et al. (1963, 1969) or by Kidybiński and Patyńska (2008). Suchodolski (1969) in Kruk et al. (1969) reports, that a total count of 1,084 CO<sub>2</sub> and coal outbursts were registered in this area between 1884 and the end of 1967. During that period, the total weight of ejected rocks was 241,668 tons, and 422 miners died during the outbursts. In the 1941 outburst alone, at Nowa Ruda Mine, as many as 180 miners died.

More recent data on the outbursts which occurred until the end of 1976 were given by Swidziński (1977). The total count of outbursts was 1506 in the Nowa Ruda district and 210 in the Wałbrzych coal district, respectively. These outbursts were provoked by evolutions of CO<sub>2</sub> and by loosening of coal: 25 outbursts were provoked by CO<sub>2</sub> and rocks tearing loose at Thorez Mine (northwards of Wałbrzych); five outbursts were connected with firedamp evolving from coal at Bolesław Chrobry Mine (situated in the central and middle parts of Wałbrzych district). Piast Mine (Nowa Ruda) experienced 70 outbursts of carbon dioxide and sandstones (Suchodolski, 1969, in Kruk et al. (1969). Thorez Mine (northwards of Wałbrzych district) was the site of 42 outbursts of CO<sub>2</sub> and rocks during the 1945–1965 period; up to 130 tons of rocks were ejected and the volumes of CO<sub>2</sub> released varied from several hundred to 4,000 m<sup>3</sup>.

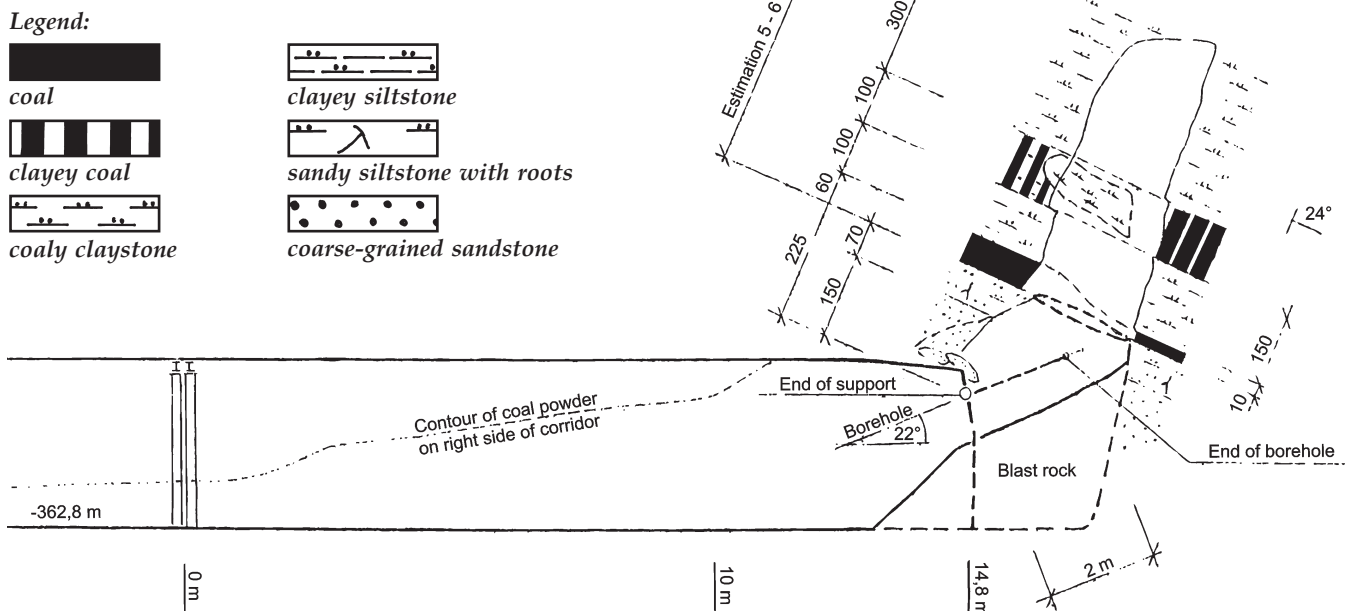


Fig. 5.8 The no. 7 mixed-type outburst (CO<sub>2</sub> and CH<sub>4</sub>) and coal. The outburst occurred on 11. 08. 1989 at 16.15 h, during a blasting operation. Geological section of the right-hand wall of gallery no. 3/6002, at the stationing point 14.8 m, at a time when the no. 3 Źdářecká coal seam was being opened at the 6th heading level, at an elevation of -362.8 m, in the SE section of the coalfield.

ODMG VUD Co. (A. Bouda), Zdeněk Nejedlý Mine in Malé Svatoňovice – adapted.

The locations of the outburst sites are shown schematically in Fig. 5.1. A more detailed map of outbursts sites in the Polish part of the Lower Silesian Basin, to which we refer, is shown by Kruk et al. (1963, drawing 1) We also refer to detailed records of individual outbursts in this mining district until 1963 and in 1969 (Kruk et al., 1963 (first part), 1969 (second part)). However, the gas, rock and coal outburst sites are distributed very unevenly across the coalfields. In the Wałbrzych part of the basin, to the SE of Wałbrzych, in the area of Sobiecin basin in the Victoria Mine exploitation area, seven different outburst sites are known which are more or less closely linked to the zones of faults of the NW-SE Sudeten direction. In the coalfield of Bolesław Chrobry Mine, to the SW of Wałbrzych, there are two zones with a close linkage to the regional structure consisting of an overthrust. Northwards of Wałbrzych, in the Thorez Mine exploitation area there

are 13 outburst-prone zones, closely linked again to the line of tectonic faults of the Sudeten direction (NW-SE), running in parallel to the Main Peripheral Sudeten fault. In the area where the Thorez Mine coalfield extends in the NE direction there is the Cezar-Zofia Mine exploitation area with its five outburst sites, again linked to tectonic faults of the Sudeten direction and to an interface with porphyres. In the Nowa Ruda mining district, in the SE part of the Waclaw Mine coalfield situated to the NW of Nowa Ruda, there are at least 40 outburst sites located in the vicinity of faults. This zone extends further on to the Bolesław Mine coalfield where there are six outburst sites. To the north of Nowa Ruda, there is the Nowa Ruda – Piast Mine exploitation area situated. Here the coal, rock and gas outbursts sites are clustered in an area of strong tectonic fissures occurring in-between the two tectonic faults of Sudeten direction or in the surroundings

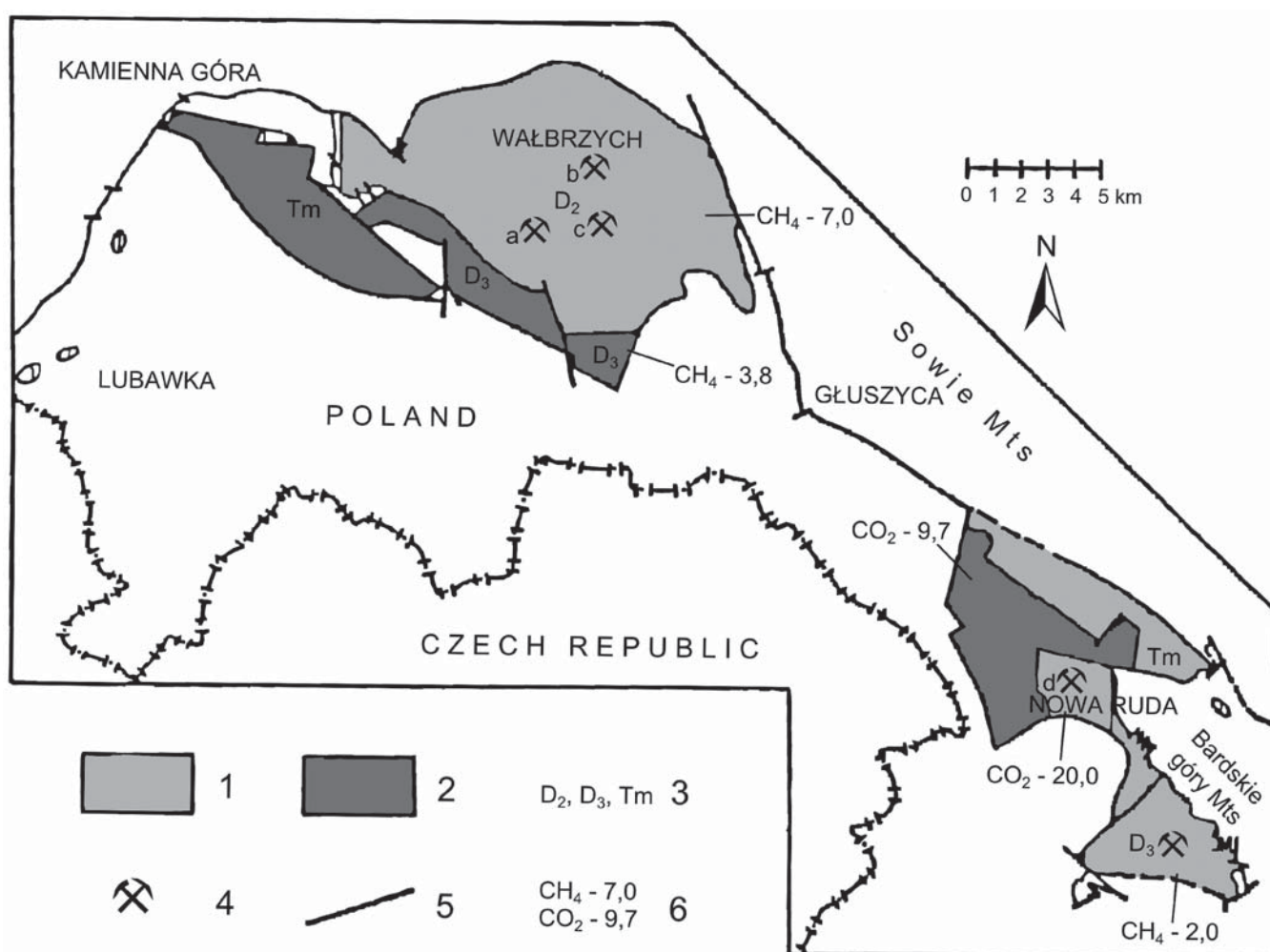


Fig. 5.9 Coalbed methane and carbon dioxide in coal seams in mines situated in the Polish part of the Intra-Sudeten Basin (adapted to Bossowski in Zdanowski et al., 1995).

- Legend:
- 1 – coalfields of abandoned mines;
  - 2 – exploration area;
  - 3 – prospective reserves of Category D<sub>2</sub> and D<sub>3</sub> coal methane; T<sub>m</sub> – theoretical reserves;
  - 4 – mines: a – Viktoria, b – Thorez, c – Wałbrzych, d – Nowa Ruda;
  - 5 – main tectonic faults;
  - 6 – coalbed methane and carbon dioxide contents converted to the carbon content, C<sup>daf</sup> [m<sup>3</sup>·ton C<sup>daf</sup>]

thereof. Thus, it follows from the works by Kruk et al., 1963 and 1969, that a close linkage exists to tectonic faults of the Sudeten direction which accompany the NE edge of the block of Sowie góry Mts. The lithological predisposition for an incidence of outburst sites derives from the properties of the Carboniferous rocks and coal there, as well as from the aforementioned tectonic structure of the Intra-Sudeten Basin in the forefield of the block of Sowie góry Mts (see Zdanowski et al., 1995). Not even a linkage to local foci of Tertiary volcanism can be excluded; these are connected with deep tectonic faults running in the Sudeten direction which accompany the Main Peripheral Sudeten fault. This seems to be also confirmed by isotopic analyses of  $^{13}\text{C}$  in  $\text{CO}_2$  from the Polish part of the Intra-Sudeten Basin reported by Kotarba, 1990. He indicates very low values of  $\delta^{13}\text{C}$   $\text{CO}_2$  ranging from -4 to -7‰, indicating that the gas originates from great depths and that magmatic activity is also involved. The outbursts of rocks, coal and gases may well be related to the contact of the Žacléř Fm with Upper Carboniferous porphyres; this is unproven but interesting (Thorez Mine, Cezar – Zofia Mine and perhaps, Victoria Mine coalfield as well).

The documentation available on the outbursts that took place on Polish territory fails to provide any information on the physical properties of coal and accompanying rocks, as well as any data on the petrography of coal and on the intensity of fissuring in the coal mass (Suchodolski, 1969; Kruk et al., 1969). Nevertheless, it ought to be appreciated that the publications by Polish authors describe the technological situations and identify the outburst sites (Jaros in Kruk et al. (1969)), also furnishing detailed data on the sorption and desorption parameters of the coal (Tarnowski, 1969 in Kruk et al. – see Chapter 2), the desorption rates (Tarnowski in Kruk et al. (1969)), the influence of geostatic pressure relief (Osmęda in Kruk et al. (1969)), etc.

It has to be borne in mind that outbursts of gases, rocks and coal are linked to the massif affected by mining adjacent to the mine workings; it is evident from the maps of coal seams (see Kruk et al. (1963, 1969)) that the outbursts tend to occur in the vicinity of the mine workings in the seams and need not always be strictly linked to faults existing in those coal seams (but are only linked to the wider, disturbed, massif of regional faults). This means that in the gas phase the coal seams contain syngenetic, thermogenous methane and, apparently, adsorbed  $\text{CO}_2$ . This has also been proved by investigations of coal bed methane in this basin (Bossowski in Zdanowski et al., 1995). In the Polish part of the Intra-Sudeten Basin the saturation of the coal seams with coal bed methane is highly uneven and the percentages of  $\text{CO}_2$  in the coal bed gases are different, too (Fig. 5.9).

#### The main factors influencing the gas production of coal seams are considered to be:

- the existence of areas around large-sized tectonic dislocations and their accompanying faults or fissure zones,
- the vicinity of rhyolite intrusions, around which the methane contained in the seams is displaced by  $\text{CO}_2$ .

The methane content increases with the depth of the coal bearing Carboniferous series; its content decreases in the vicinity of Carboniferous outcrops. The highest  $\text{CH}_4$  content was found in Victoria (Mine Witold and Barbara) and also in the SW section of Wałbrzych Mine. In some places, the methane content surpasses 20  $\text{m}^3$  per metric ton of pure coal; the average content is 8  $\text{m}^3$  per ton of pure coal but the  $\text{CO}_2$  content varies greatly. In Nowa Ruda district the  $\text{CH}_4$  contents are low; the highest contents were found in the vicinity of Przygórze, viz. 2  $\text{m}^3$  per ton of pure coal. However, high  $\text{CO}_2$  contents were found in Nowa Ruda (Piaśt) Mine – up to 20  $\text{m}^3$  per ton of pure coal. Lower contents were found in the SE part of Waclaw Mine: 9.7  $\text{m}^3$  per ton of pure coal.

The depth intervals in which  $\text{CO}_2$  outbursts or mixed  $\text{CO}_2$  –  $\text{CH}_4$  outbursts occurred correspond with the vertical component of geostatic stress (see 2.6) (for bulk weight of overburden strata of 2,350  $\text{kg}\cdot\text{m}^{-3}$ ) below or above the critical pressure for  $\text{CO}_2$ , at temperatures around 30°C prevailing at the deep mines.

#### Wałbrzych district:

- Thorez Mine: 420 to 654 m (9.7 – 15.08 MPa);
- Bolesław Chrobry Mine:  
281 to 821 m (6.5 – 18.9 MPa);
- Victoria Mine: 309 to 543 m (7.1 – 12.5 MPa);
- Cesar Zofia Mine: 320 to 390 m (7.3 – 9 MPa);

#### Nowa Ruda district:

- Piaśt Mine, Franciszek seam:  
300 to 375 m (6.9 – 8.6 MPa);
- Piaśt Mine, Anton seam:  
240 to 570 m (5.5 – 13.2 MPa);
- Piaśt Mine, Roman seam:  
295 to 625 m (6.8 – 14.4 MPa);
- Piaśt Mine, Franciszek Mine:  
390 to 625 m (9 – 14.4 MPa);
- Bolesław Mine: 200 to 426 m (4.6 – 9.8 MPa);
- Waclaw Mine: 175 to 510 m (4.1 – 11.8 MPa).

As a matter of comparison, the depths at which the outbursts occurred and the corresponding vertical components of geostatic stress at Zdeněk Nejedlý Mine in Malé Svatoňovice are the following: 620 m (14.3 MPa) to 721 m (19.7 MPa). They are of the same order as the values encountered in the Polish part as mentioned above.

In view of the fact that the Intra-Sudeten Basin is common to the Polish and Czech parts, the data on the properties of coal, first of all the data on  $\text{CO}_2$  sorption on coal and the geological data, can also be applied, with certain caution, to the Czech part of the basin on which no such data are available. For selected coal types from twelve outburst sites, Tarnowski in Kruk et al. (1969) published the isothermal sorption curves of pure  $\text{CH}_4$  and  $\text{CO}_2$  gases and of their mixtures. A commented example of this is given in Chapter 2.

## 5.4 SUMMARY

In both the Czech and the Polish parts of the Intra-Sudeten basin, the sites of occurrence of carbon dioxide, frequently accompanied by thermogenic methane, are closely connected with the geological structure. In the Czech part of the basin, the first outbursts were observed in the coal-field of Zdeněk Nejedlý Mine when extracting coal from greater depths in locations rather far removed from the Hronov-Poříčí thrust where there was no natural degassing of the massif. The carbon dioxide and methane outbursts are connected with the presence of lithologically contrasting rocks where there are coal seams, sandstones, and small tectonic zones or cracks in the massif. Adsorption of carbon dioxide and methane occurs by slow diffusion where the gases penetrate the finely structured coal matter in the coal seams which often are tectonically disturbed. However, no wide-area accumulation of carbon dioxide has occurred across the entire bulk of the coal seams, and no accumulation of CO<sub>2</sub> or methane took place in the porous sandstones or conglomerates (with secondary porosity). This is why it remains exceedingly difficult to pinpoint the exact locations where gas and coal or gas and rock outbursts could occur, and forecasting such sites would require costly verification by observation boreholes and by measurements of the CO<sub>2</sub> and methane volumes following their desorption from the coal matter of the coal seams.

In the Polish part of the Intra-Sudeten basin the two main factors are the tectonic constraint of the basin along its northern periphery by deep tectonic faults extending in the Sudeten direction (NW-SE, the Main Peripheral Sudeten Fault) and the existence of Tertiary volcanism tied up with these NW-SE fault zones.

Compared to the Czech part of the basin the frequency of outbursts in the Polish part is more frequent. And owing to the greater scale of mining activities in the Polish part of the basin coupled with difficult geological and mining conditions, the consequences were more tragic there, too. In coal seams adjacent to tectonic disturbance zones (or right on the tectonic faults) carbon dioxide together with thermogenic methane are adsorbed on and thus, accumulated in, the coal matter, just as in the pore space in rocks (sandstones, conglomerates) or in the fissures occurring in the rock bodies. Again, it is assumed that CO<sub>2</sub> penetrates by slow diffusion along deep tectonic structures, maybe connected with subvolcanic foci, and is adsorbed within the fine inner structure of coal matter in the coal seams, as is evidenced by the thorough destruction of the coal in the case of outbursts. It is highly probable that the incidence of carbon dioxide is connected with tectonic structures occurring at great depths and with sources of Tertiary volcanism (*Fig. 2.1*); this is also believed by Polish authors to be quite possible.

A



(A) Triassic – Jurassic oxidative alteration of Carboniferous rocks denoted as „Variegated beds“ type connected with fossil burning out of coal seams.

B



(B) Paleogene oxidative alteration of Carboniferous known as „Brown weathering crust“ type on Carboniferous surface (2).

The Czech part of the Upper Silesian Basin.

## 6. CARBON DIOXIDE IN THE CZECH PART OF THE UPPER SILESIAN BASIN

Geological conditions in the Czech part of the Upper Silesian Basin are described by Dopita et al. (1997); the geological condition and hydrogeological characteristics of basal clastics of Lower Badenian (so called "detritus") by Pišta (1954), Grmela in Dopita et al. (1997), and Dvorský et al. (2006); the weathering cover on the Carboniferous by Martinec and Krajčiček (1989) and Martinec in Dopita et al. (1997); and the properties of bituminous coal in Dopita et al. (1997), Martinec et al. (2005), and Martinec and Honěk (2002). The geology of Moravskoslezské Beskydy (Moravian-Silesian Beskydy) Mts. and Podbeskydská Uplands and the Varisan structural stage of the Outer Carpathian system are described by Menčík et al. (1983). Detailed analyses of the gas conditions, in particular the emissions of CO<sub>2</sub> in the mines of Ostrava-Karviná district, were presented by Jičínský (1885) as early as in 1892 and later, by Folprecht in Patteisky (1928) and by Říman (1952). The Directors' Conference Monograph (Patteisky and Folprecht, 1928) describes emissions of carbon dioxide in the mines of the western part of the Ostrava-Karviná district (see below).

### On the relatively small-sized territory of the Czech part of the Upper Silesian Basin, carbon dioxide occurs in different geological environments:

- dissolved CO<sub>2</sub> in a collector with fossil marine water in Lower Badenian basal clastics (so called detritus) in the western part of Bludovice furrow,
- gas (CO<sub>2</sub> together with CH<sub>4</sub>) adsorbed on coal matter in coal seams in the western part of Ostrava-Karviná coal district,
- dissolved CO<sub>2</sub> together with CH<sub>4</sub> as a part of isolated collectors in tectonic faults in the Carboniferous,
- CO<sub>2</sub> and CH<sub>4</sub> accumulated in the weathering cover on the buried surface of Carboniferous strata,
- CO<sub>2</sub> and CH<sub>4</sub> as a part of mine air (atmosphere) in active or closed coal mines,
- as a constituent of mine gas emissions from closed coal mines rising to the surface.

### 6.1. CARBON DIOXIDE IN BASAL CLASTICS OF LOWER BADENIAN SEDIMENTS

In the Czech part of the Upper Silesian Basin, CO<sub>2</sub> and CH<sub>4</sub> gases are an integral part of the Lower Badenian water aquifer and always have been studied as such. Occurrence of carbon dioxide in this aquifer is known only in the western part of Bludovice furrow, in basal clastics; an accident occurred there on 9 April, 1902, during the sinking of the hoisting shaft for Bedřich Mine in Zábřeh nad Odrou (Makarius and FASTER, 2008). Pumping tests connected with backfilling of the shaft were carried out and evaluated by Pišta (1961). The classification of detritic waters according to their chemical composition was first made by Jirkovský

(1953), and the basic chemical types of detritic waters were identified by Pišta (1954). Zonation of chemical composition of waters and hydrogeological conditions in Lower Badenian basal clastics (so called "detritus") were studied by Homola (1959), Michálek (1961), Dvorský and Tylčer (1969), Hufová et al. (1971) and others. Drainage of basal clastics by underground boreholes and coal mining in the Carboniferous under the Lower Badenian basal clastics reservoir were investigated by Pišta (1961), Majzlík (1965), Michálek (1961, 1980, 1983), and Schejbalová et al. (1983, 1985, 1988); liquidation of waters was investigated by Tardon et al. (1992). Hydrochemistry of deep underground water in Ostrava region was described in summary by Květ (1971, 1980); and the geology, hydrogeology, hydrochemistry, and chemical composition of Lower Badenian basal clastics were investigated by Dvorský et al. (2006). In the Czech part of the Upper Silesian Basin, methane and carbon dioxide are dissolved in highly mineralized water in the Lower Badenian basal clastics (detritus). Such clastics are deposited in Dětmarovice furrow to the north of Ostrava-Karviná ridge and in Bludovice furrow situated in the south (Fig. 6.1); the latter continues along the axis of Moravian Gate (Moravská brána) towards SW, in direction to Hranice town. The furrows are buried valleys on the surface of Carboniferous paleorelief, filled with Lower Badenian basal clastics with coarse detritic material of different sortings such as pebbles and debris, graywacke, Lower Carboniferous (Viséan) argillaceous schist, but also of different compositions (gneisses, phyllites, quartzites, granitoides).

#### Such basal clastics originated:

- by redeposition of older gravel of fluvial origin and Carboniferous weathered rocks (gravels mainly containing rocks from Nížký Jeseník Mts (from Lower Carboniferous, Devonian strata),
- by block slides on furrow slopes and by marine abrasion of stone blocks and stone debris loosened from slopes of Ostrava-Karviná ridge and Mszany-Jastrzebie ridge; such redeposited sediments lay in the lower parts of slopes of furrows and contain redeposited older submarine cones, too.

#### These sediments are divided into three basic types:

- sand with gravels, generally cemented by secondary calcite,
- coarse gravel with rocks of Lower Carboniferous (Viséan) from Nížký Jeseník Mts. or crystalline rocks deposited mainly in the deepest, axial parts of furrows,
- slope breccia containing blocks or lumps of rocks from deeply oxidized Carboniferous rocks and coal from Lower Carboniferous Ostrava Fm (Namurian A, Pendlian, Arnsbergian) and from deeply altered rocks from Karviná Fm (Namurian B,C and Westphalian A,B), known by local name as „Variegated beds“ (in Czech publications, „pestré vrstvy“).

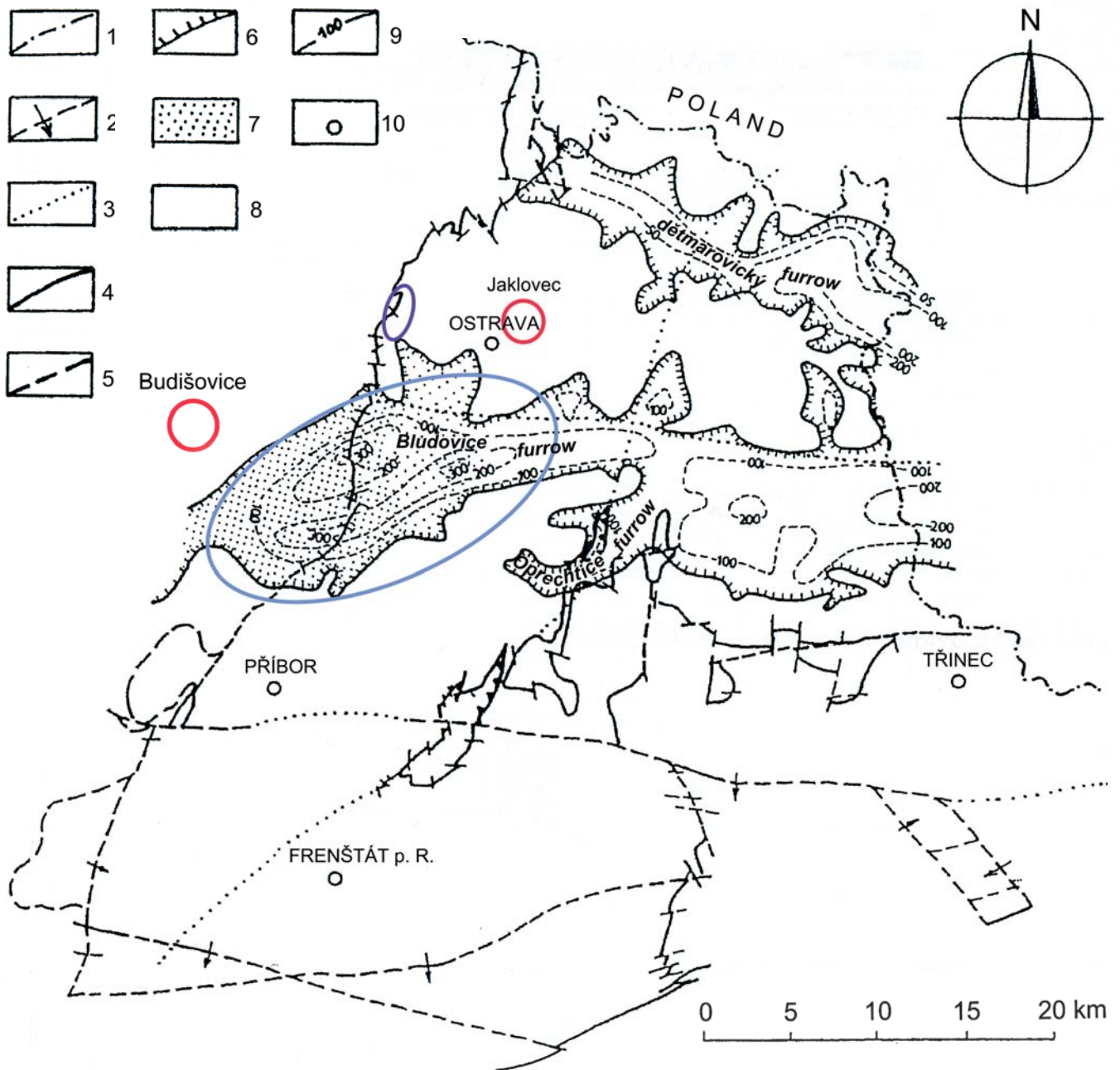


Fig. 6.1 Occurrence of Lower Badenian basal clastics (so called „detritus“) in the Czech part of the Upper Silesian Basin

Legend: Blue area - Lower Badenian fossil water in basal clastic rocks in the Western part of Bludovice valley with  $\text{NaHCO}_3$  and  $\text{CO}_2$ .

Violet - rock, coal and  $\text{CO}_2$  outburst sites in Carboniferous coal seams.

Red circle - locations of Tertiary basalts on Jaklovec Hill in Ostrava town and in old quarry in Budišovice willage.

- Legend:
- 1 state frontiers;
  - 2 proven tectonic faults;
  - 3 borders of geological areas;
  - 4 proven limits of coal-bearing Carboniferous (Namurian A);
  - 5 presumptive limits of coal-bearing Carboniferous (Namurian A);
  - 6 contour line of Lower Badenian basal clastic (so called „detritus“);
  - 7 aquifer with  $\text{NaHCO}_3$  containing water;
  - 8 aquifer with  $\text{NaCl}$  containing water;
  - 9 lines of constant thickness of Lower Badenian basal clastic sediments (thickness in [m]);
  - 10 towns and villages.

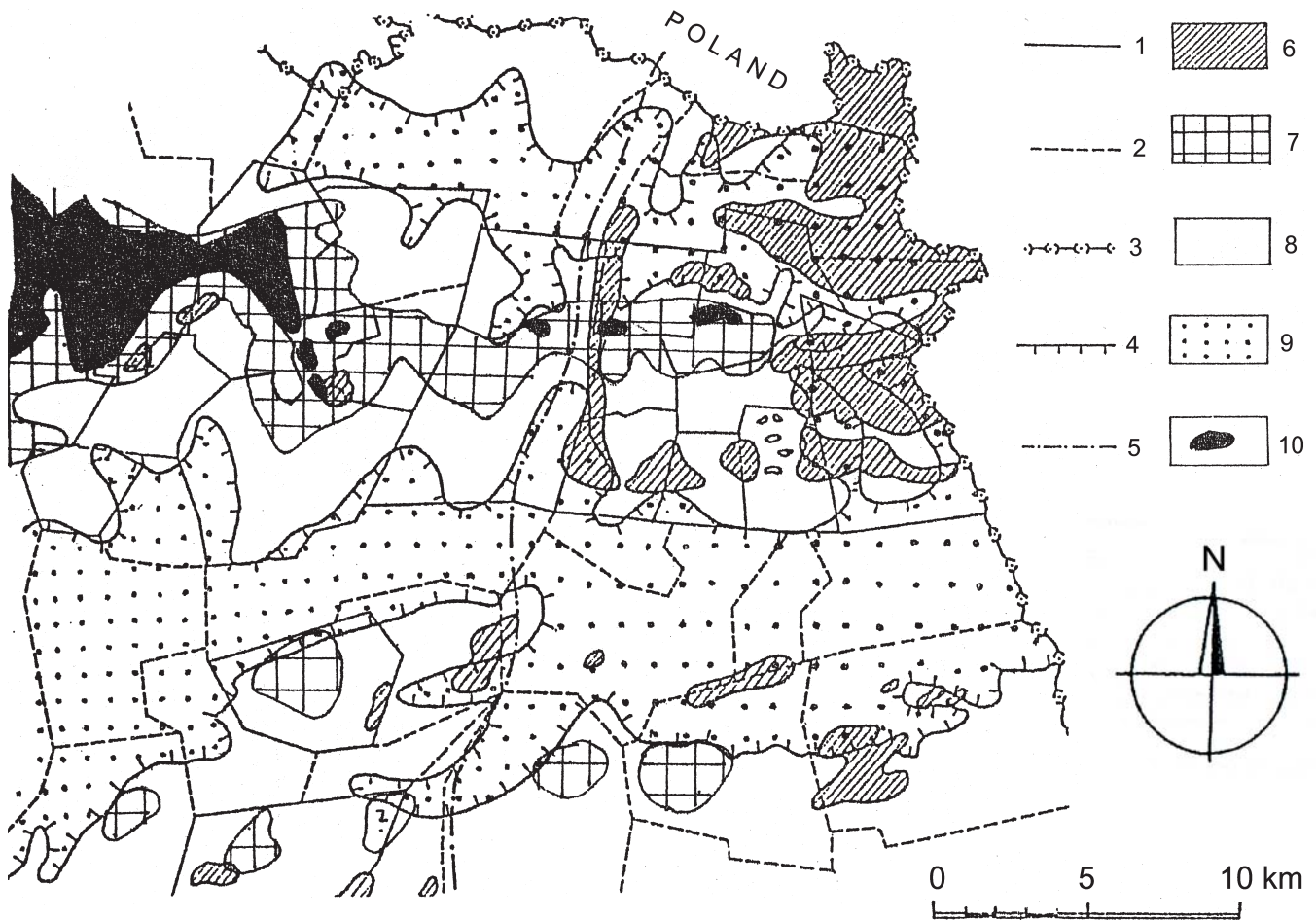


Fig. 6.2 Geomorphologic types of buried Carboniferous paleosurface in the northern section of the Czech part of the Upper Silesian Basin.

- Legend:
- 1 mine perimeters;
  - 2 exploration areas;
  - 3 Czech and Polish state frontiers;
  - 4 rim of Lower Badenian clastics (co called „detritus“) in fossil valleys;
  - 5 Orlova fault;
  - 6 outcrops of „variegated beds“ on Carboniferous surface;
  - 7 plateau on the top of Carboniferous hills;
  - 8 upper part of slopes with transition to plateau on the top of Carboniferous hills;
  - 9 lower part of valley slopes and bottom;
  - 10 outcrops of Carboniferous strata on surface.

The geomorphological types of buried Carboniferous paleorelief in the northern area of the Czech part of Upper Silesian Basin are shown in Fig. 6.2.

Water in aquifer in the Lower Badenian basal clastics is fossil marine water under pressure, the initial piezometric pressure of which at the top of collector ranges from 3.3 to 7.0 MPa (Dvorský et al. 2006) depending on where it is located. From the point of view of hydrochemistry, such a collector is a complex, closed structure of initially stagnant fossil marine waters with dissolved gas. Hydrochemically, the collector in detritus in Lower Badenian basal clastics is not homogeneous. The boundary marking the changes in chemical composition of waters and dissolved gases in aquifer in the Lower Badenian basal clastics is formed by the zone of a major narrowing of Bludovice furrow between Svinov, Zábřeh, and Radvan-

ice lateral furrows (Pišta, 1954; Tylčer, 1977; Dvorský and Tylčer, 1969; Dvorský et al., 2006). To the west from this boundary, towards Moravian Gate, the waters found are of  $\text{Na}-(\text{HCO}_3)^-$  type, with medium to low content of dissolved  $\text{CO}_2$ , up to  $\text{Na}(\text{Ca}) - (\text{HCO}_3)^- - (\text{Cl})$  type with mineralization of  $5-10 \text{ g}\cdot\text{dm}^{-3}$  or less, mainly containing  $\text{CO}_2$  alone. As an example, Homola (1959) indicates the following composition of gas from borehole no. NP 639:  $\text{CO}_2$  85.9%,  $\text{H}_2$  0.002%,  $\text{He}$  0.006%,  $\text{Ar}$  0.05%,  $\text{N}_2$  50%,  $\text{CH}_4$  8.0%, and  $\text{O}_2$  1.1%, with water / gas ratios of 1:1 to 1:2. Here, the main component of such waters is hydrogen carbonates (as much as  $7 \text{ g}\cdot\text{dm}^{-3}$ ). Dvorský and Tylčer (1969) write that waters from the western part of Bludovice furrow do not represent only one hydrochemical type, but that locally, non-transformed waters from Lower Badenian basal clastics of the basic  $\text{Na}-\text{Ca}-\text{Cl}$  type

are also preserved without dissolved CO<sub>2</sub> (lateral Zábřeh furrow, borehole no. NP 484). For discussion on the questions of occurrence of transformed waters from Lower Badenian basal clastics with dissolved CO<sub>2</sub> in the western part of Bludovice furrow, the reader is referred to works by Dvorský et al. (2006).

From the western part of Bludovice furrow, in its branch towards SW, in boreholes no. NP 611 (bedding pressure 7.3 MPa), no. NP 612 (in Jistebník), and no. NP 613 (in Studénka), all of them drilled from the surface, eruptions of free CO<sub>2</sub> were observed, as a result of a spontaneous decrease of bed pressure when the collector of Lower Badenian basal clastics was opened.

In Bludovice furrow, in direction from the hydrochemical boundary toward the east, and in the whole Dětmárovice furrow, the standard type of water from Lower Badenian basal clastics is Na–Ca–Cl with a total average mineralization above 20 g·dm<sup>-3</sup> and with dissolved CH<sub>4</sub> of biogenic origin (Dvorský et al., 2006). The following example of composition is from the borehole no. NP 753 Havířov: CH<sub>4</sub> 93.5%, C<sub>2</sub>H<sub>6</sub> 0.12, CO<sub>2</sub> 2.9%, H<sub>2</sub> 0.019%, He 0.092%, N<sub>2</sub> 3.1, and O<sub>2</sub> 0.3% (Homola, 1959).

The genesis of CO<sub>2</sub> in water from Lower Badenian basal clastics in the western part of Bludovice furrow was discussed by a number of authors (Homola, 1959; Grmela in Dopita, 1997; Pišta, 1954; Dvorský and Tylčer, 1969; Květ, 1980; Dvorský et al., 2006). They are inclined to believe that CO<sub>2</sub> is of juvenile origin, from deep sources. Such sources could be related to deep tectonic faults in the western delimitation of the Czech part of the Upper Silesian Basin and to foci of Tertiary volcanism in the western part of Ostrava-Karviná ridge (in the coalfield of Ostrava Mine – Petr Bezruč, Heřmanice) or in Budišovice village (Fig. 6.1). Cases of mixed outbursts of coal and CO<sub>2</sub> with admixture of CH<sub>4</sub> in the western part of the basin, in Jan Šverma Mine (Fig. 6.1, Fig. 6.12), could support this hypothesis on genesis of carbon dioxide.

According to authors mentioned further on, the primary water from Lower Badenian basal clastics are considered to be synsedimentary fossil marine waters (Hufová et al., 1971; Květ, 1980; Grmela in Dopita et al., 1997; Dvorský et al., 2005, 2006), isolated in the body of Lower Badenian basal clastics. Nevertheless, in western part of Bludovice furrow, such waters were transformed, to a higher or lower degree, by becoming enriched in CO<sub>2</sub>. Carbon dioxide from deep sources contributes to transformation of the composition of primary waters from Lower Badenian basal clastics and, first of all, facilitates reactions with rock-forming minerals in Lower Badenian basal clastics rich in K-micas and illites, feldspars, and carbonates. This is evidenced, e.g., by the results of investigations of the hydrochemism of waters from Lower Badenian basal clastics by Grmela, Rapantová, and Labus (2004). They show anomalies in water composition, first of all in the Na, K, and Ca contents in relation to Cl in waters of the western part of Bludovice furrow with CO<sub>2</sub>. Such differences, which can be partly explained by CO<sub>2</sub> participation in mineral reactions, stand out in case of comparison with the composition of standard marine water. In addition, it cannot be excluded that, during the transformation of water from Lower Badenian basal clastics, there could have occurred – as indicated by Dvorský and Tylčer (1969) and

Květ (1980) – an infiltration of water from higher blocks of Lower Carboniferous (Viséan) beds which form Oder-ské vrchy Uplands in the west.

As stated by all the authors, the genesis of CO<sub>2</sub> is still an object of discussion. In spite of a detailed analysis of hydrochemical conditions by Dvorský et al. (2006), it still is necessary to shed more light on this question. The persisting uncertainties are due, *i.a.*, to errors in sporadic historical data, absence of a monitoring network, detection of the routes of ascent of CO<sub>2</sub>, and lack of its deep sampling including isotopic analyses. Last but not least, the termination of a systematic hydrochemical research in this field, which could lead to the determination of potential sequestration capacity for carbon dioxide in such specific collectors, also plays a part here. Therefore, estimates of the properties of collectors and of the behavior of the system of detritic waters as regards the sequestration of gaseous CO<sub>2</sub> in collectors are unreliable.

## 6.2. COAL AND GAS OUTBURSTS IN MINES IN THE WESTERN PART OF OSTRAVA-KARVINÁ COAL DISTRICT

Emissions and outbursts of CO<sub>2</sub> and (CO<sub>2</sub>+CH<sub>4</sub>) together with the occurrence of mineral waters with dissolved CO<sub>2</sub> are described by Patteisky and Folprecht (1928), referring to a number of coal seams: Anna, Ferdinand, Bedřich, and Vladimír at the former Ignác Mine known as Jan Šverma Mine since 1947 (Fig. 6.12); in the western part of Ostrava-Karviná district this concerns Jan Šverma Mine and Odra Mine, but other cases of mine waters containing carbon dioxide also exist. Such sources manifest themselves as weak, quickly disappearing small springs of CO<sub>2</sub> mineralized water, which disappear with the advance of the mining to greater depths.

During coal mining and driving operations at the mine workings in western part of Ostrava-Karviná district, dangerous outbursts of coal and carbon dioxide with admixture of methane were recorded. In such cases, carbon dioxide with methane was adsorbed in the coal seams. While outbursts of coal and methane were registered in a number of mines in the Ostrava – Karviná district (in the mines of Heřmanice, Vítězný únor, Paskov, and Staříč), outbursts of coal with carbon dioxide occurred only in the western part of the exploitation area of Jan Šverma Mine. Data on outbursts presented further on refer only to that mine. As indicated by Šmíd et al. (1989), a total of 180 mixed outbursts of coal and (CO<sub>2</sub> + CH<sub>4</sub>), in which 11 miners died, were registered at Jan Šverma Mine during the period from 1894 until 1988. From 1889 until 1958, there were 43 outbursts; from 1958 until 1988, 137 outbursts. Outbursts registered from 1976 to 1988 in this locality occurred exclusively in the no. 6 block (15 cases in the seams of OKD code numbering (Dopita et al. 1997): 023 (Černá nevěsta), 036 (Upper Max), 056 (seam D), 068 – Bedřich) and in the no. 9 block (two cases in the seams of OKD code numbers 026 (Novodvorský) and 036 (Upper Max). (Code numbering of coal seams in the Czech

part of the Upper Silesian Basin is given in Dopita et al. (1997) and is different from the numbering of coal seams in the Polish part of the Upper Silesian Basin). Available data show that the number of outbursts increased when mining works were taken to greater depths or were intensified.

In the aforementioned mining area in the west of Ostrava-Karviná District, the coal seams of Petřkovice Mbr (Ostrava Fm, Namurian A, Pendleian) have a rather simple character from the point of view of coal petrography. They contain coal metatypes with different ratios of lustrous banded (LUP grade) coal and banded (UP grade) coal of a higher coalification (volatile matter  $V^{daf}$  around 14 %). The prevailing microlithotype is vitrinitite, macerals of liptinite are highly vitrinitized. Inertinite is often represented by sklerotinite and fusinite. Average contents

of vitrinite range from 75 to 88%, the contents of macerals of inertinite group range from 12 to 25% (Martinec et al., 2005). Due to the molecular structure of coal matter of these coals, they are prone to adsorbing high volumes of  $CO_2$  and  $CH_4$ . The macroscopic texture of the coal is mostly lustrous banded coal and banded coal. At the outburst sites, the primary coal structures are overlapped with secondary deformation structures (joints, fissures, tectonically induced plastic deformation of coal (Foldyna and Kožušníková, 1997), as a consequence of tectonic deformations. Such secondary macro-textures of coal (Martinec et al., 2005) influence not only the pore structure in the coal, coal permeability (Konečný and Kožušníková, 2011 – see Chapter 2), and the strength and deformation properties of coal, but also the susceptibility of the coal to outbursts of  $CO_2$ ,  $CH_4$  and mixed ( $CO_2 + CH_4$ ). The  $CO_2$

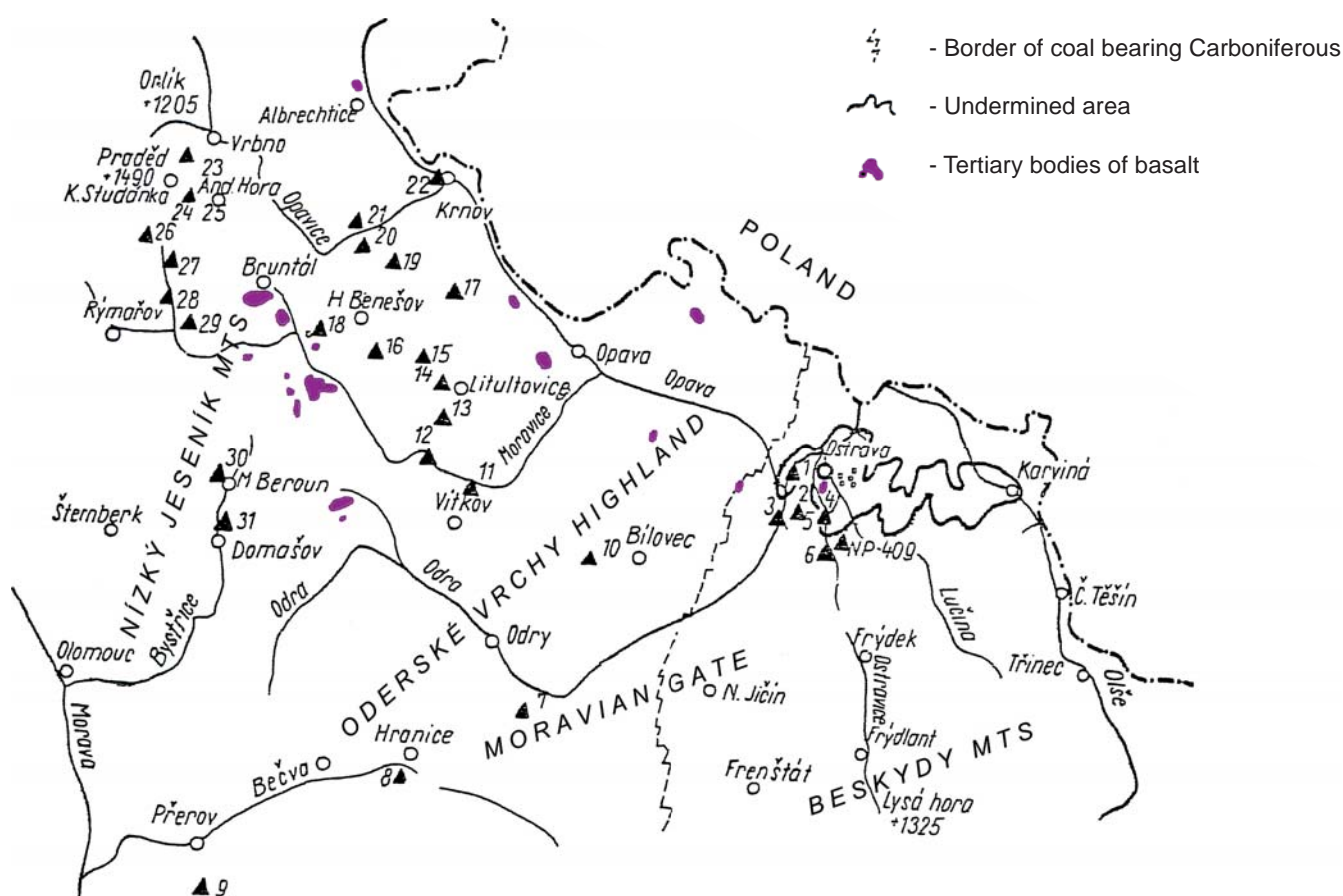


Fig. 6.3 Mineral waters with  $CO_2$  on the territory of North Moravia and Silesia (Pišta, 1954 – adapted).

Legend: Wells of mineral waters with carbon dioxide in mines and in boreholes:

- 1 – mine wells and  $CO_2$  emissions in Jan Šverma Mine; 2 – Bedřich shaft in Ostrava–Zábřeh; 3 – surface well at a borehole in Svinov (1897); 4 – mine wells with  $CO_2$  connected with Lower Badenian basal clastic sediments („detritus“) in Jeremenko Mine; 5 – boreholes from surface in Bedřich (Zábřeh) Badenian lateral valley; 6 – Hrabůvka borehole NP 32 with  $CO_2$  in Lower Badenian aquifer in Bludovice valley.

Wells and springs of mineral waters with carbon dioxide on surface (names of towns and villages):

- 7 – Jeseník nad Odrou; 8 – Teplice nad Bečvou; 9 – Horní Moštěnice; 10 – Bravinné; 11 – Dolní Víkštejn; 12 – Jánské Lázně; 13 – Lhotka u Litultovic; 14 – Mladecko; 15 – Jakartovice; 16 – Staré Heřminovy; 17 – Velké Heraltice; 18 – Rázová; 19 – Lichnov; 20 – Zátor; 21 – Loučky; 22 – Krnov (backfilled wells); 23 – Ludvíkov; 24 – Karlova Studánka; 25 – Suchá Rudná; 26 – Karlov; 27 – Moravice; 28 – Jakartovice; 29 – Stará Štáhlé (short boreholes from surface); 30 – Ondrášov; 31 – Domašov (short boreholes from surface).

sorption curves obtained in laboratory were determined on coal from Ostrava and Karviná Fm (Chapter 2); they illustrate good adsorption capacity of such types of coal, in particular if the high tectonic disturbance of coal in the seam is taken into account.

Outbursts in Jan Šverma Mine occurred only in seams of Petřkovice Mbr, Ostrava Fm (Namurian A, Pendleian), namely during the driving of crosscuts in seams and in the coalface. However, out of a total of 20 outbursts which occurred during the 1976 to 1988 period, more detailed data on the outbursts and on accompanying CO<sub>2</sub> emissions are available only for 11 mixed outbursts of coal and (CO<sub>2</sub> + CH<sub>4</sub>). In these outbursts, the minimum volume of ejected CO<sub>2</sub> was 115 m<sup>3</sup>, the maximum volume was 21,000 m<sup>3</sup> CO<sub>2</sub>, the median value was 4,340 m<sup>3</sup> CO<sub>2</sub> (Šmíd et al., 1989). The CO<sub>2</sub> outbursts in seams in this locality during the 1976 to 1988 period occurred in those zones where coal was more or less tectonically disturbed (zones with joints, coal affected by plastic deformation, and mylonitized coal) or in the vicinity of tectonic faults (apparently, in more than 65% of cases). A lesser part of outbursts in this locality occurred without any symptoms that would indicate that an outburst is impending. The tectonic predisposition of a given site for triggering an outburst is important from the point of view of deep migration of free CO<sub>2</sub> and its adsorption on coal matter in the coal seam. However any more detailed documentation of the above outbursts, first of all, any geological and petrological information, is lacking at present.

### 6.3. CARBON DIOXIDE IN ZONES OF DISTURBED TECTONICS IN THE CARBONIFEROUS MASSIF

A few cases of CO<sub>2</sub> emissions in Šverma Mine have also been related to tectonically disturbed zones or systems of fissures in the Carboniferous massif. When such zones are opened for mining, the CO<sub>2</sub> is quickly released as a „gas blower“; the volume of ejected gas as well as the volume of released water decrease quickly and their source disappears. One of such cases was observed in 1955 and is described by Pišta (1961). There the emission of carbon dioxide was accompanied by ejection of mineralized water from a cross-heading driven for transport purposes and denoted as “Peter’s transport cross-heading” in the mine documentation; it was located on the 5<sup>th</sup> level of Jan Šverma Mine. At a depth of 250 m under the buried Carboniferous surface and 410 m under the surface, this cross-heading advanced to a joint from which water saturated with CO<sub>2</sub> rose at a rate of 30 dm<sup>3</sup>·min<sup>-1</sup>, was accompanied by a swift and thunderous CO<sub>2</sub> emission. Initially, only CO<sub>2</sub> was ejected with water, but progressively, the share of CH<sub>4</sub> increased, too. Within three months, the emission of gases as well as the inflow of mineralized water disappeared.

### 6.4. CARBON DIOXIDE IN MINE AIR AND MINE GAS ASCENDING TO SURFACE

Carbon dioxide is also an integral part of mine air in active mines. The content of CO<sub>2</sub> in exhaust air in active mines in the Czech part of the Upper Silesian Basin ranges from tenths of a percent (mine gallery without ventilation) to one percent (Pošta, pers. comm.); the origin of CO<sub>2</sub> is technological, biogenic, and thermogenic. After mine closure, the composition of mine air enclosed within a massif disturbed by mining is subject to a metamorphosis (the liberation of gases adsorbed on coal continues, as does biogenic oxidation of methane). When the mines are shut down the mine gases ascend to surface in uncontrolled fashion, via the massif disturbed by previous mining underneath, as a mixture of CO<sub>2</sub> and CH<sub>4</sub>. In Ostrava-Karviná district, the composition of gases ascending from the mines is the following: in Ostrava area, CH<sub>4</sub> 0.01 to 66%, CO<sub>2</sub> 0.2 to 9%; in Petřvald area, CH<sub>4</sub> 0.1% to 42%, CO<sub>2</sub> 0.1% to 10%; in Orlová area, CH<sub>4</sub> 6.1 to 8.5%, CO<sub>2</sub>: 0.1 to 14.5%. Maps of areas threatened by gas emissions were prepared by Takla and Král (1999) and by Takla et al. (2003). An overview of the problems faced in built-up areas and the problems of safety of buildings in Ostrava region, associated with the termination of deep coal mining in the Czech part of the Upper Silesian Basin and with uncontrolled ascent of mine gases to the surface, are summarized by Martinec et al. (2006).

Mine gas contains CO<sub>2</sub> of different geneses, namely of thermogenic origin (coalification processes, processes occurring at greater depths), of technological origin (processes connected with secondary coal oxidation and with oxidation of timber supports), of biogenic origin (methane oxidation processes) and, first of all, of microbial origin. As stated by Buzek et al. (1999) on the basis of isotopic analysis of methane and CO<sub>2</sub> from gas samples taken from boreholes and underground, the share of CO<sub>2</sub> that had a highly negative value of δ<sup>13</sup>C CO<sub>2</sub> was interpreted as CO<sub>2</sub> of biogenic (bacterial) origin. A sample of gas taken from deeper seams showed high negative δ<sup>13</sup>C CO<sub>2</sub> values (-27‰) a δ<sup>13</sup>C CH<sub>4</sub> values (-40‰) and was interpreted as gas which underwent bacterial reduction in upper coal seams or were oxidized later in an oxygen-rich medium. Biogenic CH<sub>4</sub> enclosed in such locations within the mines which had access to fresh air was partly oxidized to CO<sub>2</sub>, exhibiting δ<sup>13</sup>C CO<sub>2</sub> values ranging from -30 to -50‰. The authors mentioned above did not specify any δ<sup>13</sup>C values for primary CO<sub>2</sub> from the basin and believe that the primary thermogenic CO<sub>2</sub> might originated from deep seams. According to these authors, the gases formed due to bacterial activity (CH<sub>4</sub> + CO<sub>2</sub>) can be formed as follows: thermogenic gas rich in CH<sub>4</sub>, generated deep underground, is reduced by bacteria present in coal seams; and can be degraded later by oxidation in those seams which are in contact with air.

Nevertheless, not even the ground-breaking research of isotopic composition of carbon dioxide from mine gases and from gases liberated in deep boreholes, carried out by Buzek et al. (1999), has succeeded in answering the question as to whether there exists any inflow of CO<sub>2</sub> to the

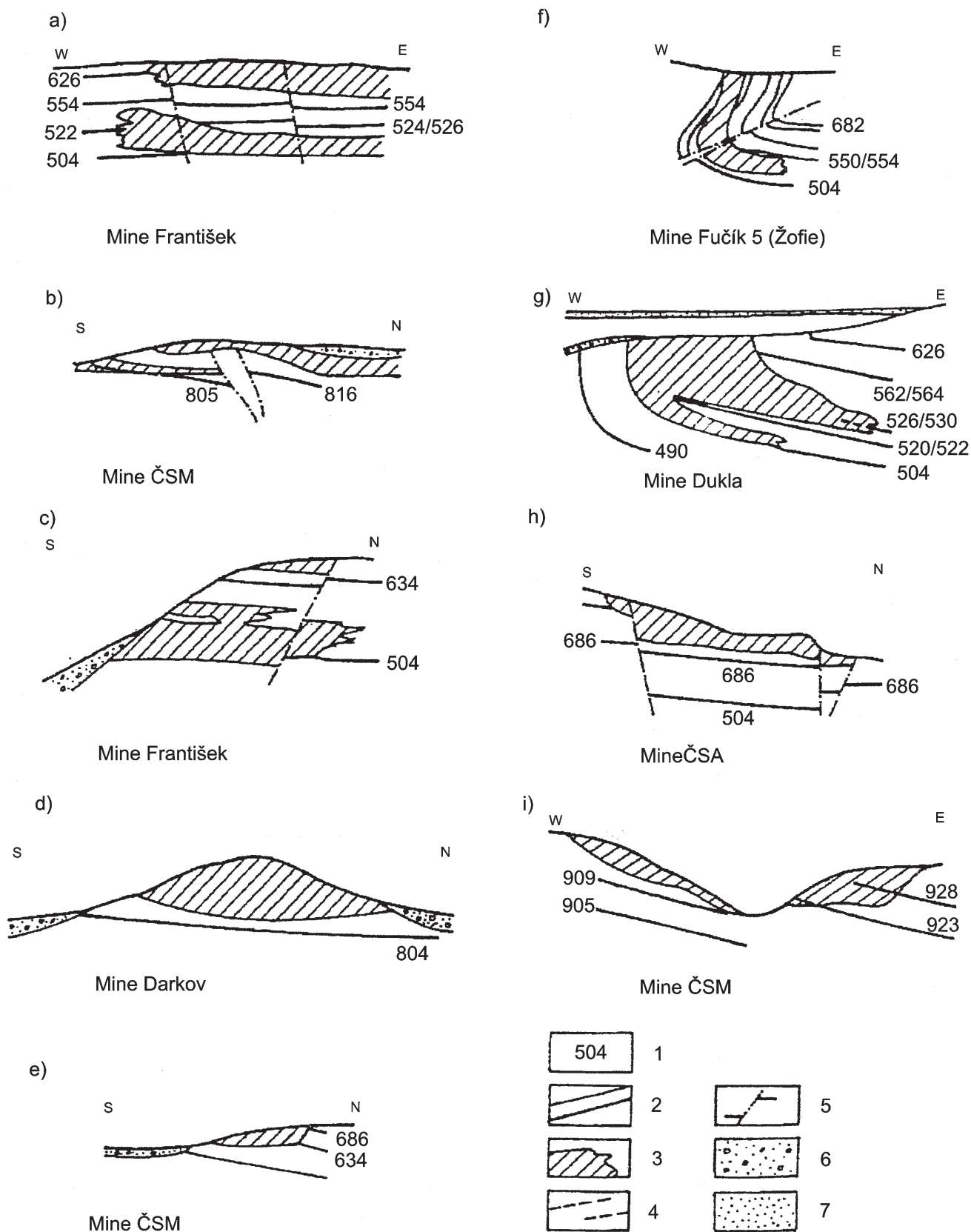


Fig. 6.4 Mezozoic weathered „variegated beds“ and their relation to Carboniferous paleo-surface in the Czech part of Upper Silesian Basin (after Dopita et al., 1987).

Legend: 1 – Code nos. designating the coal seams in Ostrava-Karviná coal district: Karviná Fm; Members: code no 500 – Sedlové vrstvy Mbr, 600 – Lower Sucha Mbr, 700 – Upper Sucha Mbr, 800 – Doubrava Mbr;  
 2 – coal seam, 3 – „Variegated bed“ bodies in Carboniferous strata;  
 4 – burned-out coal seams; 5 – Tectonic faults; 6 - 7 – Lower Badenian basal clastic sediments („detritus“).

Carboniferous massif and to its young Neogene and Quaternary cover along deep-seated faults. However, their work underlined the importance of biogenic oxidation of methane and coal matter for the genesis of carbon dioxide in mine gases or in the rock massif disturbed by mining.

## 6.5. WATER AND GAS RESERVOIRS IN WEATHERED CRUST OF THE CARBONIFEROUS

A weathered crust (cover) developed on the buried Carboniferous surface represents a polygenetic geological object of different origins and ages. Weathered crust on the Carboniferous strata is hydraulically connected with Lower Badenian basal clastics where water and gases accumulate. For the miners, this represents an anomalous structure of the Carboniferous massif (Dopita, 1988a; Takla and Ptáček, 1990). On the other hand, if an adequate isolating rock is present, such buried weathered crusts (covers) can serve as a suitable place for CO<sub>2</sub> sequestration. It should be pointed out that during the 1960 to 1980 period, i.e. at a time when prospecting for new fields in the coal basin by boreholes was in progress, no attention was paid to methodology issues that would define or determine the properties of the weathered crust (cover). These came only to be studied later, in connection with coal mining under water-bearing horizons (Schejbalová et al., 1983, 1984, 1985, 1987, 1988; Martinec and Krajíček, 1988) or when the Frenštát Mine was being developed (Mikytová et al., 1984).

### MEZOZOIC OXIDATIVE WEATHERED CRUST OF „VARIEGATED BEDS“

The surface of the Carboniferous is covered with an irregularly preserved weathered crust, the so-called „variegated beds“ or „red beds“ (Dopita and Havlena, 1962; Martinec and Dopita in Dopita et al., 1997), for the age of which we have direct geological evidence is lacking so far. According to paleomagnetic analyses and dating of red rocks from variegated beds, the origin of such solid products of weathering is to be sought during the period from Jurassic to Lower Cretaceous (Krs et al., 1993). Such dating is in line with the evolution of erosion on the Carboniferous paleosurface in the Upper Silesian Basin (Jura, 1993, 2001). It follows from works by Polish authors (Pluta, 2002; Dowgiałło, 1973; Krawiec et al., 2003) who studied the isotopic composition of sulfur  $\delta^{34}\text{S}$  and oxygen  $\delta^{18}\text{O}$  in water that the origin of those waters which infiltrated the beds of Dębowiec Mbr is rainwater of post-Triassic period on the Carboniferous paleorelief that already had undergone deep alteration and where, in a tropical climate, a deep oxidative alteration of rocks on the Carboniferous surface took place.

The red weathered cover on the Carboniferous surface, so called „variegated beds“ or „red beds“, in Czech publications as „pestré vrstvy“, appeared as an hard oxidative surface alteration of Carboniferous rocks (see photo on page 100) and coal (Dopita et al., 1997) while, at the same time, the massif was under thermal influence during the

burning of thick coal seams on the outcrops which interfered deep into the Carboniferous (Klika et al., 2000, 2004). For that reason, such rocks and adjacent coal seams are characterized by thermal and oxidative changes in their mineral composition (Králík, 1982; Klika and Osovský 1999, Klika et al., 2000, 2004, Klika and Kraussová 1993), the formation of collapsed breccia at the site of burnt-out coal seams brought about a disruption of the surrounding massif by cracking. In contact with Lower Badenian basal clastics (detritus), such solid products of weathering operate as a permeable rock body, acting as an aquifer where water and gases can collect, or as migration paths for gases within the Carboniferous massif in mines (Dopita, 1988). Owing to weathering, the physical properties of Carboniferous rocks altered by thermal and oxidative effects become different from those of rocks that had not been impacted by such specific alterations (Martinec, 1993).

### PALEOGENE-MIOCENE AND RECENT WEATHERED CRUSTS ON CARBONIFEROUS SURFACE (SO-CALLED „BROWN CRUST“)

On the surface of Carboniferous strata, an oxidative weathered crust is developed from rocks which themselves had shown no signs of weathering („grey“, unaltered rocks) or from „variegated beds“; for the sake of simplicity, this crust is termed the „brown crust“ (Martinec and Krajíček, 1989). Its residues are found under autochthon Carpathian, basal Lower Badenian clastics as well as under Quaternary glacial sediments or directly on outcrops of the Carboniferous along the Ostrava-Karviná ridge (these outcrops are locally dubbed „Carboniferous windows“). However, the primary zonal structure and thickness of such weathered crust has been reduced by erosive processes.

**The thickness and mineral transformation of rocks in this weathering crust on the surface of Carboniferous strata are influenced by:**

- 1) **Geomorphological factors:**
  - type of paleosurface on Carboniferous strata,
  - dip of beds and discontinuities (bedding, tectonic zones) in relation to the surface,
  - intensity of mechanical disruptions due to slope deformation and movements,
  - the rates of weathering, erosion, and denudation processes.
- 2) **Geochemical factors:**
  - geochemical reactivity of rocks,
  - temperature and intensity of rainfall,
  - occurrence of coal seam or of rocks with dispersed coal matter within reach of the weathering crust due to it becoming covered with younger sediments.
- 3) **Lithological and petrological factors:**
  - petrographic composition of rocks,
  - the degree of diagenetic transformation of sedimentary rocks, the degree of compaction of sediments, and porosity,
  - occurrence of unstable rock-forming minerals in the hypergenous alteration (weathering) zone.

## GEOMORPHOLOGICAL FACTORS IMPACTING THE GROWTH OF WEATHERING CRUST

The above attempts at describing the development of the brown weathered crust on the surface of the Carboniferous show that its evolution and degree of preservation are greatly modified by the morphological type of the surface of the Carboniferous.

Generally, the following types of paleorelief of the fossil landscape can be identified:

- (a) Hilltop areas, buried smooth relief peneplane with local elevations and flat depressions (Ostrava-Karviná ridge, Paskov and Staříč elevations, Frenštát-Trojanovice plateau, and also the surface peneplane of Oderské vrchy Uplands in the West). This type of relief is propitious for the penetration of the weathering crust to greater depths and for its preservation. The weathered crust is covered under younger sediments (autochthonous Carpathian, Neogene sediments of Outer Carpathian foredeep, Quaternary sediments); with intensive recent weathering in progress on the outcrops of Carboniferous rocks. On this type of relief, the weathering crust showing oxidative rock alteration is up to ca. 40 m thick; the commonly encountered thicknesses of weathered rocks are 25 to 30 m. At greater depths there are signs of weathering along joints and zones of disrupted rock communicating with the surface. The coal seams with outcrops on the surface of the Carboniferous paleorelief are weathered by oxidation (they contain humic acids). The outcrops lend themselves to direct observation on Landek Hill in Ostrava-Petřkovice, in the Lučina collision-type riverbank opposite the former Zárubek Mine (Fig. 6.5), in Trojice Valley near Ostrava Castle, as well as in Ostrava-Michálkovice and Ostrava-Hladnov.



Fig. 6.5 Outcrops of horizon of Castel conglomerate ("Zámecký slepenec"), Ostrava Fm, basal part of Poruba Mbr, on the river bank of Lučina river in an impact location opposite to the abandoned Zárubek Mine in Ostrava. Photo: Petr Martinec. An example of deeply weathered Carboniferous sandstones on the plateau atop the Ostrava-Karviná ridge where outcrops of Carboniferous sediments reach the surface („Carboniferous windows“).

- (b) The slopes of Carboniferous strata in deep paleo-valleys of the Dětmarovice and Bludovice furrows and in the transversal valleys thereof are ragged and rather broken morphologically. Bulged beds and big blocks of stable sandstones may even form of big rocks blocks on the valley slope. The jagged character of slopes is also influenced by the dip of beds in relation to surface. In the lower part of the slope there are slope debris and slope sediments (debris of Carboniferous rocks, sand and gravels cemented by calcite), e.g., basal Lower Badenian clastics. The thickness of the weathered crust is very variable. As a result of erosion, it may be missing completely or may be preserved in patches only. The coal seams with surface outcrops show minimum or no alteration. At the lower slopes, a weathering crust (cover) of a thickness of ca. 10 m has been preserved locally.
- (c) The furrow beds and adjacent slopes are covered in debris and sandy sediments (Eggenburgian) or basal clastics of Lower Badenian. Due to severe erosion, the weathered crust has been fully removed here or is preserved only in relicts of a up to 10m thickness. The furrows show a certain tendency to preservation of the weathered crust in the eastward sections.

It is evident from the above overview that in locations where long-lasting and deep erosion of the Carboniferous strata has occurred (furrows, transversal valleys and slopes), the thickness of the crust is minimal and the crust if any is preserved only to a limited extent and in geomorphologically advantageous locations out of reach of erosion.

## GEOCHEMICAL FACTORS

It is assumed that weathered crust was formed by a continuous process on the surface of Carboniferous peneplain, under conditions of warm and wet climate of the Tertiary or in humid climate of the Quaternary. According to chemical rock analyses (Martinec and Krajíček, 1989) the rocks of Ostrava Fm and Karviná Fm (Sedlové vrstvy Mbr) exhibit a geochemical stability of which is low or medium (0.05 to 0.15) if measured by the rocks alkalinity index (Rieche, 1943), or low to high (3 to 8) if measured by the reactivity of rocks based on the potential weathering index after Dubánek (1986), as is illustrated in Fig. 6.6.

## MINERAL TRANSFORMATION IN CARBONIFEROUS WEATHERING CRUST

From the point of view of the changes that occurred to the minerals involved, the brown weathering crust of Carboniferous rocks seems to be a rock environment where mineral transformations are limited, due above all to their petrographic and chemical composition and structure. In the whole Ostrava Fm and Karviná Fm, the association of clastic components in the rocks, i.e., both of minerals and of rocks fragments, much the same regardless of the rock genesis. Clastic quartz and fragments of stable rocks (quartzites, chlorite-muscovite quartzites, lydites etc.) are common. Sandstones and conglomerates from Sedlové vrstvy Mbr (Karviná Fm) are also richer in quartz –

		Index of rock alkalinity									Potential weathering index									
		0	0.025	0.050	0.075	0.1	0.125	0.150	0.175	0.2	1	2	3	4	5	6	7	8	9	10
Karviná FM		Rieche 1943									Dubánek 1986									
Sedlové vrstvy Mbr	conglomerate			■									■							
Sedlové vrstvy Mbr	sandstones				■	■	■						■	■	■	■				
Sedlové vrstvy Mbr	siltstones and claystones					■	■	■						■	■	■	■			
Ostrava Fm																				
Poruba Mbr Jaklovec Mbr Hrušov Mbr petřkovic Mbr	sandstones							■												■
	siltstones							■	■										■	
	claystone																		■	

Fig. 6.6 Rock alkalinity index (Rieche, 1943) and potential weathering index (Dubánek, 1987) according to the chemical analysis of rocks from Ostrava and Karviná Fms in the Czech part of the Upper Silesian Basin.

Legend: Rieche, 1943:  $R.I. = [100 \text{ moles } (Na_2O + K_2O + CaO + MgO - H_2O)] / [moles ((Na_2O + K_2O + CaO + MgO + SiO_2 + Al_2O_3 + Fe_2O_3))]$

Dubánek, 1987:  $X_{alk} = (mNa + mK + mCa + mLi + mSr + mBa) / \Sigma_{ni}$

where:  $m$  – molar concentration of element       $n$  – number of components determined (except  $H_2O$ )

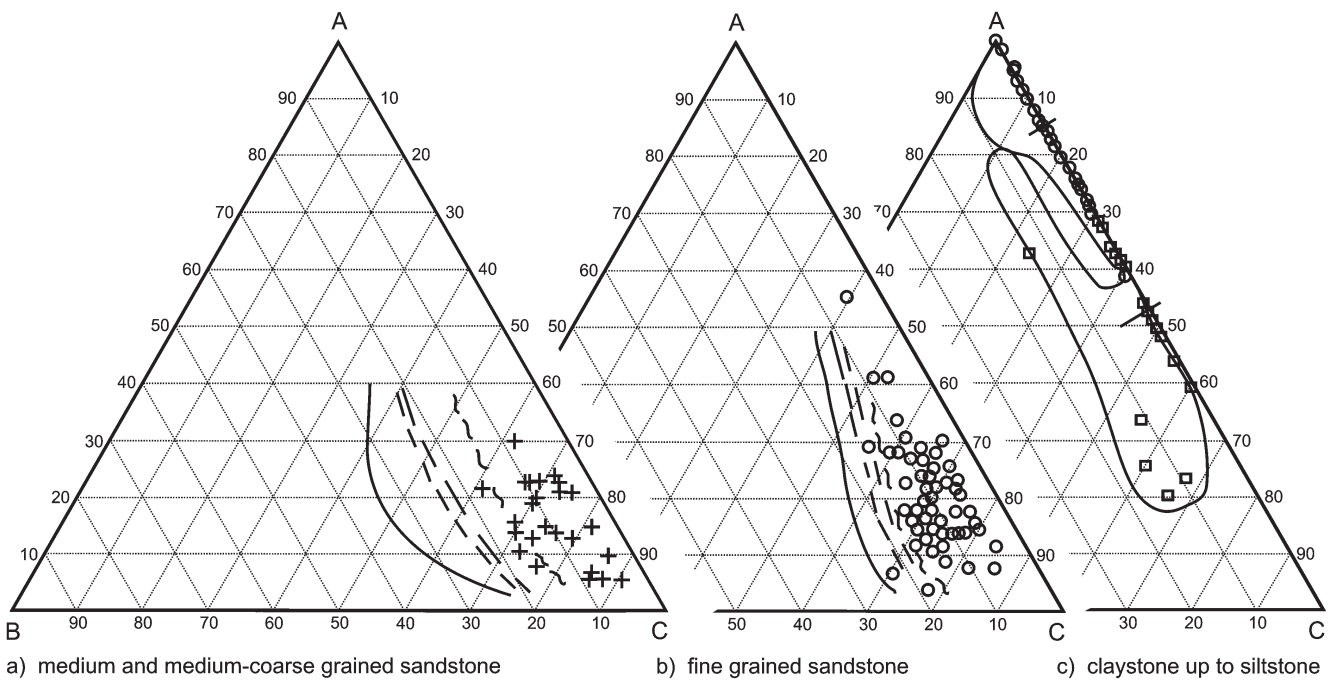


Fig. 6.7 Modal composition of Carboniferous clastic rocks from the Czech part of the Upper Silesian basin in ternary diagram: A (silt and clay component) – B (unstable components (feldspars, micas, unstable rock fragments) – C (clastic quartz fragments, stable rock fragments rich in quartz).

Legend: OSTRAVA FM:   Petřkovic Mbr      KARVINÁ FM: ≈ ≈ ≈ Sedlové vrstvy Mbr.  
  Hrušov Mbr  
- - - Jaklovec and Poruba Mbrs

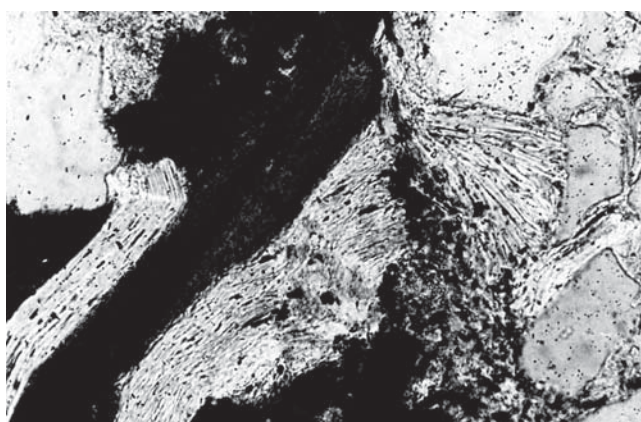
quartz-feldspar aggregates from gneisses and granitoides. Feldspars are represented by orthoclase, microcline, and plagioclases (acidic oligoclase-andesine). Biotite and muscovite, and to a lesser extent, also detritic Fe-Mg chlorite, are common components of the clastic phase. Unstable fragments are represented by bituminous coal, claystones and siltstones, phyllites, acidic igneous rocks, quartz-feldspar grains (granites, gneisses ?); amphibolite or chlorite schists are very rare. The modal composition is shown in *Fig. 6.6*.

Clayey matter is a normal component of all sediments. However, the association of clayey minerals is highly influenced by the stage of diagenetic transformation of sediments and by petrographic types in those cases where diagenetic transformations in sandstones outstrip transformations in claystones and siltstones (Králík, 1982a,b; Uher in Dopita et al., 1997). Associations of minerals in the cement of rocks in reducing environments are com-

monly represented by siderite and pyrite, in marine and brackish sediments by Fe-dolomite and in continental sequences by Mg-siderite to Fe-dolomite and pyrite. The modal composition of Carboniferous rocks of Ostrava and Karviná Fms is shown in *Fig. 6.7*.

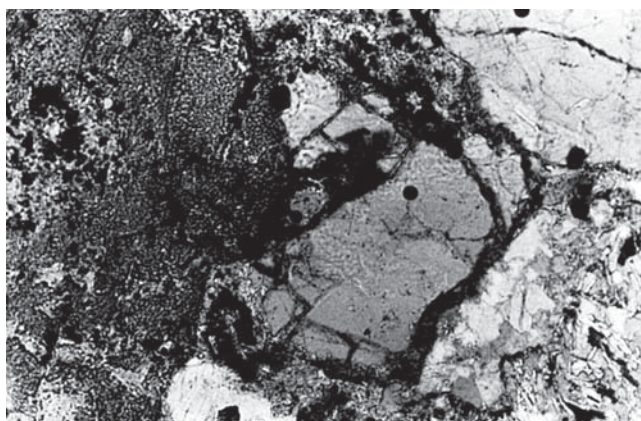
The zone of oxidation forms the uppermost part of weathering crust. Recent weathering of the Carboniferous is accessible to direct observation only on outcrops of the Carboniferous; the buried oxidation zones can be observed only in boreholes.

Unstable minerals in Carboniferous rocks include pyrite, biotite, muscovite, detritic chlorite and feldspars, detritic Fe-Mg, chlorites more or less pre-sedimentation altered (sericitization, kaolinization) (*Fig. 6.7*), disintegrated and transformed micas (*Fig. 6.8*), and carbonates. Secondary minerals provide the filling in-between the rock grains; and secondary cementation of the rocks is due mainly to limonite (*Fig. 6.9*) and carbonates.



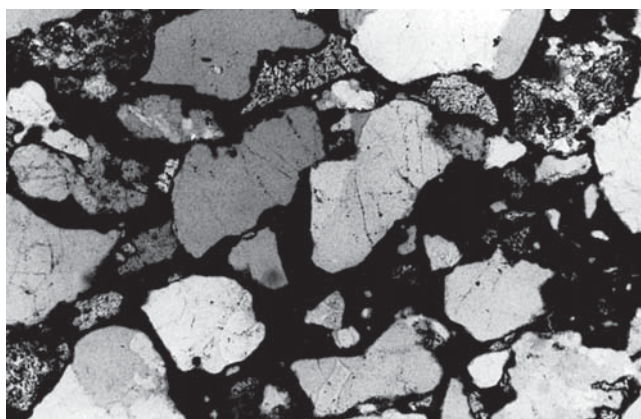
*Fig. 6.8* Hard kaolinization of feldspar, destruction of mica flakes and limonitization of matrix in hard weathered sandstone from outcrops of Zámek horizon on the river bank of Lučina river in an impact location opposite to the abandoned Zárubek Mine in Ostrava. Optical transmission microscopy. Magnification 100x.

Photo: Petr Martinec.



*Fig. 6.9* Hydration of detrital micas (smectitization and illitization) accompanied by limonitization of sandstone matrix; these are mineral transformations highly characteristic of hard weathered sandstones from outcrops of Zámek horizon on the river bank of Lučina river in an impact location opposite to the abandoned Zárubek Mine in Ostrava. Optical transmission microscopy. Magnification 100x.

Photo: Petr Martinec.



*Fig. 6.10* Intensive limonitization (Fe - oxyhydrite) around the clastic grains of quartz is a feature which is highly characteristic of the oxidative reaction taking place in hard weathered sandstone from outcrops of Zámek horizon on the river bank of Lučina river in an impact location opposite to the abandoned Zárubek Mine in Ostrava. Optical transmission microscopy. Magnification 100x.

Photo: Petr Martinec.

The oxidation-reduction zone already reflects the changes in pH and Eh of solutions in the deeper part of the weathering crust but we find it directly on the paleorelief due to surface erosion. In this zone which in terms of the intensity of its alteration processes, barely differs from unaltered rocks of grey color, can be differentiated mainly by deposition of Fe-oxohydrates (as "limonite") in fissures and minor rock veins (Fig. 6.10), by deposition on the surface of clastic grains, and by precipitation of secondary carbonates and pyrite in the pore space. Muscovite on the surface of flakes is very irregularly hydrated (illitized), but illitization has not attained the same intensity on all flakes (Fig. 6.9). Biotite is chloritized, most probably via the mixed-layered structure of biotite-chlorite yielding Fe-Mg chlorite (clinochlore).

Typomorphic minerals for oxidative part of the weathering crust include goethite, Fe-oxohydrates („limonite“), hematite, and kaolinite. However, the presence of kaolinite need not be an indicator of weathering processes since in the young Karviná Fm, kaolinite is a primary mineral, too. For the oxidation-reduction part of the weathering crust, typical minerals are chloritized biotite, deposited secondary pyrite, carbonate, goethite or Fe-oxohydrates („limonite“) in the rock structure. In both cases, attention has to be paid to changes in dispersed coal matter in rocks and to oxidative changes in the coal matter found in coal seams.

In locations where the weathered crust or its residues are covered by Lower Badenian clastics, secondary calcite is present in the contact zone with underlying Carboniferous. This occurrence of calcite has nothing to do with weathering processes on the surface of Carboniferous strata.

#### **POROSITY, PORE SIZE DISTRIBUTION AND PERMEABILITY OF CARBONIFEROUS ROCKS UNALTERED BY WEATHERING AND OF ROCKS FROM WEATHERING CRUST**

Total porosity of unaltered Carboniferous rocks (mostly of grey or light green/grey color) is low and in fact the secondary pores formed in diagenetic processes related to coalification of coal matter. Total porosity is the sum of effective porosity (communicative, open *i.e.*, accessible pores) and closed (non-communicative *i.e.*, inaccessible) pores. As a result of mineral changes, the pore space undergoes changes linked with rock weathering, and a new, tertiary porosity comes into existence. Due to weathering, the total porosity of rocks tends to be higher in the weathered crust. In altered sandstones, total porosity increases as much as 13%, which can be accounted for by an increased number of pores having more than 0,5  $\mu\text{m}$  in size (Fig. 6.10). In claystones and siltstones, total porosity tends to increase up to 14%, with extreme values up to 25%, which corresponds to rocks finely disrupted by fissures with thin oxohydrate layers.

Effective porosity varies in the same way as total porosity. In sandstones in the weathered crust, effective porosity attains extreme values of up to 9%; in claystones and siltstones it is up to 9% and, in extreme cases, up to 16%. It follows from a detailed analysis of the mechanisms capable of modifying the pore space of the samples that in sandstones, the main factor is that the cement of second-

ary carbonates is leached out (removed by elution) and replaced simultaneously by Fe oxides and Fe oxohydrates. The degree of filling of the cavities is not always the same; it differs from sample to sample. In claystones and siltstones, the network of fine fissures running in a direction sub-parallel to the plane of orientation of flakes of phyllosilicates (micas) and additional deposition of Fe oxohydrates and carbonates play dominant roles. Changes in rock properties caused by weathering can be observed in the brown weathering crust of the peneplain extending over the hillcrests, to depth of ca. 40 to 50 m, this is more pronounced near the lower boundary and less prominent on furrow slopes and in valleys. It applies analogously to total pore volumes determined by high pressure mercury porosimetry (for conditions of analysis, see Chapter 3). In fresh sandstones, the values of cumulative pore volume ( $V_{\text{COP}}$ ) are 0.007 to  $0.030 \cdot 10^{-3} \text{ m}^3 \cdot \text{kg}^{-1}$  for the so-called "grey sandstones"; in sandstones from the brown weathering crust, the interval is wider, from 0.007 to  $0.065 \cdot 10^{-3} \text{ m}^3 \cdot \text{kg}^{-1}$ . In claystones, the situation is similar; in claystones and siltstones from the brown weathering crust, the values range of  $V_{\text{COP}}$  from ca. 0.005 to ca.  $0.095 \cdot 10^{-3} \text{ m}^3 \cdot \text{kg}^{-1}$ . However, numerous samples show values that overlap with those for rocks exhibiting no signs of weathering.

Permeability of fresh, no altered sandstones was studied Konečný et Kožušníková (2011) – see Chapter 2).

Permeability testing of rocks from weathered massif using rock samples taken in a direction perpendicular to the stratification plane confirm that this parameter is highly sensitive to rock structure and texture. For a group of sandstone samples having a structure little disturbed by weathering or subsequently filled with newly formed minerals, the values of permeability fall into the same field as for grey, non-weathered rocks. Samples with open pores due to elution of unstable minerals and without secondary cementation differ from the above group. Claystones can probably be divided into three groups of samples: those showing no substantial structural changes; those affected by partial alteration and deposition of newly formed minerals (with permeabilities of ca. 1 mD); and those with a structure and texture disturbed by subparallel orientation of phyllosilicate flakes. The relationship between permeability and depth the Carboniferous cover interface shows that the outreach of changes is up to ca. 60 m under the contact level (Martinec and Krajčůček, 1989).

#### **PHYSICAL PROPERTIES OF CARBONIFEROUS ROCKS FROM WEATHERING CRUST**

Weathering also impacts the physical properties of rocks. A comparison of the physical properties of fresh, non-weathered sandstone from Zámek conglomerate horizon (Ostrava Fm, basal part of Poruba Mbr) and weathered sandstone of similar granularity in the oxidation zone on the outcrops of Zámecký conglomerate horizon in Lučina riverbank opposite Zárubek Mine is given in Table 6.1, near from the Ostrava-castle. It is worth pointing out that due to different degree of weathering, the properties of rocks from that weathered crust are very variegated, even over short distances. Therefore, owing to the limited number of samples available, only interval values could be specified for selected parameters (Table 6.2).

**WEATHERING CRUST ON THE SURFACE OF CARBONIFEROUS STRATA FROM THE POINT OF VIEW OF GEOTECHNICAL PRACTICE**

Secondary accumulation of CH<sub>4</sub> and CO<sub>2</sub> in the surface zone of the brown weathering crust with Tertiary sedimentary insulating cover also takes place thanks to natural migration of methane and carbon dioxide; subsequently, these gases accumulate in locations where the massif is disturbed by open joints. This is also reflected in the increased gas production at the mines (Škuta and Vítek, 1969; Janas, 1968). Equally, outbursts of coal and CH<sub>4</sub> (Rakowski et al., 1983; Kaisar and Pavlíček, 1984; Martinec et al., 1987) as well as outbursts of rocks and gases (Martinec et al., 2008) are more frequent in the surface zone of Carboniferous strata. Viewed from this angle, the surface zone has to be regarded as a zone that is primarily predisposed to outbursts of coal, rocks and gases. Exploitation of the accumulation potential of the

weathered crust on the surface of the Carboniferous in the capacity of a gas collector poses a complicated geotechnical problem. According to data from works connected with the construction of a map of the weathering crust on the Carboniferous surface in the coalfield of Frenštát-Trojanovice (Mikyťová et al., 1984), a new map of the weathering crust on Carboniferous surface should respect unified lithological criteria for alteration of Carboniferous rocks; it should incorporate a morpho-structural analysis of the buried Carboniferous surface; and, first of all, a lithological analysis of the covering sediments including an analysis of their isolating and collector properties (their hydraulic function), as mentioned in the present Chapter. An example of a detailed analysis of the weathering crust located in the southern part of the exploitation area of ČSM Mine is given by Štřelec and Martinec (1992).

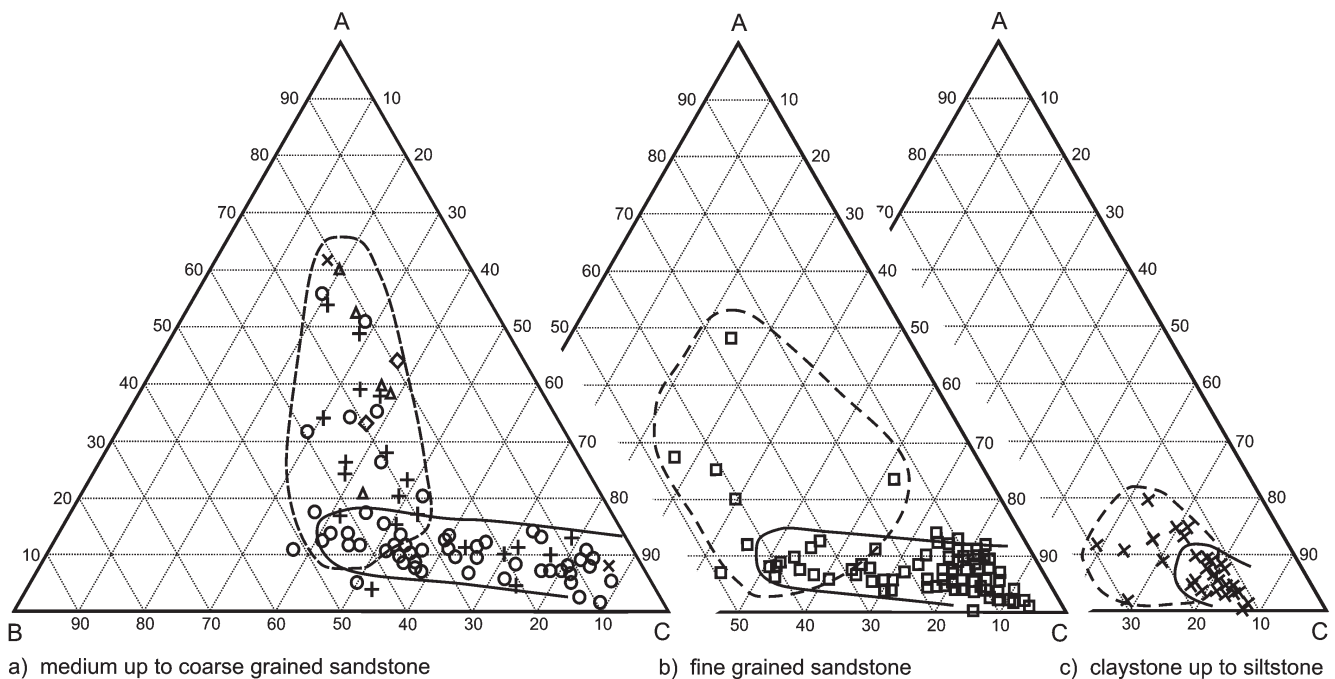


**Fig. 6.11** Volumetric percentages of pores of different size,  $V_A + V_B + V_C = V_{COP} (100 \%)$ , for pore diameter categories A ( $> 0.5 \mu m$ ), B ( $0.5-0.05 \mu m$ ), and C ( $< 0.05 \mu m$ ) in Carboniferous rocks of the Czech part of the Upper Silesian basin: rocks which suffered no alteration, or rocks from the basal part of the weathering zone where reducing conditions prevailed, and Carboniferous rocks with a highly weathered crust subject to intensive oxidation (the "brown" weathering crust).

Legend:

a) Sandstone and conglomerates:

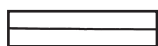
- - fine-grained sandstones;
- + - ine-grained and medium-grained sandstones;
- ◇ - coarse-grained sandstones and conglomerates;

b) Fine grained sandstones:

c) Claystone, silty claystone:



field of altered rocks from the oxidative weathering crust and from the rims of fractures (the „brown weathering crust“ with occurrences of limonite or Fe-oxohydrate)



field of fresh rocks not subject to any alteration („grey“ Carboniferous rocks) and of rocks from the oxidation-reduction zone of the weathering crust (with occurrences of pyrite, siderite, and chlorite)

Parameter		Increase in the values for weathered rocks in relation to fresh sandstones (= 100%)	Weathered sandstones on outcrops	Fresh (grey) sandstones from mine
Total porosity $p_c$	[%]	125	10.8	8.7
Effective (capillary) porosity $p_{ef}$	[%]	150	8.4	5.6
$V_{COP}$ (A) > 0.5 $\mu\text{m}$	[%]	138	55	40
$V_{COP}$ (B) 0.5 - 0.05 $\mu\text{m}$	[%]	66	25	38
$V_{COP}$ (C) < 0.050 $\mu\text{m}$	[%]	91	20	22
Uniaxial compressive strength $\sigma_D$	[MPa]	69	39	64
Splitting tensile strength $\sigma_T$	[MPa]	24	0.76	3.2

Table 6.1 Comparison of average values of selected parameters characterizing weathered (brown) sandstones from surface outcrops and fresh (grey) sandstones from the Zámek horizon (Ostrava Fm, Poruba Mbr). Deep weathered sandstones originate from Zámek horizon outcrops in Lučina riverbank, near Zárubek Mine in Ostrava; the fresh (grey), unaltered sandstone originates from Zámek horizon in Zárubek Mine. Average values and standard deviations.

Parameter		Rock types	Oxidative weathering zone (brown)	Oxidative-reductive zone with transition to fresh (grey) rocks
Uniaxial compressive strength $\sigma_D$	[MPa]	sandstone	40-80	80-140
		siltstone and claystone	10-60	60-140
Splitting tensile strength $\sigma_T$	[MPa]	sandstone	3-7	6-12
		siltstone and claystone	2-7	6-11
Tangent modulus $E_{pt}$	[MPa]	sandstone	5,000-60,000	16,000-30,000
		siltstone and claystone	11,000-3,000	11,000-27,000
Total porosity $p_c$	[%]	sandstone	6-13	1-6
		siltstone and claystone	5-25	1-5
Effective (capillary) porosity $p_{ef}$	[%]	sandstone	3.5-9	1-3.5
		siltstone and claystone	3.0-16	0.5-3.0
$V_{COP}$ (A) > 0,5 $\mu\text{m}$	[%]	sandstone	5-65	5-15
		siltstone and claystone	5-50	0-10
$V_{COP}$ (B) 0,5 - 0,05 $\mu\text{m}$	[%]	sandstone	20-50	5-50
		siltstone and claystone	15-55	5-45
$V_{COP}$ (C) < 0,05 $\mu\text{m}$	[%]	sandstone	10-50	40-90
		siltstone and claystone	20-65	50-95
Permeability [mD]	[mD]	sandstone	3-35	0.05-3
		siltstone and claystone	1-8	0.005-1
Cumulative volume of pores $V_{COP}$	[ $10^{-3} \cdot \text{m}^{-3} \cdot \text{kg}^{-1}$ ]	sandstone	0.025-0.07	0.005-0.025
		siltstone and claystone	0.015-0.12	0.005-0.015
Poisson ratio $\mu$	[-]	sandstone	0.15-0.40	0.1-0.2
		siltstone and claystone	very variable	very variable
Indent strength (point loading test) $\sigma_{VTL}$	[MPa]	sandstone	500-1000	1000-1700
		siltstone and claystone	200-500	500-1400

Table 6.2 Intervals for selected physical parameters of Carboniferous rocks from young, so-called „brown“ weathering zone on Carboniferous surface and from the transition of oxidative-reductive zone to fresh rocks, in the Czech part of the Upper Silesian basin (Martinec and Krajiček, 1989). Explonary notice:  $V_{COP}$  – see Fig. 6.1

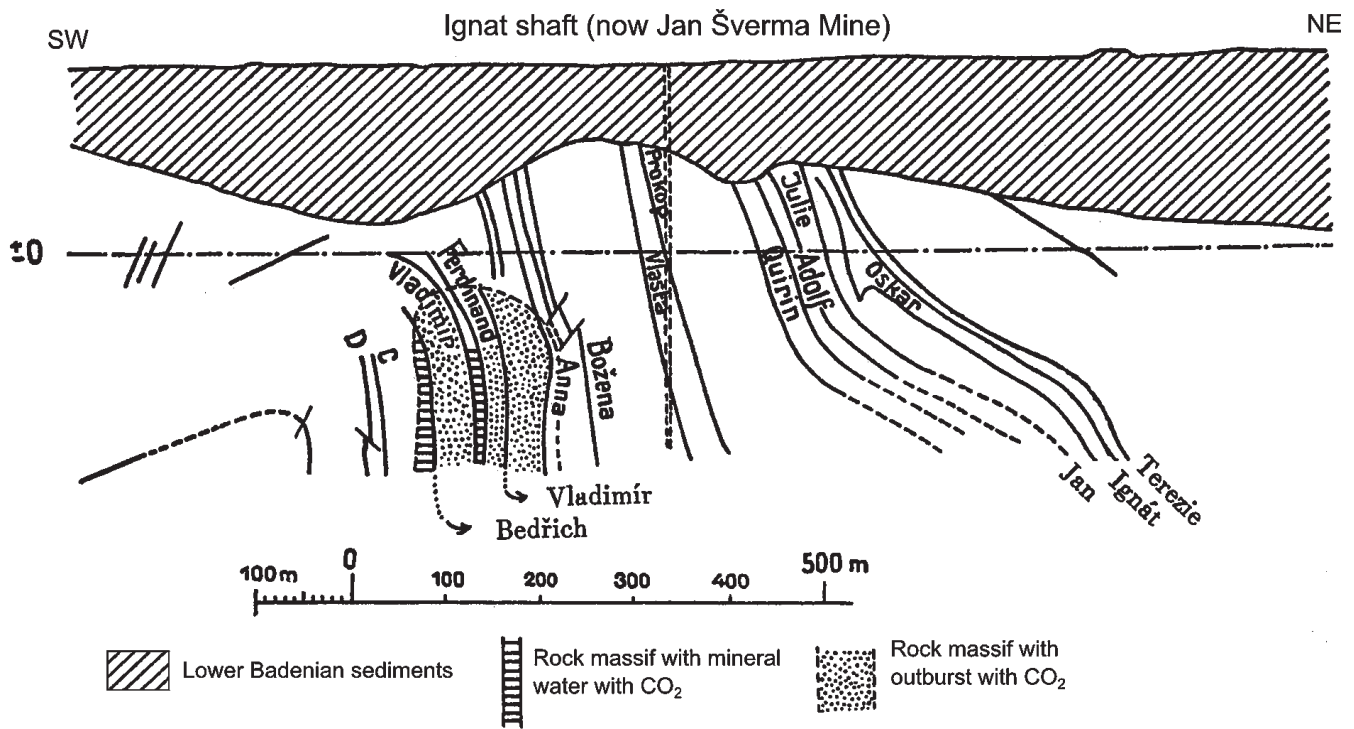


Fig. 6.12 Historical places of carbon dioxide occurrences in coal mine in western part of Ostrava-Karviná coal district historical mine: Ignac Mine.  
 After: Pateisky and Folprecht, 1928, fig. 198:256.  
 Czech part of the Upper Silesian basin, Carboniferous, Petřkovice Mbr., Ostrava Fm.

## 6.6. SUMMARY

At variance with the other coal basins described in the Chapters 2 through 5 where only one type of carbon dioxide accumulation in the massif is dominant, the Czech part of the Upper Silesian basin is characterized by variegated, numerous carbon dioxide sites.

The following cases can be encountered:

- carbon dioxide accumulations linked with the Western part of the aquifer represented by the Bludovice furrow;
- accumulations of migrating carbon dioxide in the weathering crust of Carboniferous strata;
- accumulations of adsorbed carbon dioxide in the coal seams where they occur together with thermogenic methane in the Western part of Ostrava-Karviná Coal District (Jan Šverma Mine) and in mineral water springs with dissolved carbon dioxide occurring in the mines;
- in the tectonic zones of the Carboniferous massif;
- in those parts of the massif influenced by abandoned and closed deep coal mines where there is evidence of carbon dioxide and methane rising to the surface.

It would be difficult to pass an unequivocal judgment of the suitability of the rock massif of Carboniferous or of the young covering strata for carbon dioxide sequestration. A particularly careful assessment would be required for the abandoned mine sites where there is a sufficient isolation by the covering strata (Martinec et al., 2006, 2008) or for the natural gas deposits already exploited within the weathered Carboniferous crust or its covering strata (Strakoš et al. in Dopita et al., 1997).

# 7. INFLUENCE OF CARBON DIOXIDE ON CORROSION OF CONCRETE STRUCTURES IN MINES AND UNDERGROUND CONSTRUCTIONS

Concrete structures erected or installed at major shafts of coal or ore mines – e.g., at ventilation shafts and galleries – are directly affected by atmospheric CO<sub>2</sub>, i.e., by air having at natural concentration of CO<sub>2</sub> (≈ 386 ppm ≈ 0.04 vol.%). Extreme situations are encountered in ventilation shafts and drainage tunnels where the exiting mine air already is enriched in carbon dioxide of which the concentration can be as high as 1%. For model computations, the following input data were used: mine air exit temperatures ranging from 20 to 30°C, mine air humidity 85% (±5%), and CO<sub>2</sub> contents from 0.04% to 1%.

Direct contact of the concrete supports with mineralized groundwater or with service mine water is another danger. All the aforementioned factors represent a very specific situation impacting the long-term stability of concrete structures. **Carbonation of the cement matrix of concrete is one of the most important corrosion processes impacting all types of concrete placed in underground structures, at all mines.** This **carbonate corrosion**, so-called corrosion of the 2<sup>nd</sup> type, is provoked by aggressive CO<sub>2</sub> in presence of water. Due to the reaction of Ca(OH)<sub>2</sub> (portlandite) with CO<sub>2</sub> (or (HCO<sub>3</sub>)<sub>2</sub>) producing calcite (CaCO<sub>3</sub>), the pH of the cement matrix decreases from 12.75 to ca. 8.5-8. This reaction may continue, dissolving portlandite from the cement matrix of concrete in water and yielding soluble CaHCO<sub>3</sub>. Due to decreasing pH of the cement matrix in the presence of water, and **after dissolution of Ca(OH)<sub>2</sub>, hydrolysis of calcium hydrosilicates occurs** (i.e., corrosion of the 1<sup>st</sup> type). These two types of corrosion are the most common ones; they can be examined by subjecting the concrete to laboratory tests and the severity of corrosion can be predicted by model computations.

**Corrosion of reinforced concrete** (containing rebars) is another case of corrosion. Chloride corrosion occurring when concrete is in contact with salt containing mine waters, which proceeds hand in hand with carbonation, is also common (this is so-called corrosion of the 3<sup>rd</sup> type, caused by expansion of new formed salts which crystallize from solution). **Sulfate corrosion** occurs locations where the mine waters contain sulfate ions, e.g., in mine

waters with dissolved sulfates produced by oxidation of sulfides. Cases of corrosion connected with accumulation and crystallization of salts (halite NaCl, CaCl<sub>2</sub>, bassanite CaSO<sub>4</sub>·0.5H<sub>2</sub>O, gypsum CaSO<sub>4</sub>·2H<sub>2</sub>O, etc.) by action of aggressive media expanding in the pore space and in capillary systems of the cement matrix of concrete are common, too. In these cases, corrosion is provoked by the high pressures due to the growth of salt crystals in the cement matrix from which water evaporates.

Cases of corrosion of concrete by the alkaline-silicate reaction due to the use of aggregates containing reactive rock grains from chert, certain types of greywacke, arkoses, etc. are known, too. The corrosion of concrete structures and the processes of carbonation of concrete are described in a number of works, e.g., by Dobrý and Palek (1988), Šmerda et al. (1999), Roy and Poh (1999), Drochytka et al. (2005) and others.

## 7.1 MODEL OF CONCRETE CORROSION

The software used to compute the model of concrete carbonation was *RC LifeTime - Concrete Cover Assessment* (<http://rc-lifetime.stm.fce.vutb.cz>) (Keršner et al., 2004; Rovnaník et al., 2005; Chromá, 2006, 2007; Králová and Teplý, 2001, 2002; and P. Rovnaník, 2010 – pers. comm.). *RC LifeTime* program serves for modeling the process of carbonation of concrete and for estimating the duration of the period of initiation of carbonation, i.e., the time required for the pH in the area of contact of the cement matrix with the steel rebars within the reinforced concrete to decrease below ca. pH 9.

The model used is based on the model of carbonation after Papadakis et al. (1992, 2002). It serves for computing the depth of carbonation  $x_c$  in concrete with Portland cement as a function of time. It issues from the mass balance of CO<sub>2</sub>, Ca(OH)<sub>2</sub>, and hydrated calcium silicates (CSH); changes of volume occurring in the concrete are not taken into account.

The formula for computing the carbonation depth is as follows:

$$x_c = \psi 0.35 \rho_c \frac{\left(\frac{w}{c} - 0.3\right)}{\left(1 + \frac{\rho_c w}{1000 c}\right)} f(RH) \sqrt{\left(1 + \frac{\rho_c w}{1000 c}\right) + \frac{\rho_c a}{\rho_a c}} c_{CO_2} \frac{23.8}{44} 10^{-6} t \quad (7.1)$$

where:

$x_c$  - depth of carbonation [mm] at time  $t$  [years];  
 $\psi$  - coefficient of uncertainty [-];  
 $\rho_c$  - density of cement [kg.m<sup>-3</sup>];  
 $\rho_a$  - density (bulk density of rock) of aggregates [kg.m<sup>-3</sup>];  
 $a/c$  - aggregates / cement ratio [-];

$w/c$  - water/cement ratio [-];  
 $RH$  - relative atmospheric humidity [%];  
 $c_{CO_2}$  - atmospheric concentration of CO<sub>2</sub> in the surroundings of the concrete structure under scrutiny [mg.m<sup>-3</sup>];  
 $t$  - time [years].

It should be pointed out that at high humidity values, the original function by Papadakis (1992, 2002) fails to yield correct results; therefore, correction was made using the function by Matoušek (1977). The model computations of carbonatation were performed for the type of concrete used at VOKD Co. for monolithic concrete linings (so-called „mine concrete“). The results of the model computations are shown in Figs. 7.1. and 7.2.

In spite of the fact that this is purely a model case of corrosion of concrete involving only one type of corrosion, it is evident that the impact of CO<sub>2</sub> on the propagation of corrosion in concrete under analogous conditions should be taken into account. The model case shows that for monolithic shaft concrete linings 300 mm thick, the time

period of 100 years is not critical inasmuch they were affected by carbonate corrosion to a depth of 40 mm. However, in the case of steel reinforced concrete 600 mm thick, the depth of corrosion of 160 mm could already be critical from the point of view of corrosion of the steel supports (particularly considering the existence of salty mine waters which can contact the supports). The carbonatized layer provides the main pathway for the initiation and propagation of other types of corrosion. Thus, the impacts of corrosion on the concrete structures have to be assessed in a comprehensive fashion, bearing in mind the long service periods of the given mine working under its specific operating conditions (Fig. 7.3).

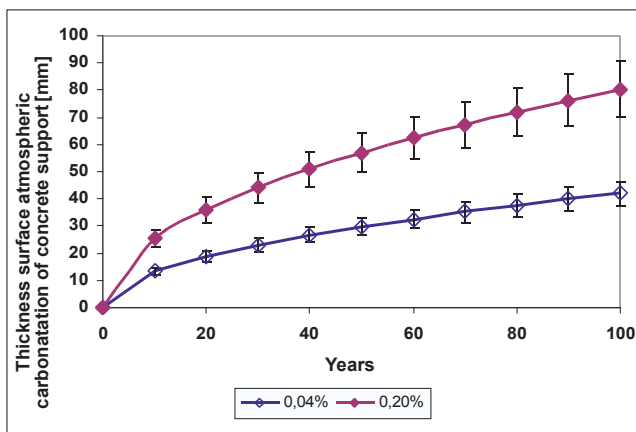


Fig. 7.1 Prognostic computation model of thickness surface atmospheric carbonatation of concrete support in shaft (condition see Tab. 7.1) for fresh air with content of CO<sub>2</sub> (0.04 %) (downcast shaft) and for exit mine air with content of CO<sub>2</sub> (0.2 %) (up cast shaft), a case of ore mines. Model is computed for time interval of 100 years.

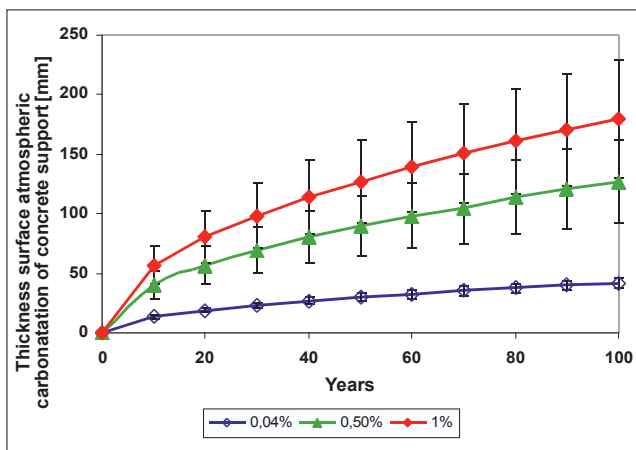


Fig. 7.2 Prognostic computation model of thickness of surface atmospheric carbonatation of concrete support in shaft (input data see Tab. 7.1) for fresh air with content of CO<sub>2</sub> 0.04 %) (downcast shaft) and for exit mine air with content of CO<sub>2</sub> (1 %) (up cast shaft), a case from hard coal mines. Model is computed for time interval of 100 years.

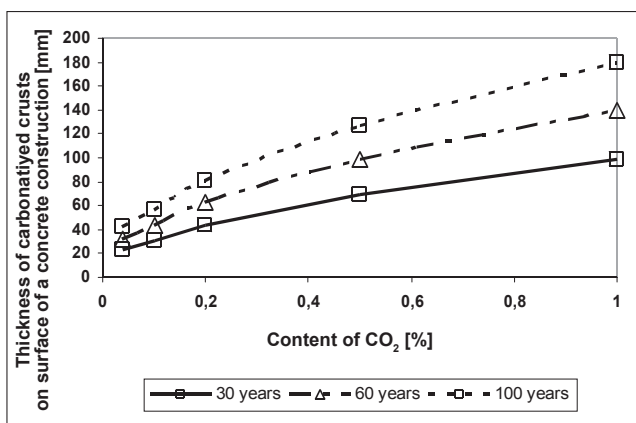


Fig. 7.3 Comparison of thickness of carbonatized crusts on surface of a concrete construction in relation to the content of CO<sub>2</sub> in air (fresh air and exit mine air) in periods of 50, 75 and 100 years of influence of CO<sub>2</sub> on concrete construction.

On the whole, experience with corrosion of concrete structures in mines is scarce. Analyses of samples of concrete taken in downcast and upcast air shafts of coal and ore mines indicate that carbonate corrosion is the dominant mode which however is accompanied by simultaneous elution of portlandite,  $\text{Ca(OH)}_2$  from concrete and by hydration of calcium silicates. Where ground waters rich in sulfates flow down the shafts, sulfate corrosion is common. This type of corrosion also appears where shafts become flooded with water from abandoned areas following the closure of mines (this has been the case for the shafts in the Rosice-Oslavany and Ostrava-Karviná coal districts).

Corrosion of concrete caused by the presence of NaCl (possibly also with sulfates) takes place in those locations where the salt-containing waters flow over the shaft walls or where the shaft walls are immersed in these waters. In the Czech part of the Upper Silesian basin, in the Ostrava-Karviná coal district, the concrete supports of the shafts come into frequent contact with such fossil salty waters infiltrating from the basal clastic sediments of Lower Badenian.

Carbonate corrosion affecting the surface of concrete is the most frequent type of which evidence was found in all concrete shaft structures (monolithic concrete lining, concrete-block walling, reinforced concrete linings), mainly in coal mines. Here, carbonate corrosion appears unevenly on the surface of supports, depending on the quality of compaction of concrete and on the integrity of the concrete surface. Corrosion is more frequent in places where mine waters flow down the concrete walls of the shaft and around the points where steel cross-beams are fixed in the shaft lining. The corrosion attack of concrete tends to be severe in shaft sumps and, above all, in the subsurface parts of lining under the shaft mouth.

## 7.2 SUMMARY

When designing concrete structures for underground locations where concrete can be affected by carbon dioxide, it is imperative that due attention be paid to the origins of the carbonate corrosion of concrete. **The existence of this type of corrosion and its propagation during the course of time as well as with progressing depth is a proven fact.**

Under the conditions prevailing in the mines, carbonate corrosion is attendant on other types of corrosion processes, with potential negative synergies.

**No thorough, systematic exploration of the corrosion of concrete that is part of various structures erected in mine shafts has been performed yet.** This type of corrosion is not reckoned with when old mine structures are liquidated, in spite of its proven effects on the stability of such structures. In those cases where the concrete structures erected in mines are accessible and are still being actively operated, the study of the corrosion processes affecting such concrete structures would be extremely desirable.

Condition	$c_{\text{CO}_2}$	$w_r$	T °C
	[mg·m <sup>-3</sup> ]	[%]	[%]
Air			
Input air	800	60 (5)	10
Exhaust mine air	19 800	85(5)	30
Components of concrete	Weight	Density	Coefficient
	[kg]	[kg·m <sup>-3</sup> ]	[-]
Cement CEM I (PC 400)	360	3100	
Aggregates 0-4 mm	690	2650	
Aggregates 4-16 mm	460	2680	
Aggregates 8-22 mm	460	2690	
Water	220		
Coefficient			1
Assessment period			100 years

Table 7.1 Input data for model computation of carbonatation of concrete components and structures installed or erected in underground mines

Legend:  $c_{\text{CO}_2}$  – concentration of carbon dioxide;  $w_r$  – relative atmospheric humidity; T °C – air temperature

## 8. CONCLUSIONS

The present work renders a description of the **cases of occurrence of carbon dioxide registered in the mines of the Bohemian Massif on Czech Republic territory (Fig. 2.1)** and also in neighbouring Poland where the geological conditions are very similar. In the cases described, it has been possible, **thanks to mining activities, to establish direct and immediate contact with the natural environment of carbon dioxide reservoirs in more or less permeable rocks, rock massif and / or in coal seams to obtain first-hand information and understanding of how carbon dioxide is stored in the massif under natural conditions.** The information derived from such investigations, the level of which corresponds to the period in which the pertinent data were collected, was not designed for dealing with issues relating to CO<sub>2</sub> sequestration underground, but rather, first of all, for the purposes of ensuring safety at work in the mines. Nevertheless, thanks to the authenticity of these investigations, they continue to represent, even today, useful information that can serve as an inspiration for further orientation of the research.

**Chapter 2** provides a summary of the general knowledge available on the behaviour of the H<sub>2</sub>O – CO<sub>2</sub> – NaCl – (CH<sub>4</sub>) system under temperature and pressure conditions existing in the coal basins in question. New information has been gleaned from laboratory experiments of carbon dioxide adsorption on coal from the Czech part of the Upper Silesian Basin, and this has been compared with the results of studies of CO<sub>2</sub> and methane adsorption on coal matter in coal seams in the Polish part of the Intra-Sudeten Basin.

The best-known locality where carbon dioxide complicated mine development and operations in the Perm-Carboniferous basin in Central Bohemia was Slaný coal deposit (1979–1990). The description of CO<sub>2</sub> and rock outbursts which occurred therein during the sinking of skip and hoisting shafts for Slaný Mine is given in **Chapter 3**. The gas reservoir from which the gas outbursts were sourced was represented by the Mirošov horizon in Nýřany Fm, composed of a complex of conglomerates and sandstones with pore space filled with mineralized water and carbon dioxide (low permeable sandstones and conglomerates). The mining problems encountered when the shafts were being opened under such adverse conditions, compounded with other unfavourable circumstances, have led to closure of the mine and to liquidation of the shafts.

The sinking of a drainage shaft for Obránců Míru Open Pit Mine in Komořany near Most in the Northern Bohemia basin (**Chapter 4**) was another case where mining works encountered and crossed a natural reservoir of carbon dioxide. In that locality, carbon dioxide is accumulated in the weathered surface of a buried gneiss complex constituting the immediate underlying strata of Cretaceous and Tertiary deposits by which these gneisses are isolated.

Miners also had to cope with occurrences of carbon dioxide adsorbed, together with methane, on coal seams in other bituminous coal basins in the Czech part of the Intra-Sudeten Basin as well as in the neighbouring Polish

part thereof. These occurrences manifested themselves as outbursts of coal and carbon dioxide with methane or outbursts of carbon dioxide and rocks. They were observed not only during the mining operations conducted within the Intra-Sudeten Basin (in the Czech part of the basin, in the area formerly exploited by East Bohemian Coal Mines Corp.) but, first of all, in the Polish part of the Intra-Sudeten Basin where extensive outbursts of carbon dioxide or carbon dioxide and methane in the Wałbrzych Mine District of the basin and in Nowa Ruda Mine District were prominent (**Chapter 5**). Outbursts involving carbon dioxide and coal and carbon dioxide with methane and coal were registered in the Ostrava-Karviná Coal District, too (**Chapter 6**).

**From the point of view of incidence of carbon dioxide, the Czech part of the Upper Silesian Basin (Chapter 6) is a very special area. Carbon dioxide occurs there in the following locations and forms:**

- *Lower Badenian groundwater body, in the Western part of Bludovice furrow – fossil valley where carbon dioxide is dissolved in water;*
- *Adsorbed onto coal matter in coal seams of the Western part of Ostrava-Karviná coal district (outbursts of coal, rock, and gases);*
- *In fissures or tectonic zones in the Carboniferous together with mineralized water; such water is drained rapidly after the fault is opened during mine activities;*
- *Together with carbon dioxide of biogenous origin existing in mine air in active mines and in gases ascending to the surface from closed mines where mining for coal was terminated.*

For selected localities, **Chapters 3, 4, 5, and 6** give detailed descriptions of the petrological properties of rocks, the character of pore space, some physical properties of rocks and coal as well as the characteristics of the structure and texture of the rocks that make it possible for carbon dioxide to accumulate. **The influence of tectonic patterns is also explained, as is their possible relation to Tertiary volcanism in the Bohemian massif influencing the distribution of natural carbon dioxide sites at mines or on the surface in the form of springs of warm and cold mineral water or as outlets of dry, gaseous CO<sub>2</sub> (moffetts) – see Chapter 2.**

**Chapter 7** describes a model situation where CO<sub>2</sub> provoking the corrosion of concrete as a result of the formation of carbonates impacts the concrete structures installed or erected underground. In addition to the effects of carbon dioxide (carbonates), such structures tend to deteriorate, in the long term, due to the extreme operating conditions in the mines, coupled with additional factors (e.g., the influence of mineralized mine waters containing sulfates, chlorides etc.; the pressure of the massif acting upon the supports; temperature changes, etc.).

**Under the natural conditions prevailing within the rock massif, carbon dioxide migrates or is accumulated mainly if the following geological situations are encountered:**

- In the Bohemian massif, the locations of the carbon dioxide sites are closely linked to the area of Tertiary volcanic activity (see Fig. 2.1).
- Carbon dioxide ascends from the depth, from mantle sources, along deep faults towards the surface; it emerges on the surface as dry gas (moffetts) or is dissolved in warm or cold mineralized water.
- Carbon dioxide is accumulated in permeable rocks, in the pore space of rocks, or in such joints or fissures of the rock massif which are isolated from the overlying strata by impermeable rocks; this type of gas reservoirs is often represented by buried weathering crust.
- Migrating carbon dioxide is adsorbed, frequently together with thermogenic methane from the coal seams, on the pore space of coal matter within the coal seams or on rocks rich in finely dispersed coal matter.

**Carbon dioxide and its migration in the massif are also related to the technology of coal mining and to the reduced extent of coal mining:**

- Carbon dioxide is liberated and enters the mine air from the surrounding massif (e.g., adsorbed on coal); it is generated within the mines by the operation of combustion engines and, last but not least, by biogenic activities related to the oxidation of both coal matter and methane and also of higher hydrocarbons (from coalification processes). Carbon dioxide is also evolved from mineral waters present in the mines in which it was dissolved. The concentration of gas in mine air is monitored and is regulated by mine ventilation. It also is the underlying cause of corrosion of concrete structures in the mines.
- In the case of any disruption of overlying strata, the carbon dioxide preserved in an isolated system of a closed mine ascends to the surface together with methane; it is recorded as gas emissions that directly impact the environment as well as the safety of structures.

**In principle, the following alternatives can be used for the storage (sequestration) of carbon dioxide in the rock massif using geotechnical methods:**

- Storage of carbon dioxide in the joints or pore space of rock bodies or rock massif (in gaseous form in fissures and pores, or as gas dissolved in aquifers), as long as these are isolated by impermeable rocks, mainly in the overlying strata. These can be e.g., stratified bodies of more or less permeable porous sandstones or conglomerates and, first of all, buried weathering crusts with cracks, open secondary pore space, etc.

- Dissolution of carbon dioxide in water in the pore space of permeable rocks in groundwater bodies isolated by impermeable rocks in the overlying strata.
- Carbon dioxide can also be stored in mine workings opened for that very purpose or in abandoned mine workings and/or in a massif affected by mining, provided that propitious natural conditions for such storage exist.

**The present work also demonstrates some specific features of the natural processes leading to the sequestration of carbon dioxide in the rock massif. Such features are the following:**

- Transport and migration of carbon dioxide take place preferentially along tectonic faults and failure zones.
- Migration of carbon dioxide in the massif takes place at pressures higher than the geostatic pressure and at velocities measured in terms of geological timescales.
- Diffusion processes participate in the distribution of carbon dioxide in pores of the rock mass; this leads to an uneven distribution of carbon dioxide in the pore space of rocks or of coal seams.
- Reaction of carbon dioxide with aqueous solutions occurring in the pores (where carbon dioxide and calcium form carbonate) and reactions with other rock-forming minerals, giving rise to new mineral transformations or to secondary porosity.

**In the case of a carbon dioxide reservoir where coal seams are the gas collector, the following factors should be taken into account:**

- The petrographical composition of the coal, i.e., the degree of coalification, its maceral composition, ash content, the humidity of deposited coal and the degree of coal fracturing caused by contraction cleats within the coal formed in the zone of the coalification jumb of coal, as well as the joints and fractures due to coal becoming crushed by the tectonic processes.
- In depth penetration of carbon dioxide into the macromolecular structure of coal by diffusion (associated with changes in coal volume), which manifests itself whenever there is a sudden departure from equilibrium (state of stressing) in the surroundings of the mine working by an outburst accompanied by a profound disintegration of the coal (giving rise to coal dust).
- When carbon dioxide is adsorbed onto the coal matter or when free gas accumulates in cracks within the coal while humidity is also present, methane is displaced due to competition with carbon dioxide.
- The permeability of coal and rocks decreases rapidly with increasing stress in the adjoining rock mass.

**In the case of carbon dioxide reservoirs constituted by more or less permeable clastic rocks with well-developed pore space, attention shall be paid to the following:**

- *Porosimetric analysis of the rocks involved (total volume of pores; pore size distribution; and percentages of pores belonging to different size categories).*
- *Analysis of the permeability of rocks and coal, and the influence of stress thereon.*
- *Analysis of mineral associations in the rocks, mainly in order to identify minerals which modify the pore space or minerals that can be removed by a suitable process by which the permeability of the rocks will be increased (e.g., removing carbonates by an acid solution).*
- *Detailed analysis of the „water – CO<sub>2</sub> – NaCl – (CH<sub>4</sub>)“ system at the pore pressure and temperature prevailing in the deposit under scrutiny or in the entire locality.*

**In case of adsorption collectors such as coal seams, these can be confronted with the results of laboratory testing of sorption processes. It is evident that:**

- *In laboratory adsorption tests, both carbon dioxide and methane become adsorbed onto the surface of coal particles.*
- *Under laboratory conditions, the sorption process is highly dependent on the specific surface area of the coal sample or, directly, on the size of the coal particles (i.e., on the particle size of the prepared ground coal sample or on the degree of disintegration of the natural coal sample taken).*
- *For that reason, the sorption volumes of gases as well as the desorption rates determined in situ and in laboratory will be different.*
- *For the results of laboratory measurements to be applied to situations encountered in a natural environment it is imperative that the orientation and intensity of the cleats naturally occurring in the coal seams be determined and their type of mineralization identified.*  
*Core sampling from oriented boreholes or withdrawal of suitably oriented samples of coal from the seam is recommended.*

The data acquired in actual cases of gas dynamic effects or of coal, rock, and gas outbursts mentioned in the present work cannot be regarded as exact experimental data; rather, they are data not always determined under precisely defined conditions and immediately after the outburst. Nevertheless, they characterize each phenomenon under scrutiny at the conditions actually observed, using such technical means as were available at the time. Nevertheless, they represent the unique and sole data acquired, whether as single points or as interval values and this have to be taken into account when working with the data.

The information presented in this monograph can find application not only for the purpose of identifying localities suitable for underground storage (sequestration) of carbon dioxide and for modelling the related processes, but also for the purpose of specifying mine safety measures in cases where mine workings are opened in a rock massif potentially loaded with carbon dioxide.

PLATE - A

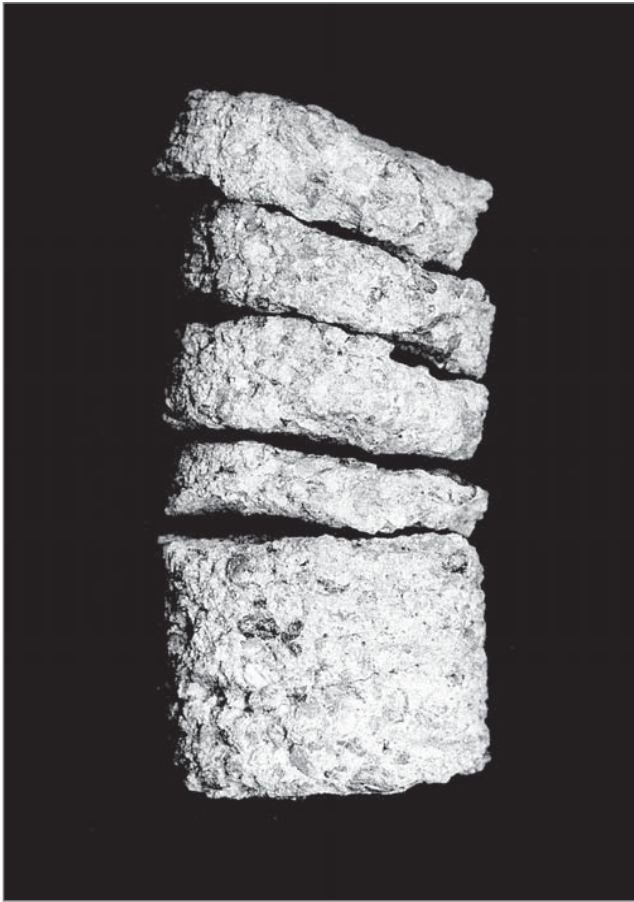


*Plate A/1*

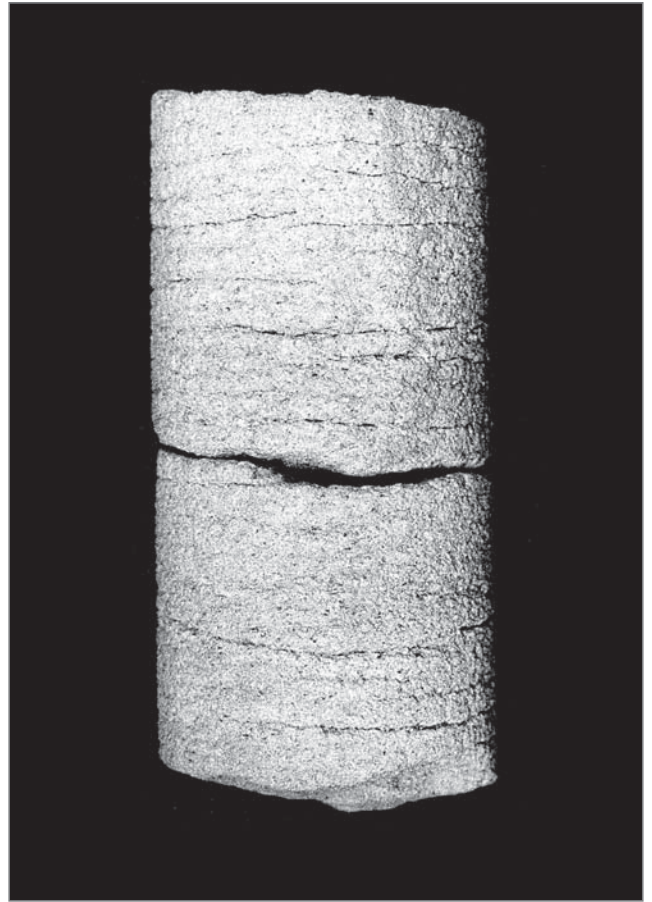


*Plate A/2*



*Plate A/3*

**PLATE A/1**

Fracture in drill core having the character of „conchoidal fracture“ in conglomerates.

Conglomerates, Nýřany Mbr, Mirořov horizon, Slaný Mine skip shaft.

Core drill of 46 mm dia.

*Photo: Petr Martinec.*

**PLATE A/2**

Fine-grained to medium-grained sandstone, very fine fracturing of sandstone drill core; „conchoidal“ fracture.

Sandstones, Nýřany Mbr, Mirořov horizon, Slaný Mine.

Core drill of 46 mm dia.

*Photo: Petr Martinec.*

**PLATE A/3**

Fine-grained to medium-grained sandstone with fracture planes in drill core („conchoidal fracture“).

Nýřany Mbr, Mirořov horizon, Slaný Mine skip shaft.

Core drill of 46 mm dia.

*Photo: Petr Martinec.*

# PLATE - B

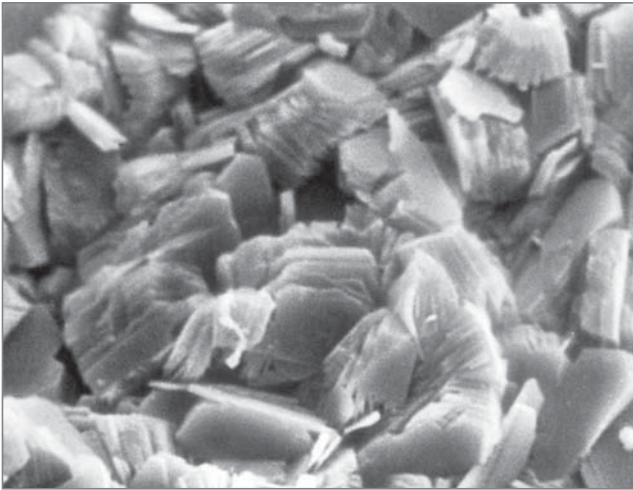


*Plate B/1*

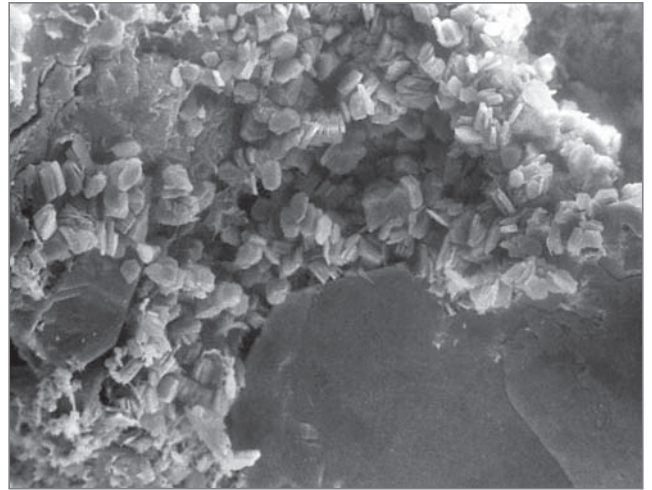


*Plate B/2*

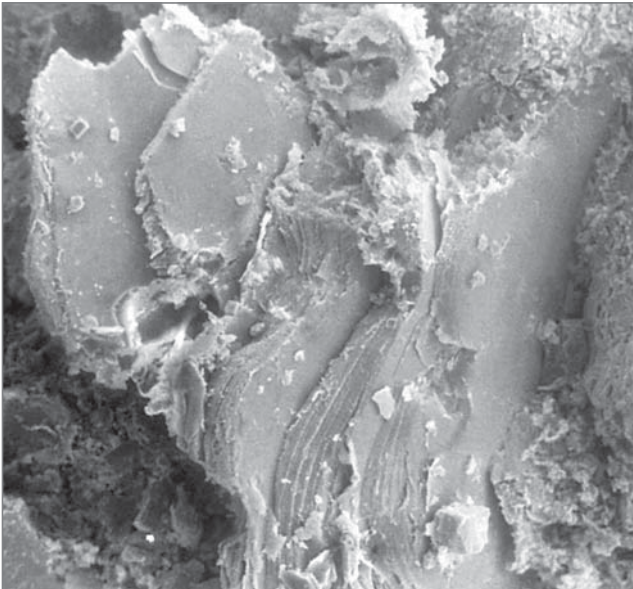


*Plate B/3*

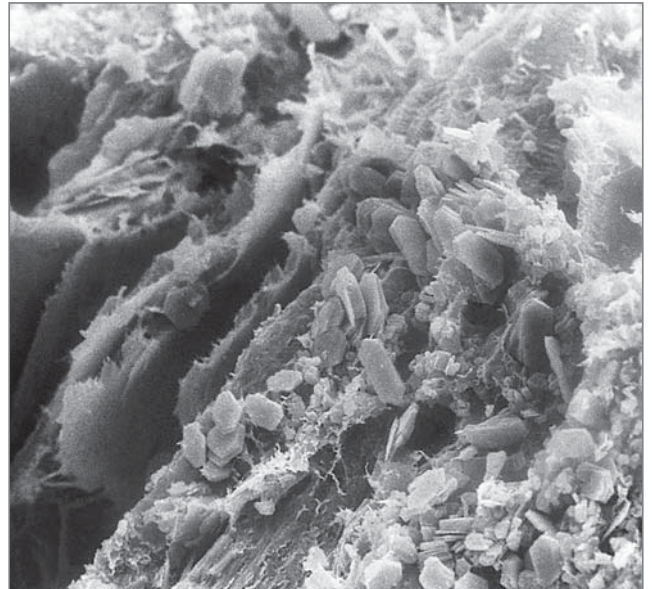


*Plate B/4*



*Plate B/5*

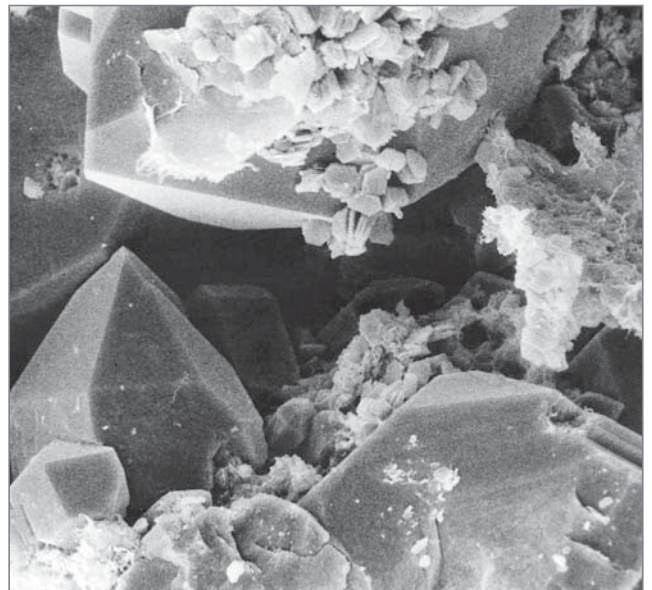


*Plate B/6*

**PLATE B/1**

Kaolinite aggregates of perfect crystallinity and crystal morphology in sandstone matrix.

Sandstones. Nýřany Mbr, Mirošov horizon.  
Slaný Mine skip shaft.

SEM, magnification 1250.

*Photo: Antonín Uher.*

**PLATE B/2**

Quartz grain with kaolinite aggregates of perfect crystallinity and crystal morphology in sandstone matrix.

Sandstones, Nýřany Mbr, Mirošov horizon.  
Slaný Mine skip shaft.

SEM, magnification 250.

*Photo: Antonín Uher.*

**PLATE B/3**

Flakes of detrital muscovite with hydrated surface in sandstone.

Nýřany Mbr, Mirošov horizon.  
Slaný Mine skip shaft.

SEM, magnification 800.

*Photo: Antonín Uher.*

**PLATE B/4**

Heavy exfoliation in flakes of hydrated and illitized muscovite in sandstone.

Sandstones, Nýřany Mbr, Mirošov horizon.  
Slaný Mine skip shaft.

SEM, magnification 1000.

*Photo: Antonín Uher.*

**PLATE B/5**

Detrital quartz and feldspar grains showing surface corrosion.  
Sandstone.

Nýřany Mbr, Mirošov horizon.  
Slaný Mine skip shaft.

SEM, magnification 650.

*Photo: Antonín Uher.*

**PLATE B/6**

Crystals of newly formed quartz growing on detrital quartz grains, with exposed tabular crystals of kaolinite in macropores.  
Sandstones.

Nýřany Mbr, Mirošov horizon.  
Slaný Mine skip shaft.

SEM, magnification 650.

*Photo: Antonín Uher.*

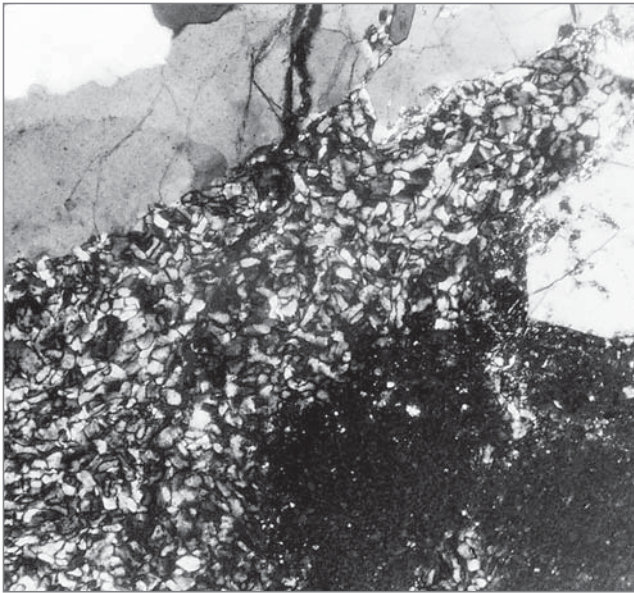


*Plate B/7*

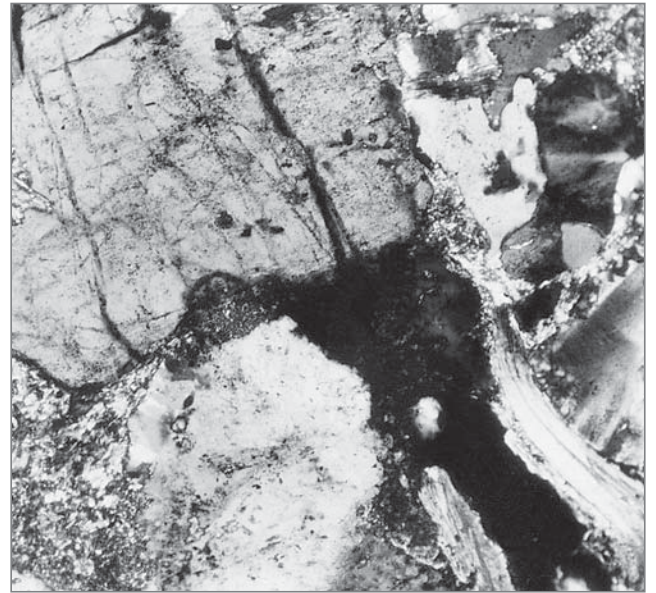


*Plate B/8*

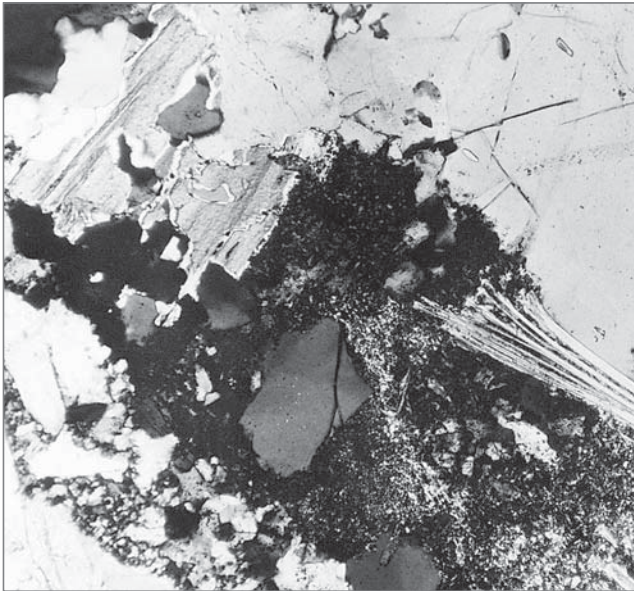


*Plate B/9a*

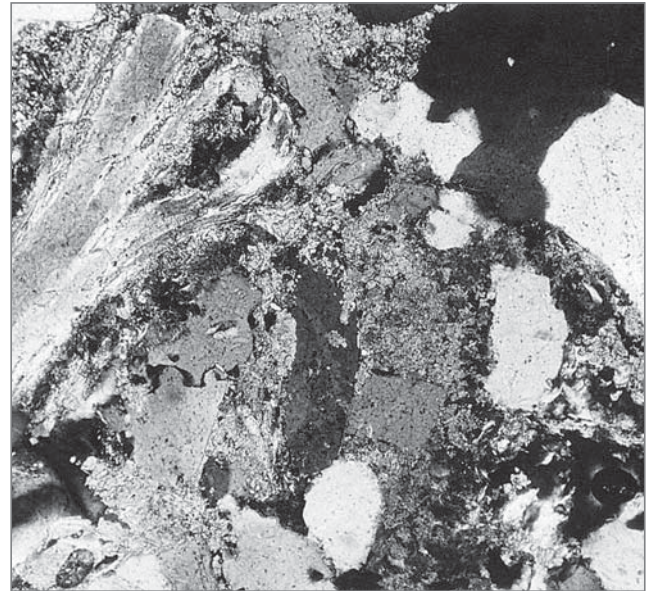


*Plate B/9b*

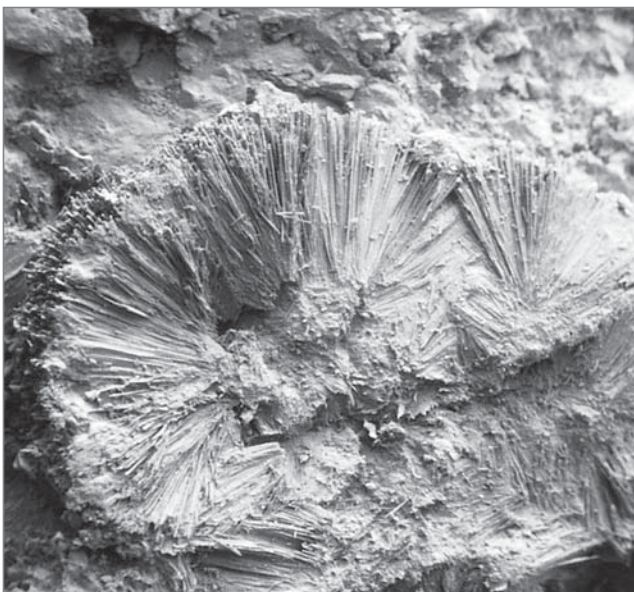


*Plate B/10a*

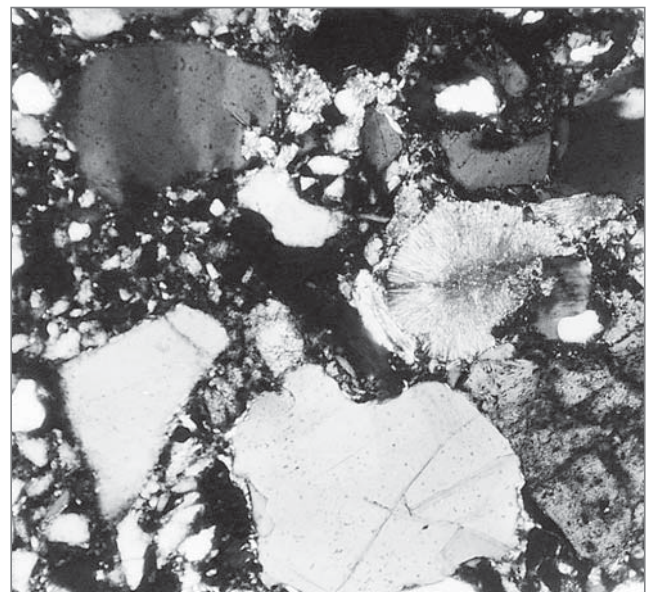


*Plate B/10b*

**PLATE B/7**

Newly formed fine-grained quartz is deposited (as microquartzite) in pores situated in-between the clastic quartz grains.  
The crack planes correspond to „conchoidal fracture “.

Sandstones, Nýřany Mbr, Mirořov horizon.  
Slaný Mine skip shaft.

Optical microscopy, magnification 400, crossed nicols.

*Photo: Petr Martinec.*

**PLATE B/9a**

Exfoliated flakes of clastic micas (muscovite), illitized on the surface. Quartz of magmatic origin containing gas-water bubbles and rutile crystals.  
Hard, silicified matrix.

Sandstones, Nýřany Mbr, Mirořov horizon.  
Slaný Mine skip shaft.

Optical microscopy, magnification 100, crossed nicols.

*Photo: Petr Martinec.*

**PLATE B/10a**

Radial crystal aggregates of dawsonite  
 $\text{NaAl}[(\text{OH})_2 \cdot \text{CO}_3]$  on a fissure in sandstone.

Nýřany Mbr, Mirořov horizon.  
Slaný Mine skip shaft.

SEM, magnification 60.

*Photo: Antonín Uher.*

**PLATE B/8**

Hard, altered clastic feldspar showing signs of both corrosion and mechanical damage. Fine-grained, flaky, mainly kaolinite clay matter with newly formed carbonates is deposited around the original grains.

Sandstones, Nýřany Mbr, Mirořov horizon.  
Slaný Mine skip shaft.

Optical microscopy, magnification 100, crossed nicols.

*Photo: Petr Martinec.*

**PLATE B/9b**

Clayed, carbonaceous matrix deposited between detritic quartz grains. Exfoliated detritic flakes of micas with illite surface crust.

Medium-grained sandstones, poorly sorted.  
Nýřany Mbr, Mirořov horizon.  
Slaný Mine skip shaft.

Optical microscopy, magnification 63, crossed nicols.

*Photo: Petr Martinec.*

**PLATE B/10b**

Radial crystal aggregates of dawsonite  
 $\text{NaAl}[(\text{OH})_2 \cdot \text{CO}_3]$  on a fissure in sandstone.

Sandstones, Nýřany Mbr, Mirořov horizon.  
Slaný Mine skip shaft.

Optical microscopy, magnification 100, crossed nicols.

*Photo: Petr Martinec.*

# PLATE - C

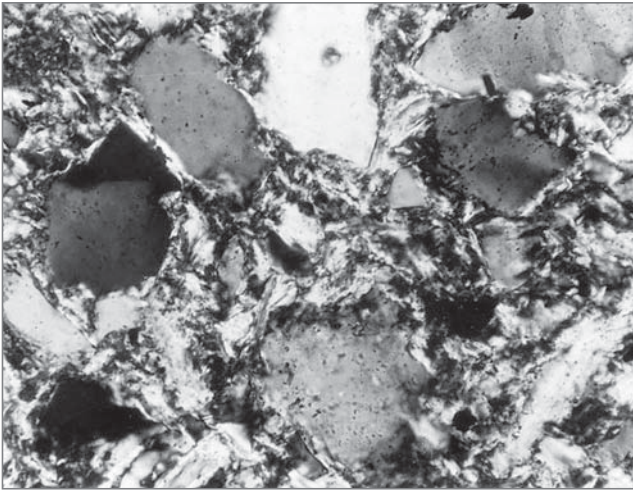


*Plate C/1*

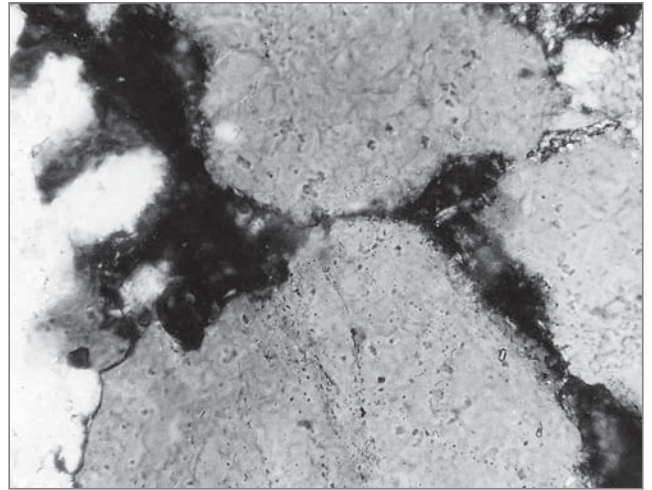


*Plate C/2*

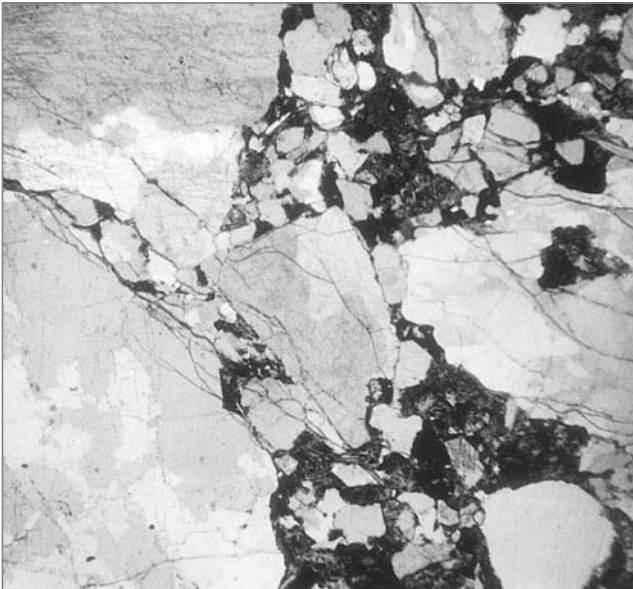


*Plate C/3*

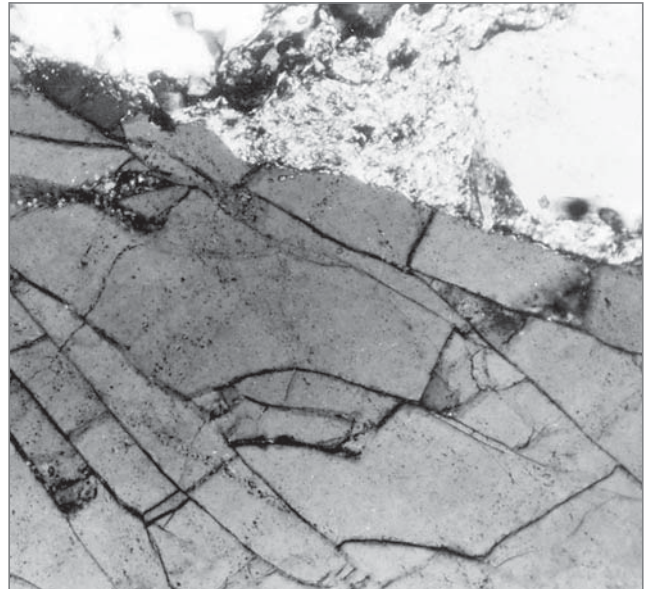


*Plate C/4*

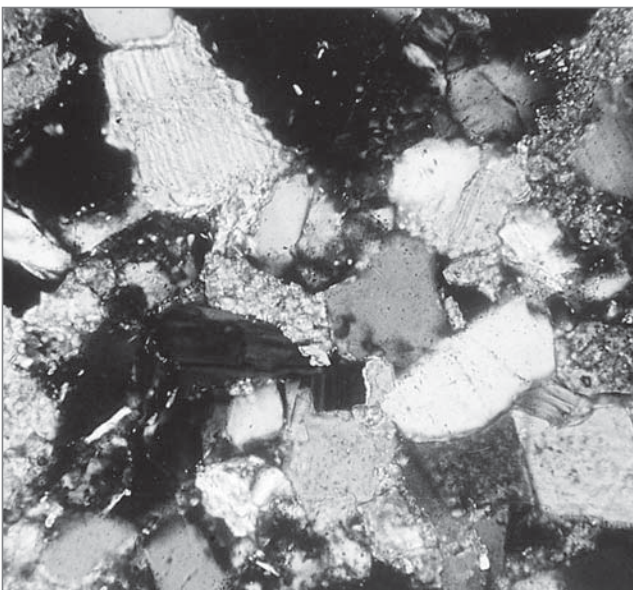


*Plate C/5*

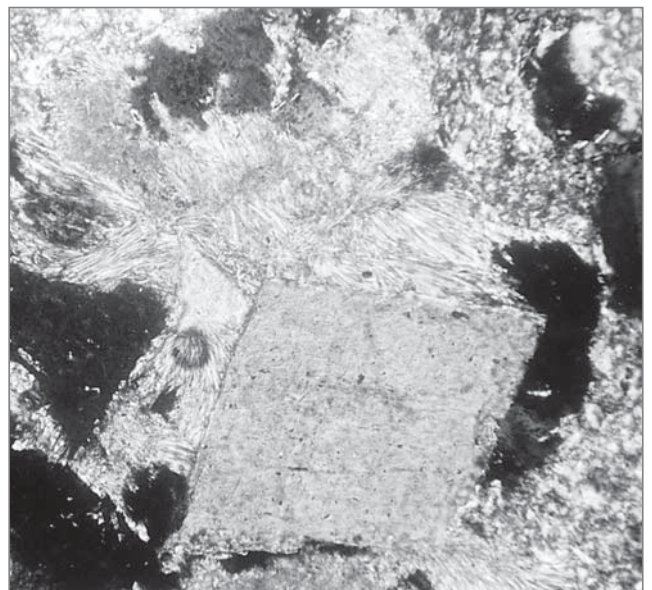


*Plate C/6*

#### **PLATE C/1**

Microtexture of sandy siltstone with matrix formed by fine flakes of argillized micas.

Nýřany Mbr, Mirošov horizon.  
Slaný Mine.

Optical microscopy, magnification 100, crossed nicols.

*Photo: Petr Martinec.*

#### **PLATE C/3**

Specific fracturing of detritic quartz grains. Cracks and crushing across the quartz grains. Sandstone drill core. Fracture in drill core having the character of "conchoidal fractures" in sandstone (see *Plate A/2, A/3*).

Nýřany Mbr, Mirošov horizon.  
Slaný Mine skip shaft.

Optical microscopy, magnification 100, crossed nicols.

*Photo: Petr Martinec.*

#### **PLATE C/5**

Sandstone from Mirošov horizon. In pores between the detritic grains there are idiomorphous, rhombohedral crystals of carbonate which stop off the pore mouths.

Nýřany Mbr, Mirošov horizon.  
Slaný Mine cage shaft.

Optical microscopy, magnification 100, crossed nicols.

*Photo: Petr Martinec.*

#### **PLATE C/2**

Detritic quartz grains with short contact planes. Detritic grains showing surface corrosion and local diagenetic regeneration.

Medium-grained sandstone, Nýřany Mbr, Mirošov horizon. Slaný Mine.

Optical microscopy, magnification 250, crossed nicols.

*Photo: Petr Martinec.*

#### **PLATE C/4**

Detail of fractured detritic quartz grains. Cracks across the quartz grains, „conchoidal“ fracture. Sandstone drill core. Fracture in drill core having the character of "conchoidal fractures" in sandstone (see *Plate A/2, A/3*).

Nýřany Mbr, Mirošov horizon.  
Slaný Mine skip shaft.

Optical microscopy, magnification 100, crossed nicols.

*Photo: Petr Martinec.*

#### **PLATE C/6**

Sandstone from Mirošov horizon. In pores between the detritic grains there are idiomorphous, rhombohedral crystals of carbonate which stop off the pore mouths.

Nýřany Mbr, Mirošov horizon.  
Slaný Mine cage shaft.

Optical microscopy, magnification 250, crossed nicols.

*Photo: Petr Martinec.*



*Plate C/7*

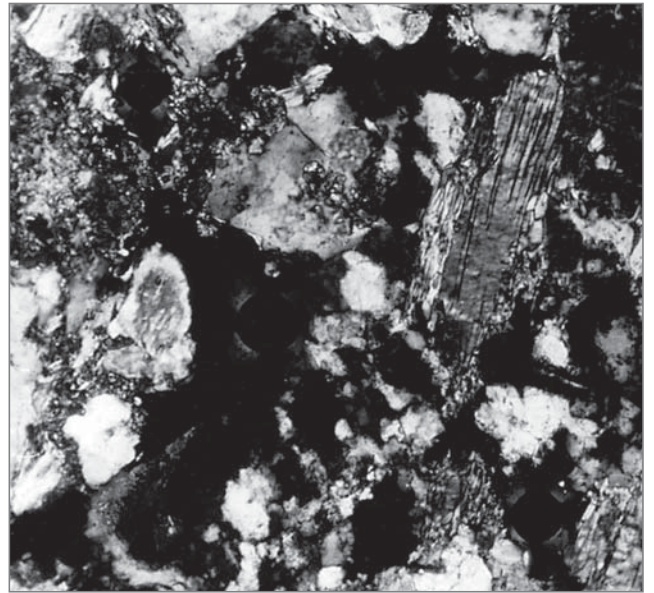


*Plate C/8*



*Plate C/9*

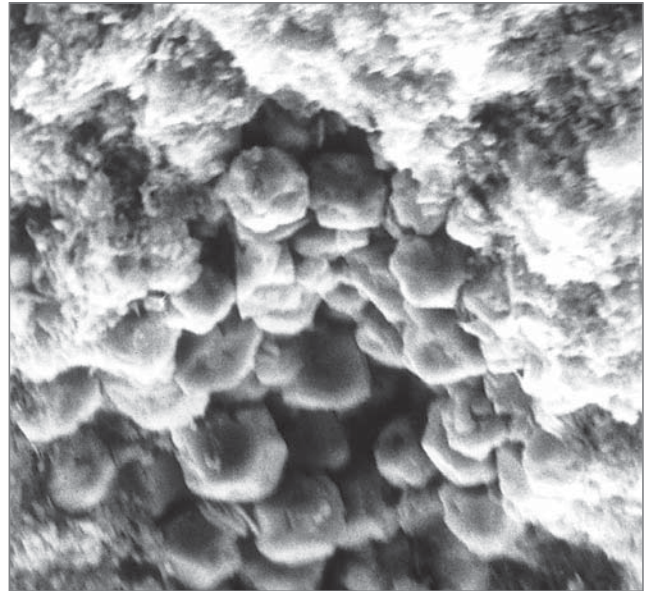


*Plate C/10*



*Plate C/11*

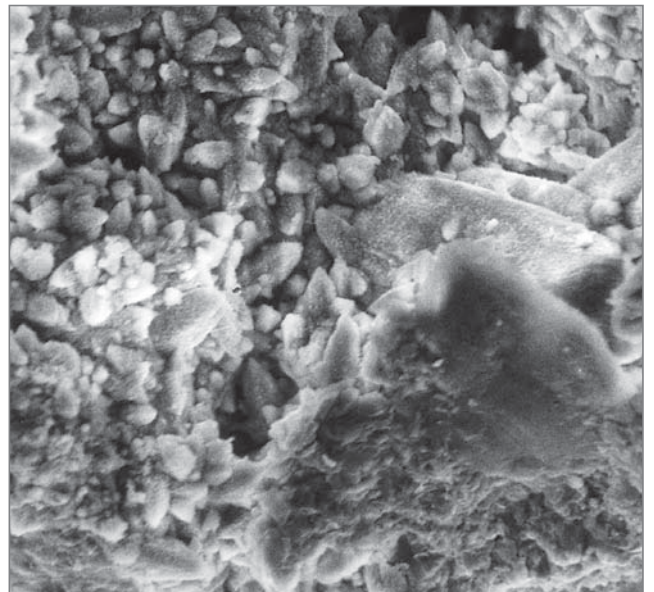


*Plate C/12*

#### **PLATE C/7**

Specific fracturing of detritic quartz grains. Cracks across the quartz grains connected by a „conchoidal“ fracture. Sandstone drill core.

Drill core, medium-grained sandstone.  
Nýřany Mbr, Mirořov horizon.  
Slaný Mine cage shaft.

Optical microscopy, magnification 100, crossed nicols.

*Photo: Petr Martinec.*

#### **PLATE C/8**

Extended exfoliation and surface alteration of muscovite flakes connected with illitization or with mixed layers of illite and smectite.

Drill core, medium-grained sandstone.  
Nýřany Mbr, Mirořov horizon.  
Slaný Mine cage shaft.

Optical microscopy, magnification 100, crossed nicols.

*Photo: Petr Martinec.*

#### **PLATE C/9**

Marlstone (Lower Turonian), sample 4465a.

Komořany drainage shaft, borehole KO-16,  
depth 82.5-84.7 m.

SEM, magnification 600.

*Photo: Antonín Uher.*

#### **PLATE C/10**

Marlstone with framboidal grains of pyrite (Lower Turonian), sample 4465a.

Komořany drainage shaft, borehole KO-16,  
depth 82.5-84.7 m.

SEM, magnification 2500.

*Photo: Antonín Uher.*

#### **PLATE C/11**

Conglomerate from Cretaceous base (Cenomanian) with hard silicification.

Komořany drainage shaft, borehole KO 16,  
depth 89.8-91.2 m.

SEM, magnification 500.

*Photo: Antonín Uher.*

#### **PLATE C/12**

Glauconitic sandstone from Cretaceous base (Cenomanian) with silty matrix showing cementation of quartz.

Komořany drainage shaft,  
depth 845 m.

SEM, magnification 500.

*Photo: Antonín Uher.*

# PLATE – D

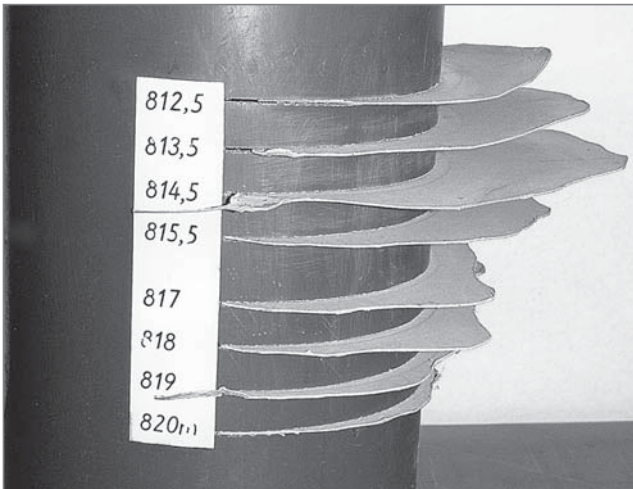


Plate D/1

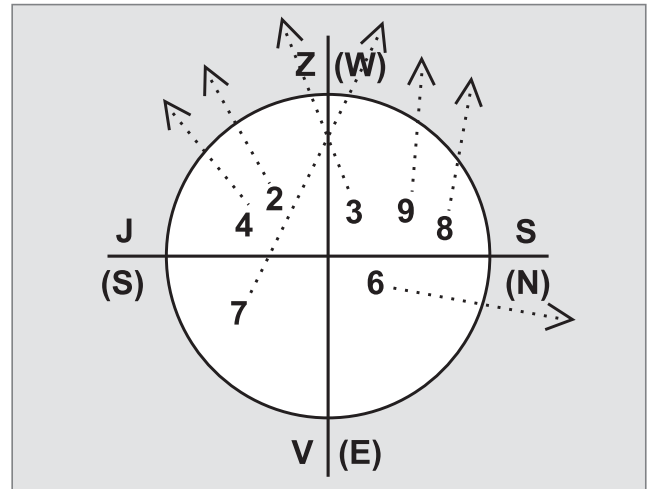


Plate D/2



Plate D/3



Plate D/4



Plate D/5



Plate D/6

#### **PLATE D/1**

Model of skip shaft with outburst caverns after the no. 1 gas and rock outburst in the skip shaft, at a depth of 812.5 – 820 m.

Simulates the Slaný Mine skip shaft.

*Model and photo: HBZS Corp.  
(Central Mine Rescue Station), Kladno.*

#### **PLATE D/3**

Cavern rim in the SSW segment of skip shaft after the no. 1 gas and rock outburst at the depth of 812.5 – 820 m. Direction „4“.

Slaný Mine skip shaft.

*Photographic documentation in Plates D3 - D18:  
HBZS Corp. (Central Mine Rescue Station), Kladno.*

#### **PLATE D/5**

Cavern in the W segment of skip shaft after the no. 1 gas and rock outburst at the depth of 812.5 – 820 m.

Direction „3“. One day after the outburst.

Slaný Mine skip shaft.

*Photographic documentation in Plates D3 - D18:  
HBZS Corp. (Central Mine Rescue Station), Kladno.*

#### **PLATE D/2**

Schematic representation of the directions in which photographs were taken after the no. 1 gas and rock outburst occurred within the skip shaft at the depth of 812.5 – 820 m.

Slaný Mine skip shaft.

*Photographic documentation in Plates D3 - D18:  
HBZS Corp. (Central Mine Rescue Station), Kladno.*

#### **PLATE D/4**

Cavern in the SW segment of skip shaft after the no. 1 gas and rock outburst at the depth of 812.5 – 820 m. Direction „2“.

Slaný Mine skip shaft.

*Photographic documentation in Plates D3 - D18:  
HBZS Corp. (Central Mine Rescue Station), Kladno.*

#### **PLATE D/6**

Midpoint of cavern in the W segment of skip shaft after the no 1 gas and rock outburst at the depth of 812.5 – 820 m. Direction „7“.

One day after the outburst.

Slaný Mine skip shaft.

*Photographic documentation in Plates D3 - D18:  
HBZS Corp. (Central Mine Rescue Station), Kladno.*



*Plate D/7*



*Plate D/8*



*Plate D/9*

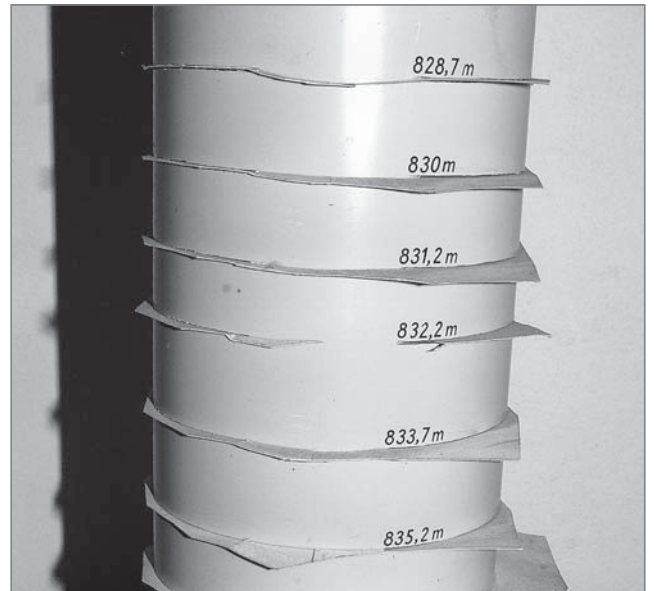


*Plate D/10*

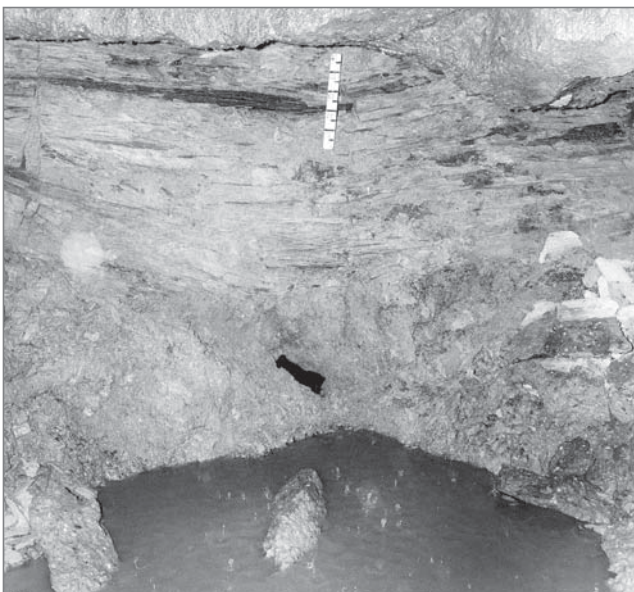


*Plate D/11*



*Plate D/12*

**PLATE D/7**

Midpoint of cavern in the WNW segment of skip shaft after the no. 1 gas and rock outburst at the depth of 812.5 – 820 m. Direction „9“.  
One day after the outburst.

Slaný Mine skip shaft.

*Photographic documentation in Plates D3 - D18:  
HBZS Corp. (Central Mine Rescue Station), Kladno.*

**PLATE D/8**

Cavern rim in the NW segment of skip shaft after the no. 1 gas and rock outburst at the depth of 812.5 – 820 m. Direction „8“.  
One day after the outburst.

Slaný Mine skip shaft.

*Photographic documentation in Plates D3 - D18:  
HBZS Corp. (Central Mine Rescue Station), Kladno.*

**PLATE D/9**

Cavern in the N segment of skip shaft after the no. 1 gas and rock outburst at the depth of 812.5 – 820 m. Direction „6“.  
One day after the outburst.

Slaný Mine skip shaft.

*Photographic documentation in Plates D3 - D18:  
HBZS Corp. (Central Mine Rescue Station), Kladno.*

**PLATE D/10**

Model of skip shaft with outburst caverns after the no. 2 gas and rock outburst in the skip shaft, at the depth of 828.7 – 838.4 m.

Slaný Mine skip shaft.

*Photographic documentation in Plates D3 - D18:  
HBZS Corp. (Central Mine Rescue Station), Kladno.*

**PLATE D/11**

Situation after the no. 3 gas and rock outburst in the skip shaft, at the depth of 848.3-850.00 m.

Slaný Mine skip shaft.

*Photographic documentation in Plates D3 - D18:  
HBZS Corp. (Central Mine Rescue Station), Kladno.*

**PLATE D/12**

Detail of the destruction of sandstone layers in the roof of cavern formed in the NW segment of the skip shaft. Situation after the no. 3 gas and rock outburst in the skip shaft, at the depth of 848.3 m.

Slaný Mine skip shaft.

*Photographic documentation in Plates D3 - D18:  
HBZS Corp. (Central Mine Rescue Station), Kladno.*

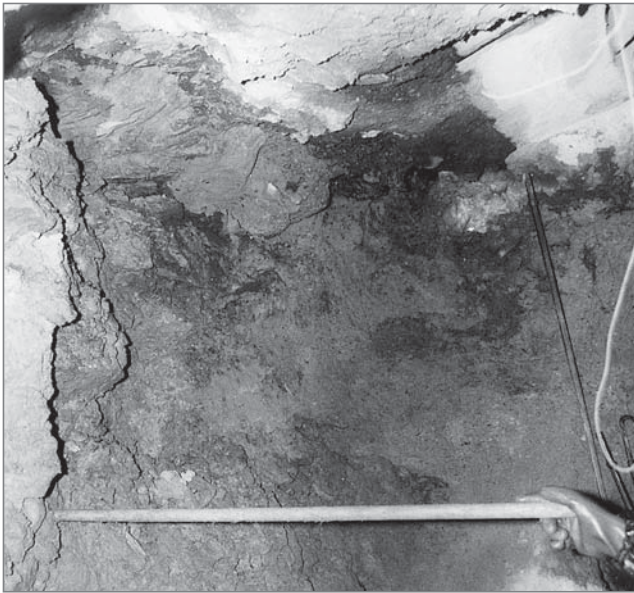


Plate D/13



Plate D/14

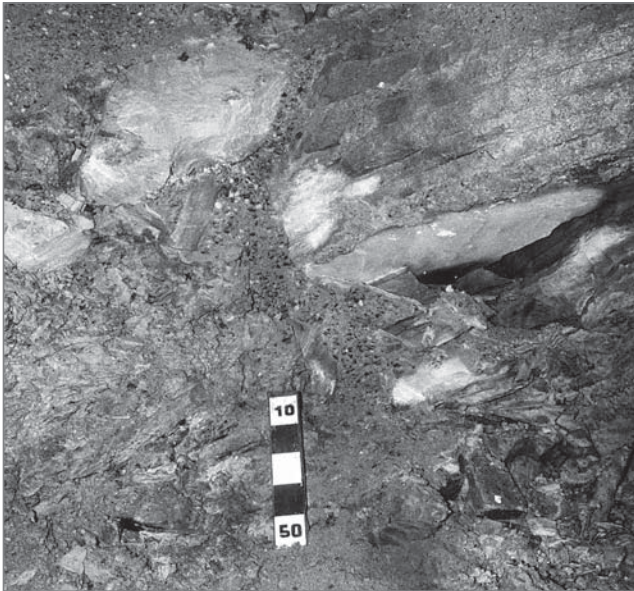


Plate D/15



Plate D/16

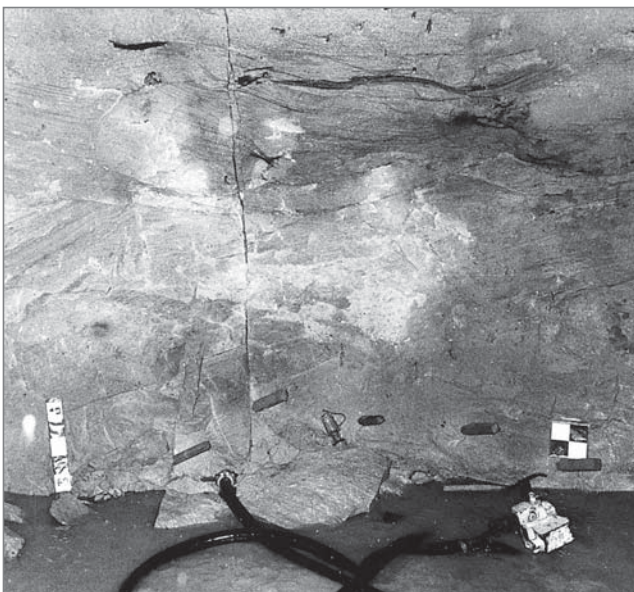


Plate D/17



Plate D/18

**PLATE D/13**

Detail of cavern in the N segment of the skip shaft with a coarse sandstone bed.

Situation after the no. 3 gas and rock outburst in the skip shaft, at the depth of 851.5-854.5 m.

Slaný Mine skip shaft.

*Photographic documentation in Plates D3 - D18:  
HBZS Corp. (Central Mine Rescue Station), Kladno.*

**PLATE D/14**

Detail of cavern formed in the W-NE segment of the skip shaft (depth in rock massif  $\approx$  4 m).

Situation after the no. 3 gas and rock outburst in the skip shaft, at the depth of 851.5- 854.5 m.

Slaný Mine skip shaft.

*Photographic documentation in Plates D3 - D18:  
HBZS Corp. (Central Mine Rescue Station), Kladno.*

**PLATE D/15**

Detail of cavern (depth  $\approx$  1.6-2 m) formed in the skip shaft after the no. 3 gas and rock outburst took place at the depth of 854.5-857.0 m.

Slaný Mine skip shaft.

*Photographic documentation in Plates D3 - D18:  
HBZS Corp. (Central Mine Rescue Station), Kladno.*

**PLATE D/16**

Detail of cavern (depth  $\approx$  3-4 m) formed in the NNW segment of the skip shaft after the no. 3 gas and rock outburst took place at the depth of 860 m.

Slaný Mine skip shaft.

*Photographic documentation in Plates D3 - D18:  
HBZS Corp. (Central Mine Rescue Station), Kladno.*

**PLATE D/17**

Skip shaft wall in the SE segment affected by rock mucking following the no. 3 gas and rock outburst which occurred at the depth of 863.5-866.5 m.

Slaný Mine skip shaft.

*Photographic documentation in Plates D3 - D18:  
HBZS Corp. (Central Mine Rescue Station), Kladno.*

**PLATE D/18**

Detail of cavern formed in the NNE segment (depth  $\approx$  3-4 m) of the skip shaft after the no. 3 gas and rock outburst at the depth of 863.5-866.5 m.

A case of destruction of the sandstone beds.

Slaný Mine skip shaft.

*Photographic documentation in Plates D3 - D18:  
HBZS Corp. (Central Mine Rescue Station), Kladno.*

# PLATE - E



*Plate E/1*

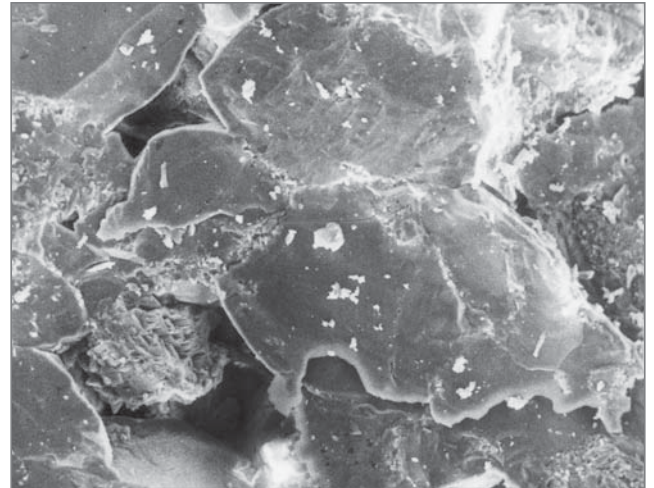


*Plate E/2*

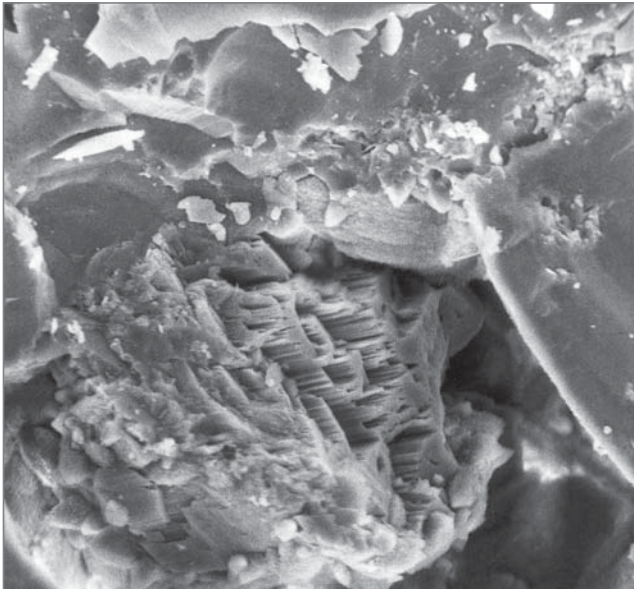


*Plate E/3*



*Plate E/4*



*Plate E/5*

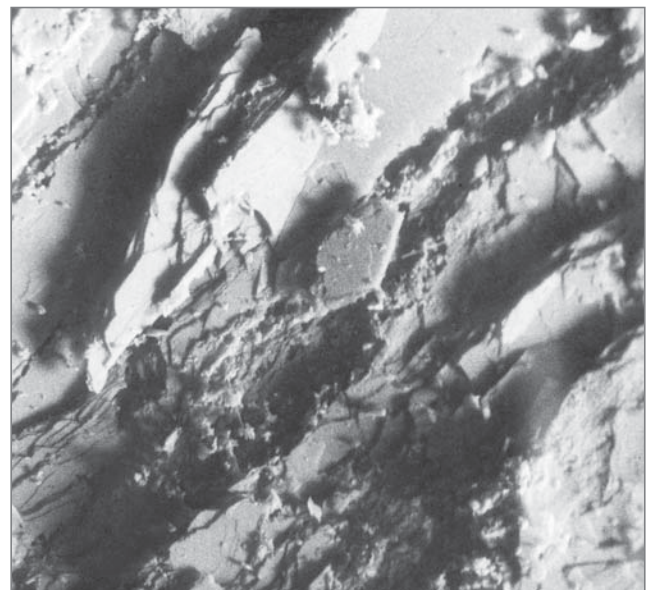


*Plate E/6*

**PLATE E/1**

Conglomerate with hard silicification (sample 4468a) and newly formed (dark) pyrite. The light-coloured areas correspond to quartz newly formed in matrix and in pores. Cenomanian – Lower Turonian (?).

Komořany drainage shaft, depth 89.4-90.4 m.

X-ray positive photo, core drill diameter 48 mm, thickness 1-3 mm.

*Photo: Petr Martinec.*

**PLATE E/3**

Conglomerate with hard silicification (sample no. 4468a) showing severe corrosion of feldspars located within the large-sized pore between regenerated quartz grains with regeneration. Cenomanian – Lower Turonian (?).

Komořany drainage shaft, depth 89.8-91.2 m.

SEM, magnification 750.

*Photo: Antonín Uher.*

**PLATE E/5**

Kaolinized muscovite-biotite gneiss (sample no. 4450a) with newly formed carbonate in argillized clastic feldspars.

Komořany drainage shaft, borehole 2A.

X-ray positive photo, diameter 48 mm, thickness 1-2 mm.

*Photo: Petr Martinec.*

**PLATE E/2**

Conglomerate with hard silicification (sample 4468a) and newly formed quartz. Cenomanian – Lower Turonian (?).

Komořany drainage shaft, depth 89.8-91.2 m.

SEM, magnification 230.

*Photo: Antonín Uher.*

**PLATE E/4**

Conglomerate with hard silicification (sample no. 4468a). Intensive silicification of quartz grains. Pores filled with newly formed quartz. Cenomanian – Lower Turonian (?).

Komořany drainage shaft, depth 89.8-91.2 m.

SEM, magnification 900.

*Photo: Antonín Uher.*

**PLATE E/6**

Decomposition of feldspars and onset of kaolinization in muscovite-biotite gneiss. Sample no. 4469a.

Komořany drainage shaft, borehole KO 16, depth 99-101.6 m.

SEM, magnification 610.

*Photo: Marie Heliová.*



*Plate E/7*



*Plate E/8*



*Plate E/9*



*Plate E/10*



*Plate E/11*

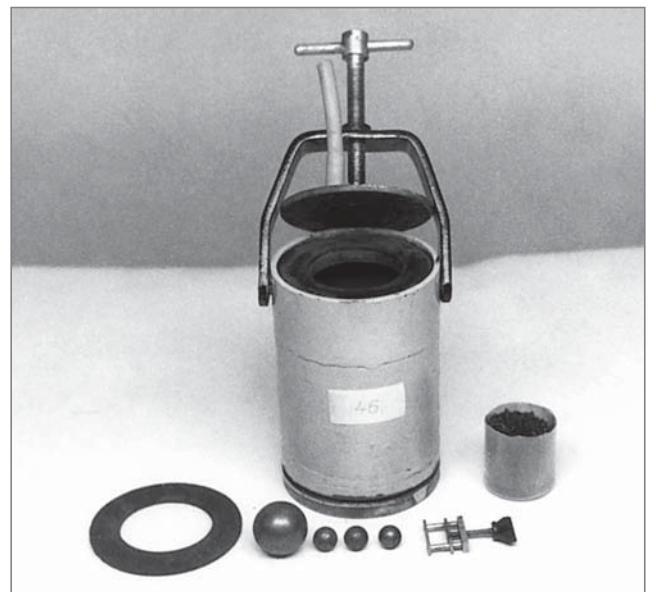


*Plate E/12*

**PLATE E/7**

Kaolinization of clastic feldspars along the cleavage planes in muscovite-biotite gneiss (sample no. 4508a).

Komořany drainage shaft, borehole KO-16, depth 162.2-163.3 m.

SEM, magnification 550.

*Photo: Marie Heliová.*

**PLATE E/9**

Kaolinite aggregates (vermi-form) of perfect crystallinity and crystal morphology in hard kaolinized muscovite-biotite gneiss.

Komořany drainage shaft, borehole KO-16, depth 162.2-163.3 m.

SEM, magnification 3600.

*Photo: Marie Heliová.*

**PLATE E/11**

Kaolinite aggregates (vermi-form) of perfect crystallinity and crystal morphology in hard kaolinized muscovite-biotite gneiss.

Komořany drainage shaft, borehole KO-16, depth 162.2-163.3 m.

SEM, magnification 3100.

*Photo: Marie Heliová.*

**PLATE E/8**

Kaolinite aggregates of perfect crystallinity and crystal morphology in intensely kaolinized muscovite-biotite gneiss (sample no. 4470a).

Komořany drainage shaft, borehole KO-16, depth 101.8-110.0m.

SEM, magnification 850.

*Photo: Marie Heliová.*

**PLATE E/10**

Kaolinite aggregates (vermi-form) of perfect crystallinity and crystal morphology in hard kaolinized muscovite-biotite gneiss.

Komořany drainage shaft, borehole KO-16, depth 162.2-163.3 m.

SEM, magnification 3600.

*Photo: Marie Heliová.*

**PLATE E/12**

Canister for rock sampling and for determination of content and composition of gas entrapped in rock. Canister design and construction: Coal Research Institute in Ostrava-Radvanice (VVUÚ Ostrava-Radvanice).

*Photo: Petr Martinec.*

# PLATE – F



*Plate F/1*



*Plate F/2*



*Plate F/3*



*Plate F/4*



*Plate F/5*



*Plate F/6*

**PLATE F/1**

Outburst no. 2 of 7<sup>th</sup> July 1987. Face of no. 3/5001 gallery after the outburst which occurred at the distance of 1548.5 m in the SE part of the coalfield.

Zdeněk Nejedlý Mine in Malé Svatoňovice.

*Scan photo: Václav Jirásek, OBZS Odolov.*

**PLATE F/2**

Outburst no. 2 of 7<sup>th</sup> July 1987. Right-hand side of face in no. 3/5001 gallery after the outburst which occurred at the distance of 1548.5 m in the SE part of the coalfield.

Zdeněk Nejedlý Mine in Malé Svatoňovice.

*Scan photo: Václav Jirásek, OBZS Odolov.*

**PLATE F/3**

Outburst no. 2 of 7<sup>th</sup> July 1987. Left-hand side of face in no. 3/5001 gallery after the outburst which occurred at the distance of 1548.5 m in the SE part of the coalfield.

Zdeněk Nejedlý Mine in Malé Svatoňovice.

*Scan photo: Stanislav Straka, OBZS Odolov.*

**PLATE F/4**

Outburst no. 2 of 7<sup>th</sup> July 1987. Right-hand side of face in no. 3/5001 gallery after the outburst which occurred at the distance of 1548.5 m in the SE part of the coal field.

Zdeněk Nejedlý Mine in Malé Svatoňovice.

*Scan photo: Stanislav Straka, OBZS Odolov.*

**PLATE F/5**

Outburst no. 4 of 23<sup>th</sup> July 1988. Ejected rock and coal after an outburst which occurred in the no. 3 Žďárecká coal seam, in the face of no. 3/5212 gallery, at the distance of 45.2 m in the SE part of the coalfield.

Zdeněk Nejedlý Mine in Malé Svatoňovice.

*Scan photo: Václav Jirásek, OBZS Odolov.*

**PLATE F/6**

Outburst no. 4 of 23<sup>th</sup> July 1988. Ejected rock and coal after an outburst which occurred in the no. 3 Žďárecká coal seam, in the face of no. 3/5212 gallery, at the distance of 45.2 m in the SE part of the coalfield.

Zdeněk Nejedlý Mine in Malé Svatoňovice.

*Scan photo: Václav Jirásek, OBZS Odolov.*



## REFERENCES

- Atkins, P., de Paula, J. (2002): Atkins' Physical Chemistry. 7th edition. – Oxford University Press, London.
- Augustiniak, K. (1970): Geological atlas of the Lower Silesian Coal Basin. 1:100 000. Part 2. – Panstw. Inst. Geol. Warszawa.
- Augustiniak, K., Grocholski, A. (1968): Geological structure and outline of the development of the Intra-Sudetic Depression. – *Biul. Inst. Geol.*: 227. Warszawa.
- Babuška, V., Plomerová, J. (2010): Mantle lithosphere control of crustal tectonics and magmatism of the western Ohře (Eger) Rift. – *J. Geosciences*, Vol. 55, no. 3:171, Praha.
- Battistutta, E., van Hemert, P., Lutynski, M., Bruining, H., Wolf, K.-H. (2010): Swelling and sorption experiments on methane, nitrogen and carbon dioxide on dry Selar Cornish coal. – *Int. J. Coal Geol.* Vol. 84: 39–48, Issue 1.
- Busch, A and Gensterblum, Y. (2011): CBM and CO<sub>2</sub>-ECBM related sorption processes in coal: A review. – *Int. J. Coal Geol.* Vol. 87: 49-71, Issue 2.
- Buzek, F., Holub, V., Boháček, Z., Franců, J. (1999): Carbon isotope composition of methane emissions in the Czech Republic-preliminary results. – *Věst. Čes. Geol. Ústavu*, Vol. 74, no. 2: 191-196, Praha.
- Cajz, V., Valečka, J. (2010): Tectonic setting of the Ohře/Eger Graben between the central part of the České středohoří Mts. and the Most Basin, a regional study. – *J. of Geosciences*, Vol. 55, no.3: 201, Praha.
- Ceglarska-Stefańska, G., Zarębska, K., Aleksandrowicz, K. (2002): Displacement sorption of CO<sub>2</sub> and CH<sub>4</sub> on low rank hard coal within gas low pressure range. – *Archives of Mining Sciences*, Vol. 47: 157-173, Katowice.
- Ciembronowicz, A., Marecka, A. (1990): Sorption kinetics of CO<sub>2</sub> in hard coal with different granual size. – *Archives of Mining Sciences*, Vol. 35: 253-261, Katowice.
- Cílek, V. (1971): Nové poznatky o výskytu plynů a vod sycených plynem ve slánské depresi (*New knowledges about gas and water in Slaný mine area*). – *Sbor. Geol. Věd, HIG*, Vol. 8: 67-95, Academia, Praha.
- Clark, P, Jr., edit. (1966): Handbook of physical constants. – *Geol. Soc. America, Inc. Memoir 97*, Yale Univ, New Haven (in Russian edition: Mir, Moskva 1969).
- Cuřín, M., Kautský, J. (1988): Základní faktory otvírky černouhelného ložiska Slaný – hydrogeologické a plynové poměry (*Main factors for opening of bituminous coal deposit Slaný*). – *Geologický průzkum*, Vol. 9, Praha.
- Čichovský, L. (1987): Mirošovský obzor – litologická studie. (*Mirošov horizon - lithological study*). – Tech. Report, Geindustria Praha. Report no. SÚ P-01-125-808, VVUÚ Ostrava-Radvanice. MS.
- D'Amore, F., Fancelli, R., Nuti, S., Richard, G., Pačes, P. (1989): Origin of Gates in Variscan massifs of Europe. – In: Miles (ed.) *VI<sup>th</sup>. Intern. Symp. On Water-Rock Interaction*. Molvern, 6 : 177-180.
- Day, S., Sakurovs, R., Weir, S. (2008): Supercritical gas sorption on moist coals. – *Int. J. Coal Geol.*, Vol. 74, no. 3-4: 203-214.
- Dobry, O., Palek, L. (1988): Koroze betonu ve stavební praxi. (*Concrete corrosion in praxis*) – SNTL, Praha.
- Dopita, M., Havlena, V. (1962): Dvojí stáří pestrých vrstev v Ostravsko-karvinském revíru. (*Two etaps variegated beds origine in the Ostrava-Karviná Basin*). – *Přírod. Sbor. Ostravského kraje*, Vol. 23, no. 3: 329-371, Ostrava.
- Dopita, M., Pešek, J., Havlena, V. (1988): Geologie uhelných ložisek (*Geology of coal deposits*). SNTL a ALFA, Praha
- Dopita, M., with: Aust, J., Brieda, J., Dvořák, P., Fialová, V., Foldyna, J., Hřmela, A., Grygar, R., Hoch, I., Honěk, J., Kaštovský, V., Konečný, P., Kožušnicková, A., Krejčí, B., Kumpera, O., Martinec, P., Merenda, M., Müller, K., Novotná, E., Ptáček, J., Purkyňová, E., Řehoř, F., Strakoš, Z., Tomis, L., Tomšík, J., Valterová, P., Vašíček, Z., Venc, J., Žídková, S.: Geologie české části hornoslezské pánve a Aust, J., Čechová, S., Hozza, L., Kaštovský, V., Krůl, M.: Odkrytá geologická mapa paleozoika české části hornoslezské pánve 1:100 000. (*Geology of the Czech part of the Upper Silesian Basin with Geological map of Paleozoic in the Czech part of the Upper Silesian Basin 1:100 000*). Min. živ. Prostředí ČR, Praha (in Czech and English sumary), pp. 1-274 and Plate I-XXVI.
- Dowgiallo, J. (1973): Pochodzenie siarczanów w niektórych polskich wodách podziemnych w świetle oznaczen δ<sup>34</sup>S. – *Przegląd Geologiczny*, Vol. 21: 282-284, Warszawa.
- Drochytka et al. (2005): Atmosférická koroze betonu (*Atmospheric corrosion of concrete*). – Grada, Praha.
- Dvorský, J., Tylčer, J. (1969): Hydrogeologické mapování části listu Ostrava (M-34-XIX). (*Hydrogeological map Ostrava (M-34-XIX)*). – Tech. Rep. Geologický průzkum n.p. Ostrava, Ostrava.
- Dvorský, J., Grmela, A., Malucha, P., Rapantová, N. (2006): Ostravsko-karvinský detrit (*Lower Badenian basal sediments („detrit“) in Ostrava-Karviná Basin*). – Montanex, Ostrava.
- Dubánek, V. (1986): Odhad chemické reaktivity horninového prostředí. (*Estimation of reactivity of rock environment*). – *Věstn. Ústř. Úst. Geol.*, Vol. 62, Praha.
- ENERGIE KLADNO, a.s. (2002): I. Závěrečná zpráva o likvidaci hlavních důlních děl I. fáze báňsko-geologického průzkumu ložiska černého uhlí Slaný (*Tech. report about final liquidation of shaft Slaný Mine*). – Tech. Report no. 2860/00, Kladno.

- Ettinger, I. L., Šulman, N. V. (1975):** Raspredelenie metana v porach iskopaemych uglej. – AN USSR, Nauka, Moskwa.
- Fitzgerald, J.E., Pan, Z., Sudibandriyo, M., Robinson, J.R.L., Gasem, K.A.M., Reeves, S. (2005):** Adsorption of methane, nitrogen, carbon dioxide and their mixtures on wet Tiffany coal. – *Fuel*, Vol. 84, no. 18: 2351–2363.
- Franke, M., Středa, J. (1975):** Výskyt ropy na dole Jan Šverma v Lamprechticích u Žacléře. (*Occurrence of crude oil in Jan Šverma Mine*) – *Technol. lož. geol.*, Vol. 7: 15–22, Geindustria, Praha.
- Foldyna, J., Kožušníková, A. (1997):** Some remarks on coal substance behaviour in tectonic stress fields: comparison with the results of triaxial compression tests. Interlayer deformation in Ostrava-Karviná coal seams. – In: *Proceedings of the 13<sup>th</sup> International Congress on Carboniferous-Permian*, CLVII, part 2, Panstwowy Instytut Geologiczny: 217–227, Warszawa.
- Folprecht, J. (1928):** in Kamenouhelné doly ostravsko-karvinského revíru (*Coal Mines in Ostrava-Karviná coal district*). – Ředitelská konference Ostravsko-karvinského kamenouhelného revíru v Mor. Ostravě v X. roce Československé republiky. Prometheus Praha.
- Gehrig, M., Lentz, H. and Franck, E. U. (1986):** The system water – carbon dioxide – sodium chloride to 773 K and 300 MPa. – *Ber. Bunsenges. Phys. Chem.* Vol. 90: 525–533, Berlin.
- Goebel, St. (1985):** Sorpce methanu a oxidu uhličitého na uhlí (*Sorption of CH<sub>4</sub> and CO<sub>2</sub> on coal*). – Tech. Rep. VVUÚ Ostrava-Radvanice, Ostrava.
- Goodman, A.L., Busch, A., Bustin, R.M. et al. (2007):** Inter-laboratory comparison II: CO<sub>2</sub> isotherms measured on moisture-equilibrated Argonne premium coals at 55°C and up to 15 MPa. – *Int. J. Coal Geol.*, Vol. 72: 153–164, Issue 3–4.
- Gregg S. J., Sing K. S. W. (1982):** Adsorption, Surface Area and Porosity. – Academic Press, London.
- Grmela, A., Rapantová, N., Labus, K. (2004):** Chemizm wód podziemnych w gruboklastycznych utworach dolnego badenu na terenie Ostravsko-Karwinskiego Zagłębia Weglowego. – *Zeszyty Naukowe Politechniki*, Katowice.
- Gustkiewicz, J. (1990):** Deformacja i wytrzymałość skal w trojosowym stanie naprężenia z uwzględnieniem plynów porowych. Strata as Multiphase Media (Ed. by Litwiniczin J.) – Instytut Mechaniki Gorotworu PAN. Wydawnictwo AGH, Kraków.
- Havlena, V. (1964):** Geologie uhelných ložisek (*Geology of coal deposits*). – ČSAV-Academia, Praha.
- Havlena, V., Pešek, J. (1975):** Stratigrafie, paleografie a základní strukturální členění limnického permokarbonsu Čech a Moravy. – *Sborník Příroda*, Vol. 34, Západočeské muzeum, Plzeň.
- Hepnar, P., Květoň, P., Kautský, J. (1987):** Hydrogeologické a plynové poměry ložiska kamenného uhlí Slaný a perspektivy jeho otvírky (*Hydrogeology and gas conditions in Slaný coal deposit*). – Tech. Rep. Geindustria n.p., Praha.
- Hepnar, P., Květoň, P., Kautský, J. (1988):** Slaný, předběžné vyhodnocení hydrogeologických vrtů. (*Slaný area - preliminary evaluation of hydrogeological deep wells*). – Tech. Rep. Geindustria n.p., Praha.
- Holub, V., Pešek, J. (1991):** Návrh stratigrafického členění mladopaleozoických pánví oblasti středních a západních Čech. (*Proposal of stratigraphy of Young Paleozoic basin in Central and West Bohemia*) – *Věstn. Ústř. Úst. Geol.*, Vol. 66: 31–41, Praha.
- Homola, V. (1959):** Příspěvek k hydrogeologii a plynovosti podbeskydské části ostravsko-karvinského revíru. (*Hydrogeology and gas occurrences in Sub-Beskydian part of the Upper Silesian Basin*) – In: *Sborník prací Konference o geologii OKR:153-172*. VŠB, Ostrava.
- Homola, V., Klír, S. (1975):** Hydrogeologie ČSSR III. Hydrologie ložisek nerostných surovin (*Hydrogeology of the Czech Republic, part III, Hydrogeology of coal and ore deposits*). – Academia, Praha.
- Honěk, J., Schejbal, C. (1972):** Mikropetrografická a technologická charakteristika žďareckých slojí na dole Zdeněk Nejedlý v Malých Svatoňovicích (československá část dolnoslezské pánve) (*Micropetrographical and technological parameters of Žďárky coal seams, Zdeněk Nejedlý Mine*). – *Sbor. věd. Prací Vys. Šk. Báň. v Ostravě, Ř. horn.-geol.* 18, 4., 332, Ostrava.
- Hošek, M. (1968):** Nové poznatky z geologického průzkumu permokarbonských souvrství na Svatoňovicu (*Geology of Permo-Carboniferous on Svatoňovice area*). – *Acta Mus. reginaehradec., S.A. Sci, natur.*, Hradec Králové.
- Hufová, E. (1971):** Hydrogeologický průzkum vymýtin ostravsko-karvinského revíru. (*Hydrogeology of fossil valleys on Carboniferous surface in Ostrava-Karviná Coal District*). – Tech. Rep., Geologický průzkum n.p., Ostrava.
- Hurník, S. (2004):** Minerální a ostatní podzemní vody na Mostecku. (*Mineral and other water in Most area*). – Sb. Oblastního muzea v Mostě, řada přírodovědná, Vol. 26, Most.
- Hynie, O. (1963):** Hydrogeologie ČSSR II, Minerální vody (*Hydrogeology of the Czech Republic, part II: Mineral waters*). – Academia, Praha.
- Chodot, V. V. (1961):** Vnězapynye vybrosy uglja i gaza. – GNTI, Moskwa.
- Chromá, M. (2006):** Modelování karbonatace betonu. – Sb. konf. CONSTRUMAT 2006, Brno.
- Chromá, M. (2007):** Accelerated carbonation studies. MS, Thesis, Faculty of Civil Engineering, Brno, University of Technology, Brno.

- Janas, J. (1968):** Prognóza plynodajnosti dolů OKR (*Prognosis of mine gas productivity in Ostrava-Karviná Coal District*). – VVUÚ Ostrava-Radvanice, 1-136 pp., Ostrava.
- Jetel, J., Rybářová, L. (1979):** Minerální vody Východočeského kraje (*Mineral water in district of East Bohemia*). – Ústř. Úst. Geol., Praha.
- Jiráňková, J. (1989):** Petrologická charakteristika hornin ze skipové a klecové jámy dolu Slaný (*Petrology of rocks from skip and hoisting shafts, Slaný Mine*). – Tech. Rep. Geindustria s.p., Praha.
- Jičínský, W. (1885):** Monographie des Ostrau-Karwiner Steinkohlenrevieres. – Teschen: Berg-und Hüttenmännischen Vereine in Mähr-Ostrau. 1-487 pp.
- Jirkovský, R. (1953):** Minerální prameny ve Slezsku. (*Mineral water in Silesia*). – *Přírod. Sbor. Ostr. Kraje*, Vol. 14, nos. 1-2., Slez. stud. Ústav, Opava.
- Joubert, J. I., Grein, T., Bienstock, D. (1974):** Effect of moisture on the methane capacity of American coals. – *Fuel*, Vol. 53:186–191.
- Jura, D. (2001):** Morfotektonika i ewolucja roznowiekowej niezgodności w strope utworów karbonu Gornosląskiego Zagłębia Węglowego. – Wyd. USI, 1-176pp., Katowice.
- Kačura, G. (1980):** Minerální vody Severočeského kraje (*Mineral water in District of Central Bohemia*). – Ústř. Úst. Geol., Praha.
- Kaisar, E., Pavlíček, J. (1984):** Průtrže uhlí a plynů v dolech ostravsko-karvinského revíru v letech 1976-1983 (*Outbursts of coal and gas in mines in the Ostrava-Karviná Coal District*) – *Uhlí*, Vol. 32, no. 12: 460-466, Praha.
- Keršner, Z., Rovnaníková, P., Teplý, B., Novák, D. (2004):** Design for durability: An interactive tool for RC structures. – Proc. of Int. Conf. on Life cycle assessment, behaviour and properties of concrete structures LC 2004.: 172-182, Brno.
- Kidybiński, A., Patyńska, R. (2008):** Analiza zjawisk gazodynamicznych w kopalniach węgla kamiennego w Polsce i na świecie. – Główny Instytut Górnictwa, Katowice.
- Klika, Z., Kraussová, J. (1993):** Properties of altered coals associated with carboniferous red beds in the Upper Silesian Coal Basin and their tentative classification. – *Int. J. Coal Geol.*, Vol. 22, nos. 3-4: 217-235.
- Klika, Z., Osovský, M. (1999):** Thermally altered coal from the Upper Silesian Coal Basin. – *J. Czech Geol. Soc.*, Vol. 44, nos. 3-4.: 343-352, Praha.
- Klika, Z., Kozubek, E., Martinec, P., Kliková, Ch., Dostál, Z. (2004):** Mathematical modeling of bituminous coal seams burning contemporaneously with the formation of a variegated beds body. – *Int. J. Coal Geology*, Vol. 59, nos. 1-2: 137-151.
- Kolář, P. (1989):** Metodika stanovení distribuce pórů rtuťovou porometrií pro sedimentární klastické horniny (*Methods for determination pore distribution of by means of high pressure mercury porosimetry*) – In Martinec P. et al. (1989).
- Kolář, P., Martinec, P. (1989):** Rtuťová pórometrie cementačně klastických sedimentárních hornin (*High pressure mercury porosimetry for clastic sedimentary rocks*). – In: Fyzikální vlastnosti hornin a ich využitie v geofyzike a geológii III. (Ed. by Kapička, A., I. Túnyi): 113-17. Jednota československých matematiků a fyziků, Praha.
- Kolář, P., Martinec, P. (1994):** The system H<sub>2</sub>O-CO<sub>2</sub>-NaCl in natural conditions of the Slaný basin. – Proc. Geomechanics 93 (Rakowski Z. ed.): 89-93, Balkema Rotterdam.
- Kolář, P., Martinec, P., Benš, P. (1991):** Methodological instructions for merkury porosimetry of clastic sedimentary rocks. – *Ceramics*, Vol. 35: 379-390, Praha.
- Kolářová, M. (1978):** Minerální vody Středočeského a Jihočeského kraje (*Mineral water in in the Districks Central Bohemia and South Bohemia*). – Ústř. Úst. Geol., Praha.
- Kolářová, M., Myslil, V. (1979):** *Minerální vody Západočeského kraje* (Mineral water in District West Bohemia) – Ústř. Úst. Geol., Praha.
- Konečný, P. Jr. and Kožušníková, A. (1998):** Permeability of Coal of the Upper Silesian Basin. – In: Proc. VIII. Uhelně geologická konference, Pešek J. (ed.), Univerzita Karlova, Praha.
- Konečný, P. jr., Kožušníková, A. and Martinec, P. (1999):** Rock mass as a porous medium: Gas filtration ability in triaxial state of stress. – Proc. 9th International Congress on Rock Mechanics, 761-764pp., Paris.
- Konečný, P., Kožušníková, A., Nowakowski, A. (2000):** Gas Permeability Changes in the Rock Specimen during the Triaxial Compression Test. – Proc. 14. Nationale Symposium für Tunnelbau, Aachen.
- Konečný, P., Mlynarczuk, M. (2002):** Discontinuities: Filtration properties in triaxial state of stress. – In: Rock-mec'2002 - VI<sup>th</sup> Regional Reck Mechanics Symposium, Konya.
- Konečný, P., Kožušníková, A. (2010):** Srovnání propustnosti uhlí ze sloje 504 (sedlové vrstvy) a ze sloje 080 (petřkovické vrstvy) pro různé plyny (*Comparison of permeability of coal from coals seam no. 504 and 080 for different gasess*). – Proc. XXXIII. Symposia „Geologia Formacji Węglonosnych Polski“, 21. - 22. 4. 2010, Krakow.
- Konečný, P., Kožušníková, A. (2011):** Influence of stress on the permeability of coal and sedimentary rocks of the Upper Silesian basin. – *Int. J. Rock Mechanics and Mining Sciences* Vol. 48: 347-352.

- Kopecký, L. (1978):** Neoid taphrogenic evolution and zouny alkaline volcanism of the Bohemian Massif. – *Sbor. Geol. Věd, Geol.* Vol. 31: 91-107, Praha.
- Kopecký, L. (1986-1988):** Mladý vulkanismus Českého masivu (strukturně geologická vulkanologická studie) (*Young volcanism of Bohemian Massif (structural and volcanological study)*). – *Geologie a metalurgie uranu*: Vol. 11, no. 3:30-67, Vol. 11, no. 4: 3-44, Vol. 12, no. 1: 3-40, Vol. 12, no. 4: 3-40. Stráž pod Ralskem.
- Kotarba, M. (1990):** Geneza gazów akumulowanych w górnośląskiej serii Węglonosne Górnoszląskiego Zagłębia Węglowego i południowej szesti ROW.- In: *Górotwor jako odrodem wielofazowy*. Wydaw. AGH, Kraków.
- Kotarba, M. (2001):** Composition and origin of coalbed Gases in the Upper Silesian and Lublin Basis, Poland. – *Organic Geochemistry*, Vol. 32, Issue 1:163-180, London.
- Krajča, J. (1977):** Plyny v podzemních vodách (jejich vlastnosti, průzkum a využití) (*Gases in underground water*). – SNTL/Alfa, Praha a Bratislava.
- Králík, J. (1982a):** Mineralogie pestrých vrstev v ostravsko-karvinské černouhelné pánvi. (*Mineralogy of the variegated beds in Ostrava -Karviná basin*). – *Čas. Slez. Muz., Sér. A* 31: 149-171, Opava.
- Králík, J. (1982b):** Relationship between clay mineralogy and coalfication rock in sediments of Ostrava-Karviná coal basin and the Nížký Jeseník Mts. – In: *Sb. 9. konf. jíl. mineral. a petrol.*, 107-118, Zvolen.
- Králová, H., Teplý, B. (2001):** Koncentrace oxidu uhličitého - karbonatace betonu - koroze výztuže. (*Concentration carbon dioxide-carbonatation of concrete-support corrosion*). – *Beton - Technologie - Konstrukce - Sanace*. Vol. 5: 44-45, Brno.
- Králová, H., Teplý, B. (2002):** Časový profil oxidu uhličitého a jeho vliv na trvanlivost železobetonových konstrukcí. – *Beton - Technologie - Konstrukce - Sanace*, Vol. 5, no. 4: 43-44, Brno.
- Krawiec, A., Halas, S., Pluta, I. (2003):** Skład izotopowy siarki i tlenu w siarczanach wód leczniczych antyklinorium pomorskiego. – In: *Współczesne problemy hydrogeologii*, Vol. XI, no. 2: 193-200, Gdansk.
- Krooss, B. M., Bergen, F., Gensterblum, Y., Siemons N., Pagnier, H.J.M. and David, P. (2002):** High-pressure methane and carbon dioxide adsorption on dry and moisture-equilibrated Pennsylvanian coals. – *Int. J. Coal Geol.*, Vol. 51: Issue 2: 69-92.
- Krs, M., Krsová, M., Martinec, P., Prunel, P. (1993):** Paleomagnetism of carboniferous and variegated layers of the Moravan-Silesian region. – *Geol. Carpatica*, Vol. 44: 301-314. Bratislava.
- Kruk, E., Swoboda, A., Suchodolski Z., Tomkowski, W. (1963):** Materiały z prac Komisji dla spraw zagrożeń związanych z wyrzutami gazów i skal w kopalniach węgla kamiennego: Evidencja wyrzutów gazów i skal i wybrane prace z zakresu wyrzutów gazów i skal w kopalniach węgla kamiennego w dolnośląskim zagłębiu węglowym. Zeszyt 1 – Dolnośląskie zjednoczenie przemysłu węglowego, Wydawnictwo geologiczne, Warszawa.
- Kruk, E., Osmęda, J., Schinohl, A., Suchodolski Z., Swoboda, A, Jaros, Z. (1969):** Materiały z prac Komisji dla spraw zagrożeń związanych z wyrzutami gazów i skal w kopalniach węgla kamiennego: Evidencja wyrzutów gazów i skal i wybrane prace z zakresu wyrzutów gazów i skal w kopalniach węgla kamiennego w dolnośląskim zagłębiu węglowym. Zeszyt 3. – Dolnośląskie zjednoczenie przemysłu węglowego, Wydawnictwo geologiczne, Warszawa.
- Květ, R. (1971):** Hydrochemie a sedimentární geochemie vídeňské pánve (*Hydrochemistry and sedimentary geochemistry of Vienna Basin*). – *Sbor. Geol. Věd, HIG*, Vol. 8: 141-200. Academia, Praha.
- Květ, R. (1980):** Hydrochemie Ostravska (*Hydrochemistry of region of Ostrava*). – *Studia Geographica*, Vol. 66, ČSAV, Geografický ústav AV, Brno.
- Květ, R., Kačura, G. (1978):** Minerální vody Severomoravského kraje (*Mineral water of Nord Moravia District*). – Ústř. Úst. Geol., Praha.
- Kukal, Z. (1985):** Návod k pojmenování a klasifikaci sedimentů. Metodické příručky 2 (*Description and classification of sediments*). – Ústř. Úst. Geol., Praha.
- Kurial, J. et al. (eds) (2006):** Dobývání uhlí na Kladensku (*Bituminous coal mining in Kladno basin*). – OKD a.s. Ostrava, Kartis + Co, 1-751pp., Praha.
- Lama, R. D., Bodziony, J. (1996):** Outburst of gas, coal and rock in underground coal mines. – R.D. Lama & Associates.
- Lama, R. D., Bodziony, J. (1998):** Management of outburst in underground coal mines. – *Int. J. Coal Geology*, Vol. 35: 83-115.
- Lát, J., Čech, J., Novotný, I., Maršálek, Z. (1987):** Způsoby ovlivňování vlastností horninového masivu v lokalitě Slaný pro snížení rizika průtrži hornin a plynů (*Methods for influence of rock massif properties on Slaný Mine*). – Tech. Rep. no. HS 784/87, VŠB-TU, Ostrava.
- Lempp, Ch. (1993):** Influence of fluids on mechanical rock properties in low-porosity crystalline rocks. – *Annales Geophysicae I: Supplement I*, Springer Int. Europ. Geophys. Soc.

**Leopold, L. (1985):** Báňsko-geologický průzkum Slaný – I. fáze. Aktualizace projektu geologické části. (*Geological and mine survey in Slaný Mine - actualization of geological part of the Project*). – Tech. Report Výstavba Dolu Slaný, Slaný.

**Leopold, L. (1986):** Báňsko-geologický průzkum Slaný – I. fáze. Dokumentace o zabezpečovacím vrtu SJ-2 z počvy SJ v hl. 800m (-483m n.m.Bpv). (*Geological and mine survey in Slaný Mine the 1st phase – documentation of SJ-2 borehole in Slaný Mine skip shaft in depth 800 m*). – Tech. Rep. no. SO 201 SJ, Výstavba Dolu Slaný, Slaný.

**Leopold, L. (1987):** Báňsko-geologický průzkum Slaný – I. fáze. Výroční zpráva za rok 1986 (*Geological and mine survey in Slaný Mine the 1st phase. - Annual Rep. 1986*). – Tech. Rep., Výstavba Dolu Slaný, Slaný.

**Leopold, L., Živor R. (1986):** Báňsko-geologický průzkum Slaný – I. fáze. Projekt geologicko-průzkumných prací na rok 1987 (*Geological and mine survey in Slaný Mine the 1st phase. - Geological project for 1987 yr.*) – Tech. Rep., Kladno Mine. Důl Slaný, Slaný.

**Logviněnko, N. V. (1968):** Postdiagenetičeskije izmenenija osadočnych porod. – Nauka, Leningrad.

**Majewska, Z., Ceglarska-Stefanska, G., Majewski, S., Zietek, J. (2009):** Binary gas sorption / desorption experiments on a bituminous coal: simultaneous measurements on sorption kinetics, volumetric strain and acoustic emission. – *Int. J. Coal Geol.* Vol. 77, Issue 1-2: 90-102.

**Majzlík, J. (1965):** Závěrečná zpráva o výsledku průzkumu vodních a plynových poměrů v severní části bedříšského a svinovského výmolu prováděného v zatopené těžní jámě Bedřich v Ostravě-Zábřehu (*Hydrogeology and gas occurrence in Bedřich shaft in Ostrava-Zábřeh*). – Tech. Rep., OŘ OKD-ZDO, Paskov.

**Makarius, R., Faster, P. (2008):** Memento důlních nehod v českém hornictví (*Mine accidents in Czech mining*). – OKD, HBZS, a.s., Montanex, Ostrava.

**Malinin, S. D. (1979):** Physical chemistry of hydrothermal systems with carbon dioxide. – Nauka, Moskva.

**Malkovský, M. et al. (1985):** Geologie české severočeské hnědouhelné pánve a jejího okolí. Regionální geologie ČR. (*Geology of North Bohemian lignite basin and its surroundings - Regional Geology of the Czech Republic*) – Ústí. Úst. Geol, Praha.

**Markham, A. E., K. A. Kobe (1941):** The solubility of carbon dioxide and nitrous oxide in aqueous salt solutions. – *J. Am. Chem. Soc.* Vol. 63: 449-454.

**Martinec, P. (1987):** Mirošovský obzor (litologická studie) (*Mirošov horizon - lithological study*). – Tech. Rep. no. SÚ P 01-125-808, DÚ 06, E 03, VVUU Ostrava-Radvanice.

**Martinec, P. (1988):** Petrologie a litologie mirošovských slepenců ve skipové a klecové jámě Dolu Slaný ve vztahu k PHP (s použitím dat z vrtu SJ 847 m) (*Petrology and lithology of conglomerates from the Mirošov horizon from point of view outburst rock and gasses (Slaný Mine)*). – Tech. Rep. no. SÚ P 01-125-808, VVUU Ostrava-Radvanice.

**Martinec, P. (1988):** Petrologie a litologie mirošovských slepenců ve skipové a klecové jámě Dolu Slaný ve vztahu k PHP. Mirošovský obzor II., vrt Dn – 3. (*Petrology and lithology Mirošov horizon in the Slaný Mine borehole Dn -3*). – Tech. Rep. No. SÚ P 01-125-808 VVUU Ostrava-Radvanice.

**Martinec, P. (1993):** Geotechnical classification of carboniferous rock mass with alteration of the variegated beds types. – Proc. Int. Conf. Geomechanics 93 (*Rakowski Z. ed.*): 105-111, Balkema Rotterdam.

**Martinec, P. et al. (1987):** Náchylnost uhlí k průtřím. Srovnávací studie uhlí z československé části hornoslezské pánve a maďarské pánve Mecsek (*Liability of coal to outbursts. Comparison of coal from Czech part of the Upper Silesian basin and Mecsek Basin in Hungary*) – Monography VVUU no. 33, VVUU Ostrava-Radvanice.

**Martinec, P., Krajčůček, J. (1988):** Litologie kontaktní zóny karbonu s pokryvem a její geomechanické vlastnosti. (*Lithology of contact zone of Carboniferous with covering strata and its geotechnical properties*). – Tech Rep. no. SÚ P-01-125-401, VVUU Ostrava Radvanice.

**Martinec, P. et al. (1989):** Petrografie a litologie obzoru mirošovských slepenců ve skipové a klecové jámě Dolu Slaný ve vztahu k PHP (*Petrology and lithology Mirošov horizon in the Slaný skip and hoisting shafts in a relation to outburst rocks and gasses*). – Final Tech. Rep. No. SÚ P 01-125-808, VVUU Ostrava-Radvanice.

**Martinec, P., Kolář, P. (1989):** Petrologie a litologie obzoru mirošovských slepenců v jamách Dolu Slaný (*Petrology and lithology Mirošov horizon in the shaft of Slaný Mine*). – Tech. Rep. no. P-01-125-808. VVUU Ostrava-Radvanice.

**Martinec, P., Kolář, P. (1989):** Pórové charakteristiky hornin mirošovského obzoru a radnických vrstev ve slánské pánvi (*Porosimetry of rocks from Mirošov horizon and Radnice Mbr.*) – In: Fyzikální vlastnosti hornin a ich využitie v geofyzike a geológii III. (Ed. by Kapička, A., I. Túnyi): 125-128. Jednota československých matematiků a fyziků, Praha.

**Martinec, P., Krajčůček, J. (1989):** Vlastnosti hornin svrchního karbonu na kontaktu s pokryvnými útvary (*Properties of Carboniferous rocks on the contact with covering strata*) – Monography VVUU no. 43, VVUU Ostrava-Radvanice.

**Martinec, P., Kolář, P. (1990):** Vyjádření ke geologické situaci a petrografii hornin ve hloubené jámě Komořany v hl. 84,3-111 m (*Geological situation and petrography in the Komořany shaft in depth 84,3-111m*). – Tech. Rep. no HS 17 531, VVUU Ostrava-Radvanice.

- Martinec, P., Krajčůek, J. (1990a):** Vlastnosti hornin slánské pánve. (*Properties of rocks from Slaný Basin*). – Monography no. 49, VVUÚ Ostrava-Radvanice.
- Martinec, P., Krajčůek, J. (1990b):** Pokryvné útvary karbonu čs. části hornoslezské pánve. (*Covering strata of the Carboniferous in Czech part of the Upper Silesian Basin*). – Monography VVUÚ no. 50, VVUÚ Ostrava-Radvanice.
- Martinec, P., Pipek, R. (1990):** Hloubení jámy „Komořany“ – vyhodnocení úseku č. 1. (*Sinking work of Komořany shaft – interval of sinking no.1*) – Tech. Rep., VVUÚ Ostrava-Radvanice.
- Martinec, P., Pipek, R. (1991):** Vliv vlhkosti na mechanické vlastnosti hornin slánské pánve. (*Influence of humidity on rock mechanical properties from Slaný Basin*) – In: Fyzikální vlastnosti hornin a ich využití v geofyzice a geologii IV. (Ed. by Křišťáková, Z.): 46-51. Jednota československých matematiků a fyziků, Praha.
- Martinec, P., Pipek, R. (1991):** Fyzikální vlastnosti kaolinizovaných migmatitů v podloží sedimentární výplně severočeské hnědouhelné pánve (*Physical properties of kaolinized migmatites from base of sedimentary covering strata in the North Bohemian Lignite Basin*) – In: Fyzikální vlastnosti hornin a ich využití v geofyzice a geologii IV. (Ed. by Křišťáková, Z.): 97-100, Jednota československých matematiků a fyziků, Praha.
- Martinec, P., Honěk, J., Staněk, F. (2002):** Bituminous Coal of the Upper Silesian Basin, The Czech Republic – Relation Between Mean Vitrinite Reflectance  $R_o$ , Volatile Matter  $V^{daf}$  and Content of Carbon, Hydrogen and Nitrogen. – *Carboniferous and Permian of the World: XIV. ICCP Proceedings*. (Edit.: Len V. Hilus et al.), Canadian Society of Petroleum Geologists Calgary, April 2002: 902-909, Alberta.
- Martinec, P., Jirásek J., Kožušníková, A., Sivek (ed.) (2005):** Atlas uhlí české části hornoslezské pánve (*Atlas of Coal from the Czech part of the Upper Silesian Basin*). – ÚGN AV ČR Ostrava in Anagram, 1-64pp., Ostrava.
- Martinec, P., Honěk, J., Živor, R. et al. (2006):** Termination of underground coal mining and its influence on environment. – ÚGN AV ČR in Anagram, 1-174pp., Ostrava.
- Martinec, P., Dvořák, D., Kolcun, A., Malík, J., Schejbalová, B., Staš, L., Šňupárek, R., Vašíček Z. (2008):** Geologické prostředí a geotechnické vlastnosti pokryvu karbonu v české části hornoslezské pánve (*Geological environment and geotechnical properties of covering strata of Carboniferous in the Czech part of the Upper Silesian Basin*) – ÚGN AV ČR, Ostrava: 1-148, Fig. 57, Tables. 33 (Czech with English resumé), Ostrava.
- Matoušek, M. (1977):** Effects of some Environmental Factors on Structures. – MS, Thesis, VUT Brno.
- Medek, J. (1971):** Povrchové vlastnosti uhlí a koksů (*Properties surface of coal and coke*) – Acta Montana, No. 15, Praha.
- Menčík, E. et al. (1983):** Geologie Moravskoslezských Beskyd a Podbeskydské pahorkatiny. Oblastní regionální geologie ČSR. (*Geology of Morava-Silesian Beskydy Mts. and Sub-Beskydy Highland - Regional Geology of the Czech Republic*) – Ústř. Ust. Geol. in Academia, Praha.
- Michálek, R. (1961):** Hydrogeologie bazálních miocénních klastik v Odrách (*Hydrogeology of Miocene basal clastic in Odry - town*). – *Přírodovědný časopis slezský, Zprávy č. 1*, Opava.
- Michálek, R. (1980):** Problematika ostravsko-karvinského detritu (*The Ostrava-Karviná Lower Badenian basal clastics*). – *Zpravodaj TEI*, no. 10, Báňské projekty, Ostrava.
- Michálek, R. (1983):** Báňsko-hydrogeologické předpoklady odvodňování detritu ve vymýtinách OKR (*Hydrogeological an mine problems with Lower Badenian basal clastics dewatering in Ostrava-Karviná Coal District*) – *Zpravodaj TEI*, nos. 7-8, Báňské projekty, Ostrava.
- Mikyťová, M., Polický, J., Honěk, J., Vrbová, V., Chvístek, A., Pauková, V., Huřová, E., Prokop, I. (1984):** Frenštát - Trojanovice. Studie zvětralinového pláště karbonu (*Frenštát-Trojanovice. Weathering crust on Carboniferous*) – Tech. Rep. no. 02 82 2308 59 201 3804 1, Geologický průzkum, Ostrava.
- Nodzienski, A. (2000):** Wysokociśnienowa desorpca ditlenku węgla i metanu z węgla kamiennego. Zagłębia Dolnośląskiego. – *Rozprawy orografie*, No. 95, AGH, Krakov.
- Novák, J. P., Malijevský, A., Šobr, J., and Matouš, J. (1972):** Plyny a plynné směsi (*Gasses and gaseous mixtures*) – Academia, Praha.
- Nowak, G. J. (1992):** Środowiska depozycji pokładów węgla warstw Źaclierskich w depresji środsudeckiej w oparciu o badania petrologii węgla – *Przew. Seminarium Sedymetol.*, Poznań.
- Nowak, G. J. (1993):** Macerały i mikrolitotypy jako wskaźniki facji węgla. Przykład z warstw Źaclierskich niecki środnosudetskiej. – 2. *Symp. Sedymetologiczna*. Wrocław.
- Nowakowski, A., Konečný, P. jr. (2002):** Wpływ obciążeń termicznych na zmiany przepuszczalności próbek skał w trójosiowym stanie naprężenia. – XXV. Zimowa szkoła mechaniki górotworu. Krakov.
- Novotný, M., Skácelová, Z., Mlčoch, B. (2010):** Crustal structures beneath the Saxonian Granulite Massif, the České středohoří and Doupovské hory Mts. based on the depth-recursive tomography – *J. of Geosciences*, Vol. 55, No.3: 1987-1992, Praha.
- Ottiger, S., Pini, R., Storti, G., Mazzotti, M. (2008):** Competitive adsorption equilibria of CO<sub>2</sub> and CH<sub>4</sub> on a dry coal – *Adsorption*, Vol.14, nos. 4–5: 539–556.

- Pačes, T. (1974):** Sprinte of carbon-dioxide waters in northwestern Bohemia. Field-trip guide – Intern. Symp. Water-Rock interaction, Czech Geol. Surv., Praha.
- Pačes, T. (1987):** Hydrochemical evolution of saline waters from crystalline rock of Bohemia Massif (Czechoslovakia) – In: Saline water and Gates in crystalline rocks ed. P. Fritéz, S. K. Frappe. Geol. Assoc. Canad. Spec. Pap. 33, 145-156.
- Papadakis, V.G., Fardis, M.N., Vayenas, C.G. (1992):** Effect of composition, environmental factors and cement lime mortar coating on concrete carbonatation – *Material and Structures*. Vol. 25: 293-304, N.Y.
- Papadakis, V.G., Tsimas, S. (2002):** Supplementary cementing materials in concrete, part I: efficiency and design – *Cement and Concrete Research*, Vol. 32, No. 10: 1525-1532.
- Patteisky, K. in Folprecht (1928):** in Kamenouhelné doly ostravsko-karvinského revíru. – Ředitelská konference Ostravsko-karvinského kamenouhelného revíru v Mor. Ostravě v X. roce Československé republiky, Prometheus Praha.
- Perera, M.S.A., Ranjith, P.G., Choi, S.K. et al. (2011):** – *Environmental Earth Science*, Vol. 64: 223-235.
- Pešek, J. (1996):** Geologie pánví středočeské svrchnopaleozoické oblasti (*Geology of Upper Paleozoic basins in Central Bohemia*) – Česká Geol. Služba, Praha.
- Pipek, R., Martinec, P. et al. (1990):** Vyhodnocení vrtu KO 16 - Komořany v hloubkovém intervalu 92 až 245,6 m (*Borehole KO 16 - Komořany shaft - interval 92 - 245.6 m*). – Tech. Rep. VVUÚ Ostrava-Radvanice.
- Pišta, J. (1954):** Oblast výronu juvenilního CO<sub>2</sub> v OKR (*Areas of carbon dioxide emissions in the Ostrava-Karviná Coal District*) – *Uhlí*, Vol. 30, no.4, Praha.
- Pišta, J. (1961):** Ostravsko-karvinský detrit (*Lower Badenian basal clastics in the Ostrava-Karviná Coal District*) – Monography for Ministerstvo paliv a energetiky: 1- 276, Praha.
- Plášil, M. et al. (1987):** Závěrečné zhodnocení úkolu VČSA – odvodnění USOM (*Final report VČSA – dewatering of USOM*) – Tech. Rep. no. 01-87-1041. Geoindustria, Praha.
- Plášil, M. (1989):** Popis vrtného jádra vrtu 2A v hloubené jámě Komořany (*Description of borehole no. 2A in Komořany shaft*) – personal comm., Geoindustria, závod Dubí u Teplíc ze dne 21.12.1989.
- Pluta, I. (2002):** Jakost wód południowo-zachodniej czesci HP na podstawie badań hydrochemicznych i izotopowych w kopalni „Morcinek” – *Przegąd Górniczy*, no. 9: 42-54. Warszawa.
- Polyak, B. G., Prasolov, E. M., Čermák, V., Verkhovskiy, A. B. (1985):** Isotopic composition of noble gases in geothermal fluids of the Krušné hory Mts., Czechoslovakia, and the nature of the local geothermal activity – *Geochim. Acta*, Vol. 49: 695-699.
- Pone, J.D.N., Halleck, P.M., Mathews, J.P. (2009):** Sorption capacity and sorption kinetic measurements of CO<sub>2</sub> and CH<sub>4</sub> in confined and unconfined bituminous coal – *Energy & Fuels*, Vol. 23, no. 9: 4688-4695.
- Příbyl, O., Weishauptová, Z. and Kolář, F. (2009):** Factors influencing the amount of CO<sub>2</sub> sorbed on coal – *J. GeoLines*, Vol. 22: 52-57, Praha.
- Rakowski, Z., Lát, J., Hruzík, B., Dvořáček, J. (1983):** Nové poznatky v problematice průtržní uhlí a plynů v OKR (*New knowledges in problems of outbursts coal and gas*) – Monography GR OKD Ostrava.
- Rieche, R. (1943):** Graphic representation of chemical weathering – *J. Sed. Petrology*, Vol. 13: 58-68, London.
- Rovnaník, P. et al. (2005):** RC LifeTime-software tool for designing of durability of RC structures. - Centre for Integrated Design of Advanced Structures – Projekt no. 1 M0579, VUT Brno.
- Roy, S. K., Poh, K.B. (1999):** Nortwood: Durability of concrete-accelerated carbonation and weathering studies. – *Building and Environment*, Vol. 34: 557-606.
- Říman, A. (1955):** Základy mechaniky hornin a důlních tlaků (*Rock mechanics and mine stresses*) – SNTL Praha.
- Sakurovs, R., Day, S., Weir, S., Duffy, G. (2007):** Application of a modified Dubinin-Radushkevich equation to adsorption of gases by coals under supercritical conditions – *Energy and Fuels*, Vol. 21: 992-997.
- Sakurovs, R., Day, S., Weir, S., Duffy, G. (2008):** Temperature dependence of sorption of gases by coals and charcoals – *Int. J. Coal Geol.*, Vol. 73, Issue 3-4: 250-258.
- Schejbalová, B., Endel, K., Majzlík, J. et al. (1983):** Stanovení ochranných celíků pod detrity I (*Determination of safety pillar under Lower Badenian clastics, part I.*) – Tech. Rep. no. 204, VVUÚ Ostrava-Radvanice.
- Schejbalová, B., Endel, K., Majzlík, J. et al. (1984):** Technicko-ekonomická studie úkolu RVT Dobývání uhlí pod vodonosnými horizonty (*Coal mining under water-bearing horizon - Technical and Economical Study*) – Tech. Rep. no. P 10-125-401, VVUÚ Ostrava-Radvanice.
- Schejbalová, B., Endel, K., Majzlík, J. et al. (1985):** Bezpečnostní opatření pod detrity a zvodněnými horizonty (*Safety arrangement in case mining under water-bearing horizon*) – Tech. Rep. no. P 10-125-401, VVUÚ Ostrava-Radvanice.
- Schejbalová, B., Endel, K., Majzlík, J. et al. (1987):** Dobývání uhlí pod vodonosnými horizonty II (*Coal mining under water-bearing horizon, part II*) – Tech. Rep. no P 10-125-817 VVUÚ Ostrava – Radvanice.
- Schejbalová, B., Endel, K., Majzlík, J. et al. (1988):** Dobývání uhlí pod vodonosnými horizonty I (*Coal mining under water-bearing horizon, part I*) – Tech. Rep. no. P 10-125-109, VVUÚ Ostrava-Radvanice.

- Střelec, T., Martinec, P. (1992):** Analýza zvětralinového pláště na povrchu karbonu (Důl ČSM) (*Analysis of weathering crust on Carboniferous surface (ČSM Mine)*) – Tech. Rep. no. P 10-125-109, VVUÚ Ostrava-Radvanice.
- Suchodolski, Z. in Kruk (1969):** Wpływ struktury i zwiezłości węgla oraz ciśnienia górotworu na zagrożenie wyrzutami CO<sub>2</sub> i skal w rejonie wałbrzyskim – *Archiwum Górnictwa*, Vol. XII, no. 2, Katowice.
- Swidzinski, A. (1977):** Charakterystyka głównych czynników wpływających na możliwość zaistnienia wyrzutów setli, gazów i skal – *Zeszyty Naukowe Politechniki Śląskiej. Seria Górnictwo*, Vol. 87, Katowice.
- Škuta, K., Víték, J. (1969):** Zonálnost plynů v OKR (*Zonal distribution of gasses in the Ostrava-Karviná Coal District*) – Monography no. 72, VVVÚ Ostrava-Radvanice.
- Šmejkal, V., Hladíková, J., Pfeiferová, A., Melková, J. (1976):** Isotopic composition of carbon and oxygen in speleotherms from Karst Caves in Norten Moravia – Proc. Int. Symp. On Water-Rock International 1974 (Čadek, J. a Pačes, T. eds.), Ústř. Úst. Geol., 356-366. Praha.
- Šmerda, Z. et al. (1999):** Životnost betonových staveb (*Durability of concrete construction*) – Technická knihnice autorizovaného inženýra a technika č. 4., Čes. svaz stavebních inženýrů, Praha.
- Šmíd, M., Jelen. B., Složil, J., Rakowski, Z. (1978):** Instrukce k provádění prognózy a prevence průtrží uhlí a plynů na dolech s nebezpečím průtrží v OKR – Monography no. 33, Vědeckovýzkumný uhelný ústav Ostrava-Radvanice.
- Šmíd, M., Kaiser, E., Pavlíček, J., Martinec, P. (1989):** Databanka průtrží hornin a plynů a možnost jejího dalšího vývoje (*Database of coal, rock and gasses and possibility its development*) – Monography no. 39 VVUÚ Ostrava-Radvanice.
- Šmíd, M. a kol. (1990):** Posouzení aktuálnosti nebezpečí průtrže hornin a plynů v odvodňovací jámě VČSA Komořany (*Outburst of rock and gas in Komořany dewatering shaft - actual state of danger*) – VVUÚ Ostrava-Radvanice.
- Štěpán, J., Šmíd, M. (1989):** Návrh metod prevence průtrží hornin a plynů a průvalů vod trhačí prací pro odvodňovací jámu Velkodolu ČSA v Komořanech u Mostu (*Proposal methods for prevention of gas and water outburst after rock blasting in Komořany shaft*) – Tech. Rep., VVUÚ Ostrava-Radvanice.
- Takla, G. et al. (2003):** Komplexní řešení problematiky výstupu důlních plynů na povrch. (*Mine gas emission on surface - methods for prevention*) – Tech. Rep. DPB Paskov, Paskov.
- Taraba, B. (2008):** Tech. Rep. Project ČBÚ, no. 57-2008, Praha.
- Tardon, S. et al. (1992):** Likvidace důlních slaných vod v OKR (*Liquidation of mine salty water in Ostrava-Karviná Coal District*) – Tech. Rep. no. TP-817-93-DÚ 03, VVUÚ Ostrava-Radvanice.
- Tarnowski J. (1969):** Wpływ ilości gazu zasorbowanego przez węgli na szybkość desorbcji – In: Kruk et al. (1969): Komisja dla Spraw Zagrożeń Związanymi z Wyrzutami Gazów i Skal w Kopalniach Węgla, Materiały z prac komisji - zwięzek 3, 162-202, Warszawa.
- Tarnowski, J. (1969):** Własności sorpcyjne dolnośląskich węgli sklonnych do wyrzutów gazu i skal – In: Kruk et al. (1969): Komisja dla Spraw Zagrożeń Związanymi z Wyrzutami Gazów i Skal w Kopalniach Węgla. Materiały z prac komisji - zwięzek 3, 202-248. Warszawa.
- Tásler, R. et al. (1979):** Geologie české části vnitrosudetské pánve (*Geology of the Intra-Sudeten Basin. Regional geology of the Czech Republic*) – Ústř. Úst. Geol. in Academia, Praha.
- Teplý, B., Chromá, M., Rovnaník, P. (2010):** Durability assessment of concrete structures: Reinforcement depasivation due to carbonation – *Structure and infrastructure engineering*, Taylor & Francis, Colchester, Essex, CO<sub>3</sub> 3LP, UK, Essex.
- Tesař, J. (1986):** Zusammensetzung der für therapeutische Zwecke genutzten natürlichen Quellgase in der Westbömischen Heibädern – *Balneol. Bohem.*, vol. 15, no 2: 51-59
- Tylčer, J. (1977):** Polanka nad Odrou - hydrogeologický průzkum (*Polanka nad Odrou - hydrogeological survey*) – Tech. Rep.. Geol. Průzkum, Ostrava.
- van Krevelen, D.W., Schuyer, J. (1957):** Coal Science – Elsevier PC, 1-136 pp., Amsterdam.
- van Krevelen, D.W. (1993):** Coal: Typology-Physics-Chemistry-Constitution – Elsevier 1-1002 pp., Amsterdam.
- Weinlich, F.H., Tesař, J., Weise, S.M., Bräuer, K., Kämpf, H. (1998):** Gas flux distribution in minerál springs and tectonic structure in the western Eger Rift – *J. Czech Geol. Soc.* Vol. 43, no.1-2: 91-110, Praha.
- Wiebe, R., Gaddy, V. L. (1941):** Vapor phase composition of carbon dioxide-water mixtures at various temperatures and at pressures to 700 atmospheres – *J. Am. Chem. Soc.* Vol. 63: 745-747.
- Zang, A., Stephanson, O. (2010):** Stress Field of the Earth's Crust – Springer, Dordrecht, Heidelberg, NY.
- Zdanowski, A., Zakowa, H. et al. (1995):** The Carboniferous system in Poland (Karbon w Polsce) – *Prace Panstwowego Instytutu Geologicznego*, CXLVIII, Warszawa.
- Zelvenskij, U. D. (1937):** *Žurnal. chim. promyšlennosti*, Vol. 14: 1253, Moskva.

**Zolcinska-Jezerska, J., Lason, M., Otowska, A. (1980):** The physico-chemical properties of coal with respect to outburst phenomenon – *Archivum Gornictwa*, Vol. 25: 19-26, Katowice.

**Žbánek, J. et al. (1978):** Závěrečná zpráva Slánsko (*Final report „Slaný area“*) – Tech. Rep., Geofond Praha.

**Žižka, J. (1989):** Popis vrtného jádra vrtu V1 v hloubené jámě Komořany (*Description of core in bore V1A in Komořany shaft*) – Personal comm 7.12.1989.

**Živor, R., Leopold, L. (1986):** Hydrogeologická zpráva za období 1979-1986 (*Hydrogeological report - Slaný shafts 1979-1986*) – Tech. Rep., Geindustria, Praha.

**Živor, R. (1988):** Báňsko-geologický průzkum Slaný I. fáze (*Geological and mine survey, locality Slaný – Phase I: Annual report 1987*) – Tech. Rep., Výstavba Dolu Slaný.

**Živor, R. (1988):** Báňsko-geologický průzkum Slaný I. fáze. (*Geological and mine survey, locality Slaný – Phase I: Annual report 1988*) – Tech. Rep., Výstavba Dolu Slaný.

**Živor, R. et al (1989):** Výroční zpráva za rok 1988. Báňsko-geologický průzkum Slaný - I. fáze. (*Geological and mine survey locality Slaný - Phase I: Annual report 1988*) – Tech. Rep. Výstavba Dolu Slaný.

**Živor, R. (1989):** Báňsko-geologický průzkum Slaný I. fáze. (*Geological and mine survey locality Slaný - Phase I: Annual report 1989*) – Tech. Rep. Výstavba Dolu Slaný.

#### **STANDARDS:**

EN 1992-1 Eurocode 2: Design of Concrete Structures - Part 1.1: General Rules and Rules for Buildings. CEN, 2003.

EN 1990 Eurocode - Basis of Structural Design.

EN 206-1 Concrete - Part 1: Specification, Performance, Production and Conformity (incl. ČNI Amendment Z1/2002 and Z2/2003).

#### **INSTRUCTIONS:**

Instruction VUD to reglement of ČBÚ 6000/77 (Outburst prevention).

Instruction for forecasting and preventing coal and gas outbursts in mines prone to outbursts – VVUÚ Ostrava -Radvanice.

Institute of Geonics ASCR  
Studentská 1768  
708 00 Ostrava-Poruba  
Czech Republic  
[www.ugn.cas.cz](http://www.ugn.cas.cz)

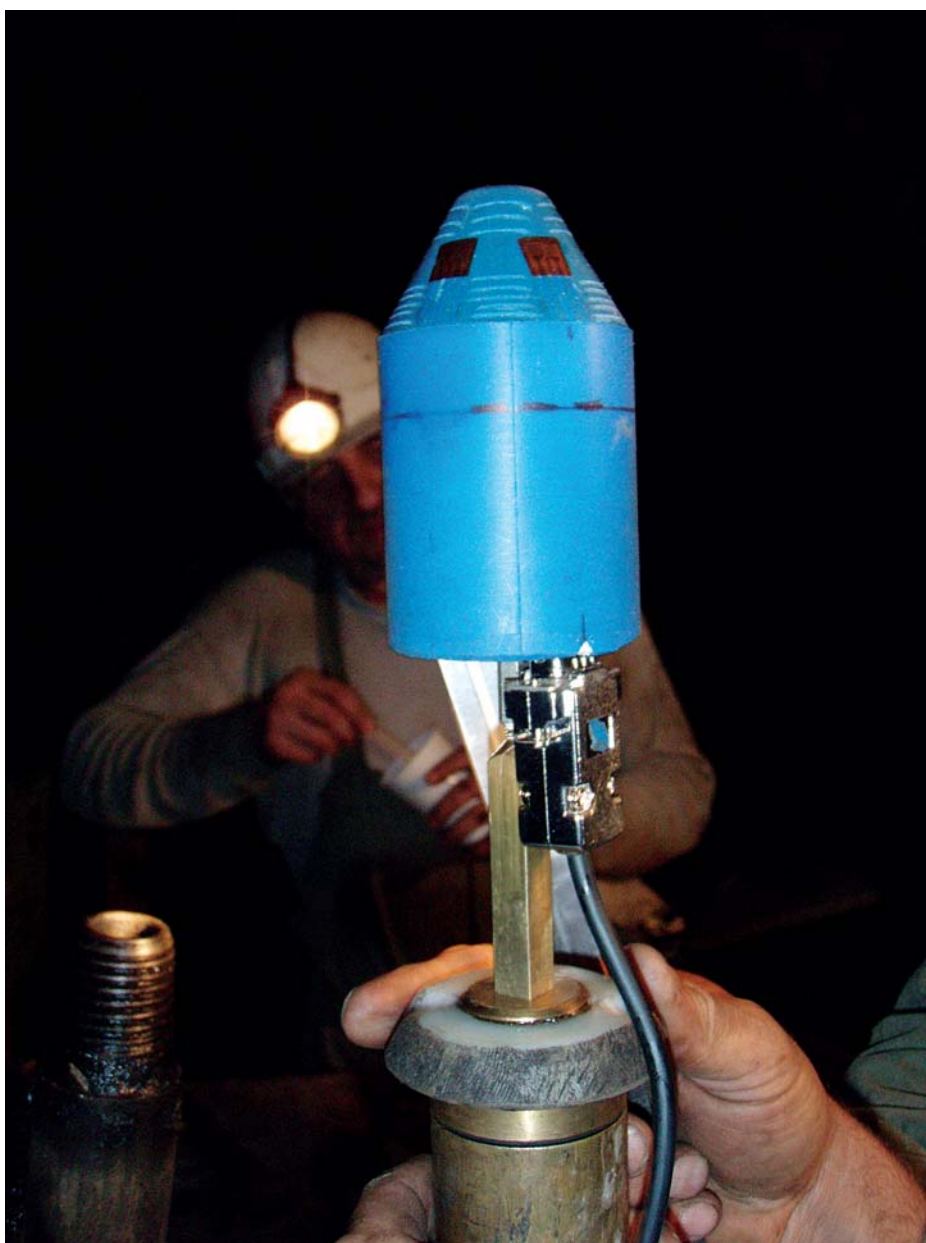


For centuries, the energy requirements lead to the use of the Earth's crust as a source of coal, oil, gas, uranium or geothermal power. Nowadays, rock mass is also key in gas storage and future plans for reposition of pollutants from energy production, such as carbon dioxide or nuclear waste. These reasons motivate research activities of the *Institute of Geonics of the Academy of Sciences of the Czech Republic*.

The Institute was founded in Ostrava, the centre of the Czech part of the Upper Silesian Coal Basin, and much its research concerned coal mining at great depths. Gradually, the Institute's focus expanded substantially, and now includes coal and uranium mining, construction of gas reservoirs, carbon dioxide sequestration and deep deposition of spent nuclear fuel. Besides solving geotechnical problems, such as rock burst prevention, the Institute contributes to rock stress measurements, seismic monitoring, systematic investigations of geomaterials, development of new mathematical modelling tools and investigation of social aspects of the energy.

The Institute's investigations are currently supported by the Academy and many research projects, and its results benefit the Czech Mining Authority, Czech Radioactive Waste Repository Authority, mining companies and others.

It participates in the worldwide DECOVALEX project devoted to reliably modelling processes in rocks crucial for nuclear waste deposition, and in EU projects on coal carbonization and brownfields. The Institute is also involved in two large EU-supported projects started in 2011, which provided new equipment for rock mechanics and establishment of a new laboratory on X-ray tomography of geomaterials, further development for high pressure water-jet technology **and involvement in a new supercomputing facility.**



# ČEZ GROUP

is an environmentally responsible group of companies headed by ČEZ Corporation,  
with focus on providing the best available yet economical technologies,  
to progressively mitigate any impacts harmful to the environment and to human health.

ČEZ initiated a research and development program oriented on innovative technologies for power engineering,  
which also aims to further reduce the sector's environmental impacts.

Development of new ways of abatement of CO<sub>2</sub> emissions from the combustion of fossil fuels,  
which is the essence of CCS (carbon capture and storage) technology, is an integral part of the program.  
Safe underground storage of CO<sub>2</sub> in bedrock is an inseparable, ultimate component of the system.

This is why it is very important to identify geological areas which are out  
of reach of the natural sources of juvenile CO<sub>2</sub>;  
this is done by prospecting for new locations where the final storage of carbon dioxide  
could be sited in the Bohemian Massif.

CEZ is a member organization of the European Technology Platform in this field  
(ZEP - Zero Emission Platform)  
and has supported several international projects  
(e.g., Geocapacity and CO<sub>2</sub> EuroPipe).



## SKUPINA ČEZ



ISO - 9001

Tiskárna AG TYP  
Rudé armády 1468  
514 71 Kostelec nad Orlicí  
Czech Republic

phone: 00420 494 321 275  
e-mail: [agtyp@agtyp](mailto:agtyp@agtyp)  
[www.agtyp.cz](http://www.agtyp.cz)

Printing haus produced:  
books, booklets, trade printed materials, regional press ...



